

BIOTIC COMPOSITION AND TAPHONOMY OF AN UPPER CRETACEOUS
KONSERVAT-LAGERSTÄTTE: THE INGERSOLL SHALE,
EUTAW FORMATION, EASTERN
ALABAMA

Except where reference is made to the work of others, the work described in this thesis is my own or was done in collaboration with my advisory committee. This thesis does not include proprietary or classified information.

Terrell Keith Knight

Certificate of Approval:

Charles E. Savrda
Professor
Geology and Geography

Ronald D. Lewis, Chair
Associate Professor
Geology and Geography

David R. Schwimmer
Professor
Chemistry and Geology
Columbus State University

Joe F. Pittman
Interim Dean
Graduate School

BIOTIC COMPOSITION AND TAPHONOMY OF AN UPPER CRETACEOUS
KONSERVAT-LAGERSTÄTTE: THE INGERSOLL SHALE,
EUTAW FORMATION, EASTERN
ALABAMA

Terrell Keith Knight

A Thesis

Submitted to

the Graduate Faculty of

Auburn University

in Partial Fulfillment of the

Requirements for the

Degree of

Master of Science

Auburn, Alabama
August 4, 2007

BIOTIC COMPOSITION AND TAPHONOMY OF AN UPPER CRETACEOUS
KONSERVAT-LAGERSTÄTTE: THE INGERSOLL SHALE,
EUTAW FORMATION, EASTERN
ALABAMA

Terrell Keith Knight

Permission is granted to Auburn University to make copies of this thesis at its discretion, upon request of individuals or institutions and at their expense. The author reserves all publications rights.

Signature of Author

Date of Graduation

VITA

Terrell Keith Knight, son of Kenneth Malloy and Martha Fay Knight, was born on September 19, 1974, in Birmingham, Alabama. He graduated from Bradshaw High School in 1992. On June 28, 1995, he became the proud father of Anastasia Jade Knight. He attended Columbus State University, Columbus, Georgia, and graduated in December 2003 with a Bachelor of Science degree in Geology. He entered the Graduate School at Auburn University in the Fall of 2004.

THESIS ABSTRACT

BIOTIC COMPOSITION AND TAPHONOMY OF AN UPPER CRETACEOUS

KONSERVAT-LAGERSTÄTTE: THE INGERSOLL SHALE,

EUTAW FORMATION, EASTERN

ALABAMA

Terrell Keith Knight

Master of Science, August 4, 2007
(B.S., Columbus State University, 2004)

237 Typed Pages

Directed by Ronald Lewis

The Ingersoll shale is a thin (<1m), laterally restricted clay lens within the Upper Cretaceous (Santonian) Eutaw Formation, Russell County, eastern Alabama. The clay lens represents abandoned tidal creek fill within an estuarine environment. Excavation of this marginal marine *Konservat-Lagerstätte* has produced an abundant, diverse, and extraordinarily well-preserved biotic assemblage, which is dominated by terrestrial plants but includes invertebrates and vertebrates. The macroflora consists of leaves from dicotyledon and monocotyledon angiosperms (over two dozen species), gymnosperms, and a variety of water plants (ferns and lycopsids). Many of these plants represent riparian vegetation that was introduced to the site via wind transport; they have minimal

signs of damage from being transported by water. Although most plant tissues are carbonized and/or pyritized, some leaf cuticle is unmineralized, flexible, and easily removed from the matrix. Conifer stems are often preserved in three-dimensions via early authigenic pyritization. Some of these reveal *in situ* amber rods. The shale lens also contains a variety of plant reproductive organs (e.g., cones, and seedpods), megaspores from heterosporous isoetalean lycopsids and water ferns, a variety of fungal spores, pollen, acritarchs, and marine dinoflagellates. Many of these fossils were transported into the depositional site. Amber is very abundant in the lower portions of the lens and often contains inclusions, some of which are insect appendages, mites, and fungal hyphae. In the reducing environment represented by the Ingersoll shale, carbonates are completely absent, and phosphatic components such as vertebrate bones have not yet been found. However, well-preserved vertebrate integumentary structures, such as theropod feathers and fish scales, have been found. These structures represent the preservation of originally protein-based tissues (e.g., beta-keratin and collagen). Feathers are preserved by replacement by fossilized bacilliform bacteria and are especially significant.

The Ingersoll-shale biota is more diverse than any previously documented Gulf coast Santonian deposit and provides a unique look into Late Cretaceous terrestrial plant and animal communities. In particular, the Ingersoll shale has yielded the largest collection of fossil feathers from the Mesozoic strata of North America. Furthermore, understanding the taphonomy of the Ingersoll shale biota provides insight into the conditions that govern the preservation of refractory soft tissues, thus enhancing future prospecting methods for other nearshore *Konservat-Lagerstätten*.

ACKNOWLEDGMENTS

The author would like to thank the Geological Society of America and the National Science Foundation for grants that supported this research. Michael Ingersoll allowed the author access to his property, and fellow Auburn University geology student Patrick Sean Bingham, who discovered this wonderful fossil deposit, acted as a sounding board for ideas and inspired me through his dedication and hard work on the project. The following individuals assisted in the field: Jerry Smith, Carl Mehling, John Interlandi, David Grimaldi, Tracy Hall, David Leuth, Dent Williams, William Frazier, William Montante, Robert Monrreal, Dennis Ruez, Will Newton, Nichole Kirksey, Dan Evans, Tom Hart, and Bobby Norris. The following individuals prepared, identified, analyzed, and/or photographed specimens for this thesis: Brian Axsmith, Richard Lupia, David Grimaldi, Mary Schweitzer, Raymond Christopher, Michael Miller, and Barton Prorok. Chuck Savrda and Ronald Lewis acquired NSF support for this work and provided guidance with field work, laboratory analyses, and writing. David Schwimmer inspired the author to study paleontology and provided guidance with excavation and fossil identification. Anastasia Knight provided patience, love, support, and encouragement throughout the course of this project. Dear friend Jennifer Glidewell provided her love, support, and encouragement while writing this thesis. The author dedicates this thesis and M.S. degree to his daughter Anastasia Jade Knight.

Journal style used: Palaios

Computer software used: Microsoft Word 2003, Microsoft Excel 2003, Adobe Photoshop
7.0.

TABLE OF CONTENTS

LIST OF FIGURES	xii
LIST OF TABLES	xix
OBJECTIVES	1
INTRODUCTION	3
Fossil <i>Lagerstätten</i> and Exceptional Preservation	3
Taphonomic Investigations of Fossil <i>Lagerstätten</i>	4
SOUTHEASTERN GULF COASTAL PLAIN (EUTAW FORMATION).....	9
General Stratigraphy	9
Depositional Environments.....	9
Eutaw Formation Fossils (Chattahoochee Valley)	11
LOCATION OF STUDY	14
GENERAL METHODOLOGY	18
Introduction.....	18
Field Work for Discovering Macrofossils	18
Field and Lab Methods for Extracting Mid-Size Fossils	21
OVERVIEW OF FINDINGS	22
Biotic Composition	22
Fossil Distribution.....	25
DESCRIPTION OF PALYNOMORPHS AND MEGASPORES.....	31
Palynomorph Results	31
Megaspores	33
MACROFLORA.....	38
Introduction.....	38
Methodology	40
Results.....	41
Description and Discussion of Fossil Remains.....	42
<i>Equisetum</i> (?)	42
Ferns.....	42
Monocotyledon Angiosperm Leaf Morphotypes.....	48

Dicotyledon Angiosperm Leaf Morphotypes	50
Conifer Foliage Morphotypes	82
Conifer Reproductive Organs	89
Flowers, Seeds, and Fruits	92
Roots	99
Modes of Preservation Observed in the Ingersoll Flora	101
Interpretation and Discussion	105
Closing Remarks	110
AMBER	111
Introduction	111
Previous Work	111
Methodology	115
Results	116
Interpretation and Discussion	124
Conclusion	128
INVERTEBRATES	130
Marine Invertebrates	130
Terrestrial Invertebrates	132
CTENOID FISH SCALES	133
Introduction	133
Fish Scale Anatomy	133
Methodology	136
Results and Description	136
Taphonomic Summary and Discussion	141
FEATHERS	142
Introduction	142
Feather Anatomy	142
Feather Types	146
Feather Taphonomy	150
Feathers from Mesozoic Strata	153
Methodology for Collecting and Examining Fossil Feathers	156
Results and Descriptions	157
Taphonomic Processes	170
Interpretation and Discussion	172
Closing Remarks	180
FOSSIL CONTENT AND PRESERVATION ON RELATION TO THE DEPOSITIONAL HISTORY OF THE INGERSOLL SHALE	181

COMPARISONS WITH SIMILAR <i>KONSERVAT-LAGERSTÄTTEN</i> AND A MODERN ANALOG	192
Introduction.....	192
Similar Fossil Deposits	192
Modern Analog to the Ingersoll Shale	198
Closing Remarks.....	200
 SUMMARY AND FUTURE RESEARCH.....	 202
 REFERENCES	 207
 APPENDIX.....	 CD

LIST OF FIGURES

- FIGURE 1—Stratigraphic correlation chart of Upper Cretaceous deposits spanning from central Alabama (west) to western Georgia (east). The red square indicates the stratigraphic location of Ingersoll shale (modified from Savrda et al., 1998)10
- FIGURE 2—Study location of the Ingersoll shale. Red arrow (left) points to Upper Cretaceous deposits (green), blue dot (right) shows approximate location of the study site off State Highway 43115
- FIGURE 3—Stratigraphic column of the measured section at the study location showing the location of the Ingersoll shale (red box) located ~1 m above the Tuscaloosa/Eutaw disconformity (modified from Bingham, 2007)16
- FIGURE 4—Quarrying technique used to remove blocks of Ingersoll shale. (A) Wedges were driven into preexisting fractures. (B) Top blocks were removed. (C) Wedges were driven to base. (D) Bottom blocks were removed20
- FIGURE 5—Ingersoll shale quarry map (11x20 m grid). Shows the approximate location of proteinaceous fossils. Dashed line represents thickest portions of the clay lens26
- FIGURE 6—General stratigraphic column of the Ingersoll shale lens divided into six zones based on the relative abundance of fossils. Relative fossil abundance of each layer is based on qualitative data and indicated by the thickness of the red bars. Included in zone 5 are two intervals (cross-hatched) denoting subzones with bundles containing multiple layers of macerated plant detritus. Shown in zone 6 are *Thalassinoides*- and *Rhizocorallium* burrows. The dashed lines represent sand dominated lamina. Blue dotted line represents the vertical datum27
- FIGURE 7—Lateral distribution of fossils within the clay lens. Thickness of red bar indicates relative abundance of fossils. Note that fossils are most abundant along the inferred channel-thalweg and decrease in abundance toward the east (from Bingham, 2007)29
- FIGURE 8—Ingersoll shale palynomorphs, assignable to the *Sohlipollis* Taxon Range Zone (mid-Turonian-Santonian). (A) Pollen (B) Marine dinoflagellate. (C) Acritarch. (D) Fungal spore. Photographs taken by Richard Lupia (Clemson University). *Sohlipollis* Taxon Range Zone assignment and general palynomorph identifications made by Ray Christopher (University of Oklahoma)32

FIGURE 9—Megaspores from the Ingersoll shale. (A) <i>Molaspora lobata</i> . (B) <i>Ariadnasporites</i> sp. (C) <i>Arcellites</i> sp. (D) <i>Paxillitriletes</i> sp. (E) Unidentified megaspore. (F) <i>Erlansonisporites</i> sp. Identifications courtesy of Richard Lupia (Clemson University).....	34
FIGURE 10—(A) Sporocarp from Marcileaceae. (B) Close-up of sporocarp showing articulated megasporangia and microsporangia; megasporangia (me), microsporangia (mi), main vein (mv), lateral vein (lv).....	35
FIGURE 11—Possible Ingersoll shale <i>Equisetum</i> . (A) Pyritized pith cast. (B) Strobilis spicate axis	43
FIGURE 12—Ingersoll shale ferns. (A) Fern morphotype 1 (KIS-220). (B) Fern morphotype 2 (KIS-607). (C) Fern morphotype 3 (KIS-203). (D) Fern morphotype 4 (KIS-051). (E) Fern morphotype 5 (KIS-009A). (F) Fern morphotype 6 (KIS-200). (G) Fern morphotype 7 (KIS-276)	44
FIGURE 13—Ingersoll shale monocotyledon leaf morphotypes. (A) Monocotyledon leaf morphotype 1. (B) Monocotyledon leaf morphotype 2	49
FIGURE 14—Ingersoll shale dicotyledon leaf morphotypes. (A) Morphotype 1 from the Columbus State University collection. (B) Morphotype 2 (KIS-085). (C) Morphotype 3 (KIS-159). (D) Morphotype 4 (KIS-002). (E) Morphotype 5 (KIS-084). (F) Morphotype 6 (KIS-606). (G) Morphotype 7 (KIS-608). (H) Morphotype 8 (KIS-048). (I) Morphotype 9 (KIS-049).....	51
FIGURE 15—Ingersoll shale dicotyledon leaf morphotypes. (A) Morphotype 10 (KIS-603). (B) Morphotype 11 (KIS-086). (C) Morphotype 12 (KIS-145). (D) Morphotype 13 (KIS-272A). (E) Morphotype 14 (KIS-092). (F) Morphotype 15 (KIS-033). (G) Morphotype 16 (KIS-600B). (H) Morphotype 17 (KIS-146). (I) Morphotype 18 (KIS-268)	60
FIGURE 16—Ingersoll shale dicotyledon leaf morphotypes. (A) Morphotype 19 (KIS-268). (B) Morphotype 20 (KIS-045). (C) Morphotype 21 (KIS-054). (D) Morphotype 22 (KIS-148). (E) Morphotype 23 (KIS-705). (F) Morphotype 24 (KIS-149). (G) Morphotype 25 (KIS-139). (H) Morphotype 26 (KIS-073). (I) Morphotype 27 (KIS-512)	66
FIGURE 17—Ingersoll shale dicotyledon leaf morphotypes. (A) Morphotype 28 (KIS-006). (B) Morphotype 29 (KIS-062). (C) Morphotype 30 (KIS-275). (D) Morphotype 31 (KIS-153). (E) Morphotype 32 (KIS-205). (F) Morphotype 33 (KIS-025). (G) Morphotype 34 (KIS-072). (H) Morphotype 35 (KIS-037). (I) Morphotype 36 (KIS-082)	73

FIGURE 18—Ingersoll shale dicotyledon leaf morphotypes. (A) Morphotype 37 (KIS-156). (B) Morphotype 38 in the Columbus State University collection. (C) Morphotype 39 (KIS-046B)	80
FIGURE 19—Ingersoll shale conifers. (A) Conifer foliage morphotype 1 (KIS-212). (B) Conifer foliage morphotype 2 (KIS-231). (C) Conifer foliage morphotype 3 from the Columbus State University collection. (D) Conifer foliage morphotype 4 (KIS-112A). (E) Close-up of KIS-112A showing the helically arranged, acicular leaves.....	83
FIGURE 20—Ingersoll shale conifers. (A) Conifer foliage morphotype 5 (KIS-223). (B) Conifer foliage morphotype 7 (KIS-185). (C) Conifer foliage morphotype 5 (KIS-182). (D) Conifer foliage morphotype 6 (KIS-106).....	87
FIGURE 21—Ingersoll shale cones. (A) Taxodiaceous cone (cone morphotype 1) from the Columbus State University collection. (B) Cone morphotype 2 from the Columbus State University Collection. (C) Cone morphotype 3 (KIS-225B). (D) Cone morphotype 4 (KIS-282B).....	91
FIGURE 22—Ingersoll shale cone morphotype 5 (KIS-225A and 225B).....	93
FIGURE 23—Ingersoll shale angiosperm reproductive organs. (A) Flower morphotype 1 (KIS-163). (B) Flower morphotype 2 (KIS-513A). (C) Flower morphotype 3 (KIS-165). (D) Flower morphotype 4 (KIS-163). (E) Angiosperm fruit. (F) Seed/fruit coating. (G) Miscellaneous seed type 1 (KIS-184). (H) Fruit wing (KIS-105). (I) SEM image of miscellaneous seed type 2	94
FIGURE 24—Rare Ingersoll shale roots. Note they are not cutting through lamina.....	100
FIGURE 25—SEM images of leaf cuticle and wood, and light microscopy of leaf cuticle. (A) SEM image of angiosperm leaf cuticle showing detailed preservation. Note the preserved stomata and guard cells (arrow). (B) SEM image of miscellaneous seed type 1, showing completely pyritized organic matter. (C) SEM image of leaf cuticle showing a layer of original cuticle and internal structure (note the void space and the pyritized cell walls). (D) Lignitized remains of wood. (E) Translucent leaf cuticle under binocular microscope; note empty cell and the preservation of stomata (arrow).....	103
FIGURE 26—Detailed photographs of mummified fossil leaves. (A) Leaf showing insect herbivory and subsequent reactivation tissue. (B) Brown leaf cuticle showing venation patterns and stomatal preservation.....	104

FIGURE 27—Representative samples and inclusions within Ingersoll shale amber. (A) Two flat pieces (arrows) were polished to reveal internal cracking and coloration. (B) Large pieces with their natural shape; note the rounded edges. (C) Large fragments collected from the outcrop; note the light yellow color. (D) Small pieces with natural shapes. This is the most abundant size. (E) Alternating clear and dark amber flows. Dark, thin layers are possibly the result of rapid drying by sunlight and wind (see Martínez-Delclòs et al., 2004, p. 39). (F) Rare bubble inclusion; note the adjacent organic inclusion indicated by the black arrow (possibly a mite). Figures A-E were photographed by David Grimaldi (American Museum of Natural History), and Figure F was photographed by Patrick Bingham (Auburn University).....118

FIGURE 28—Plant macrofossils directly associated with amber. (A) Conifer foliage type 4 (KIS-118) showing *in situ* amber rods inside the stem (indicated by the red arrow). (B) Poorly preserved conifer fossil (KIS-127), possibly a cone or cone scale, showing *in situ* amber rods. (C) Close-up of amber rods from Fig. 1B. (D) “*Dammara*” cone-scale (KIS-161)120

FIGURE 29—Inorganic amber inclusions. (A) Opaque white mineral in tufts of acicular crystals (gypsum?). (B) Pyrite infilling shrinkage cracks (indicated by red arrow). (C) Pyritized organic fossil within amber nodule (indicated by red arrow). (D) Unidentified fibrous organic fossils (possibly moss or bark fibers)121

FIGURE 30—Non-arthropod amber inclusions. (A) Unidentified organic particles in a turbid piece. (B) Fungal mycelia and fine bubbles. (C) Detail of mycelia. (D) Wood fragment with mycelia overgrowth. (E) Wood and/or plant inclusions. (F) Wood and/or plant fibers and insect fecal pellets (indicated by red arrows). Photographed and identified by David Grimaldi (American Museum of Natural History)122

FIGURE 31—Fungal, plant, and arthropod inclusions. (A) Possible fungal hyphae (indicated by black arrow). (B) Fibrous organic inclusions (possibly a seed or flower). (C) Disarticulated insect appendage; well preserved spines indicate tibia. (D) Disarticulated flagellum segment of an insect antenna; notice the well-preserved sensory hairs. Photographed by Patrick Bingham (Auburn University).....123

FIGURE 32—Arthropod inclusions. (A and B) Unidentified mites. (C) Spider webbing; notice the sticky droplets adhering to the silk strands. (D) Disarticulated araneoid spider and associated webbing. (E) Details of spider appendage. (F) Female coccoid (scale) insect. Photographs and identifications made by David Grimaldi (American Museum of Natural History).....125

FIGURE 33—Invertebrates. (A) Cast of infaunal bivalve on the underside of a bedding plane, oriented dorsal edge up, lying almost perpendicular to bedding. Anterior end is on the left (B) Possible beetle elytron showing irregular, coarse pitting (notice the blue iridescence)131

FIGURE 34—Photograph of ctenoid fish scale with most of the descriptive terms used in this chapter (modified from Cavanihac, 2002).....	134
FIGURE 35—Ingersoll shale fish scales (external molds). (A) Fish scale morphotype 1 preserved as an external mold with residual carbon. (B) Fish scale morphotype 2 preserved as an external mold with residual carbon (notice the asymmetry). (C) Fish scale morphotype 3 preserved as an external mold with residual carbon (notice the brown film between the black carbonized remains and the matrix). (D) SEM image of KIS-228 (morphotype 2) showing fine detail of the circuli and carbon-filled grooves.....	137
FIGURE 36—Rostral field of morphotype 1 and 2 (both are external molds). (A) KIS-209B showing circuli intersecting and crossing the radii (right) forming a reticulate pattern. (B) KIS-205B showing fine circuli curving sharply toward the caudal field at the midline (note the absence of radii). On the right, along the margin, the circuli become confluent.....	138
FIGURE 37—Close-up pictures of fish-scale morphotype 3. (A) KIS-227A showing circuli curving sharply toward the caudal field and prominent midline (red dashed line). (B) Portion of the caudal field of KIS-230A showing the ctenii (center) and granulation (right). (C) KIS-227A showing carbonized remains and external mold preserving regular circuli (left) and irregular circuli (right). (D) Preserved annuli on specimen KIS-230A (individual annuli are numbered).....	140
FIGURE 38—Structures found on a typical body contour feather (from Lucas and Stettenheim, 1972).....	143
FIGURE 39—Segment of a contour feather in an oblique ventral view, showing the internal structure of the rachis, the attachment of the barbs to the rachis, and the orientation and structure of the barbs (from Lucas and Stettenheim, 1972).....	145
FIGURE 40—Two interlocking pennaceous barbs showing the structure of the ramus and the structure of the distal and proximal barbules (from Lucas and Stettenheim, 1972).....	147
FIGURE 41—Different structural types of feathers (modified from Chatterjee, 1997).....	148
FIGURE 42—Body contour feathers. (A) CSUK-03-05-1F. (B) CSUK-03-05-2F. (C, D) CSUK-03-05-3F part and counterpart, respectively. (E) KIS-700. (F) KIS-701. Photographed by Patrick Bingham (Auburn University).....	160

FIGURE 43—Partial contour feathers. (A) KIS-702. (B) KIS-703. (C) KIS-704. Figures A and C photographed by Patrick Bingham (Auburn University)	163
FIGURE 44—Body contour feathers. (A) KIS-705. (B) KIS-707. (C) KIS-708. (D) KIS-710. Figure D was photographed by Patrick Bingham (Auburn University).....	165
FIGURE 45—Structural and taphonomic features of Ingersoll shale feathers. (A) Tip of the barbs on CSUK-03-05-1F, showing a decrease in length of the distal and proximal barbules. (B) “Unzipping” of the proximal and distal barbules in KIS-706. (C) Close-up photograph of distal barbules on KIS-705 (red arrow points to barbicels). (D) Barb on the right vane of KIS-705 showing degradation of the barbules prior to deposition.....	166
FIGURE 46—Composite image of KIS-706, the longest contour feather discovered in the Ingersoll shale (possibly a rectrix). Photographs and composite image made by Patrick Bingham (Auburn University).....	167
FIGURE 47—Part and counterpart of KIS-709 (A) Asymmetry of the left and right vanes. (B) Three-dimensionally preserved rachis	169
FIGURE 48—SEM images of KIS-706 and KIS-709. (A) SEM image of KIS-706 showing rachis (center), barbs, and barbules. (B) SEM image of KIS-709 showing the “flow-mat” alignment of bacilliform bacteria at a branching intersection of the ramus (lower right) and a barbule (notice how the bacteria have reoriented themselves at the intersection). (C) Close-up image of the bacilliform bacteria in KIS-706. (D) SEM image of KIS-709 showing framboids and cluster of pyrite crystals	171
FIGURE 49—SEM of barbules on KIS-709. Notice the fine clay between the barbules and the void space between bacteria. Inset image shows coccoid forms of bacteria (indicated by the red arrow) on the tips of bacilliform bacteria	173
FIGURE 50—EDS results of KIS-706. (A) EDS results from the bacteria. (B) EDS results from the surrounding clay matrix. (C) EDS results from an associated pyrite crystal.....	174
FIGURE 51—False-color SEM image of KIS-706 showing EDS results from analysis on EDS results on bacteria (right), clay (middle), and pyrite (left)	175

FIGURE 52—Reconstruction of estuary development in relation to the study area (red dot). (A) Subaerial erosion of the Tuscaloosa Formation during sea-level low stand. (B) Initial transgression with flooding of the incised valleys and development of the estuary and bayhead delta. (C) Creation and filling of the Ingersoll tidal creek in the bayhead-delta plain as transgression continues. (D) Landward migration of shoreline and deposition of central-bay deposits on top of the Ingersoll shale (from Bingham, 2007).....182

FIGURE 53—Detailed view of the interpreted estuarine setting of the Ingersoll shale. (A) Estuarine complex includes bayhead delta (red dot indicates inferred tidal creek for the deposition of the Ingersoll shale). (B) Outcrop scale reconstruction of Ingersoll tidal creek in relation to the quarry and trenches (both figures from Bingham, 2007).....183

FIGURE 54—General stratigraphic column of the Ingersoll shale lens divided into six zones based on the relative abundance and taphonomic condition of fossils. Curves show weight percent sand and total organic carbon (modified from Bingham, 2007). Relative fossil abundance is based on qualitative data and indicated by the thickness of the red bars. Included in zone 5 are two intervals (cross-hatched) denoting subzones with multiple layers of macerated plant detritus. Shown in zone 6 are *Thalassinoides* and *Rhizocorallium* borrows. The dashed lines represent sand-dominated lamina. Blue dotted line marks the triplet of sand layers used as a vertical datum. TOC represents total organic carbon185

LIST OF TABLES

TABLE 1—Confirmed occurrence of fossil feathers from Mesozoic strata
(modified from Kellner, 2002).....154

TABLE 2—Measurements of Ingersoll shale feathers and their structures158

CHAPTER 1: OBJECTIVES

A new fossil *Konservat-Lagerstätte* deposit containing a rare assemblage of flora and fauna occurs within the Upper Cretaceous Eutaw Formation of east-central Alabama. This deposit was discovered in 2003 by Patrick Bingham while working on a mapping project for Columbus State University (Columbus, Georgia). Preliminary observations of the carbonaceous clay lens, informally named the Ingersoll shale, revealed an abundance of well-preserved plant fossils including leaves, stems, reproductive organs, and some articulated remains (Knight et al., 2004; Bingham and Knight, 2005). Many fossils are carbonized and pyritized, some in three dimensions, but decay-resistant tissues (e.g., waxy leaf cuticle and sporopollenin) appear to be unaltered in some specimens. Fish scales were also discovered, demonstrating the carbonization of collagen-based tissues. In addition, the Ingersoll shale lens exhibits exceptional preservation of originally proteinaceous tissues such as theropod feathers (originally β -keratin), preserved via replacement by bacteria.

This thesis and a companion study by colleague Patrick Bingham describe the new *Lagerstätte*. The objectives of Bingham's study were to establish the paleoenvironmental setting of the clay lens and to interpret the depositional and early diagenetic conditions that contributed to fossil preservation. The goals of my study were to describe the diverse fossil biota preserved within the Ingersoll shale, to document the

taphonomic condition of the fossil assemblage, and to reconstruct its taphonomic history.

A final goal was to use this information on the fossil biota to clarify the depositional setting and to provide new clues as to the conditions required for the preservation of refractory soft-tissues in general and the formation of marginal marine *Konservat-Lagerstätten* in particular.

CHAPTER 2: INTRODUCTON

FOSSIL *LAGERSTÄTTEN* AND EXCEPTIONAL PRESERVATION

Some fossil deposits are extraordinary, whether because of exceptional fossil abundance or unusual preservation. Fossils found within these deposits reveal detailed information about the diversity of ancient life that is not typically preserved in the fossil record (Bottjer et al., 2002; Briggs, 2003). In addition, these extraordinary deposits provide clues to the specific geochemical and sedimentologic conditions that are required for their formation.

Rock bodies that are unusually rich in paleontological information were first termed *Fossil-Lagerstätten* by Seilacher (1970). Seilacher further classified *Fossil-Lagerstätten* into two types: deposits that preserve an abundance of fossils, or “*Konzentrat-Lagerstätten*” (concentration deposits), and deposits that contain exceptionally preserved fossils, or “*Konservat-Lagerstätten*” (conservation deposits).

Conservation deposits can either consist of articulated multi-element skeletons, or they may contain preserved “soft-bodied” or non-biomineralized tissues, the later being the focus of this study. The preservation of soft tissues varies according to the particular tissue’s resistance to decay. Labile tissues (e.g., muscle and ligaments) are very susceptible to rapid decay and are usually preserved only during very early authigenic mineralization (Allison, 1988a). In contrast, refractory tissues (e.g.,

sporopollenin, lignin, and cuticle) are more decay resistant and can be preserved as the original material (Butterfield, 1990).

Allison (1988a) describes how detailed analyses of soft-bodied fossils can provide an abundance of information. In addition to documenting the occurrence of species not normally seen, preservational states and taphonomic signatures can provide insight into the physical and chemical processes at the depositional site. This is especially true for *Konservat-Lagerstätten* with soft tissues because most preservation occurs shortly after deposition (Plotnick, 1986; Briggs and Kear, 1994; Grimes et al., 2002).

TAPHONOMIC INVESTIGATIONS OF FOSSIL *LAGERSTÄTTEN*

Seilacher (1970) was the first to classify *Konservat-Lagerstätten* on the basis of inferred preservational mechanisms. He distinguished among *Konservat-Lagerstätten* formed by anoxic conditions, rapid burial, early diagenetic concretion growth, and the occurrence of a decay-inhibitory medium such as tar, amber, or permafrost. Seilacher later added conservation deposits wherein preservation was related to cyanobacterial sealing (Seilacher et al., 1985). Allison (1988a) performed actualistic taphonomic studies on the decomposition of soft tissues to reveal the decay-inhibiting factors of *Konservat-Lagerstätten*. He discovered that obrution (rapid burial) and stagnation (anoxia) slow decay, but they are rarely formative agents in long-term, soft-tissue preservation. He affirmed that preservational traps (e.g., amber, ice, and tar sands) are the most effective preservational medium for preserving soft parts. Amber is remarkable in preserving soft tissues, including cellular details such as mitochondria and muscles, but amber remains largely unexplored (Henwood, 1992). Aside from preservational traps, Allison (1988b)

concludes that early diagenetic mineralization is the only way to completely halt decay-induced information loss; hence, it is the key factor in the formation of *Konservat-Lagerstätten*.

Nearshore *Konservat-Lagerstätten* somewhat similar to that of the Ingersoll shale have been studied to some extent. Briggs et al. (1983) described the soft-tissue remains of a conodont deposited in a nearshore Carboniferous shale in Edinburgh, Scotland. They do not address the modes of preservation in detail. However, they describe the absence of bioturbation and presence of pyrite, suggestive of an anoxic depositional environment. Feldman et al. (1993) explored the origins of a tidally influenced, estuarine, Carboniferous *Konservat-Lagerstätten* of the mid-continental United States. They revealed that high rates of deposition found in tidally influenced areas cause rapid burial and increase anoxia of pore waters. In turn, these factors prevent scavenging, bioturbation, and colonization of marine invertebrates. Three *Konservat-Lagerstätten* that are similar in age and biota as well as depositional setting are discussed later (Chapter 14): the Messel Oil Shale of Germany, the Grès à Voltzia Formation of France, and the South Amboy Fire Clay of New Jersey.

Several studies have been conducted on the precipitation of authigenic minerals due to bacterially mediated processes in anoxic environments (Plotnick, 1986; Briggs and Wilby, 1996; Grimes et al., 2001; Grimes et al., 2002; Scheiber, 2002). The chemical composition of the surrounding sediment, mediated by bacterial decay, dictates which minerals will precipitate around and within the decaying carcass (Briggs, 2003). Calcium phosphate preserves the most detail of labile (muscle) tissues, including three-dimensional preservation, and is thought to be the result of slow depositional rates

(Allison, 1988b). Phosphatization can also be triggered by the initial lowering of pH during decay in an anoxic environment, inhibiting the precipitation of calcium carbonate (Briggs and Wilby, 1996). Calcium carbonate preserves less detail but is often found in close association with calcium phosphate. Briggs and Wilby (1996) found that calcium carbonate bundles encrusted phosphatized soft tissue as a result of a rise in pH after initial decay, whereas Allison (1988b) believes calcium-carbonate precipitation is a result of rapid burial and limited residence time at the oxic/anoxic boundary. Clay minerals such as illite also can preserve soft tissues in very acidic environments. This is exemplified by the Soom Shale of South Africa, where metabolizing bacteria form nucleation sites for the adsorption of potassium or the direct precipitation of clays on soft tissues (Gabbott et al., 2001). Early diagenetic silicification sometimes leads to exceptional preservation of soft-tissue microorganisms in peats (Allison, 1988a). However, this silicification is related to sediment permeability, availability of silica, and high organic-matter concentrations, not microbial-induced decay (Knoll, 1985).

Pyritization is common in *Konservat-Lagerstätten*, particularly in the preservation of plant remains (Grimes et al., 2002). Pyrite can form early in the diagenetic history of a sediment and be strongly controlled by sedimentation rates and environmental geochemistry (Allison, 1988a). Precipitation of pyrite within plant tissues protects them from later compaction. One important actualistic study of the preservation of pyrite in an anoxic environment was conducted by Grimes et al. (2001). By replicating the fossilization process in the laboratory using bacterially-mediated decay under various chemical regimes, they were able to infer the mechanisms and controls of pyritization. This study found that FeS_{aq} (aqueous iron-monosulfide, a precursor to pyrite) appeared

within plant tissues in less than 80 days and that pyritization occurred first on the cell walls and, subsequently, in the void space within the cells. As decay continued, more void space was made available for pyrite precipitation. Brock et al. (2006) conducted experiments designed to mimic pyritization within twigs of *Plantus acerifolia* under variable marine conditions. Sulfate reduction occurred within all systems; however, only 2 of the 18 experiments resulted in the pyritization of the twigs. This study shows that the pyritization within the sedimentary matrix and pyrite formation within the decaying twigs were significantly different. They concluded that the pyritization process of organic matter is local and possibly limited by nucleation sites on the twigs rather than the availability of sulfate and iron ions within the system.

Grimes et al. (2002) also examined pyritization of plant material (twigs and roots) preserved in the Eocene London Clay. They investigated the quality of preservation and provided detailed descriptions of pyrite textures in relation to cell type using thin section analysis and scanning electron microscopy (SEM). They found that the highest quality of preservation was associated with the rapid nucleation of microcrystalline pyrite on, and within, cell walls, pit-closing membranes, and the middle lamella. The cell was subsequently infilled by framboidal or octahedral crystals. The range of pyrite textures observed is attributed to changes in pore-water chemistry, ion availability, and microbial decay during the burial process.

Microbial communities responsible for decay also can become fossilized. Closely packed rod-shaped bacteria, resembling a “flowing mat,” were described from the Eocene Messel Shale, where the bacteria were replaced by siderite (Wuttke, 1983; Franzen,

1985). Preservation of bacteria also was documented in feathers from the Cretaceous Crato Formation, Brazil, and from Oligocene strata in France (Davis and Briggs, 1995).

CHAPTER 3: SOUTHEASTERN GULF COASTAL PLAIN (EUTAW FORMATION)

GENERAL STRATIGRAPHY

Outcrops of the Eutaw Formation (Upper Santonian and Lower Campanian), first described by Hilgard (1860), occur in the eastern Gulf of Mexico Coastal Plain Province in an arc-shaped belt that extends from northern Mississippi, through Alabama, and into western Georgia (Savrda and Nanson, 2003). This heterolithic package of micaceous sands and laminated clays unconformably overlies the Cenomanian Tuscaloosa Formation, which consists predominately of fluvial deposits (Fig. 1). The Eutaw Formation is disconformably overlain by the siliciclastic Blufftown Formation in western Georgia and eastern Alabama, and the Mooreville Chalk in central-western Alabama and eastern Mississippi (Smith and Johnson, 1887; Reinhardt et al., 1994; Frazier, 1997). Westward, the Eutaw Formation is divided into a lower, unnamed member and the upper Tombigbee Sand Member (Hilgard, 1860). The Eutaw Formation records a major transgression during the Santonian (Reinhardt and Donovan, 1986).

DEPOSITIONAL ENVIRONMENTS

The Eutaw Formation was deposited in estuarine or restricted shallow-marine environments represented by back-barrier, barrier-island, lower-shoreface, inner-shelf

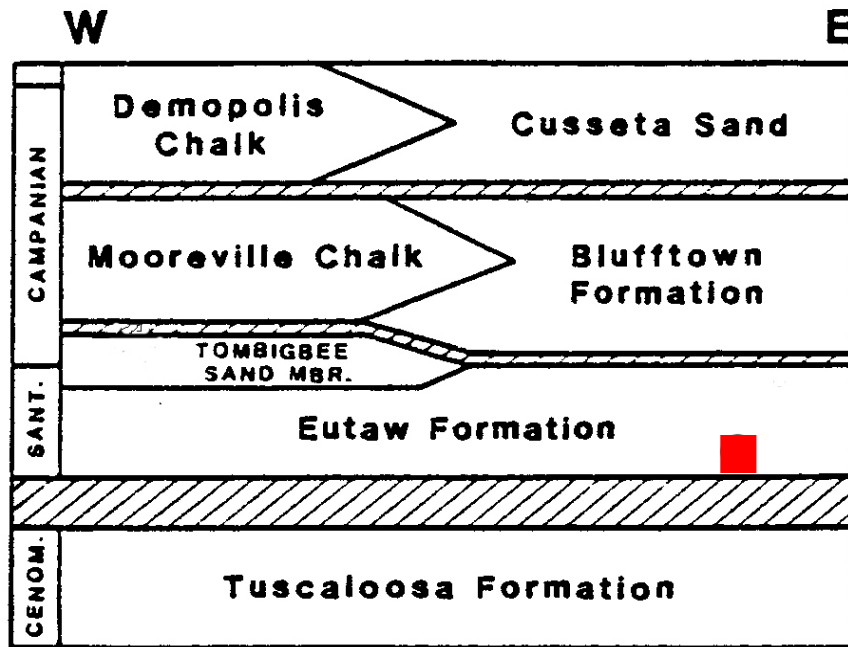


FIGURE 1—Stratigraphic correlation chart of Upper Cretaceous deposits spanning from central Alabama (west) to western Georgia (east). The red square indicates the stratigraphic location of Ingersoll shale (modified from Savrda et al., 1998).

facies (King and Skotnicki, 1986; King, 1990; Frazier, 1997). The 35-to-40-m-thick Eutaw Formation strikes east-west and dips gently to the south. Frazier (1997) found that the coarse, cross-bedded sandstones with associated *Ophiomorpha* burrows in northern or up-dip areas represent a coastal, tide-dominated environment. The Eutaw Formation is considered to be an incised valley fill formed in response to a transgression (Mancini et al., 1995). Frazier (1997) attributes the gray, clay-rich fossiliferous mudstones and the thin, fine-grained sandstone interbeds in southern (down-dip) areas to have formed by deposition in a bay or lagoonal setting. The Ingersoll shale is located in the up-dip, tide-dominated portion of the Eutaw Formation.

EUTAW FORMATION FOSSILS (CHATTAHOOCHEE VALLEY)

Marine invertebrate fossils are very abundant in the Eutaw Formation. Early studies of these invertebrates were conducted in the Chattahoochee Valley by Stephenson (1957). Stephenson describes 16 genera of bivalves, including *Nucula*, *Protarca*, *Breviarca*, *Trigonarca*, *Pseudoptera*, two species of *Ostrea*, *Gryphaea*, *Exogyra*, *Anomia*, *Cardium*, *Legumen*, *Cymbophora*, and three species of *Caryocorbula*; however many of these names have been replaced. Stephenson also recognized the ammonite *Placenticerias benningi*.

Ichnofossils were described by Savrda and Nanson (2003) from fair-weather and storm deposits in the Eutaw Formation of western Georgia. Fair-weather sedimentary suites are dominated by *Terebellina*, *Teichichnus*, and *Planolites*, whereas storm generated sands are dominated by *Ophiomorpha*.

Recent studies on vertebrate fossils in the Chattahoochee Valley were conducted primarily by Schwimmer (1981, 1988) in the Blufftown Formation. However, some of Schwimmer's work has been directed toward fossils found in the Eutaw Formation. He described the common occurrence of *Scapanorhynchus texanus*, *Cretolamna appendiculata*, *Cretodus semiplicatus*, and *Squalicorax falcatus* (Schwimmer et al., 1997, 2002). Pycodont teeth and jaws also were described from the Santonian deposits of Alabama and Georgia (Hooks et al., 1999). Other vertebrates include pterosaur remains, which were discovered in the banks of Ochilee Creek, Chattahoochee County, Georgia (Schwimmer et al., 1985).

Plant remains from the Eutaw Formation were mentioned only briefly in sediment descriptions (Hilgard, 1860) prior to the extensive study done by Berry (1919) in which he described 43 floral species. He described the Eutaw Formation species as being only a small representation of the flora that flourished when the Eutaw Formation sediments were laid down. In addition, Berry noted that the flora in the Eutaw Formation were not remarkably different from that found in the Tuscaloosa Formation. Most of the plant remains in the Eutaw Formation had undergone fragmentation due to transportation, and this process destroyed all but the coriaceous (leathery) forms. Berry could find no close comparisons with modern plant communities but used the term "temperate rain forest" to describe the paleoenvironment associated with the Eutaw Formation flora.

Megaspores, microspores, and sporocarps from heterosporous water ferns and lycopsids from the Eutaw Formation sediments were discovered in unconsolidated clays and silts on the banks of Upatoi Creek, Fort Benning Military Reservation, Georgia (Lupia et al., 2000). Preliminary analysis of this outcrop and palynological evidence

suggest that the depositional environment was nonmarine, but close to the coast. From this locality, the megaspore, *Regnellidium upatoiensis*, extends the first stratigraphic appearance of the genus back to the Late Cretaceous (Lupia et al., 2000). The Upatoi Creek exposure also contains fossil species of *Molaspora* and its associated microspore, *Crybelosporites*.

CHAPTER 4: LOCATION OF STUDY

The study site is located in Phenix City, Russell County, Alabama, east of highway 431 (Fig. 2). At this site, the upper portions of the fluvial Tuscaloosa Formation sediments are overlain disconformably by the basal 11.60 m of the Eutaw Formation. Within this exposure, a shale lens of variable thickness (0-76 cm) occurs within the basal Eutaw Formation, ~1 m above the Tuscaloosa/Eutaw Formation contact (Fig. 3). The clay lens is informally named the Ingersoll shale in reference to Michael Arnold Ingersoll, the property owner who provided access to the site. The Tuscaloosa Formation sediments are characterized by fining-upward sequences of fluvial sands and muds. The most basal Eutaw Formation sediments are composed of coarse-grained, poorly indurated, cross-bedded and planar-bedded sandstone, with clay drapes and *Ophiomorpha* burrows. The next facies upward was described as part of a channel-form complex, which includes the Ingersoll shale (Bingham, 2007). The Ingersoll shale lens is a fossiliferous, olive-gray to black, sulfur-rich, non-calcareous, carbonaceous shale that fills a NNW-trending channel that is ~20 m in width. Throughout the shale lens, there are alternating lamina of sand and clay, which suggest a tidal influence during deposition. The shale lens is disconformably overlain by bioturbated sandy muds and muddy sands, which are interpreted to be central bay deposits (Bingham et al., 2006). These sediments contain reworked Ingersoll-shale clasts and the internal and external molds of ammonites

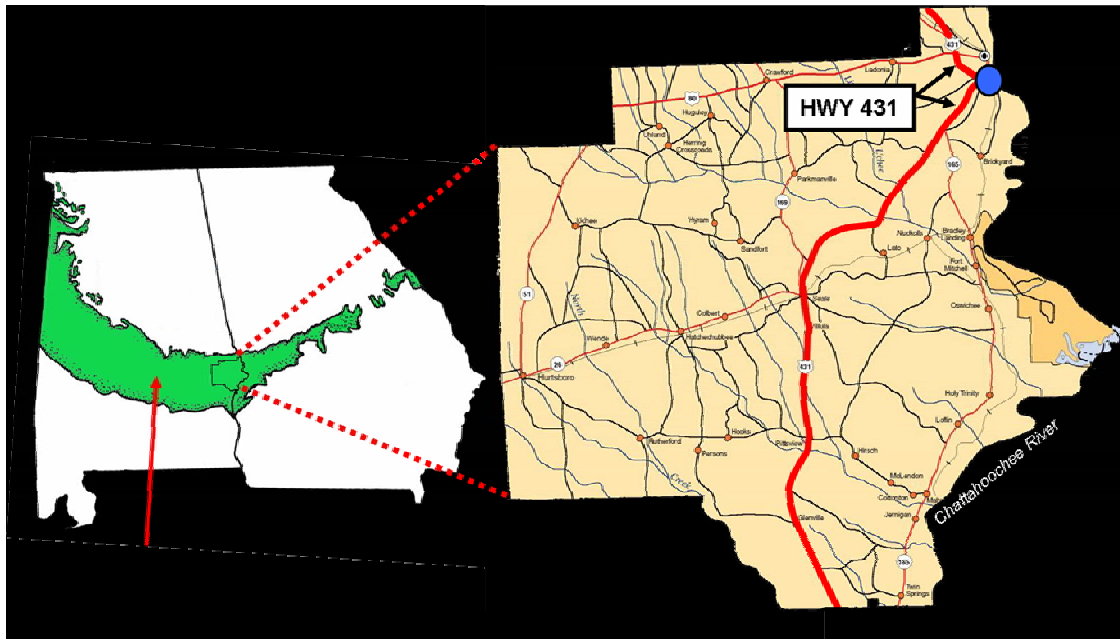


FIGURE 2—Study location of the Ingersoll shale. Red arrow (left) points to Upper Cretaceous deposits (green), blue dot (right) shows approximate location of the study site off State Highway 431.

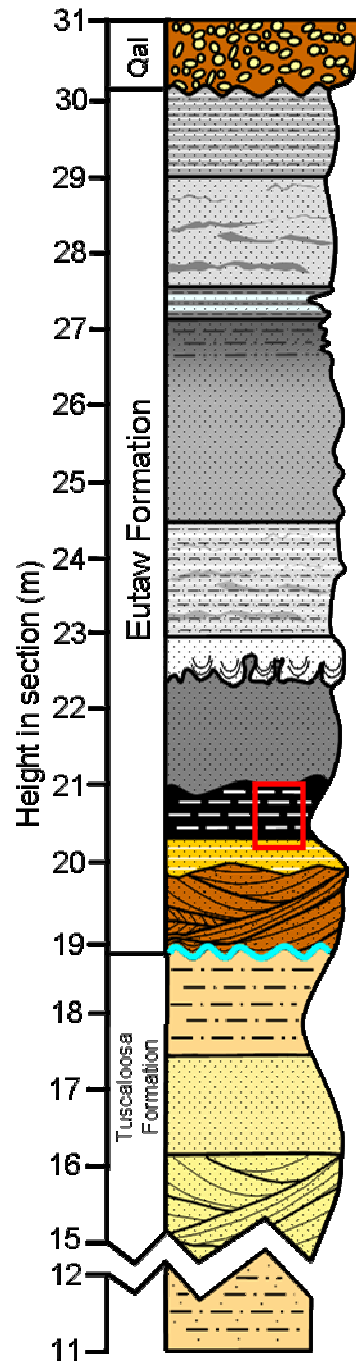


FIGURE 3—Stratigraphic column of the measured section at the study location showing the location of the Ingersoll shale (red box) located ~1 m above the Tuscaloosa/Eutaw disconformity (modified from Bingham, 2007).

(including *Placenticerus benningi*), gastropods, bivalves, crustaceans, amber, and rounded pieces of *Teredolites*-bored wood. The sedimentology and stratigraphy of the clay lens is described in more detail in the companion study by Bingham (2007).

CHAPTER 5: GENERAL METHODOLOGY

INTRODUCTION

The Ingersoll shale lens was excavated over the course of four years. The first phase of excavation (2003-2006) was limited to exposures with minimal overburden. The second phase was a conservation phase (March, 2006) in which a quarry was established in order to keep a horizontal reference on blocks removed from the site and stored at CSU for future research. Volunteers from the paleontologic community participated in a group effort to archive bulk samples for future research. In the third phase (July, 2006), external funding was provided by the National Science Foundation, allowing us to remove overburden with heavy equipment and to expand the quarry to its present size.

FIELD WORK FOR DISCOVERING MACROFOSSILS

During all phases, field work consisted of mechanically quarrying large blocks of the Ingersoll shale in a systematic fashion. The overburden was removed initially by pick and shovel, and later by bulldozer and backhoe. An 11 x 20 m grid was established in the quarry for horizontal control in recording discoveries. Because the shale lens is bounded on top by an irregular, erosional surface and bounded on the bottom by a gradational, iron-cemented surface overlying the lower leached zone, a internal vertical datum was needed. Three closely spaced, easily identifiable, laterally continuous sand layers

(“the triplet”) served this purpose. Wedges and/or crowbars were driven into preexisting fractures in order to extract blocks from the clay lens (Fig. 4A). The top blocks were separated using the top sand layer of the “triplet” as their base (Fig. 4B). Wedges were then driven through the shale to the oxidized zone below (Fig. 4C), and the blocks were removed (Fig. 4D). The blocks were split in the field or were numbered and placed in air-tight plastic containers to slowly dry and to minimize oxidation. The containers were transported to the Department of Geography and Geology at Auburn University.

Delicate fossils were digitally photographed in the field to capture their appearance at the time of discovery before they were distorted or otherwise damaged by drying, oxidation, or transport. Once photographed, some fossils were coated with polyvinyl alcohol (PVA). Fossils were placed in air-tight containers to slow mineral oxidation, and their vertical and horizontal position in the quarry was recorded. Feathers and other rare fossils remained uncoated to facilitate taphonomic analysis using SEM. Fossils were tentatively identified and described via a literature review, cataloged with the prefix KIS (Cretaceous Ingersoll shale), and temporarily stored at Auburn University. Fossils studied are listed in the appendix and assigned by morphotypes.

In the laboratory, sample blocks were split along bedding planes to recover any macrofossils. The newly exposed shale was examined with a binocular microscope under normal light.

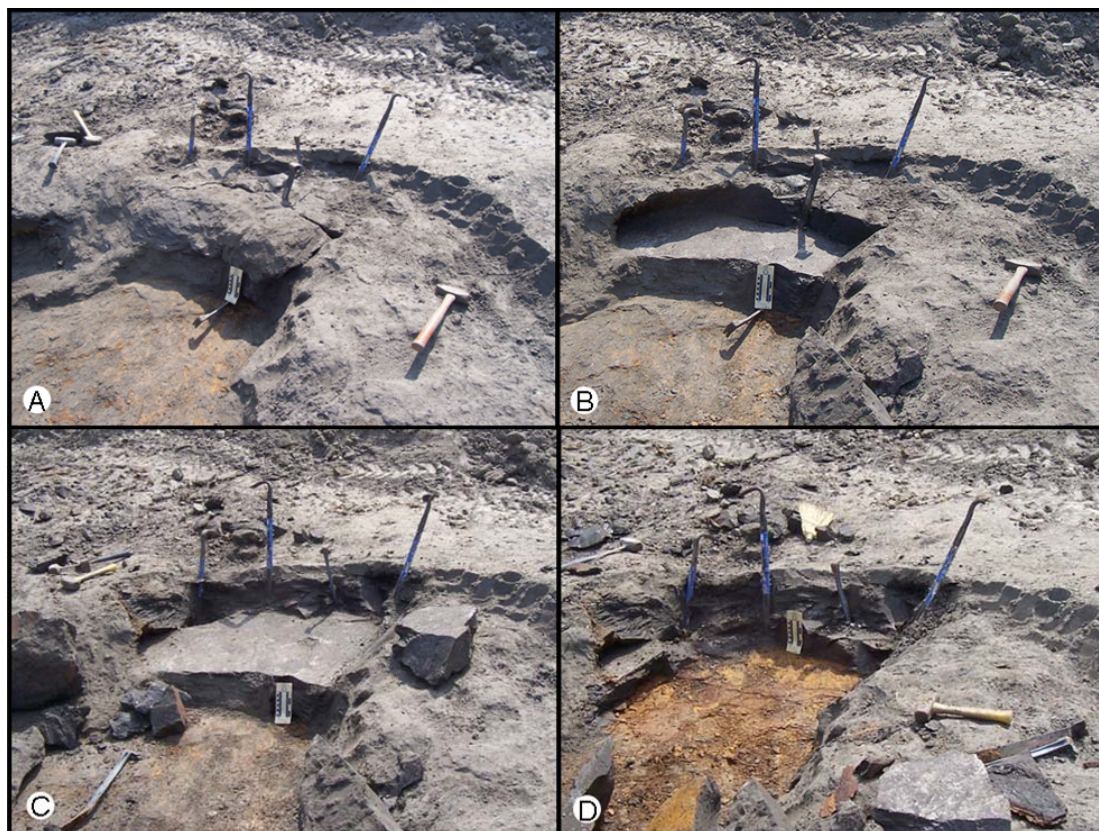


FIGURE 4—Quarrying technique used to remove blocks of Ingersoll shale. (A) Wedges were driven into preexisting fractures. (B) Top blocks were removed. (C) Wedges were driven to base. (D) Bottom blocks were removed.

FIELD AND LAB METHODS FOR EXTRACTING MID-SIZE FOSSILS

To release mid-size fossils from the matrix, subsamples were collected in 3-cm intervals using the sandstone triplet for vertical reference. Once in the laboratory, each individual subsample was washed with distilled water. Any cracks or crevasses were cut away to prevent contamination from modern organisms. The sediment was then thoroughly oven dried for two days and immediately placed in distilled water. After a short time, this process disaggregated the clay particles, releasing the fossils from the matrix. The disaggregated sample was wet sieved through a 2-phi screen to isolate plant fragments from the clay and fine sand. During sieving, Borax© (sodium borate) was added to aid in washing away the clay and sand. Plant macerals were placed in a petri dish with distilled water and were visually examined with a binocular microscope. Identifiable plant reproductive organs, such as megaspores and sporocarps, were picked out with a moistened fine-tip brush and placed on a slide so they could be analyzed, photographed, and identified.

CHAPTER 6: OVERVIEW OF FINDINGS

BIOTIC COMPOSITION

During the excavation, 321 macrofossils were recovered from the deposit, and additional meso- and microfossils were recovered from sediment and amber samples. Some samples contained multiple specimens on a single bedding plane. The Ingersoll biota includes gymnosperm foliage, seeds, cones, fruit/seed capsules, a variety of dicotyledon and monocotyledon angiosperm leaves, palynomorphs, marine and terrestrial invertebrates, fish scales, and feathers. Biologic inclusions in amber include fungal hyphae, arthropods, webbing, and plant debris. This chapter provides a general overview of the Ingersoll biota and their distribution within the deposit.

Palynomorphs

Palynomorphs are assignable to the *Sohllipollis* Taxon Range Zone (mid-Turonian-Santonian) and include pollen, marine dinoflagellates, acritarchs, and fungal spores. Megaspores from heterosporous water ferns and isoetalean and selaginellean lycopsids were recovered, as were rare sporocarps with articulated micro- and megasporangia. Spores typically exhibit three-dimensional preservation.

Lower Vascular Plants

Lower vascular plants are represented by rare horsetails and seven fern-like leaf morphotypes, including one possibly representing a water fern. Fern remains are rare but diverse morphologically and are commonly carbonized and locally pyritized.

Angiosperm Leaves

Fossilized angiosperm leaves are the most abundant and morphologically diverse fossils found within the deposit. Thus far, 41 distinctly different leaf morphotypes (39 dicotyledon and 2 monocotyledon) have been identified based on descriptive architectural classification schemes of the Leaf Architecture Working Group (1999). Fossil leaves are commonly whole and, in some cases, are found articulated on branched stems. Some leaves show evidence of post-depositional feeding damage on margins caused by insects and associated reactivation tissue, while others exhibit evidence of parasitism (e.g., fungi-induced leaf spot). The leaf cuticle is commonly unmineralized, remarkably flexible, and can be separated easily from sediment matrix. Leaves locally are carbonized and/or variably pyritized.

Gymnosperm Foliage

Gymnosperms are represented by 7 morphotypes, representing 4 form genera, which have been defined on the basis of their leaflet morphology and arrangement, as described by Harris (1969). These morphotypes are tentatively assigned to 3 families: the extant Araucariaceae and Cupressaceae (including Taxodiaceae) and the extinct Cheirolepidiaceae. All of these forms are either manifested as isolated leaflets or as articulated leaflets on stems.

Conifer Reproductive Organs

Both the Araucariaceae and Cupressaceae, and possibly also the Cheirolepidiaceae, are represented by isolated or articulated cones and cone scales. Gymnosperm elements are variably carbonized and pyritized, and three-dimensional preservation is common.

Flowers, Seeds, and Fruits

Plant organs tentatively attributed to angiosperms include seeds, seed pods, fruit wings, and small flowers, some of which are articulated on stems. Most angiosperm reproductive organs are variably carbonized and/or pyritized.

Amber and Inclusions

Isolated amber clasts 1-15 mm in diameter are common within the lowermost 5 cm of the Ingersoll shale. However, amber clasts also can be found in other parts of the lens. To date, systematic processing of this interval indicates amber concentrations as high as 362 g/m³ of sediment. Inclusions within amber pieces are commonly dominated by plant debris but also include fecal pellets, well-preserved fungal mycelia, mites, a female scale insect with well developed legs and antennae, and an araneoid spider that may be the oldest found in association with its web. The lower part of the Ingersoll shale hosts weakly compacted conifer remains, possibly from the family Cupressaceae. Ducts in some of these plant specimens contains have *in situ* amber rodlets.

Invertebrates

Marine invertebrate remains within the Ingersoll shale lens are rare. They are represented by articulated, infaunal bivalves, preserved mainly as external molds and casts, and rarely preserved by pyritization. Remains of possible terrestrial invertebrates

(beetle elytra) were found in association with plant macrodetritus. These remains are rare but are easily recognizable by their iridescence. They quickly deteriorate and lose their coloring and iridescence once they have been exposed to open air.

Fish Scales

Ctenoid scales are commonly found in the Ingersoll shale. They measure 1.5-4 cm in maximum diameter and have 3 different morphologies. The scales preserve the fine fingerprint-like texture (circuli) on the external mold and contain some carbonized material. Fish scales were found in close proximity to the inferred channel axis (Fig. 5).

Feathers

Excavations thus far have yielded fourteen isolated feathers, the largest collection known from Mesozoic strata of North America. Feather specimens range from 0.4 to 16.5 cm in length. Some are complete specimens and include all structural features, while others are partial specimens. Twelve of the feathers are body contour feathers, one is a tail feather, and one is asymmetrical and interpreted to be a wing feather. The feathers have been replaced by mats of small ($\sim 1 \mu$) rod-shaped structures that resemble bacteria and by pyrite. All feathers were found in close proximity to the inferred channel axis (Fig. 5).

FOSSIL DISTRIBUTION

Figure 6 shows the study interval divided vertically into six zones based on observations of fossil composition, relative fossil abundance, and taphonomic condition. The highest abundance of fossils was generally concentrated in the lower, high-energy

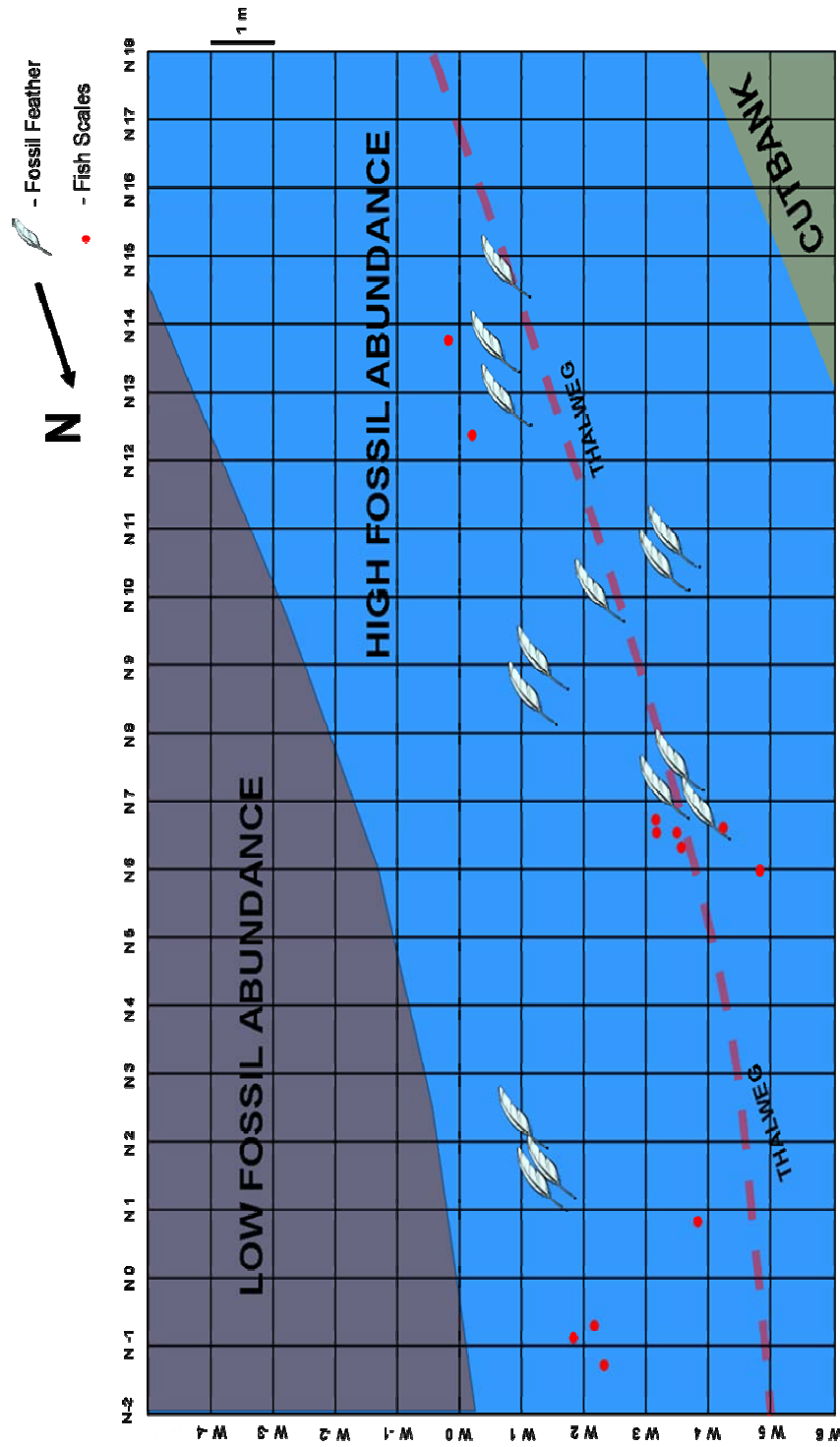


FIGURE 5—Ingersoll shale quarry map (11 m x 20 m grid). Shows the approximate location of proteinaceous fossils. Dashed line represents thickest portions of the clay lens

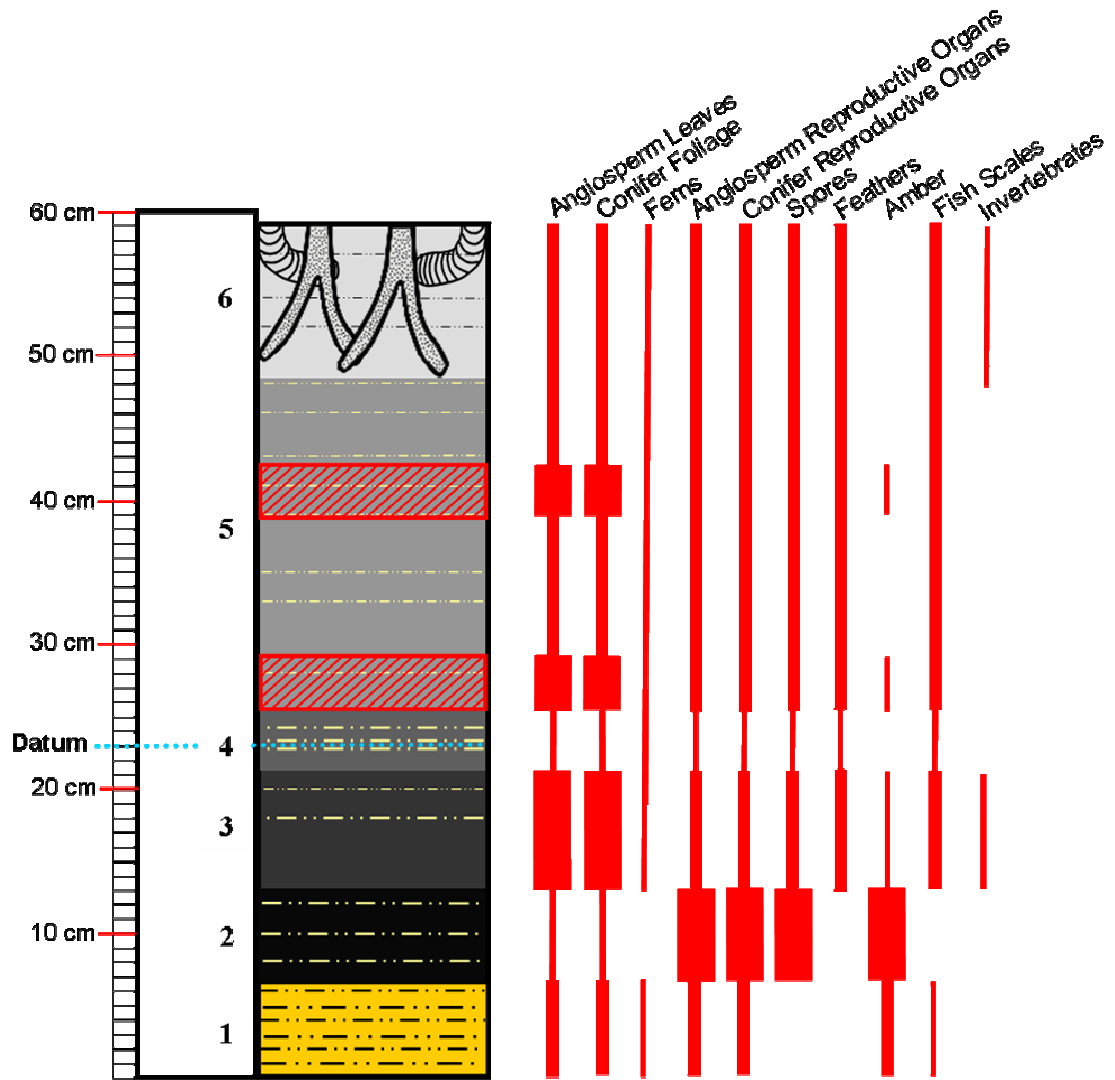


FIGURE 6—General stratigraphic column of the Ingersoll shale lens divided into six zones based on the relative abundance of fossils. Relative fossil abundance of each layer is based on qualitative data and indicated by the thickness of the red bars. Included in zone 5 are two intervals (cross-hatched) denoting subzones with bundles containing multiple layers of macerated plant detritus. Shown in zone 6 are *Thalassinoides*- and *Rhizocorallium* burrows. The dashed lines represent sand dominated lamina. Blue dotted line represents the vertical datum.

portions of the lens, and abundance of fossils decreases upward. The distribution of each component also varies laterally across the lens. Most well-preserved fossil specimens, including most proteinaceous fossils, were discovered along the inferred channel-thalweg. The inferred channel thalweg also contained the highest abundance of fossil specimens (Fig. 7). Below are descriptions of each of these zones.

Zone 1

The lowermost zone of the clay lens, zone 1, was interpreted as having the highest energy during deposition (Bingham et al., 2006). It is ~6 cm thick and has interbedded layers of sand/silt and clay. It includes whole leaves, large cones, and large clasts of red, oxidized amber. Fossils are limited to the upper few cm and preserved as impressions with iron stains and rarely as carbonized remains. Locally, leaf cuticle is preserved. However, much of the organic carbon originally in this zone apparently has been leached by groundwater.

Zone 2

Zone 2 is ~6 cm thick and includes bundles layered macerated plant detritus and abundant amber clasts interbedded with clay and silt lamina. Identifiable plant matter includes reproductive organs such as seeds, megaspores, cones, and rarely sporocarps. Whole leaves are locally preserved on and within lamina. This zone also contains pyrite layers as well as large pieces of rounded pyritized wood. Overall, this zone is very similar to zone 1 except that leaching has not occurred.

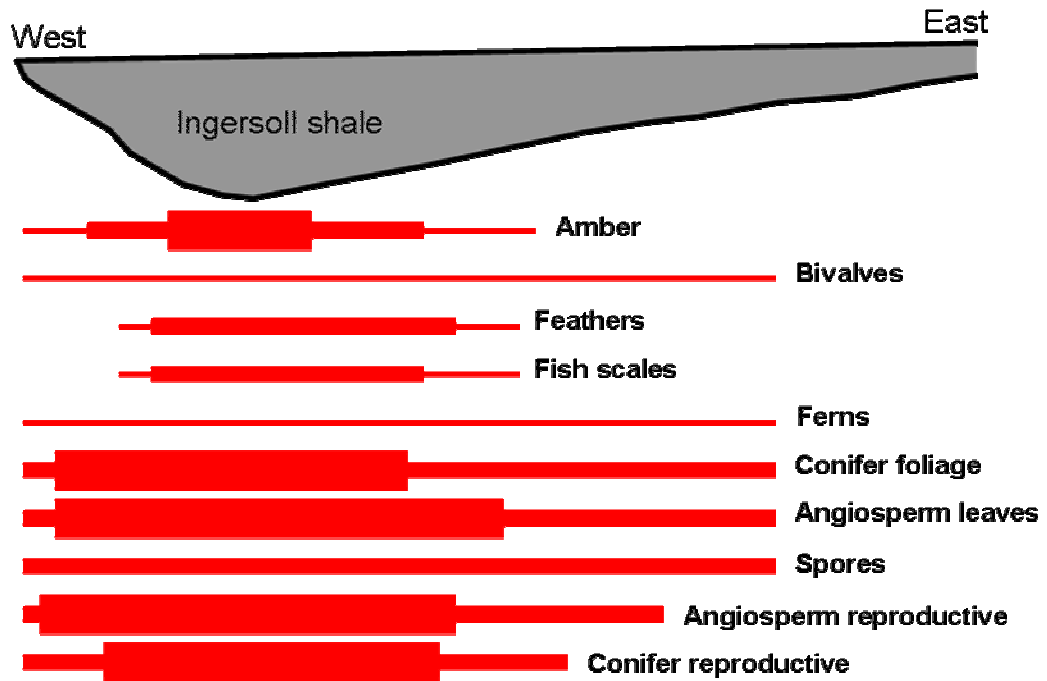


FIGURE 7—Lateral distribution of fossils within the clay lens. Thickness of red bar indicates relative abundance of fossils. Note that fossils are most abundant along the inferred channel-thalweg and decrease in abundance toward the east (from Bingham, 2007).

Zone 3

This zone is ~8 cm thick and has layers of large, well-preserved plant remains such as angiosperm leaves and conifer foliage. Amber clasts within this zone are rare and smaller than those of zone 2. Many of the leaves are complete and appear to have undergone very limited transport. Conifer fossils are sometimes preserved in three dimensions, in part because of pyritization.

Zone 4

This zone is ~4 cm thick and contains the vertical datum (the triplet). Fossils within this zone are sparse but include all elements of the Ingersoll shale biota with the exception of amber. Some laminae contain macerated plant detritus.

Zone 5

This zone is ~19 cm thick and contains few sand/silt lamina, most of which are concentrated in two subzones. These subzones have bundles with multiple layers of macerated plant detritus including seeds, small amber clasts, small cones, and whole leaves. Outside of these subzones, the clay is dominated by well-preserved angiosperm leaves that are commonly mummified, as well as conifer foliage, flowers, megaspores, and feathers.

Zone 6

This zone is similar to zone 5. However, it contains a firmground ichnofossil assemblage dominated by *Thalassinoides* and *Rhizocorallium*. Burrowing has damaged many of the fossils. This zone has an average thickness of 8 cm thick but *Thalassinoides* locally pipe down into the lens to a depth 20 cm.

CHAPTER 7: DESCRIPTION OF PALYNOMORPHS AND MEGASPORES

PALYNOMORPHS

Palynomorphs from the Ingersoll shale (Ray Christopher, personal communication, 2006) include pollen (Fig. 8A), among which are “newer” forms of *Complexiopollis*, *Sohlipollis* sp., *Taxodiaceapollenites hiatus*, *Plicapollis* sp., and *Peromonolites allenensis*; a diverse and moderately abundant assemblage of marine dinoflagellate cysts (Fig. 8B), possibly including *Palaeohystrichophora infusorioides*; acritarchs (Fig. 8C), including *Michrystidium* sp.; and fungal spores (Fig. 8D). Marine palynomorphs (mainly marine dinoflagellate cysts) are more abundant than the terrestrial palynomorphs, indicating proximal marine deposition (Richard Lupia, personal communication, 2006). Some small pollen grains (<15µm) suggest insect pollination and would argue for the source plants growing in close proximity to the depositional site (Richard Lupia, personal communication, 2006).

The presence of *Sohlipollis* sp., an index fossil in the Gulf Coastal Plain Province (Christopher et al., 1999), indicates assignment of Ingersoll shale palynomorphs to the *Sohlipollis* Taxon Range Zone (mid-Turonian-Santonian). This assignment is consistent with palynomorph data from other Eutaw Formation sites in Alabama and Georgia. None of the palynomorphs indicate a pre-mid-Turonian zonal assignment, and the presence of



FIGURE 8—Ingersoll shale palynomorphs, assignable to the *Sohlipollis* Taxon Range Zone (mid-Turonian-Santonian). (A) Pollen (B) Marine dinoflagellate. (C) Acritarch. (D) Fungal spore. Photographs taken by Richard Lupia (Clemson University). *Sohlipollis* Taxon Range Zone assignment and general palynomorph identifications made by Ray Christopher (University of Oklahoma).

Sohllipollis sp. suggests an age no younger than Santonian (Ray Christopher, personal communication, 2006).

MEGASPORES

Heterosporous plants produce two types of spores: a small, male microspore and a large, female megaspore. The Ingersoll shale has produced an abundance of megaspores from heterosporous aquatic or semi-aquatic ferns (Marsileaceae) and lycopsids (Selaginellaceae and Isoetaceae). In addition, an isolated marsileaceous sporocarp with articulated megasporangia and microsporangia also was recovered. The sporocarp is possibly assignable to *Marsilea*.

The most abundant megaspore from the deposit is *Molaspora lobata* (family Marsileaceae) (Fig. 9A). These spheroidal megaspores are easily recognizable by the 5-7 twisted triangular lobes that make up the acrolamella (Lupia et al., 2000). *Molaspora lobata* was found *in situ* in a well-preserved sporocarp in the Ingersoll shale (Fig. 10A and B). Lupia et al. (2000) assign comparable sporocarps containing *in situ* *Molaspora lobata* to *Regnellidium upatoiensis*, based on findings from a contemporaneous site along the banks of Upatoi Creek, Georgia. According to Richard Lupia (personal communication, 2006) the Ingersoll sporocarp specimen is articulated in a manner unlike the Upatoi Creek sporocarps. From my observations, the sporocarp compares favorably to the *Marsilea* in overall geometry and the manner in which the megasporangia are articulated on the lateral vein within the sori (see Nagalingum et al., 2006, fig. 1A, figs. 2B and 2D). However, the Ingersoll shale specimen is different in that it has lateral veins

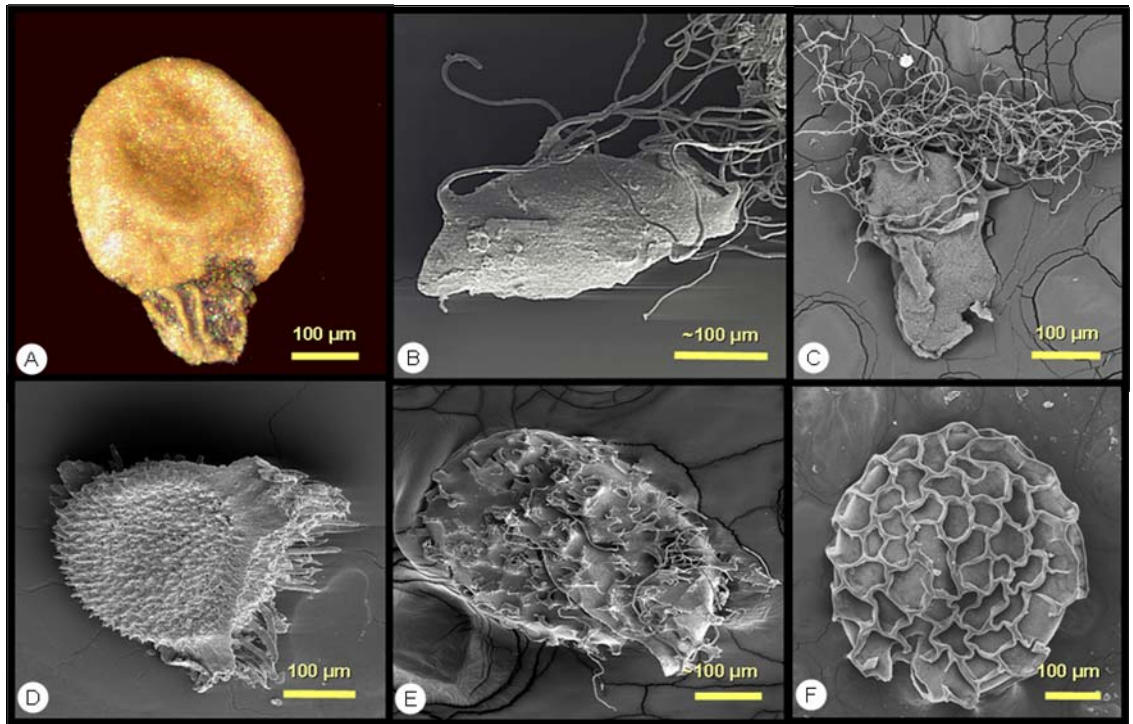


FIGURE 9—Megaspores from the Ingersoll shale. (A) *Molaspora lobata*. (B) *Ariadnasporites* sp. (C) *Arcellites* sp. (D) *Paxillitriletes* sp. (E) Unidentified megaspore. (F) *Erlansonisporites* sp. Identifications courtesy of Richard Lupia (Clemson University).

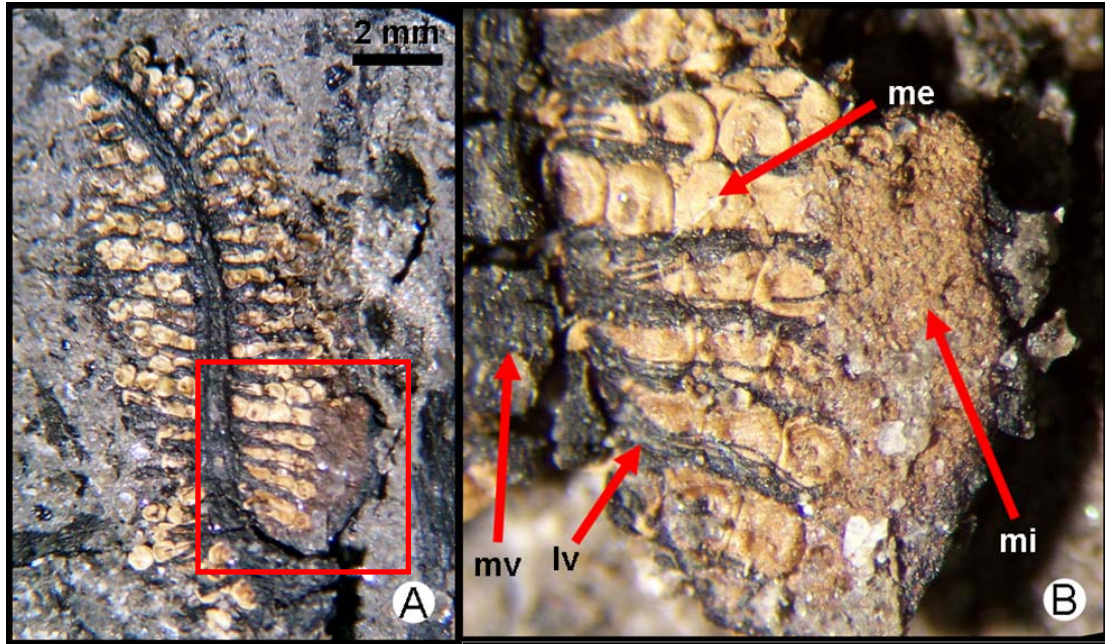


FIGURE 10—(A) Sporocarp from Marcileaceae. (B) Close-up of sporocarp showing articulated megasporangia and microsporangia; megasporangia (me), microsporangia (mi), main vein (mv), lateral vein (lv).

that are bilaterally symmetrical to the midvein, and the microsporangia lie distal to the sori and are not found in small clusters.

Other megaspores from the Ingersoll shale assignable to Marcileaceae are *Ariadnasporites* sp. (Fig. 9B) and *Arcellites* sp. (Fig. 9C). Both taxa only occur as single, isolated specimens. *Ariadnasporites* sp. and *Arcellites* sp. specimens have articulated rhizomes that are remarkably flexible and elastic. The small spore *Crybelosporites*, which is generally associated with *Molaspora* (Lupia et al., 2000) and *Arcellites* (Batten et al., 1996), has yet to be discovered or seen associated with Ingersoll shale megaspores but are possibly the microsporangia articulated with the *Marsilea* sporocarp.

Megaspores from isoltalean and selaginellean lycopsids include *Paxillitriletes* sp. (Fig. 9D) and *Erlansonisporites* sp. (Fig. 9F), respectively. Both of these megaspore types are common throughout the Ingersoll shale lens; however, to date no sporocarps and associated microspores have been discovered. Other unidentified megaspores have also been discovered from the deposit (Fig. 9E).

The quality of preservation of the Ingersoll shale megaspores is variable. *Molaspora lobata* and *Paxillitriletes* sp. are sometimes found preserved in three dimensions, but generally most megaspore fossils are flattened but whole. All megaspores are similar in color (light tan), with the exception of *Erlansonisporites* sp., and appear to be the remains of the exine layer, which is composed of the original sporopollenin. *Erlansonisporites* has an opaline iridescence that is the result of close packing of sporopollenin spheres in the megaspore wall (Takahashi et al., 2001).

The presence of megaspores in a fossil site often can be used to make paleoenvironmental interpretations. *Arcellites* is an indicator of quiet freshwater bodies

(Batten et al., 1996). Extant members of the source plants, families Marsileaceae and Isoetaceae, are not salt tolerant, although their extinct relatives could have been. It is more likely that these plants were living in nearby freshwater lakes or rivers and were washed into the depositional site (Richard Lupia, personal communication, 2006).

CHAPTER 8: MACROFLORA

INTRODUCTION

The Cretaceous is one of the most important geologic periods for plant evolution. During this time, the flora that dominated the terrain became more modern (Friis et al., 2006). The earliest evidence for the first angiosperm is from Early Cretaceous strata (Friis et al., 2006). By the end of the Cretaceous, the taxonomic diversity of cycads and ferns was in drastic decline, while angiosperms underwent a rapid diversification and radiation, producing many of the modern families we see today (Grimaldi and Engle, 2005; Friis et al., 2006). By the Late Cretaceous, older Mesozoic vegetation was virtually extinct, and angiosperms dominated many habitats worldwide (Friis et al., 2006).

Fossiliferous deposits in eastern North America provide one of the most complete records of Late Cretaceous floras in the world and have been the focus of research by paleobotanists for over one hundred years (Wolfe and Upchurch, 1987). Most of the large, monographic works on these fossiliferous deposits were published during the late 1800s and early 1900s. Although these publications are in need of taxonomic revision, they do include detailed morphologic descriptions and illustrations of Late Cretaceous floras. Some of these deposits include the Cenomanian-Turonian Amboy Clays of New Jersey (Newberry, 1896), the Cenomanian Tuscaloosa Formation in Alabama, South Carolina, and Georgia (Berry, 1914, 1919), the Santonian-Campanian deposits of the

Eutaw Formation (Berry, 1919), and the Black Creek Formation in South Carolina (Berry, 1914), to only name a few. A problem with these early works is that the authors did not recognize variations within taxonomic groups between individual fossil deposits. Furthermore, most taxonomic identifications were based on phenotypic resemblances to modern taxonomic groups; Cretaceous fossil plants were assigned indiscriminately to living genera (Brian Axsmith, personal communication, 2007). These problems led to confusing nomenclature.

Today, a description of the morphological character of leaves (e.g., size, shape, and venation) is the standard preliminary practice by most paleobotanists, prior to any fossil taxonomic identification (Brian Axsmith and Robert Gastaldo, personal communication, 2006). These detailed descriptions are useful for paleoecological studies even though the biologic affinities of the flora may remain unresolved. One example of the usefulness of leaf characters, or foliar physiognomy, is demonstrated in a study by Wolfe and Upchurch (1987) on North American, Late Cretaceous climate and vegetation. In this study, the authors used detailed morphologic descriptions and floral illustrations from some of the monographic works listed above as their database, ignoring taxonomic assignments of the original authors. They compared this data to morphologic features seen in modern plant assemblages to make inferences about the Late Cretaceous paleoenvironment. Leaf-margin analysis provided mean annual temperature estimates based on the percentage of dicotyledonous species with toothed versus entire margins. They also used leaf size to make determinations on an open-canopy versus closed-canopy forest. The morphology of leaf apices (i.e., drip-tips versus rounded apices) were used to make inferences on precipitation. The thickness of fossilized leaves indicates whether

leaves came from an evergreen tree with thick leaves indicating little temperature change or a deciduous tree with very thin leaves indicating pronounced seasonality. By taking morphological features into account, they concluded that the Late Cretaceous vegetation in southeastern North America was an open-canopy forest, dominated by angiosperms, with conifers as emergents, growing in a subhumid environment with low seasonality.

More recent publications that give detailed morphological descriptions of floral assemblages from southeastern North America include descriptions of the Santonian Allon Flora from the Gaillard Formation in central Georgia (Keller et al., 1996; Sims et al., 1999; Herendeen et al., 1999; Magallón et al., 2001). This floral assemblage is considered to be taxonomically typical of floral assemblages in the Gulf Coastal Plain in that it is dominated by a diversity of angiosperms. This assemblage also provided evidence that extant families of angiosperms had already differentiated by the Turonian-Campanian.

Southeastern North America has a virtually continuous record of Late Cretaceous flora, and it is likely that new contributions will be made with every new fossil site discovered. Within this chapter, the known Ingersoll shale macroflora is morphologically described. Although the biologic affinities of many Ingersoll taxa are still unknown, these descriptions can serve as a starting point for more detailed analyses.

METHODOLOGY

Ingersoll shale macroflora was discovered by using normal quarrying, sieving, and curating techniques as outlined in Chapter 6. Because of the time constraints of this project, the main objective when quarrying plant fossils was to collect the most diverse

assemblage possible. To avoid an overabundance of fossils of a few common taxa, many fossils encountered were not collected. However, every taxon not previously found was collected, prepared, and logged into the collection.

The manual of leaf architecture (Leaf Architecture Working Group, 1999) was used to describe dicotyledon and monocotyledon angiosperms, as well as the ferns. Form genus classification schemes by Harris (1969) were used for conifer fossils. Recent publications on Late Cretaceous mesoflora that focused mainly on reproductive organs also were used as a terminology guide for flowers and for tentative identifications (Keller et al., 1996; Sims et al., 1999; Herendeen et al., 1999; Magallón et al., 2001).

To make comparisons with other fossils from North American Cretaceous strata, the monographic works of Lesquereux (1892), Newberry (1896), and Berry (1914 and 1919) were reviewed. Although these monographic works are in need of taxonomic revision, they serve as detailed descriptions of the flora in other Late Cretaceous plant-bearing deposits.

RESULTS

During excavation, 281 plant fossils representing 70 distinct morphotypes were collected, prepared, and logged into the collection. These include the possible remains of the sphenophyte *Equisetum*, 7 fern morphotypes, 7 conifer foliage morphotypes, 5 conifer cones, 39 dicotyledon angiosperm morphotypes, 2 monocotyledon morphotypes, 4 flower morphotypes, a fruit type, fruit coatings, a fruit/seed wing, and 2 miscellaneous seed types. These fossils were preserved via a combination of lignification, pyritization, imprintization, coalification, as well as mummification.

DESCRIPTION AND DISCUSSION OF FOSSIL REMAINS

c.f. EQUISETUM

Figs. 11A and B

Description.— This taxon is described from two specimens. One specimen is less than 2 mm long and ~300 μm wide. It has what appear to be eleven nodes, but no leaves or other organic matter remains. The specimen is completely pyritized and appears to be a pith cast. The second specimen is an apical cone (strobilis) with hexagonal, peltate, sporangiophores, which are covered with cuticle. The strobilis is pyritized between the sporangiophores.

Discussion.— The possible *Equisetum* remains are very rare in the Ingersoll shale. It must be noted that this identification is tentative and made solely on comparisons with extant species. The similarities with these fossils and extant species *Equisetum* are the presence of nodes in the pyritized specimen and the presence of a strobilis with hexagonal, peltate, sporangiophores. No fossil comparisons were found in the monographic works by Lesquereux (1892), Newberry (1896), and Berry (1914 and 1919).

FERNS

Fern Morphotype 1

Fig. 12A

Description.— This fern morphotype is described from 2 pinnatifid fragments, the largest of which is 28 mm long and 15 mm wide at its widest portion. Ultimate pinnules are alternating and decrease in size toward the apex. Thick, second-order veins extend from the rachis into the ultimate pinnules at acute angles and continue to the margin of

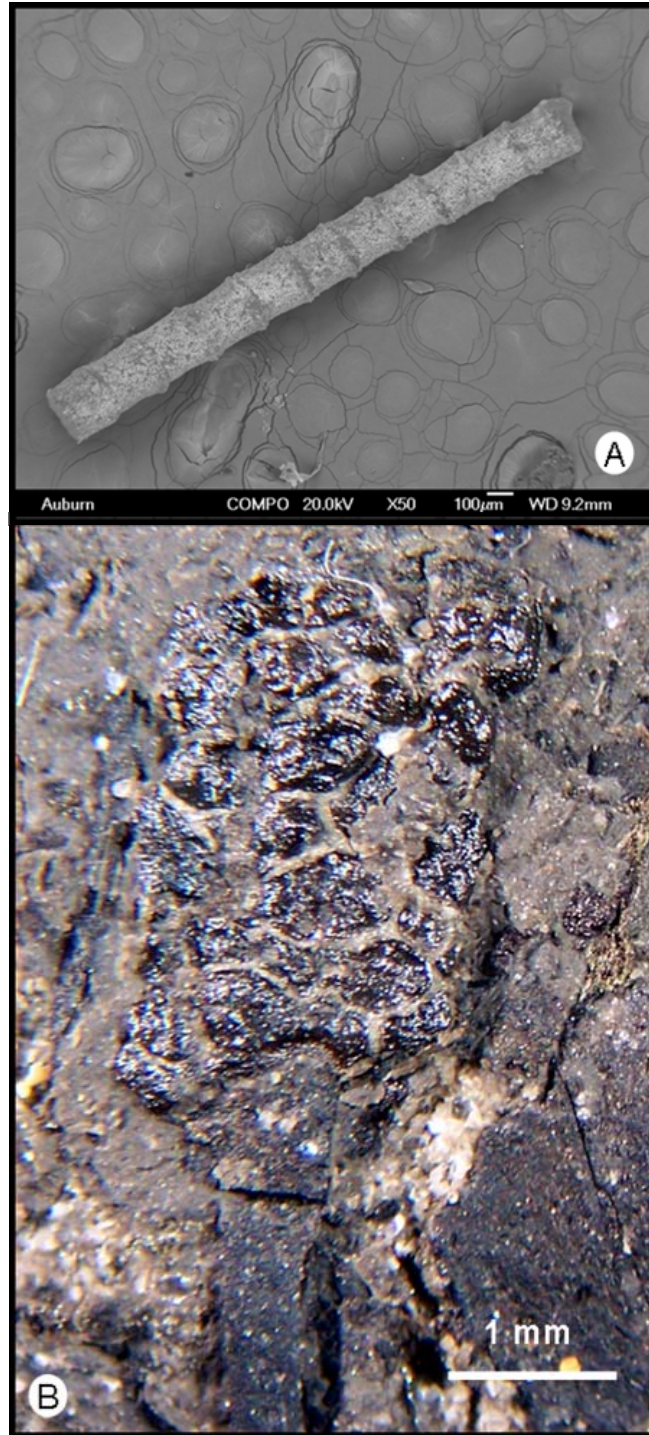


FIGURE 11—Possible Ingersoll shale *Equisetum*. (A) Pyritized pith cast. (B) Strobilus spicate axis.

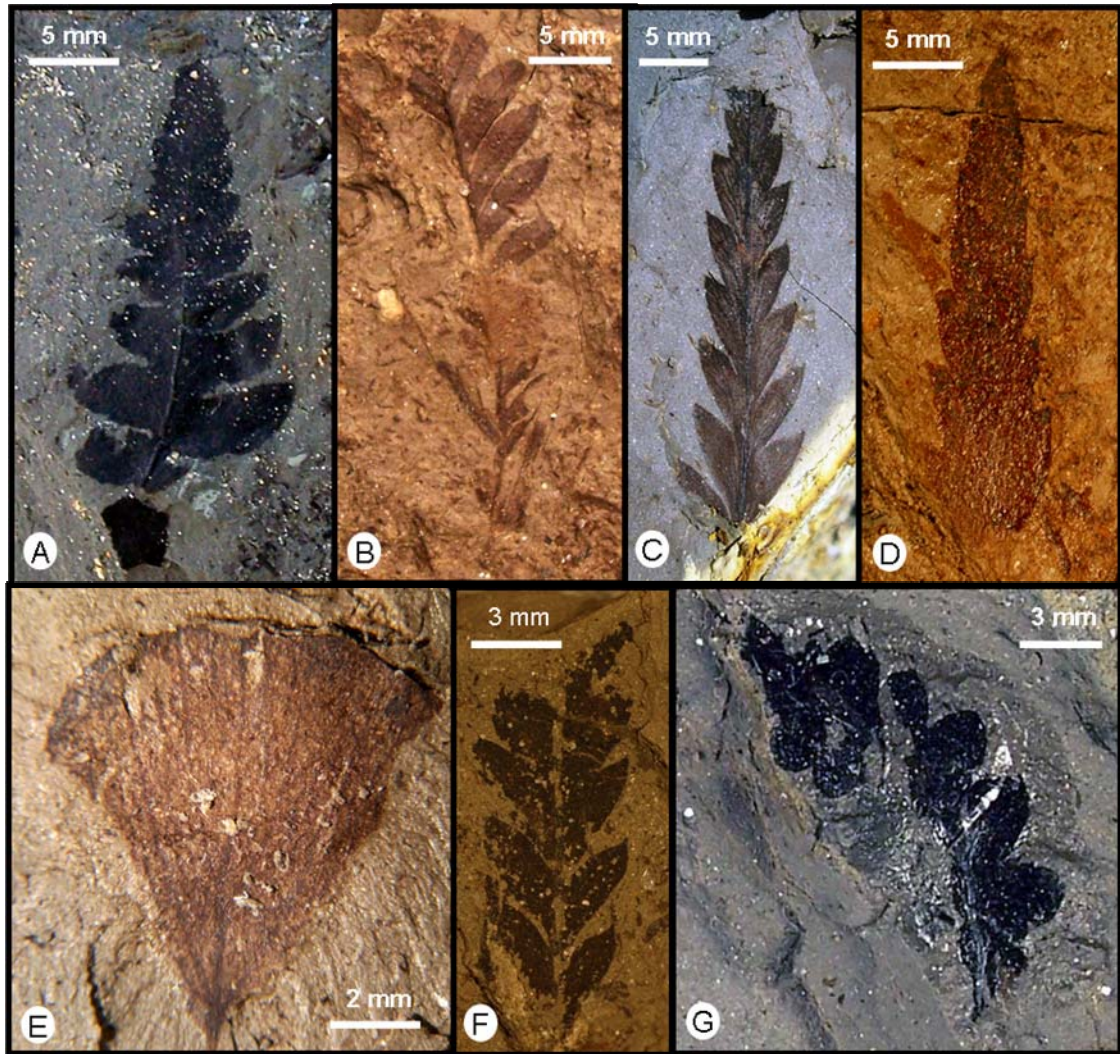


FIGURE 12—Ingersoll shale ferns. (A) Fern morphotype 1 (KIS-220). (B) Fern morphotype 2 (KIS-607). (C) Fern morphotype 3 (KIS-203). (D) Fern morphotype 4 (KIS-051). (E) Fern morphotype 5 (KIS-009A). (F) Fern morphotype 6 (KIS-200). (G) Fern morphotype 7 (KIS-276).

the apex. Tertiary veins diverge acutely and extend to the margin. Several branch into fourth-order veins before reaching the margin. The margin is irregularly toothed, bearing two orders of teeth with variable shapes. Tooth apices are simple, and the sinuses rounded. Leaf texture is coriaceous with preserved black carbonized cuticle.

Fern Morphotype 2

Fig. 12B

Description.— This type is known from one isolated pinnate fern pinna, which is 35 mm long and 12 mm wide. Ultimate pinnules are alternate and oblong, 8.2 mm long and 2.7 mm wide. Second-order veins reach the apex of the pinnule. Apex is acuminate-rounded. The specimen was preserved in a leached and oxidized portion of the shale lens, but the leaf texture appears chartaceous with some cuticle preserved.

Fern Morphotype 3

c.f. Dryopterites stephensonii

Fig. 12C

Description.— This morphotype is described from four isolated pinnate fern pinna. The longest specimen is 37.2 mm long, and all specimens have an average width of 8 mm. Ultimate pinnules average 7.6 mm long and 2.4 mm wide. Pinnule apex is acute and/or convex and pinnule margins are smooth. There is one prominent rachis with secondary veins diverging into the ultimate pinnules at acute angles ($\sim 40^\circ$). Secondary veins extend to the pinnule apex. Tertiary veins alternately branch from the secondaries with no branching of the tertiaries into fourth-order veins on the apical side. There is an average of four tertiary veins diverging from the basal side of the secondaries at $\sim 30^\circ$, with alternating forking into fourth-order veins.

Discussion.— These four specimens are similar to the form identified as *Dryopterites stephensonii* by Berry (1914, pl. XVII, fig. 1) from the Eutaw Formation. However, the branching pattern of the secondary veins described by Berry is not seen in the Ingersoll specimens.

Fern Morphotype 4
c.f. *Marsilea*
Fig. 12E

Description.— This morphotype is described from the part and counterpart of a single specimen. It is a fan-shaped obovate, symmetrical, nanophyll size (1 cm long, 1.1 cm wide) frond with entire margins. The preserved petiole measures 1.5 mm long and 0.2 mm wide. Petiole attachment appears to be marginal. The apex is obtuse and truncate (widely toothed). The shape of the base is cuneate to slightly convex. Primary venation pattern is flabellate. The leaf texture is chartaceous with cuticle preserved.

Discussion.— This plant fossil looks like a single disarticulated frond of *Marsilea*. It is the only such leaf to be found in the shale lens, however, a sporocarp of c.f. Marsilaceae has been found. Considering the relatively high salinity represented by the Ingersoll shale, and extant species of Marsilaceae being freshwater species, this leaf was probably washed into the depositional site.

Fern Morphotype 5
c.f. *Gleichenia micromera*
Fig. 12F

Description.— This type is described from one poorly preserved fragment of a pinnate fern pinna that is 11.9 mm long and 6.5 mm wide. Four opposite, broadly triangular ultimate pinnules are preserved. The ultimate pinnule apex is acuminate-

rounded. No midvein can be observed on the ultimate pinnules. Leaf texture is chartaceous and only a carbonized film remains.

Discussion.— These remains are morphologically similar to *Gleichenia micromera* (Newberry, 1896, pl. III, fig. 6) from the Amboy Clays in New Jersey.

Fern Morphotype 6
c.f. *Cladophlebis alabamensis*
Fig. 12D

Description.— This morphotype is represented by one isolated fern pinnatifid that is 25.0 mm long and 6.5 mm wide. The ultimate pinnules are alternating and their apices acute and convex. Ultimate pinnule margins are smooth. The sinus shape is angular. The rachis was preserved in the specimen but no higher order veins are seen. The leaf texture is coriaceous.

Discussion.— The shape of this fern fragment is superficially similar to *Cladophlebis alabamensis* described by Berry (1919, pl. 5, fig. 8) from the Tuscaloosa Formation. However, none of the vein patterns can be observed for closer comparison.

Fern Morphotype 7
c.f. *Booblepteris turoniana*
Fig. 12G

Description.— This morphotype is described from a single specimen that is 14 mm long and 6 mm wide, with a sinuous ultimate rachis. Alternating ultimate pinnules are rounded and obtuse. The midvein does not extend to the pinnule apex. Lateral veins are evenly spaced, some forking, and extend to margin. The margin is simple and dentate.

Discussion.— This fern morphotype is structurally similar to *Booblepteris turoniana* described by Gandolfo et al. (1997) from the Magothy Formation in Sayerville, New Jersey.

MONOCOTYLEDON ANGIOSPERM LEAF MORPHOTYPES

Monocotyledon Leaf Morphotype 1

c.f. *Doryanthites cretacea*

Fig. 13A

Description.— This morphotype is described from 7 specimens in the collection and many others observed in the field. The leaves are elongate and large (up to 75 cm long and 5-6 cm wide) and have entire margins. They are often preserved whole and appear to split into pairs ~20 cm from base. None have been found articulated to the stem. The apex shape is straight. The leaf base of this morphotype is truncate and flares outward. The leaves have very fine, longitudinal venation, with ~7 veins per cm of leaf. Microscopically, the cuticular remains show an even finer venation, ~12 veins per mm; fine veins do not terminate at the margins but converge at the apex. In the cuticular remains of some specimens, lines of stomata run parallel to the venation. Leaf texture is very coriaceous, and thickness increases towards the base, where the preserved organic matter appears to be coalified.

Discussion.— This leaf type is often preserved whole and is very common in the deposit (see Chapter 7). These leaves are very similar to what Berry (1914) described as *Doryanthites cretacea* (pl. XVII, fig. 3), also from the Eutaw Formation.

Monocotyledon Leaf Morphotype 2

Fig. 13B

Description.— Leaves are linear with entire margins. No intact leaves have been discovered. However, fragments measure up to 14 cm in length and range from 6 to 15 mm wide. The leaves show a very fine parallel venation, ~9 veins per mm, with cuticular



FIGURE 13—Ingersoll shale monocotyledon leaf morphotypes. (A) Monocotyledon leaf morphotype 1. (B) Monocotyledon leaf morphotype 2.

remains showing an even finer venation. No base attachments or apices were found. Leaf texture is coriaceous but not as thick as monocotyledon leaf type 1.

Discussion.— These leaves are very common in the deposit and are often found associated with monocotyledon leaf morphotype 1 and dicotyledon leaf morphotype 1. They have a “grass like” appearance because of their size and their shape, but they could be a smaller form of monocot leaf morphotype 1.

DICOTYLEDON ANGIOSPERM LEAF MORPHOTYPES

Dicotyledon Leaf Morphotype 1

c.f. Manihotites georgiana

Fig. 14A

Description.— These leaves are very common in the Ingersoll shale, and the morphotype description is based on many specimens. They are palmately lobed, elliptical, and macrophyll in size (typically 20 x 20 cm). The base of this leaf morphotype is wide, obtuse, and lobate. Overall angle of the apex is wide obtuse. The petiole attachment is stout with a peltate-eccentric petiolar attachment. Leaf margin is entire and palmately lobed. First-order veins are suprabasal actinodromous with 5-6 primaries radiating from the base typically at $\sim 50^\circ$. Primary veins diverge to form secondaries typically at $40-50^\circ$ and $\sim 3.0-5.5$ cm above the petiolar attachment. The middle primary vein intersects the base of the main sinus with no evidence of divergence along the margin. Second-order veins are straight or slightly curved and in some specimens diverge into tertiary veins. There are 5-6 main lobes that are unequally dichotomously sublobate. Subordinate lobes are $\sim 6-7$ cm long, ovate lanceolate, with rounded obtuse apices. The main sinuses are deep, rounded and are located an average of 3-4 cm above the base.

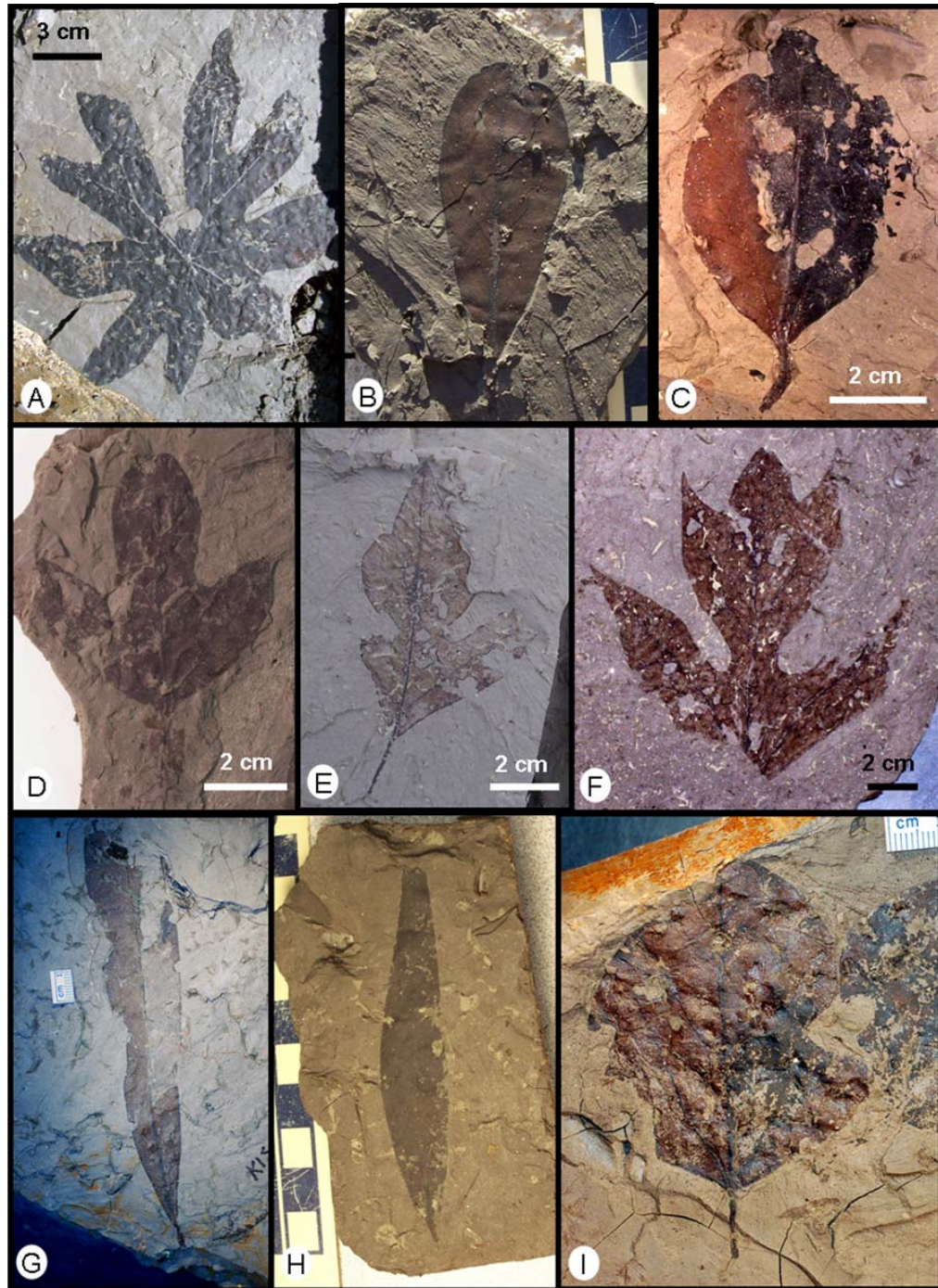


FIGURE 14—Ingersoll shale dicotyledon leaf morphotypes. (A) Morphotype 1 from the Columbus State University collection. (B) Morphotype 2 (KIS-085). (C) Morphotype 3 (KIS-159). (D) Morphotype 4 (KIS-002). (E) Morphotype 5 (KIS-084). (F) Morphotype 6 (KIS-606). (G) Morphotype 7 (KIS-608). (H) Morphotype 8 (KIS-048). (I) Morphotype 9 (KIS-049). Black and white scale (Figs. 13B and 13H) is in cm.

Subordinate sinuses on the main lobes are proportionately less deep. The leaf texture is coriaceous with cuticle often preserved.

Discussion.— This leaf type is the most abundant dicotyledon form found in the middle to upper parts of the Ingersoll shale. It almost always occurs as whole, well-preserved specimens. All mature leaf specimens are approximately the same size and are found in clusters both horizontally and vertically. Juvenile forms also have been found in the deposit, and all of these are also of nearly equal size (10x10 cm). Most of the juvenile forms were collected from a thin zone (~8 cm in thickness) directly above the triplet datum. Within this zone there are ~15 horizons, each with three or more leaves found on a single bedding plane. It is possible that the leaves are from a single plant considering their thick vertical succession and the lateral restriction.

The leaf morphology is similar to *Manihotites georgiana*, described by Berry (1919) from the basal beds of the Eutaw Formation. Berry (1919) discovered the two type specimens in a clay lens within the banks of Upatoi Creek, ~10 miles from the Ingersoll shale site. Berry related these specimens to the modern genus *Manihot*, within the Euphorbiaceae (Spurge) family. These plants are native to Central and South America today but can be grown in any frost-free, warm environment with a 10-11 month growing season (Berry, 1914).

Dicotyledon Leaf Morphotype 2

c.f. *Myrsine gaudini*

Fig. 14B

Description.— This single specimen is an obovate, symmetrical, microphyll leaf, 43 mm long and 21 cm wide. The base is acute and slightly decurrent. The apex is obtuse and rounded. The petiole is stout with a marginal petiolar attachment. The leaf margin is

entire and not lobed. Primary venation is pinnate with a massive, straight, and unbranching primary vein. Second-order venation is brochidodromous. Seven pairs of secondaries, moderate in thickness, moderately diverge alternately from the primary vein at $\sim 45^\circ$ and curve uniformly toward the apex. There are weak intersecondaries. Tertiary veins are regular pentagonal reticulate. No higher-order vein patterns were observed. Areoles formed by the tertiary veins are well developed, random, pentagonal and quadrangular, and are medium in size (0.3-1.0 mm). The leaf texture is coriaceous and cuticle is preserved.

Discussion.— This leaf closely resembles what Lesquereux (1892, p. 115; pl. 52, Fig. 4), Berry (1914, p. 98; pl. XIV, fig. 9), and Berry (1919, p. 133) described as *Myrsine gaudini* from the Dakota Group, Black Creek Formation, and the Tuscaloosa Formation, respectively. According to Berry (1919), this species is also common in the Raritan Formation in New Jersey. *Myrsine gaudini* belongs to the family Myrsinaceae.

Dicotyledon Leaf Morphotype 3
c.f. *Cinnamomum newberri*

Fig. 14C

Description.— This morphotype is described from several specimens that are microphyll-notophyll in size. Laminar shape is ovate, symmetrical, with an average length-to-width ratio of 1.7:1. The base is obtuse (85° - 90°) and concave. The apex is acute, but the exact shape could not be determined. The margin is smooth and unlobed with a marginal petiolar attachment. The petiole on specimen KIS-007 is 14.0 mm long and 2.4 mm wide. Primary veins are basal acrodromous, with 3 primaries originating at the bases. Midveins are slightly thicker than the two adjacent veins. Secondary veins are brochidodromous, irregularly spaced, with a uniform vein angle as measured to the

primaries. Tertiary veins are alternating percurrent and sinuous. Fourth-order veins are regular polygonal reticulate. Areolation is well-developed in some specimens, with 4-5 sides. The margins have a fimbrial vein. Leaf texture is coriaceous with the cuticle preserved.

Discussion.— This leaf form is similar to what Berry (1919) described as *Cinnamomum newberri* from the Tuscaloosa Formation, at Shirleys Mill and Glen Allen, Fayette County, and at Cottdale, Tuscaloosa County, Alabama, and in the basal beds of the Eutaw Formation at McBrides Ford, Chattahoochee County, Georgia.

Dicotyledon Leaf Morphotype 4
c.f. *Sassafras*
Fig. 14D

Description.— This morphotype is described from several specimens that are notophyll-mesophyll size, elliptic and symmetrical. The base is obtuse and concave-convex. The apex is odd-lobed acute. The leaf margin is entire and has three lobes. The petiole is typically 17 mm in length and 1.8 mm in width and has a marginal petiolar attachment. The lobe apex is rounded and obtuse on the center lobe, and acute and convex on the outer lobes. Both of the sinuses are rounded. Primary veins are suprabasal acrodromous. The midvein is considerably larger than the exmedial veins. No higher-order vein patterns were observed. Leaf texture is coriaceous with well-preserved cuticle.

Discussion.— See discussion for dicotyledon leaf morphotype 6.

Dicotyledon Leaf Morphotype 5
c.f. *Sassafras*
Fig. 14E

Description.— This morphologic description is based on several specimens that are mesophyll-size, elliptic-ovate, and symmetrical. The base is acute and concavo-convex. The apex is odd-lobed acute. The petiole is straight, up to 33 mm long and 2 mm wide, and has a marginal petiolar attachment. The margin is entire and sinuous. There are three lobes, with acute and convex apices. Middle lobe margins undulate inward but not enough to constitute a sinus. Both exmedial sinuses are rounded. The primary vein pattern in each specimen is suprabasal acrodromous. There are 3 primary veins; the midvein is noticeably larger than the exmedial veins. Second-order vein pattern is compound agrophic, with the lateral primaries acting as the backbone. Tertiary veins are regular polygonal reticulate. Marginal venation patterns are difficult to decipher but possibly form incomplete loops. No fourth-order veins could be established. The leaf texture is chartaceous-coriaceous with cuticle preserved.

Discussion.— See discussion for dicotyledon leaf morphotype 6.

Dicotyledon Leaf Morphotype 6
c.f. *Sassafras*
Fig. 14F

Description.— This morphotype is described from one complete specimen, which is macrophyll-size, elliptic-ovate, and symmetrical. The base is not preserved. The overall apex angle is odd-lobed acute. The margin is entire and has 5 lobes. The lobe apices are acute and rounded on the center lobe, convex on the outer 5 lobes. All sinuses are rounded. Primary veins are suprabasal acrodromous. There are 3 primary veins; the midvein is slightly larger than the exmedial veins. Second-order veins are compound

agrophic, with the lateral primaries acting as the backbone on the lower lobes. No higher-order vein patterns could be observed. Leaf texture is chartaceous-coriaceous with cuticle preserved.

Discussion.— Morphotypes 4, 5, and 6 appear to represent a continuum in leaf growth in which the morphology of their middle lobe changes as the leaf matures. The margins of morphotype 4 (Fig. 14D) are entire and unlobed; it is interpreted as being the juvenile form. Along the middle lobe margins of morphotype 5, sinuses have begun to develop ~2 cm from the apex (Fig. 14E). The sinuses are fully developed in morphotype 6, and the middle lobe is branched into 3 lobes, as seen in Figure 14F.

These 3 morphotypes share an overall similar morphology to the various species of *Sassafras* described by Newberry (1896), and Berry (1914). Both authors described their specimens as having considerable variation, even within the same species.

Dicotyledon Leaf Morphotype 7

c.f. *Ficus atavina*

Fig. 14G

Description.— This morphotype is described from many specimens that are notophyll-mesophyll size (the most complete specimen is 15 cm long and 3.2 cm wide), obovate, and symmetrical-slightly asymmetrical (asymmetrical basally). The base is acute and decurrent. The apex is obtuse and rounded-retuse. The leaf margin is entire and unlobed. First-order venation patterns are pinnate. Secondary venation patterns are cladodromous. Petioles are pulvinate, with a marginal petiolar attachment. Secondary veins are uniformly spaced ~3 mm apart and branch from the midvein uniformly at ~70°. Third-order veins are alternate, precurrent, sinuous, and are obtuse to the primary vein. Fourth-order veins are alternate precurrent between the tertiaries. No higher-order vein

patterns were observed. Areoles are well developed and 4- to 5-sided. Marginal ultimate veins are looped. The leaf texture is chartaceous with cuticle preserved.

Discussion.— This leaf form is similar to what Berry (1914) described as *Ficus atavina* (pl. X, fig. 11) from the Black Creek Formation of South Carolina.

Dicotyledon Leaf Morphotype 8
c.f. *Myrica havanensis*
Fig. 14H

Description.— This morphotype is described from several specimens that are oblong-lanceolate in outline, microphyll size (typically 8.5 cm long, 1.3 cm wide), with symmetrical lamina and an asymmetrical base. The leaf margin is entire and unlobed with a marginal petiolar attachment. Petioles average 1.3 mm in width and 4.2-5.0 mm in length, but no petiole features could be observed. The apex gradually narrows to an acute angle, and is straight and acuminate. The base is acute and cuneate. Primary venation on all specimens is pinnate with a stout, curved midvein. Secondary venation patterns are cladodromous. Second-order veins branch from the primary at 45°, are curving intramarginal, and intersect a fimbrial vein ~0.3 mm from the margin. Tertiary veins are regular polygonal reticulate and obtuse to the primary vein. No higher-order vein pattern was observed. Leaf texture on all specimens is chartaceous-coriaceous, with cuticle preserved in some specimens.

Discussion.— This leaf is similar to what Berry (1919) described as *Myrica havanensis* (pl. XI, fig. 4; pl. XXVIII, fig. 7) from the basal beds of the Eutaw Formation in Havana, Hale County, Alabama. This species belongs to the family Myricaceae. Common names for this genus include bayberry, candleberry, sweet gale, and wax-myrtle.

Dicotyledon Leaf Morphotype 9
c.f. *Menispermities integrifolius*
Fig. 14I

Description.— This morphotype is described from two specimens, which are notophyll-mesophyll size (typically 6.0 cm in length and 5.0 cm in width), deltoid ovate, and symmetrical. The base of this morphotype is obtuse and concavo-convex. The apex is obtuse and rounded. Margins are entire and unlobed. Petioles are pulvinate, stout, and straight, and are typically 2.0 mm wide and 17 mm long. Petiolar attachments are marginal. First-order venation patterns are basal actinodromous. Leaves have 7 basal veins; 1 stout midrib, 2 exmedial veins (the most basal being a simple agrophic vein), and one pair of fimbrial veins (0.03 mm, inside margin). Secondary veins are irregularly spaced, diverging from the primary veins at 45°, and increasing in number toward the apex. There are strong intersecondary veins. Tertiary veins are interior, located between the primary and secondary veins. Tertiary veins are opposite-alternate precurrent and sinuous, acute-perpendicular from midvein to intersecondaries, and increase in angle exmedially. Fourth-order veins are regular polygonal reticulate. Fifth-order veins are dichotomizing. Areoles formed by the fourth-order veins are well-developed. Leaf texture is coriaceous with cuticle preserved.

Discussion.— This leaf morphotype is similar to what Berry (1919) assigned as *Menispermities integrifolius* (pl. XX, fig. 1) from the Tuscaloosa Formation, Cottondale, Tuscaloosa County, Alabama. *Menispermities* belongs to the family Menispermaceae.

Dicotyledon Leaf Morphotype 10

Fig. 15A

Description.— This leaf morphotype is known from several specimens that are notophyll-mesophyll size (typically 6.5 cm long, 6.5 cm wide), deltoid-ovate, and symmetrical. The base is obtuse and concavo-convex. The apex is obtuse ($\sim 90^\circ$) and rounded. The leaf margin is entire and unlobed. Thin petioles preserved on two specimens average 0.10 mm in width and 6.75 mm in length, are pulvinate, and widen toward peltate eccentric petiole attachments. Primary venation pattern is suprabasal actinodromous. There are 7 basal veins; 1 stout midrib, 2 exmedial veins (the most basal being a simple agrophic vein), and 1 pair of fimbrial veins (0.12 mm inside margin). Secondary veins are irregularly spaced, diverge from the primary veins at 45° , and increase in number toward the apex. There are strong intersecondary veins. Tertiary veins are interior, located between the primary and secondary veins. Tertiary veins are opposite-alternate precurrent and sinuous, acute-perpendicular from midvein to intersecondaries, and increase exmedially. Fourth-order veins are regular polygonal reticulate. Fifth-order veins are dichotomizing. The areoles formed by the forth-order veins are well-developed. No higher-order vein patterns were observed. The leaf texture is coriaceous with cuticle preserved.

Dicotyledon Leaf Morphotype 11

Fig. 15B

Description.— This morphotype is based on 2 incomplete microphyll leaf fragments that are obovate and asymmetrical. The base angle on both specimens is obtuse ($\sim 90^\circ$), straight, but slightly concave at the base. No apices were preserved. The leaf margin is entire and unlobed. Petioles are pulvinate, averaging 1.45 mm in width and

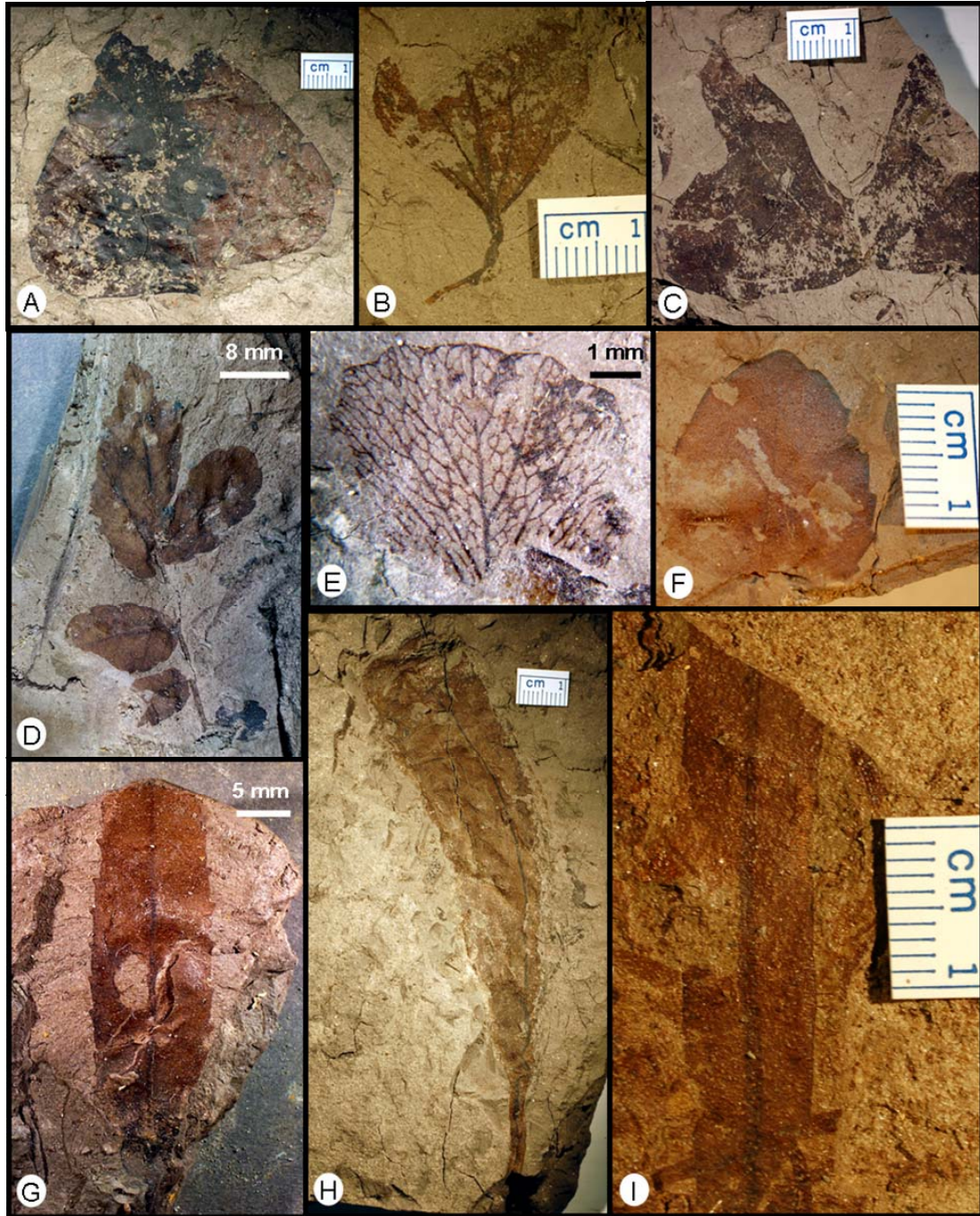


FIGURE 15—Ingersoll shale dicotyledon leaf morphotypes. (A) Morphotype 10 (KIS-603). (B) Morphotype 11 (KIS-086). (C) Morphotype 12 (KIS-145). (D) Morphotype 13 (KIS-272A). (E) Morphotype 14 (KIS-092). (F) Morphotype 15 (KIS-033). (G) Morphotype 16 (KIS-600B). (H) Morphotype 17 (KIS-146). (I) Morphotype 18 (KIS-268).

12.9 mm in length; petiolar attachments are marginal. Primary and secondary veins are basal actinodromous, composed of 1 stout primary vein and 5 secondary veins, which thin exmedially. Basal secondary veins are fimbrial and lie 0.16 mm inside the margin. Tertiary veins are opposite precurrent, slightly curved, perpendicular to the midvein, and increase exmedially. Forth-order vein patterns are regular polygonal reticulate. No higher-order vein patterns or areolation could be seen. The leaf texture is coriaceous with cuticle preserved.

Discussion.— It is possible that this specimen may be related to *Ficus fontainii* (Berry, 1914). However, due to the absence of the apex, similarities are too few to allow detailed comparison.

Dicotyledon Leaf Morphotype 12

c.f. Bauhinia alabamensis

Fig. 15C

Description.— This morphotype is described from one partial specimen, which is notophyll size, ovate, and symmetrical. The base is obtuse (~180°) and cordate. The apex is wide, obtuse, and bilobed. The leaf margin is smooth and undulating. Petiolar attachment is marginal. Primary venation is basal actinodromous. There are a total of 9 basal veins. The midvein is thin and extends into a sinus. The two most basal veins are fimbrial. Second-order venation patterns could not be determined because of poor preservation. However, one portion of the leaf showed a regular polygonal reticulate pattern in the tertiaries. Leaf texture is coriaceous with cuticle preserved.

Discussion.— This leaf is similar to the form Berry (1919) described as *Bauhinia alabamensis* (pl. XXIII, fig. 8), from the basal beds of the Eutaw Formation, Havana,

Hale County, Alabama. *Bauhinia* belongs to the family Caesalpiniaceae. Common names for this genus include the purple orchid tree, mountain ebony, and the poor man's orchid.

Dicotyledon Leaf Morphotype 13

c.f. *Celastrorhynchium*

Fig. 15D

Description.— This morphotype is described from only one specimen, which has multiple leaves attached. The leaves are articulated opposite on the petiolule, with odd-pinnate leaf organization. The leaves are nanophyll size (1.5-2.0 cm long, 0.73 cm wide), obovate, and asymmetrical. The base of this morphotype is acute-obtuse. The apex is complex and acute on the midleaf and obtuse on exmedial leaves. Petiolar attachments are marginal. The leaf margin is crenate, with irregular spacing. First-order venation pattern is pinnate. No higher-order veins or ultimate vein patterns could be discerned. The tooth shape is convex-convex with a simple apex. Sinuses are angular. Accessory veins enter the tooth. Leaf texture is coriaceous with cuticle preserved.

Discussion.— See discussion for leaf morphotype 14.

Dicotyledon Leaf Morphotype 14

c.f. *Celastrorhynchium*

Fig. 15E

Description.— This morphotype is described from several specimens that are nanophyll size (typically 7.7 mm wide and ~1.39 cm long), ovate, and symmetrical. Both the base and apex are obtuse and rounded. Petiolar attachments are marginal. The leaf margin is serrate-crenate with irregular spacing. The first-order venation pattern is pinnate. Secondary veins are cladodromous (30-40° from midvein), alternately branching, and irregular. There are weak intersecondaries. Tertiary veins are regular polygonal reticulate and have an inconsistent angle to the primary vein. No higher-order vein

patterns could be established. Marginal ultimate veins are looped. The teeth are straight-convex with a simple apex. Sinuses are rounded. Accessory veins enter the tooth. Leaf texture is chartaceous with cuticle preserved.

Discussion.— Dicotyledon Leaf Morphotypes 13 and 14 share similar morphologies. They are small and have crenate margins and both are similar to the leaves described as various species of *Celastrorhynchium* from the Amboy Clays (Newberry, 1896), the Dakota Group (Lesquereux, 1892), and the Tuscaloosa Formation (Berry, 1914).

Dicotyledon Leaf Morphotype 15
c.f. *Cissites crispus*
Fig. 15F

Description.— This leaf morphology is described from four specimens, which are nanophyll size (1.1-1.6 cm wide and 1.15-2.08 cm long), obovate, and symmetrical. The base is obtuse and concavo-convex. The apex is obtuse and rounded. The leaf margin is crenate with regular spacing. Petiolar attachments are marginal. First-order venation pattern is pinnate. No higher-order venation or ultimate vein patterns could be discerned. Teeth shapes are straight-convex with simple apices. Sinuses are rounded. Accessory veins extend into the tooth. Leaf texture is coriaceous with cuticle preserved.

Discussion.— This leaf type is morphologically similar to *Cissites crispus*, described by Newberry (1896, pl. XLII, fig. 22) from the Amboy Clay in New Jersey.

Dicotyledon Leaf Morphotype 16
c.f. *Dewalquea smithi*
Fig. 15G

Description.— This morphotype is described from one narrow, incomplete leaf fragment (1.13 cm wide), which is microphyll size, elliptic, and symmetrical. The petiole

is 0.68 mm wide. The base is acute and decurrent. The apex is not preserved. The leaf margin is crenate and not lobed. Petiolar attachment is marginal. Primary venation is pinnate; secondary venation is cladodromous (45-50° from midvein), and these veins extend into teeth. No higher order vein patterns could be established. There is a single order of teeth with three teeth per centimeters, regularly spaced; teeth are shaped straight apically and are retroflexed basally; teeth apices are simple. Sinuses are angular. Leaf texture is coriaceous with cuticle preserved.

Discussion.— This morphotype possibly is a fragment of what Berry (1919) described as *Dewalquea smithi* (pl. XIV, fig. 1; pl. XVI, figs. 2 and 3) from the Tuscaloosa Formation at Shirleys Mill, Fayette County, and Whites Bluff, Greene County, Alabama, and from the Eutaw Formation (Coffee Sand Member) at Coffee Bluff, Hardin County, Tennessee. However, more complete specimens are needed in order to confirm this. Berry tentatively assigned this species to the Ranunculaceae family, which is commonly known as the buttercup family or crowfoot family.

Dicotyledon Leaf Morphotype 17

Fig. 15H

Description.— This morphotype is described from two specimens; one is very well- preserved, and the other is poorly preserved. The description herein is based on the well-preserved specimen. It is notophyll size (10.03 cm long and 2.45 cm wide), obovate and asymmetrical. The base is acute and concave. The apex is obtuse (150°) and emarginate. The leaf margin is entire and unlobed. The petiole is pulvinate, and the petiolar attachment is marginal. First-order venation is pinnate. Secondary veins are cladodromous, numerous, and diverge from the primary at 45-70°. There are strong

intersecondary veins. Tertiary venation is regular polygonal reticulate. The fourth-order vein pattern is alternate percurrent. No higher-order venation could be observed. The margin ultimate venation has a fimbrial vein 0.6 mm inside the leaf margin. Leaf texture is coriaceous with cuticle preserved.

Dicotyledon Leaf Morphotype 18

Fig. 15I

Description.— This morphotype is from a partial, linear, incomplete, symmetrical, microphyll-size leaf (0.8 cm wide and 7.0 cm long). Base and apex are missing, but the angle of both is presumed to be acute based on the narrow width of the leaf. The leaf margin is smooth and unlobed. Primary venation is pinnate. Only 3 veins could be seen: one stout midvein and two fimbrial veins running slightly inside the leaf margin. No higher-order vein patterns could be observed. Leaf texture is coriaceous with cuticle preserved.

Dicotyledon Leaf Morphotype 19

c.f. Diospyros rotundifolia

Fig. 16A

Description.— This morphotype description is based on two specimens. The leaves have an alternate leaf attachment at each node on the petiolule. The articulated leaves are pinnately compound on the petiolule pulvinate petiole. They are microphyll size (5.37 cm long and 3.08 cm wide), oblong, and have symmetrical lamina and an asymmetrical base. Apices are not preserved. The base is widely acute and slightly convex. The leaf margin is smooth and unlobed. Petiolar attachments are marginal. Primary venation pattern is pinnate. Secondary venation is semicraspedromous, alternate, and irregular. Five pairs of secondary veins diverge from the primary vein at

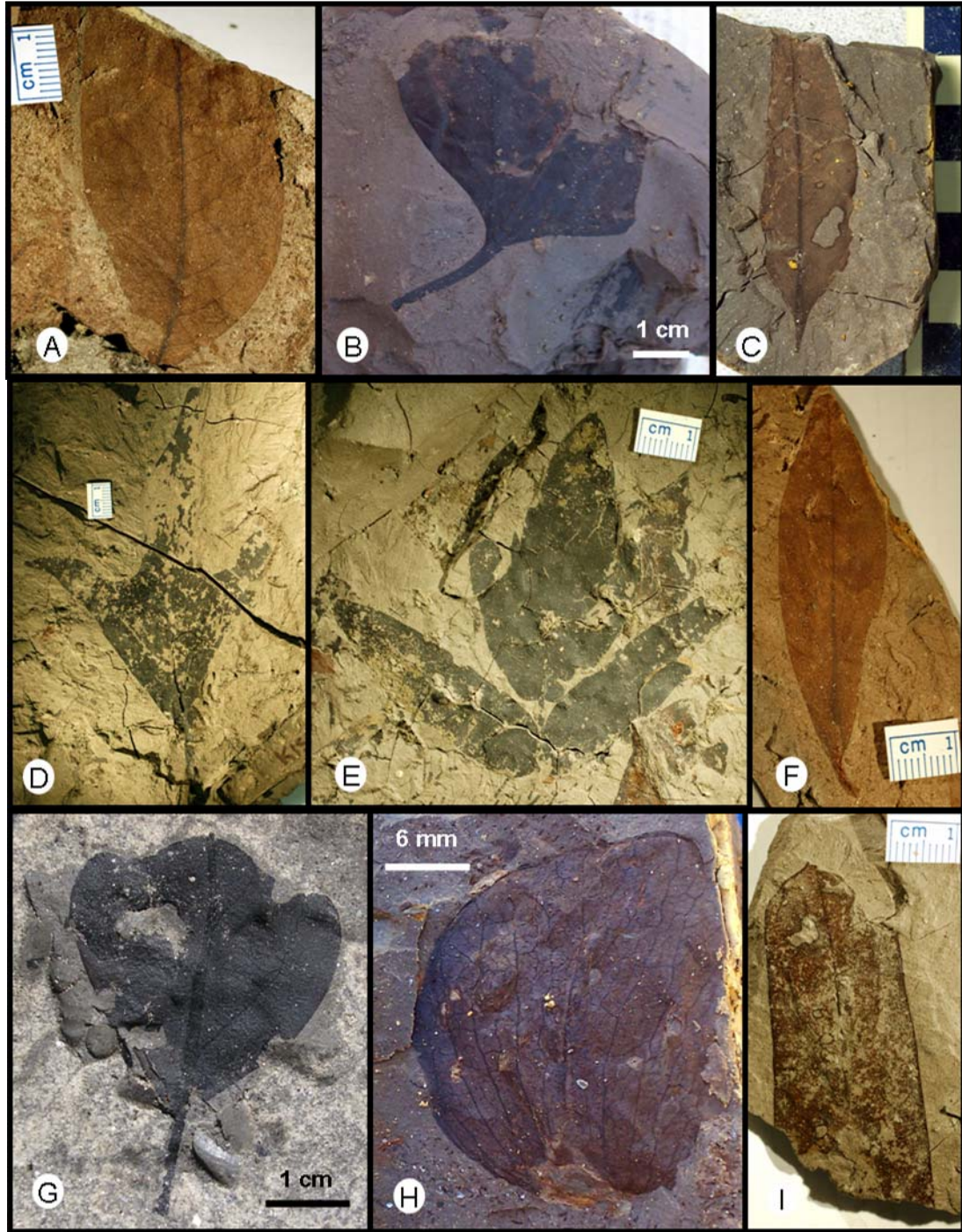


FIGURE 16—Ingersoll shale dicotyledon leaf morphotypes. (A) Morphotype 19 (KIS-268). (B) Morphotype 20 (KIS-045). (C) Morphotype 21 (KIS-054). (D) Morphotype 22 (KIS-148). (E) Morphotype 23 (KIS-705). (F) Morphotype 24 (KIS-149). (G) Morphotype 25 (KIS-139). (H) Morphotype 26 (KIS-073). (I) Morphotype 27 (KIS-512). Black and white scale (Fig. 15C) is in cm.

60° and decrease in angle basally. The leaves have weak intersecondaries. The tertiary vein pattern is opposite percurrent, sinuous, and obtuse to the primary vein. Forth-order venation is regular polygonal reticulate. Fifth-order venation could not be observed. The fimbrial veins lie on the margins. Leaf texture is coriaceous with cuticle preserved.

Discussion.— This leaf form is similar to what Lesquereux (1892, pl. XVII, figs. 8 and 11) and Berry (1919, pl. XXVII, fig. 4; pl. XXX, figs. 4 and 5) described as *Diospyros rotundifolia* from the Dakota sandstone of Kansas and the Tuscaloosa Formation at Shirleys Mill and Glen Allen in Fayette County, Alabama. The genus *Diospyros* is in the family Ebenaceae. Common names for family members include persimmon and ebony.

Dicotyledon Leaf Morphotype 20

Fig. 16B

Description.— This morphotype is described from one partial specimen with only the basal portion preserved. It is notophyll size and symmetrical. Laminal shape could not be determined. The base is obtuse (125°) and concavo-convex. The margin is entire and unlobed. Petiolar attachment is marginal. Primary venation is basal actinodromous with five basal veins. The midvein is stout; exmedially, two veins diverge at 40° from the primary vein, and two smaller fimbrial veins lie on the margin. Secondary veins diverge from the exmedial primary at 40°. Tertiary venation is opposite-percurrent, convex, and obtuse, increasing in angle exmedially. Forth-order venation is opposite-percurrent. No higher-order veins could be seen. Leaf texture is coriaceous with both cuticles preserved.

Discussion.— These remains are remarkably flexible and brown. Black carbonized material occurs (within these two cuticle layers), presumably the remains of the more labile leaf components.

Dicotyledon Leaf Morphotype 21

c.f. *Salix eutawensis*

Fig. 16C

Description.— This morphotype description is derived from two specimens, that are microphyll size (ranging between 6.98-5.3 cm in length and 2.8-1.6 cm in width), ovate, and slightly asymmetrical. The base of this morphotype is acute and gradually narrowing to an attenuate tip. The apex is acute and acuminate. The leaf margin is entire, smooth basally and finely crenate apically, and unlobed, with a marginal petiolar attachment. First-order venation is pinnate, with a stout midvein thinning apically. There are 12 pairs of cladodromous secondary veins that are alternating, branch from the primary vein at $\sim 50^\circ$, and curve upward toward the margin. Weak intersecondaries also were seen. No higher-order venation was seen. Along the margins, there are ~ 10 teeth/cm of lamina. The teeth are straight apically and convex basally, forming a simple apex. The sinuses are angular. No venation pattern or vein order could be associated with the teeth. Leaf texture is coreaceous with cuticle preserved.

Discussion.— This species is similar to what Berry (1914) described as *Salix eutawensis* (pl. XIX, fig. 3) from the basal beds of the Eutaw Formation at Broken Arrow Bend, Chattahoochee County, Georgia. However, the specimens discovered in the Ingersoll shale are slightly wider. Berry described that *Salix* leaf as being quite modern in appearance and distinctively different from any other *Salix* described from the area.

Dicotyledon Leaf Morphotype 22
c.f. *Aralia wellingtonia*
Fig. 16D

Description.— This morphotype is described from a single specimen, which is notophyll size (9.4 cm wide and 11.2 cm long), elliptic, and symmetrical. The base is acute and decurrent; the apex is odd-lobed obtuse. The petiole is stout (2.76 mm wide), straight, and intersects the leaf margin. The margin is entire and trilobed. The apex of the middle lobe is attenuate. The apices of the exmedial lobes are rounded. Primary venation is suprabasal actinodromous, with 5 primary veins. The midvein is stout; the exmedial primaries are slightly thinner, diverge from the midvein at 40°, and extend into the outer lobes. The fimbrial veins run slightly inside the margin. No higher-order venation could be determined. Leaf texture is coriaceous with cuticle preserved.

Discussion.— This leaf resembles *Aralia wellingtonia* described by Lesquereux (1892, p. 131, pl. XXI, fig. 1; pl. XXII, figs. 2 and 3) and Newberry (1896, p. 114, pl. XXVI, fig. 1) from the Dakota Group and the Amboy Clays of New Jersey, respectively. Unlike the previously described *A. wellingtonia*, marginal serrations are lacking on the Ingersoll shale specimen. However, these earlier authors indicate that the margins can be entire, as in the Ingersoll material.

Dicotyledon Leaf Morphotype 23
Fig. 16E

Description.— This morphotype is described from a single specimen, which is ternate (trifoliate) and notophyll size (middle leaflet is 5.17 cm long and 3.07 cm wide; outer leaflets are 4.79 cm long and 1.45 cm wide). The middle leaflet is elliptic, while the outer leaflets are ovate; all have symmetrical lamina. The base on the middle leaflet is

obtuse and rounded; bases on the outer leaflets are acute and rounded. Combined, all three leaflets have an odd-lobed, obtuse apex. Individual leaflets have acute apices. Leaflet margins are entire and unlobed, with a marginal petiolar attachment. Each leaflet has pinnate primary venation. No higher-order venation could be observed. Leaf texture is coriaceous with cuticle preserved.

Dicotyledon Leaf Morphotype 24

c.f. *Salix lesquereuxii*

Fig. 16F

Description.— This morphotype is based on 3 incomplete specimens, which have pulvinate petioles, typically measuring 1.7 mm in width and 4.9 mm in length, and are slightly curved. The morphotype is microphyll size (1.7-1.92 cm wide and ~6.0 cm in length if complete). Laminar shape on all three specimens is elliptic and symmetrical. The base is acute and cuneate. Apices have an acute angle, but their exact shape could not be determined. Petiolar attachments are marginal. The leaf margin is entire and unlobed. Primary venation is pinnate on all specimens. Secondary venation is brochidodromous, with many alternating secondaries diverging from the primary vein at 40-35°. Vein spacing is irregular with weak intersecondaries. Tertiary veins are regular polygonal reticulate. Fourth-order venation is alternate percurrent. No fifth-order venation could be observed, but the areolation is well-developed. Fimbrial veins lie directly on the margins. Leaf texture is coreaceous with cuticle preserved.

Discussion.— This leaf morphotype is similar to what Berry (1914 and 1919) called *Salix lesquereuxii* (p. 33, pl. VII, fig. 12) from the Black Creek Formation in South Carolina, and at several localities in the Tuscaloosa Formation and Eutaw

Formation in Georgia. Berry also indicated that this plant is common in the Dakota Sandstone.

Dicotyledon Leaf Morphotype 25

Fig. 16G

Description.— This leaf morphotype is described from a single specimen, which has a petiole that is slightly swollen and straight (0.92 mm wide and 8.42 mm long). It is microphyll in size (2.4 cm long and 2.53 cm wide), trilobed, obovate, and symmetrical. Its base is obtuse ($\sim 90^\circ$), and cuneate. The apex is odd-lobe obtuse and truncate. Petiolar attachment is marginal. The leaf margin is entire and trilobed, with wide and shallow sinuses. First-order venation is primary actinodromous, with a thick midrib, one pair of exmedial veins, and a pair of fimbrial veins. No higher-order venation could be observed. Leaf texture is coreaceous with cuticle preserved.

Dicotyledon Leaf Morphotype 26

Fig. 16H

Description.— This morphotype is described from four specimens. Leaves are rounded and microphyll size (2.5 cm long and 2.7 cm wide). No petioles are preserved. Laminal shape on all specimens is elliptic and symmetrical. The base and apices are both round and obtuse. The leaf margin is entire and unlobed. Primary venation is flabellate, with ~ 13 primary veins, which are of different sizes and irregularly spaced. Secondary and tertiary venation patterns are alternate percurrent. No higher-order venation could be established. Leaf texture is charteous-coreaceous with cuticle preserved.

Dicotyledon Leaf Morphotype 27
c.f. *Eucalyptus dakotensis*
Fig. 16I

Description.— This leaf morphotype is described from four partial specimens, which only have their apices preserved. They are mesophyll-microphyll in size, averaging 2 cm in width and can be up to 11 cm long. Laminal shape is linear, oblong, and symmetrical. Apices are acute, blunt, rounded to convex. The leaf margin is entire and unlobed. The primary venation pattern is pinnate; secondary venation is semicraspedodromous. Common fine secondaries are alternating and irregularly spaced. Tertiary veins are alternating percurrent. Forth-order veins are regular polygonal reticule. Fifth-order venation is dichotomizing. Areolation is well developed on two specimens and may have dark spots with areoles (e.g., KIS-511). They have freely ending ultimate veins with two or more branches. Fimbrial veins are looped.

Discussion.— This morphotype is similar to what Lesquereux (1892) described as *Eucalyptus dakotensis* (p. 137, pl. XXXVII, figs. 14 and 19) from the Dakota Sandstone.

Dicotyledon Leaf Morphotype 28
c.f. *Andromeda novaescaesareae*
Fig. 17A

Description.— This morphotype is described from 5 partial specimens, all of which are microphyll size (typically 1.1 cm wide and ~3 cm long). The laminal shape is oblong and symmetrical-slightly asymmetrical. The base of this morphotype is cuneate, with acute angles. The apex is not well-preserved. Primary venation is pinnate. Petiolar attachments are marginal. The leaf margin is entire and unlobed. Midveins are stout with many fine secondaries that are weakly brochidodromous. Secondary veins are alternate

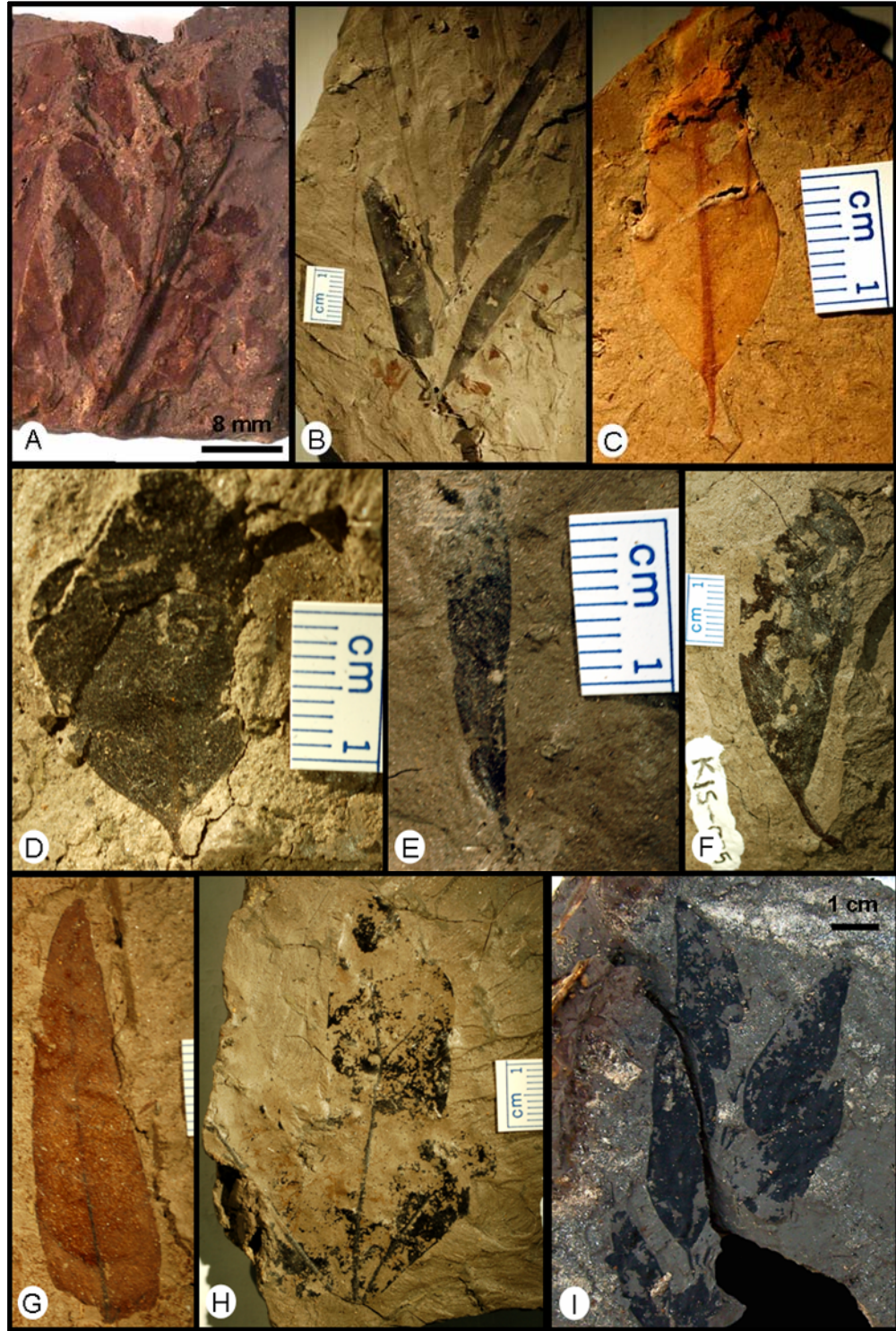


FIGURE 17—Ingersoll shale dicotyledon leaf morphotypes. (A) Morphotype 28 (KIS-006). (B) Morphotype 29 (KIS-062). (C) Morphotype 30 (KIS-275). (D) Morphotype 31 (KIS-153). (E) Morphotype 32 (KIS-205). (F) Morphotype 33 (KIS-025). (G) Morphotype 34 (KIS-072). (H) Morphotype 35 (KIS-037). (I) Morphotype 36 (KIS-082).

and uniform and diverge from the primary vein at 50°. Tertiary veins are alternate percurrent. Fimbrial veins lie ~0.01 mm inside the margin. Leaf texture is coriaceous with cuticle preserved.

Discussion.— This leaf is similar in shape and size to what Berry (1914) called *Andromeda novaecaesareae* (p. 58, pl. XIV, figs. 5 and 6) and described as common in the Middenforf Member of the Black Creek Formation in South Carolina and in the upper beds of the Raritan Formation in New Jersey, the Tuscaloosa Formation in Alabama, and in the Cusetta Sand of the Ripley Formation near Buena Vista, Georgia. He also described it as commonly occurring with *Araucaria bladenensis*.

Dicotyledon Leaf Morphotype 29

Fig. 17B

Description.— This leaf morphotype is described from one specimen, consisting of leaves articulated on a stem. It has alternate leaf attachments and one bud preserved in the upper node. Leaf organization is even-pinnately compound. Petioles are 5-6 mm long and 0.11 mm wide, narrowing toward the marginal petiolar attachment. They are microphyll size and are linear. The leaves are folded, making their symmetry hard to determine. The base of this morphotype is acute and decurrent. The apex is acute and convex/acuminate. The leaf margin is entire and unlobed. Primary venation is pinnate. Secondary venation patterns could not be determined. Leaf texture is coriaceous with cuticle preserved.

Dicotyledon Leaf Morphotype 30

Fig. 17C

Description.— This leaf morphology is described from 3 specimens. The petiole is thinner than the midrib (0.03 mm and 0.08 mm, respectively). The leaves are nanophyll

size (typically 2.7 cm long and 1.0 to 1.3 cm wide), ovate, and symmetrical. The base is acute and convex; the apex is acute and acuminate. The leaf margin is entire and unlobed. Primary venation patterns are pinnate with cladodromous secondary veins diverging from the midvein at $\sim 45^\circ$. Secondary veins are alternate and increase in number toward the apex. The tertiary veins are mixed opposite-alternate percurrent, sinuous, and obtuse to the midvein. Tertiary vein angle is uniform. No higher-order venation could be seen. Leaf texture is chartaceous with cuticle preserved.

Dicotyledon Leaf Morphotype 31

c.f. *Persoonia lesquereuxii*

Fig. 17D

Description.— This morphotype is described from 3 specimens, nanophyll in size (0.75 cm-1.25 cm wide and typically 2.2 cm long). The leaves are obovate in outline, and lamina is symmetrical. The base is acute or obtuse and narrow, becoming concavo-convex. The apex is rounded and obtuse (slightly over 90°). The leaf margin is entire and unlobed. Petiolar attachments are marginal. Primary veins are pinnate, with stout midveins. No higher-order venation could be determined. Leaf texture is coriaceous with the cuticle preserved.

Discussion.— This morphotype is similar to what Berry (1919) described as *Persoonia lesquereuxii* (pl. XIV, fig. 2) from the Tuscaloosa Formation at Shirleys Mill and Glen Allen, Fayette County, Alabama. Lesquereux (1892) also described this species from the Dakota Group of Kansas (p. 89, pl. 20, figs. 10 and 12), and Newberry (1896) referred to this species in the Amboy Clays as *Andromeda latifolia* (pl. XXXIII, fig. 9).

Dicotyledon Leaf Morphotype 32
c.f. *Dermatophyllites acutus*
Fig. 17E

Description.— This morphotype is represented by one specimen. It is nanophyll in size (2.43 cm long and 0.43 cm wide), linear, and obovate. Both the apex and base are acute; the base is decurrent. The only venation that could be observed is pinnate with a stout midvein. The leaf margin is entire and unlobed. There is a marginal petiolar attachment. Lamina shape is asymmetrical. Texture is coriaceous with cuticle preserved.

Discussion.— This leaf is similar in appearance and size to what Berry (1919) described as *Dermatophyllites acutus* (pl. XXVII, fig. 8) from the Tuscaloosa Formation, Shirleys Mill, Fayette County, Alabama. He described this species as having problematic biological affinity and only names it *Dermatophyllites* because it was the name given by the original author.

Dicotyledon Leaf Morphotype 33
c.f. *Myrica emarginata*(?)
Fig. 17F

Description.— This morphotype is described from 3 specimens. It is very similar to morphotype 17 except for a noticeable difference in size. Morphotype 33 is microphyll in size (typically 1.5 cm wide and 5.2 cm long), and obovate in outline, with asymmetrical lamina. The leaf margin is entire and unlobed. The apex is rounded and obtuse; the base is acute cuneate. The petiole is preserved on one specimen (KIS-025) and is curved, 1.3 mm wide, and 11.1 mm long. Petioles have marginal petiolar attachments. Primary venation is pinnate with ~7 pairs of alternating brachidodromous secondary veins and weak intersecondaries. Tertiary veins are alternating percurrent. Fourth-order veins are regular polygonal reticulate. Fifth-order veins are dichotomizing

and have two or more branches. Areolation of the fourth-order venation is well developed and 4- to 5-sided. Fimbrial veins are looped. Leaf texture is coriaceous with the cuticle preserved.

Discussion.— This leaf is very similar in appearance to *Myrica emarginata* from the Tuscaloosa Formation, Cottdale, Tuscaloosa County, and Shirleys Mill, Fayette County, Alabama (Berry, 1919, pl. XIII, fig. 4). It has also been reported by Newberry (1896, p. 62, pl. 41, figs. 10 and 11) and Lesquereux (1892, p. 61, pl. 41, fig. 2) from the Raritan Formation and the Dakota Sandstone, respectively.

Dicotyledon Leaf Morphotype 34
c.f. *Euginea anceps*
Fig. 17G

Description.— This leaf morphotype is described from seven specimens, two of which are articulated on a stem. Leaf attachments are alternating and oddly pinnate. Petiole base is swollen. Size is highly variable, but leaves are mainly microphyll-notophyll; most specimens are 1.63-2.21 cm wide and 9.2-12.0 cm long. Laminal shape is symmetrical, linear, and elliptical, with the widest portion in the middle. The base is acute and decurrent; the apex is acute, straight to slightly convex. Petiolar attachments are marginal. The leaf margin is entire and unlobed. Primary veins are pinnate with a stout midvein. Secondary veins are numerous, alternating, crespodromous, and increase in number toward the base. Secondary veins diverge from the midvein at 40-45°. Tertiary veins are mixed; they are both opposite and alternate percurrent, sinuous, and obtuse to midvein, decreasing in angle exmedially. Fourth-order veins are opposite percurrent. Fifth-order veins are regular pentagonal reticulate. Areolation is well-

developed and 4- to 5-sided. Marginal ultimate venation is looped. Leaf texture is thick coriaceous with the cuticle preserved.

Discussion.— This leaf is similar in shape to *Eugenia anceps* reported by Berry (1919, p. 125, pl. XXXII, figs. 3 and 5), from the McNairy Sand of the Blufftown Formation, McNairy County, Tennessee.

Dicotyledon Leaf Morphotype 35

c.f. *Ficus fontainii*

Fig. 17H

Description.— This leaf morphotype is described from one poorly preserved specimen. It is ovate, symmetrical, and of nanophyll size (7.3 cm long and 4.4 cm wide). The base is obtuse and decurrent; the apex is odd-lobed acute. It has a narrow, rounded, middle apex, and has wide complex exmedial apices. The leaf margin is entire and trilobed with shallow rounded sinuses. The midvein is stout and curves apically. Primary venation is pinnate. Secondary veins are irregularly spaced and fork from the midvein, but a category could not be determined. Leaf texture is coriaceous with some cuticle preserved.

Discussion.— This morphotype is similar in form to what Berry (1919) described as *Ficus fontainii* (p. 82, pl. XI, fig. 3) from the Tuscaloosa Formation, Cottdale, Tuscaloosa County, and Fayette County, Alabama.

Dicotyledon Leaf Morphotype 36

Fig. 17I

Description.— This morphotype is described from many specimens, two of which are articulated on branches. One of the articulated specimens also has an articulated flower. The simple leaves are alternating on the branch. Petiolar attachment is marginal;

the petiole is straight, 0.09 mm wide, and 7.3 mm long. The leaf size is microphyll-notophyll (4.41-10.33 cm long, and 1.42-2.46 cm wide. Overall shape of all specimens is ovate and their laminar shape is symmetrical. The base of this morphotype is acute and decurrent; the apex is acute and gradually narrows to a rounded tip. Primary venation patterns are pinnate. Secondary vein patterns could not be determined because they are immersed in the thick cuticle. Margins are entire and unlobed. Leaf texture is very coriaceous.

Discussion.— This morphotype is commonly found in association with dicotyledon leaf morphotype 1.

Dicotyledon Leaf Morphotype 37

Fig. 18A

Description.— This morphotype is described from 7 specimens. One specimen is articulated on the stem, with shoots at the node, and what appears to be an articulated flower. Leaves are alternately attached and are microphyll-notophyll size (6.2-14.5 cm long and 2.36-4.5 cm wide). The apex is not preserved. The leaf margin is entire and smooth. The base is round-decurrent and acute. The midvein is stout and becomes narrow distally. Primary veins are pinnate. Petiolar attachments are marginal. Petioles are 2.1 mm wide and straight; length of the petiole varies with leaf size. Secondary veins are alternate cladodromous. Tertiary veins are opposite percurrent, sinuous, and obtuse-perpendicular to the midvein. Fourth-order veins are opposite percurrent and obtuse to the midvein. No higher-order venation could be established. The marginal ultimate vein is looped. Leaf texture is coriaceous with some of the cuticle preserved.

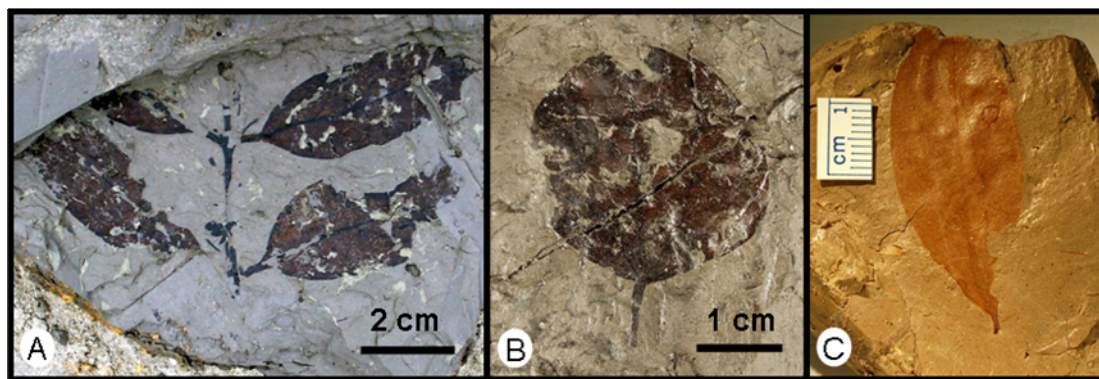


FIGURE 18—Ingersoll shale dicotyledon leaf morphotypes. (A) Morphotype 37 (KIS-156). (B) Morphotype 38 in the Columbus State University collection. (C) Morphotype 39 (KIS-046B).

Dicotyledon Leaf Morphotype 38

Fig. 18B

Description.— This morphotype is described from a single specimen. It is a round leaf, alternately articulated on a thin stem. It is of microphyll size (3.3 cm in width and length) and symmetrical. Both the apex and base are obtuse and round. The leaf margin is entire and unlobed. The petiole is 1.3 mm wide and 12.0 mm long; petiolar attachment is marginal. Primary venation is basal actinodromous. There are 7 primaries, each of which consists of one stout midvein, two pairs of exmedial veins, and one pair of fimbrial veins running along the margin. No higher-order venation could be seen. Leaf texture is coriaceous with some of the cuticle preserved.

Dicotyledon Leaf Morphotype 39

Fig. 18C

Description.— This morphotype is described from two specimens. They are nanophyll size (1.98 cm wide and 4.30 cm long), symmetrical, and elliptic. The base of morphotype is acute and decurrent; the apex is acute with a concave to rounded tip. The leaf margin is entire and unlobed. Petiolar attachment is marginal. Primary venation is pinnate. Secondary veins are brachidodromous and branch from the primary vein at 40°. Secondary veins are opposite, irregularly spaced, and increase in number basally. Tertiary veins are opposite percurrent, sinuous, and perpendicular to the midvein, increasing basally. Fourth-order veins are alternating percurrent. Leaf texture is coriaceous with some of the cuticle preserved.

CONIFER FOLIAGE MORPHOTYPES

Conifer Foliage Morphotype 1 (form genus *Brachyphyllum*) c.f. *Brachyphyllum macrocarpum*/*B. crassum*

Fig. 19A

Description.— This morphotype is described from 7 specimens that are pinnately branched, planated twigs (6-8 mm in width) with rounded apices. This morphotype has helically arranged “scale like” leaflets with broad bases, typically 3.6-5.1 mm wide and 1.6-2.5 mm long. Leaf apices are obtuse (90-100°) and straight. Leaf texture is thick coriaceous with the cuticle preserved, and it has the appearance of a succulent.

Discussion.— Most of these specimens are well-preserved, but due to the thickness of the organic remains, the surface of the fossils become highly cracked and deteriorated when dried. Because of the deterioration, leaf measurements could only be taken on two of the specimens. In one, pyrite had infilled the area between the scales preserving their dimensions (Fig. 19A). In the other, the thick organic remains were leached away, leaving behind structural details as iron stains.

These conifer shoots are similar to what Berry (1919) describes as *Brachyphyllum macrocarpum* (pl. 5, fig. 9) and what Newberry (1896) reports as *Brachyphyllum crassum* (pl. VII, figs. 1 and 7). Some of the specimens Berry described were found in the basal portions of the Eutaw Formation, east of the Chattahoochee River. These fossils are possibly of cheirolepidiaceus affinity. However, no *Classopollis* pollen has been found among the Ingersoll shale palynomorphs.

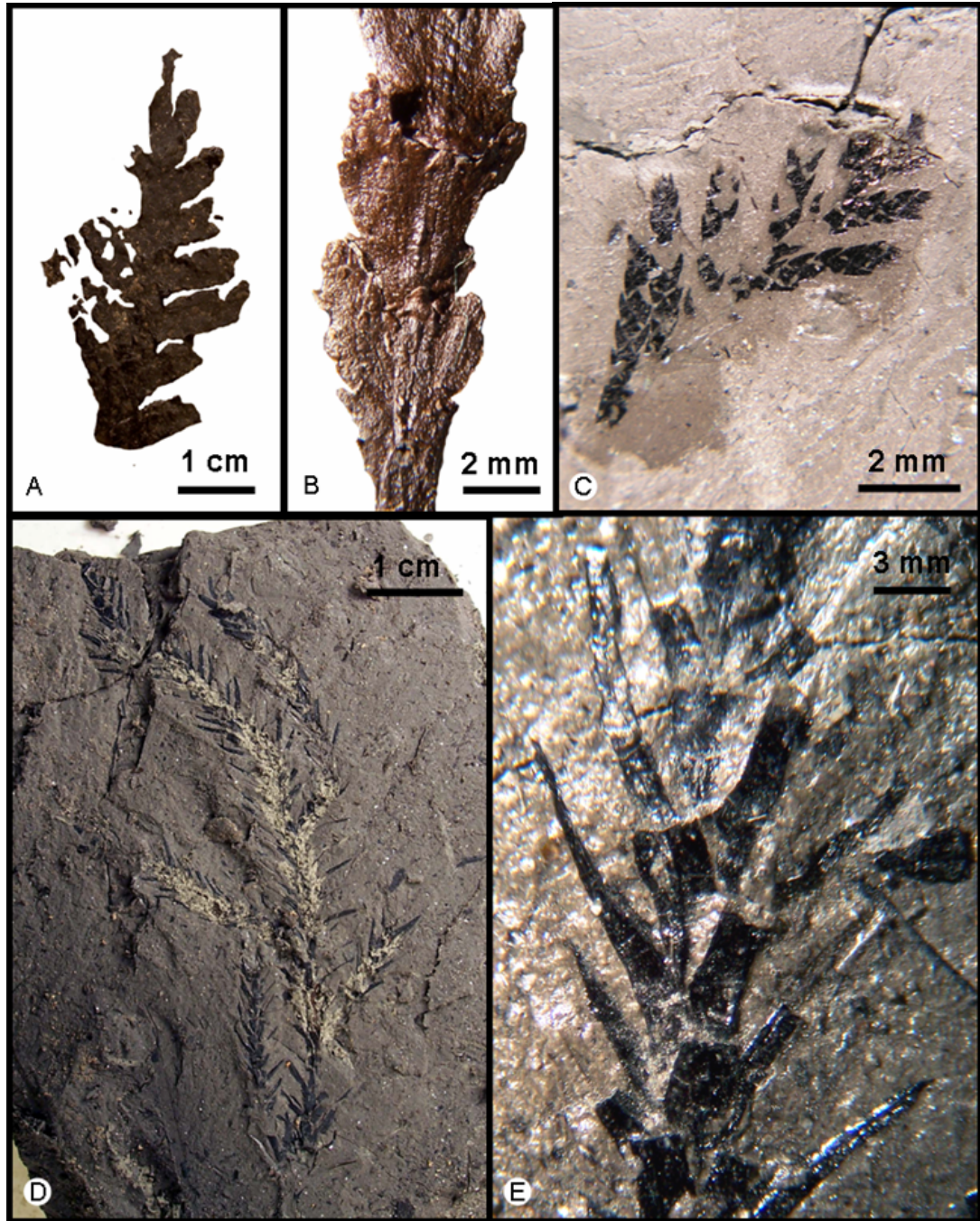


FIGURE 19—Ingersoll shale conifers. (A) Conifer foliage morphotype 1 (KIS-212). (B) Conifer foliage morphotype 2 (KIS-231). (C) Conifer foliage morphotype 3 from the Columbus State University collection. (D) Conifer foliage morphotype 4 (KIS-112A). (E) Close-up of KIS-112A showing the helically arranged, acicular leaves.

Conifer Foliage Morphotype 2 (form genus *Cupressinocladus*)
c.f. *Androvetitia elegans*
Fig. 19B

Description.— This conifer morphotype is described from 6 partial specimens that are very fern-like in appearance. Bifacial leafy twigs are arranged in an opposite, decussate manner on a prominent stem that is up to 4 cm in length. The twigs range from 4-6 mm in width. Two leaves come out from each node (opposite), and the leaf pairs are shifted 90° relative to the pair above and the pair below (decussate). One pair of leaves has reduced, blunt leaves. The other pair has multiple leaflets on the apices but becomes more elongate as the shoot matures.

Discussion.— This leaf is very similar to what Berry (1914) called *Androvetitia elegans* (pl. 18, figs. 1 and 10).

The preservation of this morphotype is very different from the preservation of other conifers in the Ingersoll shale. First, these shoot fragments are restricted to the lower, high-energy portions of the clay lens, where they are relatively common. They are probably allochthonous and do not reflect vegetation growing around the clay lens. Second, the cuticle is often brown in color, highly flexible, and easily peeled from the matrix. The cuticle is still preserved even within the leached portions of the lens.

Conifer Foliage Morphotype 3 (form genus *Cupressinocladus*)
Fig. 19C

Description.— This morphotype is described from three specimens, which can be up to 10 cm in length. The leaves are arranged in an opposite decussate manner along a wide stem (0.4 mm). Two leaves emerge from each node, opposite of each other, and the leaf pairs are shifted 90 degrees relative to the pair above and pair below (decussaate).

Nodes are ~0.8 mm apart. The leaves are typically 1.5 mm long and 0.8 mm wide, and have acute apices. The entire width of the stem and leaves is approximately 1.1 mm.

Discussion.— According to Brian Axsmith (personal communication, 2006), the only conifers that have this leaf arrangement are the Cupressaceae and Cheirolepidiaceae (non-freneloid types). However, determination of biologic affinity would require cuticular examination.

Conifer Foliage Morphotype 4 (form genus *Geinitzia*)
c.f. *Sequoia reichenbachii*
Fig. 19D

Description.— These remains are common in the Ingersoll shale and are described from 9 specimens. Shoots of the morphotype have long, needle-shaped, spiraling leaves, which are up to 7.0 mm in length and 0.4 mm in width and are not compressed. The needle-shaped leaves contract from the cushion gradually. Leaf bases extend ~2 mm down the stem. These leaves have a prominent ridge down their midline.

Discussion.— These remains are similar to *Sequoia reichenbachii* which were reported as being common in the basal Eutaw Formation in Georgia and Alabama (Berry, 1919, pl. VI, fig. 2). Herendeen et al. (1999) described similar remains from the Allon Flora of the Gaillard Formation in Georgia, and Newberry (1896) recognized this species in the Amboy Clays of New Jersey (p. 49, pl. IX, fig. 19).

These carbonized conifer remains are often found as large branches with all the leaves still attached. This indicates that they have undergone minimal transport and were probably residing near the banks of the Ingersoll shale depositor. They also are preserved in three dimensions, indicating that they may have been buried rapidly in a soupy-like substrate.

Some specimens of morphotype 3 have *in situ* amber rods within the resin ducts. This indicates that these conifers were at least one of the producers of the Ingersoll-shale amber, which will be discussed in the following chapter.

Conifer Foliage Morphotype 5 (form genus *Pagiophyllum*)
c.f. *Araucaria bladenensis*
Fig. 20A, C

Description.— This morphotype is described from many specimens. It consists of dense nanophyll-size foliage helically arranged around the branches. Leaves are ovate in outline, 0.8-2.0 cm in width, and can be over 30 cm. Leaf bases are rounded and decurrent and acute on the stem. Each leaf has a cuspidate apex. Veins are concealed by the thick cuticle and could only be observed in specimens from the leached portion of the shale. These show 17-18 thin longitudinal veins, which terminate at the leaf margin and are incurvate at the base. Leaf texture is very coriaceous.

Discussion.— These plant remains are common in the Ingersoll shale. The morphotype is similar in appearance to *Araucaria bladenensis* (Berry, 1919, pl. IX, X), which is found in the Eutaw Formation along the banks of the Chattahoochee River. This morphotype is possibly a member of the family Araucariaceae.

Conifer foliage morphotype 5 is very common in the Ingersoll shale and is always well-preserved. For example, large branches are found with all leaves still attached, so these conifers were probably living in close proximity to the depositional site.

One interesting “mystery fossil” that shares a similar morphology with these conifer remains is a large (>10 cm) circular fossil with what appear to be leaves oriented around its perimeter (Fig. 19C). The leaves share the same morphology as conifer foliage morphotype 5. In the center of this fossil are a series of thick, carbonized and pyritized

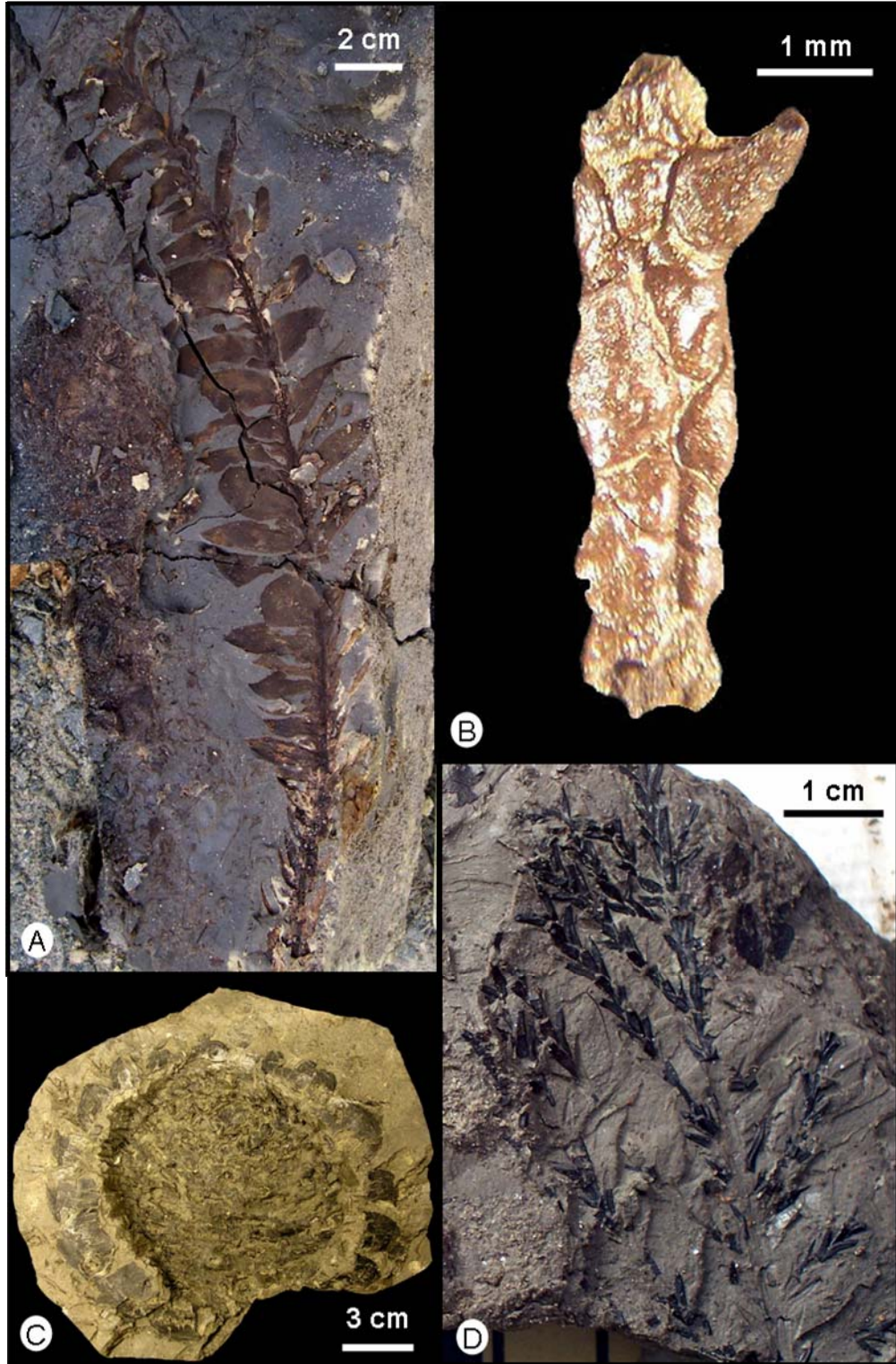


FIGURE 20—Ingersoll shale conifers. (A) Conifer foliage morphotype 5 (KIS-223). (B) Conifer foliage morphotype 7 (KIS-185). (C) Conifer foliage morphotype 5 (KIS-182). (D) Conifer foliage morphotype 6 (KIS-106).

ridges that are very similar in appearance to the “monkey puzzle bark” seen on extant species of *Araucaria*.

Conifer Foliage Morphotype 6 (form genus *Geinitzia*)
c.f. *Sequoia ambigua*
Fig. 20D

Description.— This morphotype is described from many specimens, some of which are over 30 cm long. They are composed of shoots with relatively short, sickle-shaped, spiraling leaves. Leaves average 4.4 mm in length and 0.6 mm in width, are uncompressed, and have a prominent ridge down their midline. The leaves gradually taper from the cushion into sharp apices. Leaf bases extend down the stem.

One specimen has articulated cones on the tips of the branches, preserved as external molds. Cones average 6.0 mm in length and 4.0 mm in width. They have very few, short scales. Two pollen grains were found in one specimen, but the pollen has yet to be analyzed.

Discussion.— These conifer remains are similar in morphology to *Sequoia ambigua* reported by Berry (1919, pl. VI, figs. 3 and 4) from the Tuscaloosa and Eutaw Formations in Alabama. They are also very similar in morphology to conifer morphotype 4, described above.

This morphotype is very common in the Ingersoll shale, and specimens are always well preserved with the exception of those recovered from zone 1. Large branches are found with all leaves still attached, so these conifers were probably living in close proximity to the depositional site. They, like conifer morphotype 4, are often preserved in three dimensions, which suggest that they were deposited rapidly in a soupy substrate.

**Conifer Foliage Morphotype 7 (form genus *Brachyphllum*)
c.f. *Widdringtonites subtilis*/*W. reichii***

Fig. 20B

Description.— This morphotype is described from four specimens, which measure up to 8.0 cm in length and 1.7 mm in width. Remains of this conifer consist of slender branches of appressed, scale-like leaves that are irregularly spiraling up a stem, which typically is 1.0 mm wide. Leaves are typically 1.3 mm in width and 2.0 mm in length and are flattened to the stem.

Discussion.— This morphotype is similar to what Berry (1919) describes as *Widdringtonites subtilis* (pl. VIII, fig. 3). Newberry (1896) also reported similar remains from the Amboy Clays and referred to them as *Widdringtonites reichii* (p. 57, pl. VIII, figs. 1 and 5).

Some of these conifers are preserved in three-dimensions via pyritization. This shows that they had undergone early authigenic mineralization prior to any significant compaction. Like conifer foliage morphotype 2, these conifer remains are easily peeled from the matrix and the cuticle is brown in color.

CONIFER REPRODUCTIVE ORGANS

Cone Morphotype 1

Fig. 21A

Description.— This cone type is described from one round, poorly preserved cone that is ~1.2 cm wide. The square-to-hexagonal megasporophylls are ~2 mm in diameter.

Discussion.— This is very similar in appearance to an extant cypress female cone, but nothing resembling it could be found in the literature examined.

Cone Morphotype 2
Fig. 21B

Description.— This morphotype is based on many specimens that appear to be small pollen cones. They are ~0.6 mm wide and 12.0 mm long, obovate in shape, and composed of helically arranged, overlapping cone scales. Individual scales are 1.3 mm wide and 1.5 mm long, and have rounded bases and apices.

Discussion.— These cones are common in the Ingersoll shale. They have been found articulated on conifer foliage morphotype 6, (*Sequoia ambigua* of Berry, 1919).

Cone Morphotype 3
c.f. *Strobilites anceps*
Fig. 21C

Description.— This morphotype is rare in the Ingersoll shale and is only described from three specimens of similar morphology. These cones are equidimensional, large (2.0-2.7 cm in length and width), and have spirally arranged, overlapping, obovate scales. The scales are ~5.0 mm wide and 3.5 mm long and have a longitudinal striation pattern.

Discussion.— This cone morphotype bears a strong morphological similarity to conifer foliage morphotype 1 (form genus *Brachyphyllum*) such as the scale width being greater than its height. Two similar cones were found in the Black Creek Formation, South Carolina (Berry, 1914). He was uncertain as to the true biologic affinity of these cones, so he referred them to the form genus *Strobilites*.

Cone Morphotype 4
Fig. 21D

Description.— This morphotype is rare in the Ingersoll shale; it is described from three specimens of similar morphology. They are nearly spherical cones, approximately

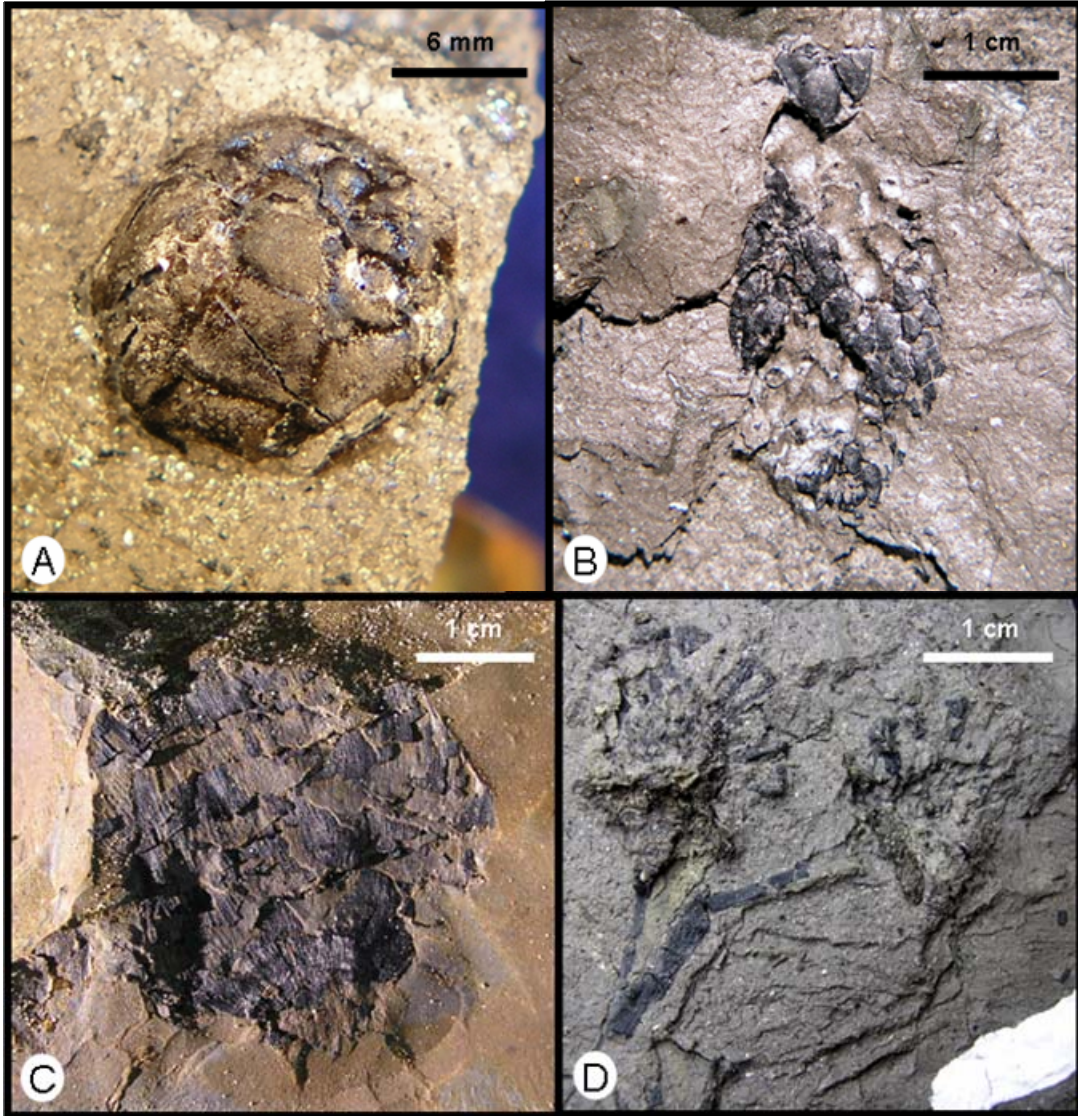


FIGURE 21—Cones (A) Taxodiaceous cone (cone morphotype 1) from the Columbus State University collection. (B) Cone morphotype 2 from the Columbus State University Collection. (C) Cone morphotype 3 (KIS-225B). (D) Cone morphotype 4 (KIS-282B).

~2.0 cm in width and length. Cones have a wedge-shaped, bract-like structure, which is 1.6 cm wide and 1.5 cm tall. The club-shaped scales are ~0.42 mm long, width expands from 0.6 mm where attached to the cone axis but expand to a maximum of 2.7 mm. Near the axis, the scales are spaced ~0.7 mm apart but contact each other distally.

Discussion.— Preservation quality within a single cone is variable. Most are carbonized, but the bract/scale complex is lignified and pyritized. Cones are articulated on the stem but are not associated with foliage.

Cone Morphotype 5
c.f. *Araucaria*
Fig. 22A-D

Description.— This morphotype is described from a single specimen found in the lower oxidized portions of the shale lens. This specimen is ~13 cm long and 2.6 cm wide and is hooked-shaped, curving more than 110°. The attachment site is very thick. The axis is composed of several horizontal segments, each with longitudinal striations. Small leaflets extend distally from the cone axis. The leaflets are very similar in appearance to conifer foliage morphotype 5.

Discussion.— These cones are morphologically similar to the male pollen cones seen in the extant species of *Araucaria* (Brian Axsmith, personal communication, 2007).

FLOWERS, SEEDS, AND FRUITS

Flower Morphotype 1
Fig. 23A

Description.— This morphotype is described from one large specimen that is preserved longitudinally. It is 1.1 cm wide and 4.9 cm long. The calyx extends past the stamen ~2.4

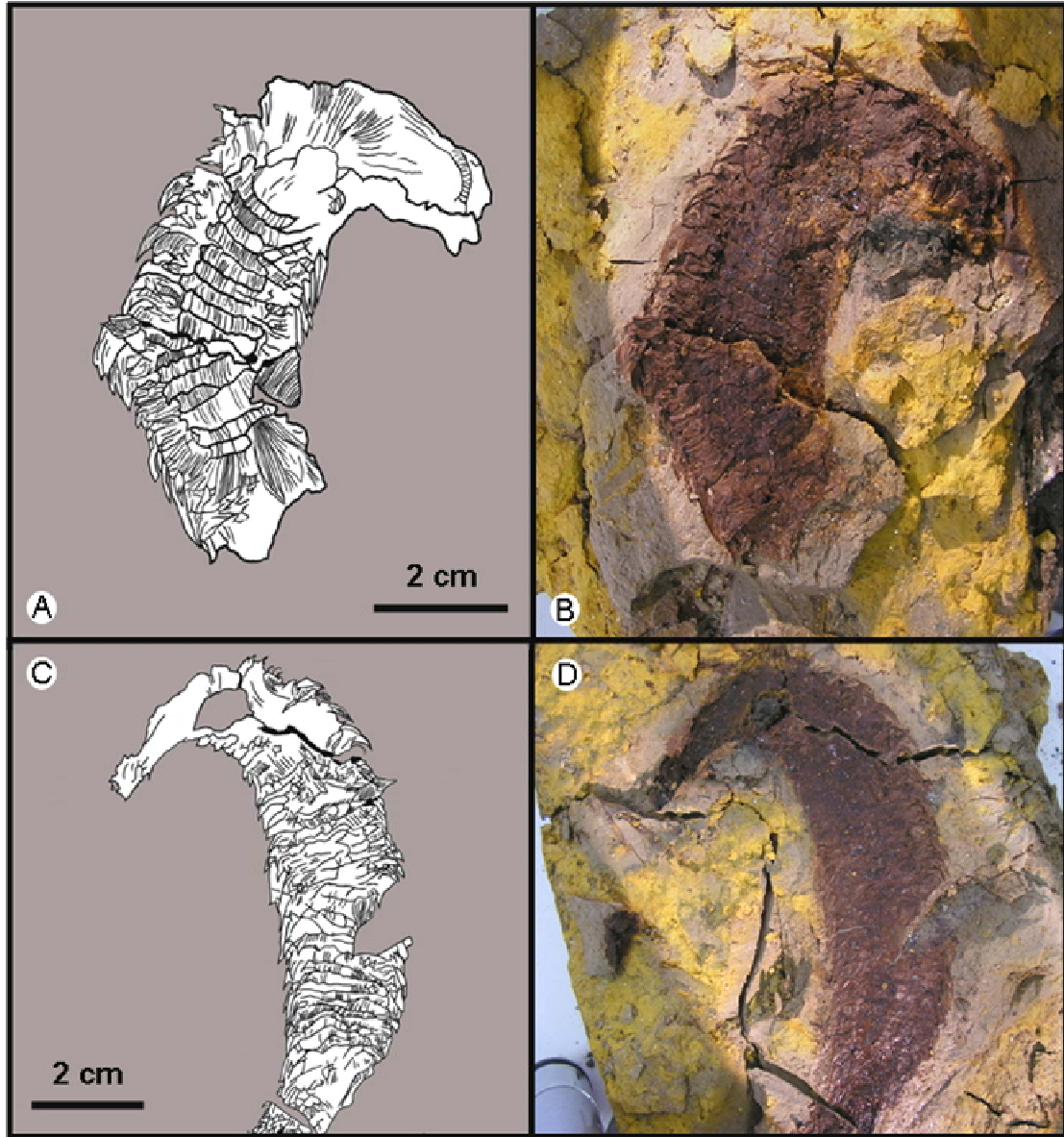


FIGURE 22—Cone morphotype 5 (KIS-225A and 225B), part and counterpart.

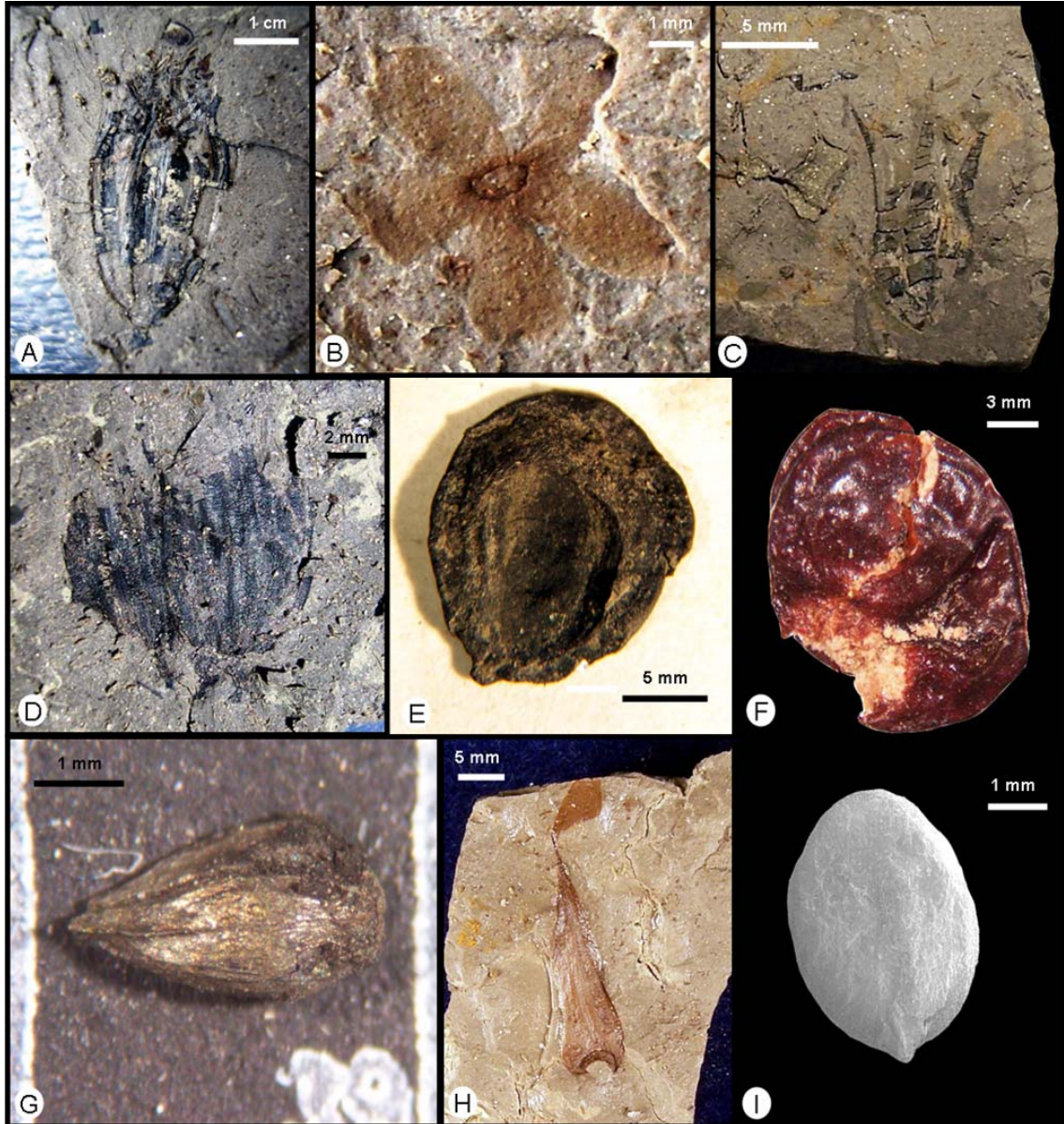


FIGURE 23—Ingersoll shale angiosperm reproductive organs. (A) Flower morphotype 1 (KIS-163). (B) Flower morphotype 2 (KIS-513A). (C) Flower morphotype 3 (KIS-165). (D) Flower morphotype 4 (KIS-163). (E) Angiosperm fruit. (F) Seed/fruit coating. (G) Miscellaneous seed type 1 (KIS-184). (H) Fruit wing (KIS-105). (I) SEM image of miscellaneous seed type 2.

cm. Highly degraded petals could be observed, but no accurate measurement could be taken. Numerous filaments are present, but no distinct anthers were preserved. No stigma could be observed.

Discussion.— This specimen is the only one of its kind to be described from the Ingersoll shale lens. This type of flower was not described in any of the monographic works that were used as guides for this thesis.

Flower Morphotype 2
c.f. *Calycites parvus* and *Calycites diospyriformis*
Fig 23B

Description.— This morphotype is described from 8 specimens. All are very small (6-10 mm in diameter), radially symmetrical, floral organs (possibly the calyx) typically with 5 petals. A carbonized disk is found in the center of some specimens, but no other floral organs are preserved. Other specimens of this morphotype lack this structure.

Discussion.— These flower-like organs are more common than any other floral organs in the Ingersoll shale. They share a similar morphologies to what Newberry (1896) described as *Calycites parvus* and *Calycites diospyriformis* (pl. XLVI, fig. 10) from the South Amboy Fire Clay, New Jersey.

Flower Morphotype 3
Fig. 23C

Description.— This morphotype is described from one specimen, preserved longitudinally. The specimen is 15.5 mm long and ~7.0 mm wide. It consists of 4 very thick, basally fused petals, which are 1.7 mm wide and have sharp-pointed apices. No other flower parts could be observed.

Discussion.— This specimen is the only one of its kind to be described from the Ingersoll shale. This type of flower was not described in any of the monographic works that were used as guides for this thesis.

Flower Morphotype 4

Fig. 23D

Description.— This description is based on a single specimen, 1.37 cm wide and 1.0 cm tall, which appears to be a composite flower. It is preserved longitudinally, rounded at the base, and truncate at the apex. It has ~17 strap-like carpels, positioned around a conical receptacle. Each of these are ~0.46 mm wide and partitioned horizontally. Along each horizontal section there are numerous appendages 0.45 mm long, branching from both sides of the carpels and are opposite to one another.

Discussion.— Identification of this specimen as a floral organ could not be confirmed. However, it is similar to what Newberry (1896) describes as *Palaeantus problematicus* (p. 12, pl. XXXV, figs. 1-9) from the Amboy Clays. It also possible that this specimen is the longitudinal section of a multicarpellate fruit similar to *Protomonimia kasai-nakajhongii* from the Late Cretaceous deposits of Japan (Friis et al., 2006). These fruits have 55 sessile carpels around a concave receptacle, with each carpel having many seeds. This could account for the appendages that are observed on both sides of the carpels.

Fruit/Seed Wing

Fig. 23H

Description.— Only one of these fossils were found in the deposit (zone 1). It is a winged-appendage that is delicately striated longitudinally. It is 2.68 cm in length and

8.56 mm in width. The base is lobate; the apex is missing. The circular disk at the attachment site at the base is ~2.5 mm in width.

Discussion.— This morphotype is similar to one of the winged-appendages that Newberry (1896) described as *Tricalycites papyraceus* (pl. XLVI, figs. 30-38) from the South Amboy Clay, New Jersey. However, a major difference is that *T. papyraceus* has 3 winged appendages surrounding the fruit/seed. Given the shape of the attachment site at the base of the Ingersoll shale fossil, it appears that there would have been room for only two of such appendages.

Fruit

Fig. 23E

Description.— This fruit is described from many specimens, which are commonly found in zone 5 of the clay lens. They are oblong, drupe-like fruit bodies that vary in size, but are typically 8.0 mm in width and 10 mm in length, and tend to split longitudinally into two parts. Internally there is a cavity, but it has yet to be determined how many seeds there are per locule.

Discussion.— These fruits are often carbonized and preserved in three-dimensions. This implies that their shape retention was not due to authigenic mineralization, but rather rapid burial in a soupy substrate.

Seed/Fruit Coating

Fig. 23F

Description.— This description is based on many specimens that vary in size. Some are 4 mm in length and 3 mm in width, whereas others are up to 1.5 cm in length and 1.2 cm in width. They are nearly spherical and are usually preserved in three dimensions. They are remarkably flexible. They are orange in color, somewhat

translucent, and have a fibrous texture. In some specimens microfibers are exfoliating from the surface. These fossils commonly contain pyrite nodules that are interpreted to be the internal, soft, fleshy fruit that has undergone authigenic mineralization.

Discussion.— The Ingersoll shale seed/fruit coatings are similar to what Grimaldi (2000a) describes from the Raritan Formation, New Jersey. Due to their variations in size, it is possible that these remains represent several types of fruit.

These remains are common in zone 5 of the Ingersoll shale lens. They are easily recognizable on the bedding planes covered by macerated plant debris.

Miscellaneous Seed Morphotype 1

Fig. 23G

Description.— This seed type description is based on a single, pyritized specimen, which is preserved in three dimensions and has remnants of carbon intermittently preserved around it. It is ovate in shape with one broadly rounded end and one acute end and is ~3.8 mm in length and 2 mm in width. It is finely striated longitudinally. A prominent ridge lies between each pair of major grooves. One end is broadly rounded and the other is acute.

Discussion.— The biologic affinity for this seed type is unknown. In general, seeds are uncommon in the Ingersoll shale. They are restricted to the high-energy portions of the clay lens (zone 5), from which they are removed with the seizing technique mentioned above.

Miscellaneous Seed Morphotype 2

Fig. 231

Description.— This description is based on a single specimen. It is a completely pyritized, flat, oblong seed, that is 4.5 mm in length, and 3.0 mm in width. It is broadly rounded on both ends. The surface is smooth.

Discussion.— The biologic affinity for this seed type is unknown. The seed was found using the seizing method in a bulk sample from zone 5 of the clay lens.

ROOTS

Fig. 24

Description.— Only two root specimens were found during the excavation. One (KIS- 516) is a very small, partial specimen, which is highly degraded. The other, KIS- 517A, was found in the leached portion of the shale lens and is only preserved as an iron stain (Fig. 24). The later specimen is 4 cm long and 2.4 mm wide with clusters of oblong nodules, approximately 5 mm long and 1.2 mm in width.

Discussion.— These preserved roots are found on bedding planes and thus do not cut through the lamina. They were found near the inferred cut bank. This suggests that the roots were not growing *in situ* but were washed into the depositional site after erosion of the soil directly adjacent to the tidal channel.



FIGURE 24—Rare Ingersoll shale roots (KIS-517A). Note that they are not cutting through lamina.

MODES OF PRESERVATION OBSERVED IN THE INGERSOLL FLORA

Floral remains from the Ingersoll shale are typically well-preserved and show a variety of preservational modes. Processes of fossilization include lignification, coalification, carbonization, compression or “mummification”, pyritization, and organic/iron staining and impression. The quality of preservation exhibited on the Ingersoll flora is not only dependent on the mode of preservation but also on the original composition of the plant organ and where it was deposited in the clay lens.

Lignification, Coalification, and Carbonization

Lignification and coalification generally occurs in floral remains that had a relatively high lignin content in life; these include wood fragments, conifer foliage stems, fruits, cones, and cone scales. Wood fragments found within the clay lens are brown (lignified) or black (coalified) or can show both modes of preservation within the same specimen. Lignification and coalification is common in the higher-energy stratigraphic zones (zones 2 and 3, Fig. 6) where in larger clasts of organic matter are concentrated. However, these preservational modes are represented throughout the entire thickness of the lens with the exception of zone 1.

The distinction between carbonized and coalified remains is an arbitrary division based on the thickness of the plant. Thus, carbonization often occurs within the parenchyma tissues of ferns, monocotyledon and dicotyledon leaves. This type of preservation is also seen in the Ingersoll flowers.

Compression

Leaf compressions are characterized by the preservation of epidermal tissue (cuticle), which is composed of the waxy substance cutin, and/or mummified parenchyma

tissue. This mode of preservation results in the highest quality: fine structural details, such as higher-order venation patterns, cell walls, and stomata are preserved (Fig. 25A, C and 26B). In some cases, leaf compressions are easily peeled from the matrix, which permits examination by transmitted light microscopy. Microscopic examination revealed intact cell walls, void cells, and the presence of stomata (Fig. 25E). Structural details (e.g., venation patterns) that are usually preserved within these compressions are commonly obscured by carbonized, black parenchyma tissue. The fruit coatings also appear to be compressions in that there is no evident carbonization or pyritization within these fossil remains. Compressions are found throughout the entire thickness of the clay lens with the exception of zone 1.

Pyritization

To one degree or another, pyrite has been precipitated in all floral remains except fruit coatings and leaf cuticle. Pyrite appears to be locally precipitated and is commonly associated with carbonized and coalified remains. One example of the apparent randomness of pyritization within the Ingersoll shale flora is that on the same bedding plane, within the same morphotype, one leaf may be completely pyritized, while an adjacent leaf will be mummified or carbonized with little or no pyritization. This process is not completely understood, but it is possible that such random pyritization is dependent on the availability plant-matter nucleation sites, such as indicated by actualistic experiments (Brock et al., 2006). In the Ingersoll shale, pyritization apparently occurred vary rapidly within the soft pith of some conifers and in the void spaces within wood fragments and seeds (Fig. 25B). The three-dimensional preservation of these plant remains is caused by rapid growth of pyrite within cellular cavities prior to any

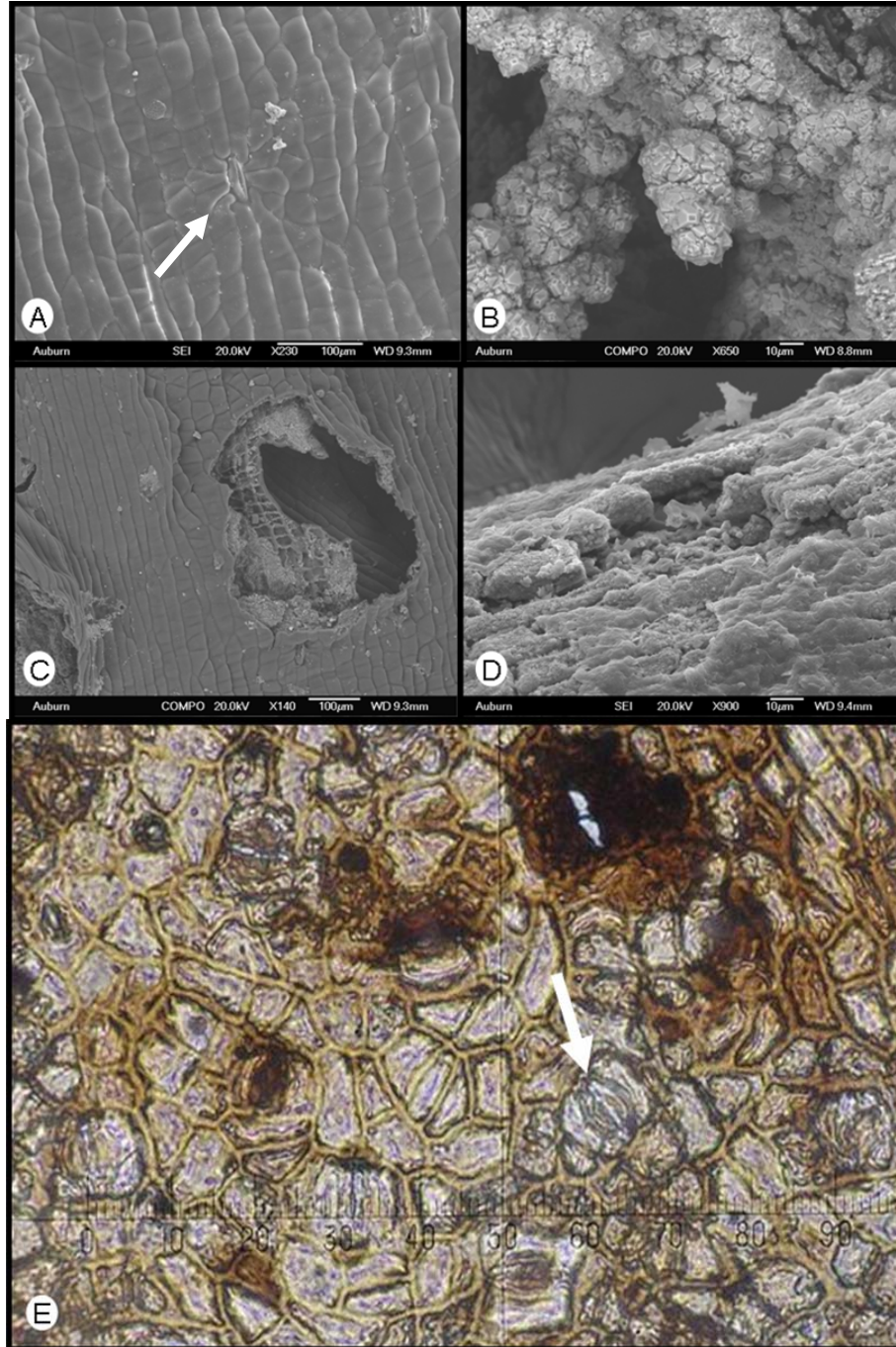


FIGURE 25—SEM images of leaf cuticle and wood, and light microscopy of leaf cuticle. (A) SEM image of angiosperm leaf cuticle showing detailed preservation. Note the preserved stomata and guard cells (arrow). (B) SEM image of miscellaneous seed type 1, showing completely pyritized organic matter. (C) SEM image of leaf cuticle showing a layer of original cuticle and internal structure (note the void space and the pyritized cell walls). (D) Lignitized remains of wood. (E) Translucent leaf cuticle under binocular microscope; note empty cell and the preservation of stomata (arrow).

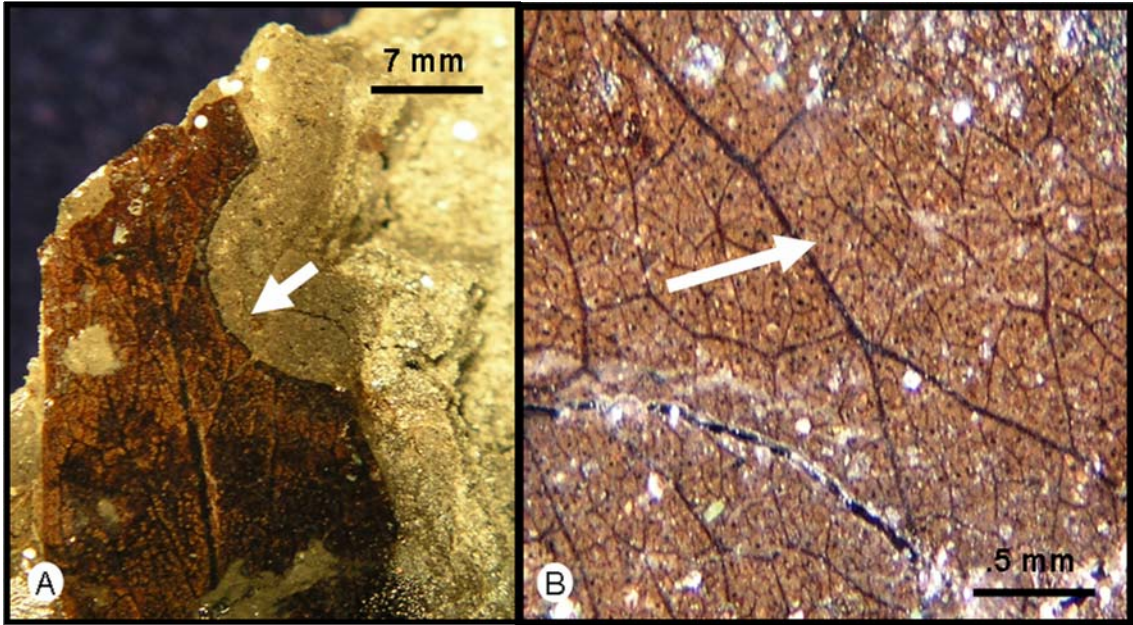


FIGURE 26—Detailed photographs of mummified fossil leaves. (A) Leaf showing insect herbivory and subsequent reactivation tissue. (B) Brown leaf cuticle showing venation patterns and stomatal preservation (brown dots).

significant compaction. Pyritization is common in zones 2 through 6 but is dominate in zone 2, where large pyrite nodules are common.

Iron/Organic Stains and Impressions

Floral remains from the oxidized/leached zone 1 are preserved as organic and/or iron stains. Most, if not all, of the original organic carbon has apparently been leached away by groundwater (Bingham, 2007), leaving an iron stain and impression. Some of these impressions preserve exceptional details, including higher-order venation patterns.

INTERPRETATION AND DISCUSSION

Floral Assemblages

Plant macrofossil assemblages are different from most animal assemblages because of the timing of disarticulation of different plant organs (Gastaldo, 1986). For example, during the life cycle of a plant there is a continual production of many different plant organs, such as leaves, stems, flowers and fruits, while other organs such as the trunk of a tree are only produced once during the life of the plant. As a whole, plant fossil assemblages commonly are the result of a mixture of plants growing both within a basin and plant fossils that have been transported into the basin.

The floral remains found in the Ingersoll clay lens represent a combination of plants living close to the depositional site - the parautochthonous assemblage (see Gastaldo, 1992) - and plant remains that were transported to the site from some distance away with some reworking (the allochthonous assemblage). The parautochthonous assemblage in the Ingersoll shale is represented by the whole dicotyledonous and monocotyledonous leaf specimens, three-dimensional conifer foliage with attached

leaflets, delicate flowers, and whole cones. The allochthonous assemblage is represented by macerated plant debris and highly durable plant organs such as seeds and disarticulated cone scales. The parautochthonous assemblage is found throughout the entire thickness of the clay lens, whereas autochthonous assemblages are found only on thin bedding planes in zone 5 (see Chapter 7) and on other bedding planes that are intermittently dispersed vertically throughout the clay lens.

Environment and History of Deposition

As discussed above (Chapter 7), the depositional environment of the Ingersoll shale was interpreted by Bingham (2007) as being a restricted tidal channel. There are several lines of evidence to suggest that the parautochthonous floral assemblage found in this channel deposit is a true representation of the nearby vegetation at the time of deposition. In the fossil record, plant assemblages with intact whole leaves and articulated leaves on stems represent plants that were growing in close proximity to the depositional site; they reflect local vegetation and syndepositional deposition with high sedimentary rates (Spicer and Greer, 1986; Greenwood, 1991; Ferguson, 2005). In addition, studies of modern analogs indicate that concentration of leaves in general only reflect local plant communities (Greenwood, 1991). In particular, vegetation in a disturbed habitat (e.g., stream-side vegetation) has the best chance of entering the fossil record because organs from these species fall directly into the depositional site and do not generally reflect species that were growing at a distance from the water's edge (Spicer and Greer, 1986).

It is also possible that some of the well-preserved plant remains in the deposit reflect vegetation that was not growing directly by the stream but rather were windblown

a limited distance from their source to the depositional site. Studies have shown that the lateral distribution of a plant organ depends on the height of the source plant (Spicer and Greer, 1986; Ferguson, 2005). In general, windblown leaves will travel laterally a distance approximately equal to the height of the tree (Ferguson, 1985). However, other factors (e.g., fall velocity in relation to leaf density and canopy height in relation to wind speeds) need to be considered.

The fall velocity of leaves is dependent on their density. For example, light leaves from deciduous trees become widely dispersed, while thicker, heavier leaves of evergreens and compound leaves fall near to the source plant (Spicer, 1989, Greenwood, 1991; Ferguson, 2005). Furthermore, leaves high in the canopy are exposed to higher wind speeds and can be dispersed further than leaves growing closer to the forest floor; thus, they have a better chance of entering a stream depositional system (Spicer and Greer, 1986). Most of the Ingersoll shale leaves are coriaceous, thus heavy evergreens, and were probably not transported very far by the wind. However, some of the lighter, chartaceous leaves were potentially high-canopy leaves, and may have been blown further from their source plant. This could possibly explain why we see a high diversity but low abundance of Ingersoll shale ferns. Ferns typically grow near the forest floor, limiting the distance that they can be transported.

During senescence, a leaf will become lighter and can be blown farther (Ferguson, 2005). However, when most leaves dry out on the source plant or on the forest floor, they roll up. If they do make it to the depositional site, they do not unroll once they are rehydrated: rather this curled state is fixed by rapid diagenesis (Ferguson, 2005). The Ingersoll shale leaves show no signs of curling prior to deposition, which indicates they

did not dry on the source plant or the forest floor and leaf litter. Furthermore, leaves that land on the forest floor usually get trapped by the surrounding plant community, limiting their mobility and their preservation potential (Ferguson, 2005).

Branches traumatically removed during high-energy events have a high potential to remain articulated because the leaves/leaflets may still be firmly attached when the branch is removed from the source plant (Ferguson, 2005). Traumatically removed flora within the Ingersoll shale can be demonstrated by the presence of long conifer branches with intact leaflets, and angiosperm stems with articulated leaves and flowers.

Once the plant organ enters the water column, the distance it can travel in a stream is dependent on its flotation time and the velocity of the current (Greenwood, 1991). Flotation times are determined by the rate at which the plant becomes waterlogged (Greenwood, 1991; Ferguson, 2005). Waterlogging begins as soon as the plant organ enters the water (Spicer and Greer, 1986). Cuticle thickness, stomatal density and size, leaf damage, and water chemistry and temperature all play a role in the process of waterlogging (Greenwood, 1991).

In general, water flow macerates plant remains (Ferguson, 2005). Once a fossil leaf is mechanically degraded in water, it will have angular tears and breaks along major veins (Spicer and Greer, 1986). Leaf fossils that have these tears are considered to have been in the water for some time prior to burial, and were probably transported under high energy (Spicer and Greer, 1986). Furthermore, such fragmentation indicates that transport was largely in the bedload (Spicer and Greer, 1986). In the Ingersoll shale, these descriptions apply to the macerated leaf fragments from zone 2 and 3 and the two subzones in zone 5 of the clay lens.

The chance of flora becoming fossilized is increased with high sedimentary rates (Gastaldo, 1986). Based on tidal laminate and textural data, Bingham (2007) interprets the depositional rates of the Ingersoll shale to have been as high as 77 cm per year. These extremely high sedimentation rates are not uncommon in deltaic settings. Plant fossils preserved as compressions can either be mummified remains or cuticular remains, and usually reflect high sedimentation rates (Gastaldo, 1986). This has been observed in modern-abandoned channels in Australia, which contain mummified leaves, carbonized plant remains, and three-dimensional preservation (Greenwood, 1991).

Further evidence to support high sedimentation rates is the general lack of trace fossils in the Ingersoll shale and the nature of traces on plant material. Plant traces indicate low residence time at the sediment-water interface. Decay by microbes will generally produce leaf skeletons (e.g., venation), and invertebrates will typically leave holes in the leaf (Spicer and Greer, 1986). Such post-mortem traces are not represented on the Ingersoll shale flora. This suggests that the plant remains were rapidly buried prior to being consumed or distorted by scavengers or microbes. The large amount of sediment at the channel floor as indicated by the high clay content of the unit would have slowed the decay process by inhibiting scavenging by invertebrates (Ferguson, 2005). The small amount of damage from invertebrates (marginal feeding) that is observed within the Ingersoll flora is also associated subsequent reactivation tissue, represented by the dark fossilized tissue (see Fig. 24A). This indicates that the leaf had healed while it was still attached to the parent plant rather than being damaged after detachment.

Foliar Physiognomy

In order to do a foliar physiognomy study on any floral assemblage, in particular leaf-margin analysis, the assemblage has to represent climax vegetation growing in an area during the time of deposition (Wolfe and Upchurch, 1987). Assemblages from channel deposits yield the least reliable mean annual temperatures because of the disruption caused by cutbank erosion and overbank flooding. This is reflected by disturbed floral succession, as indicated by a high number of toothed species (Wolfe and Upchurch, 1987). Overbank deposits yield the most reliable temperature estimates because they are undisturbed. Unfortunately, the Ingersoll flora represents vegetation from a disturbed habitat (streamside) thus making any interpretation of mean annual temperatures unreliable.

CLOSING REMARKS

The Ingersoll shale flora is very diverse and exceptionally well preserved. This study provides a detailed morphologic description of the Ingersoll flora and their preservational modes. However, a detailed taxonomic analysis on the Ingersoll flora is still needed. Due to the large amount of cuticular preservation of fossil leaves and articulated reproductive organs, future research on the Ingersoll flora may reveal species that have not been previously described or may provide more details on previously described taxa.

CHAPTER 9: AMBER

INTRODUCTION

Isolated amber clasts are common in the lowermost portions of the Ingersoll shale (zone 2) where sand and macerated plant debris are most abundant. Amber concentrations are as high as 362 g/m³ of sediment within this zone. Amber occurs as small (1 to 15 mm), highly fractile, light yellow to light red chips, drops, and rods. Biologic inclusions are common and dominated by plant debris. However, insect fecal pellets, well-preserved fungal mycelia, mites, a scale insect with well-developed legs and antennae, an araneoid spider and associated web, and various insect appendages also occur within the amber clasts.

Weakly compacted coniferous plant parts that contain *in situ* amber rods are also found within the clay lens. Amber-bearing plant parts include lignitized stems and cone scales, most of which appear to be linked to the family Cupressaceae.

PREVIOUS WORK

Amber is one of the best decay-inhibitory media known (Allison, 1988a; Poinar, 1993; Alonso et al., 2000). Amber preserves fossils in three dimensions and their microscopic anatomical details. It can preserve original color and has been shown to preserve labile tissues such as muscles (Henwood, 1992). Amber can preserve trace

fossils such as cocoons, spider webs, domiciles, and excretory products, and may preserve signs of predation on the insects trapped in the fresh resin (Poinar, 1998). The excellent preservation provided by amber facilitates comparison of extinct species with their extant relatives (Poinar, 1993). Paleobotanical inclusions have given scientists rare information on Cretaceous amber producers, as well as preserving spectacular rare fossil flowers, leaves, spores, and pollen (Alonso et al., 2000; Grimaldi et al., 2002). It appears that amber inclusions are diagenetically altered by the polymerization of cuticular waxes and internal body lipids, even altering tissues that are not directly in contact with the amber matrix (Stankiewicz et al., 1998).

Despite the exceptional preservation of biologic inclusions entombed in amber, there are limitations. Amber is found all over the world, but most deposits are often small and rarely contain amber with biologic inclusions (Ross, 1997). A preservational bias exists in the size of an organism that can be preserved in amber; for instance, large insects that become trapped in resin can struggle free, whereas smaller insects remain. This bias can limit the majority of inclusions to just a few millimeters in size (Ross, 1997).

Amber with biologic inclusions does not become abundant in the fossil record until the Early Cretaceous (Gomez et al., 2002), but several major deposits have been preserved in Cretaceous and later deposits. Lebanese amber (Barremian-Aptian) is currently considered to be the oldest amber containing biologic inclusions (Poinar and Milki, 2001). Other Cretaceous deposits that are prolific in producing fossil-bearing amber are located in the Campanian of western Canada (McAlpine and Martin, 1969), Aptian and Albian rocks of western France and northern Spain (Alonso et al., 2000;

Néradeau et al., 2003), Turonian deposits in central New Jersey (Grimaldi et al., 2000a), Turonian and Cenomanian rocks in Myanmar (Grimaldi et al., 2002), and Albian and Santonian deposits in Siberia (Zherikhin and Eskov, 1999). Many of these deposits have produced the earliest occurrences of arthropod taxa, such as the oldest bee, which was discovered in the Turonian deposits of New Jersey (Michener and Grimaldi, 1985), and the oldest ant from the Aptian deposits of western France (Nel et al., 2004).

Amber is formed by the polymerization of resins, which are produced by plants for a variety of reasons. Resin excretion may serve as a defense against herbivores, insects, and fungi, or as a consequence of physical damage to the plant. Resins also can be generated to store unwanted byproducts of growth and cellular metabolism, as a protective barrier to reduce temperatures and decrease water loss, or to attract insects for pollenization (Martínez-Delclòs et al., 2004). Resins are composed of terpenoid and phenolic compounds that are secreted by a plant's parenchyma (storage) cells and are exuded through vesicles in the plant stem, bark, leaves, and cones (Ross, 1997; Martínez-Delclòs et al., 2004). Amber clast shape is usually determined by the excretion site within the plant (Alonso et al., 2000). As examples, stalactites, rivulet pieces, and tear-shaped drops form from aerially exposed resin on branches (Martínez-Delclòs et al., 2004), while lenses and rods form within plant vessels. Since many insects and other biologic inclusions found in amber are not living within the plant, resins that are aerially exposed are more likely to trap biologic inclusions for fossilization (Ross, 1997). During polymerization, residual non-volatile terpenoids remain after volatile terpenoids are evaporated by exposure to light and air (Martínez-Delclòs et al., 2004). Amber that is

intensely polymerized is usually more brittle and also considered to be mature (Alonso et al., 2000).

Identification of the source plant of amber is often difficult because of conflicting results between foliage associated with the amber-bearing deposits versus the chemical composition of the amber in relation to resins produced by extant species (Alonso et al., 2000; Grimaldi et al., 2000a; Grimaldi et al., 2002; Perrichot, 2004). The chemical composition of most Mesozoic amber suggests an araucariacean affinity (Martínez-Delclòs et al., 2004), because it is chemically similar to modern amber producer *Agnathis* (Alonso et al., 2000). Based on associated plant fossils from significant Cretaceous amber deposits, botanical affinities have been attributed to Pinaceae (Grimaldi et al. 2000a), Araucaraceae (Grimaldi et al., 2000b, Perrichot, 2004), Cupressaceae (Grimaldi et al., 2002), Cheirolepidaceae (Gomez et al., 2002), and Taxodiaceae (David Grimaldi, personal communication, 2006). However, some amber has been attributed to the dicotyledonous angiosperm family Dipterocarpaceae (Grimaldi et al., 2000b).

“*Dammara*” fan-shaped scales, with *in situ* radiating ducts of resin, have been found in New Jersey and Wyoming (Grimaldi et al., 2000a, b). “*Dammara*” cone-scales in the New Jersey deposit are probably assignable to Taxodiaceae (David Grimaldi, personal communication, 2006) but may be Pinaceae (Grimaldi et al., 2000a). Not all resins produce amber; resins easily get broken down and washed away by rain (Ross, 1997). Today only two extant plant species produce stable amber: the Kauri pine *Agnathis australis* of New Zealand and *Hymenaea* of east Africa and south and Central America (Ross, 1997; Martínez-Delclòs et al., 2004).

METHODOLOGY

Early in the Ingersoll shale excavation, amber was hand collected using the normal quarrying methods previously described in Chapter 6. After abundant amber was discovered in the lower, high-energy portions of the shale, bulk processing began. Bulk samples were taken from the amber-rich interval, allowed to dry completely in air, placed in a 5-gallon bucket, and subsequently rehydrated with tap water. Rehydration completely disaggregated the sand and clay and formed a slurry, releasing plant debris and amber from the matrix. The slurry was physically agitated and the portion in suspension was immediately sieved through a 1-mm sieve. Because amber has a lower specific gravity, it was separated from heavier particles by this method. This process was repeated several times. The residual material remaining in the 5-gallon bucket consisted of plant matter, rock fragments, pyrite nodules, and lignite. The small plant fragments and amber that were caught in the sieve were washed under running water to remove any remaining clay and then placed in clean water. The amber was then removed with forceps and isolated in a petrie dish. Amber was thoroughly examined for biologic inclusions using a binocular stereomicroscope. If the oxidized rind of the amber nodule impeded visual examination, a small portion was chipped away in order to see into the transparent, non-oxidized amber. Any inorganic or organic inclusions that could be identified were photographed.

The amount of amber within the Ingersoll shale was estimated by weighing the amount of amber from a known volume of shale. Shale samples were collected from the lower amber-rich portions of the shale lens (zone 2), dried, and weighed. The dried shale was then subjected to the amber extracting method described above. All amber pieces

were extracted, air dried, and weighed. The results were then extrapolated to calculate the approximate amount of amber per cubic meter of sediment in zone 2.

When the screening process was complete, all amber, including pieces with biologic inclusions, were sent to David Grimaldi (Curator of Entomology at the American Museum of Natural History) for further analysis. The amber pieces with inclusions were cataloged into the American Museum of Natural History collection. Grimaldi embedded the amber with resin under vacuum in order to protect the fragile amber, prevent further oxidation, and enhance visualization; this embedding technique was described by Nascimbene and Silverstein (2000). He examined all amber pieces for inclusions and identified and photographed the biota found.

RESULTS

The Ingersoll shale amber is nearly as abundant as in other major Cretaceous amber deposits. Whereas other deposits commonly yield a kilogram of amber in 1-2 cubic meters of sediment, the Ingersoll shale yields approximately 362 grams of amber per cubic meter of shale (David Grimaldi, personal communication, 2006). To date, only 22 grams have been collected from the deposit. However, it is important to note that the collecting methods used (i.e., screening, hand-picking, washing) introduce biases in the amount, size, and type of amber collected. During screening, very tiny pieces will pass directly through the screen. Hand-picking has a bias toward clear transparent pieces; highly oxidized pieces were inadvertently sometimes passed over. Washing breaks down brittle pieces allowing them to pass through the screen.

The amber was generally found in clusters indicating that it may have settled in small depressions on the bed. The patchy distribution of amber was observed on bedding planes in the field, and is manifest by variable recovery of amber during the extraction process; sometimes processing yielded large amounts of amber and at other times only minute amounts. Pieces larger than 1 cm were rare and were usually found in the field during the process of quarrying. These large amber pieces were slightly flattened parallel to the bedding plane and were difficult to extract without shattering or splitting due to their high fractility. Small clasts (<5 mm) were common in the deposit and were easily extracted as whole pieces. Fractility also made the laboratory preparations (by David Grimaldi) difficult, due to cracking even during gentle grinding.

Amber color is commonly deep yellow to light red (Figs. 27A, 27B and 27D); light-yellow pieces are also present but are rare. Some amber pieces have a white, chalky crust or a red exterior, fading to yellow towards the interior. The chalky white crust and red exterior color of the amber pieces reflects oxidation and weathering (Grimaldi et al., 2000a; Poinar and Mastalerz, 2000). Aside from the overall oxidation on the crust of a few amber pieces, the amber is very transparent (Fig. 27D), with only a few of the pieces containing a turbid suspension of organic particles and numerous, minute, white air bubbles. Some of the rare turbid pieces show alternating dark and light flow lines (Fig. 27E), probably indicating variations in temperature and exposure to sunlight (Martínez-Delclòs et al., 2004). Most of the amber is in the form of rounded drops 2-3 mm in diameter (Fig. 27D). Some tear-shaped pieces were found, while slender rivulet pieces were rare. Irregularly-shaped amber pieces often had rounded edges (Fig. 27D). Occasionally blackened, frothy, apparently fired-damaged amber was found within

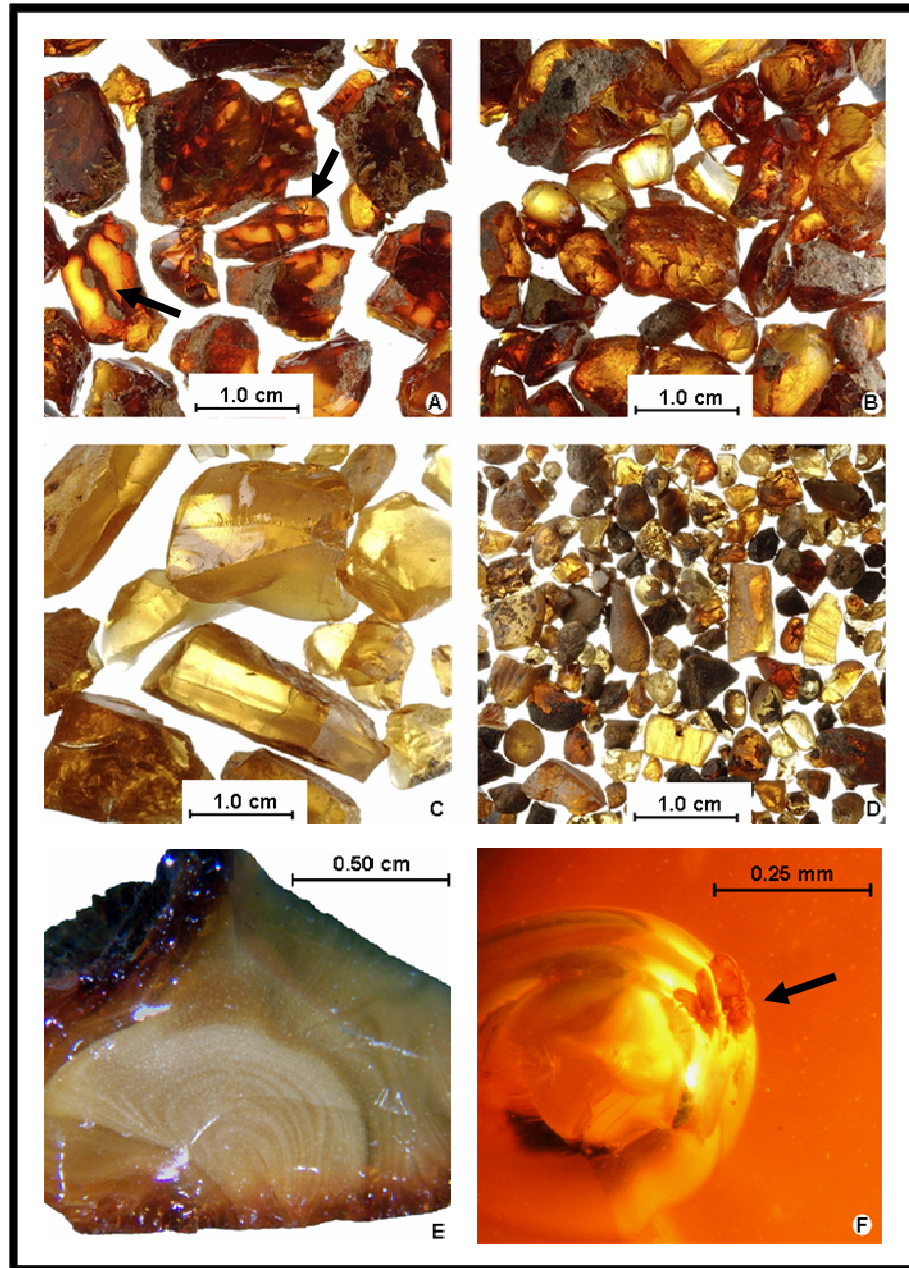


FIGURE 27—Representative samples and inclusions within Ingersoll shale amber. (A) Two flat pieces (arrows) were polished to reveal internal cracking and coloration. (B) Large pieces with their natural shape; note the rounded edges. (C) Large fragments collected from the outcrop; note the light yellow color. (D) Small pieces with natural shapes. This is the most abundant size. (E) Alternating clear and dark amber flows. Dark, thin layers are possibly the result of rapid drying by sunlight and wind (see Martínez-Delclòs et al., 2004, p. 39). (F) Rare bubble inclusion; note the adjacent organic inclusion indicated by the black arrow (possibly a mite). Figures A-E were photographed by David Grimaldi (American Museum of Natural History), and Figure F was photographed by Patrick Bingham (Auburn University).

bedding planes that also contained fusainized plant remains. Carbonized and pyritized organic matter was sometimes attached to the outside of the amber, indicating that it came into contact with the amber while it was still sticky resin. Some amber pieces exhibit polygonal shrinkage cracks, some of which are filled with pyrite.

Occasionally the amber was found in direct association with its producer. *In situ* amber rods (Fig. 28A) have been found within conifer foliage type 4 (Chapter 8). The amber rods are within the stem and the main vein of the leaf, exposed only after the fossil dried and cracked, revealing the internal plant structure. One large, poorly preserved conifer cone was found in the lower oxidized portion of the shale (Fig. 28B). Most of the organic material within this fossil cone is leached but many oxidized amber rods remain *in situ* (Fig. 28C). Two “*Dammara*” scales (see Grimaldi et al., 2000a) were found in the Ingersoll shale (Fig. 28D). One of the scales revealed the internal structure and *in situ* radiating amber ducts.

Inorganic inclusions within the Ingersoll shale amber are common. They include common air bubbles, and rare crystals of pyrite and an unidentified white mineral. The air bubbles are often clear (Fig. 27F), milky white, and rarely black. Inclusions and fractures are occasionally filled with pyrite (Fig. 29B and 29C). The opaque, white mineral occurs in clusters or tufts of needle-shaped crystals (Fig. 29A). The latter mineral may be gypsum.

Organic amber inclusions are common and consist mostly of wood fragments and plant debris (Figs. 30A, 30D, and 29B) that are sometimes associated with insect fecal pellets (Fig. 30F). Well-preserved fungal mycelia are also common (Figs. 30B, 30C, and 31A) and were sometimes associated with wood fragments (Fig. 30D). Insect fecal pellets

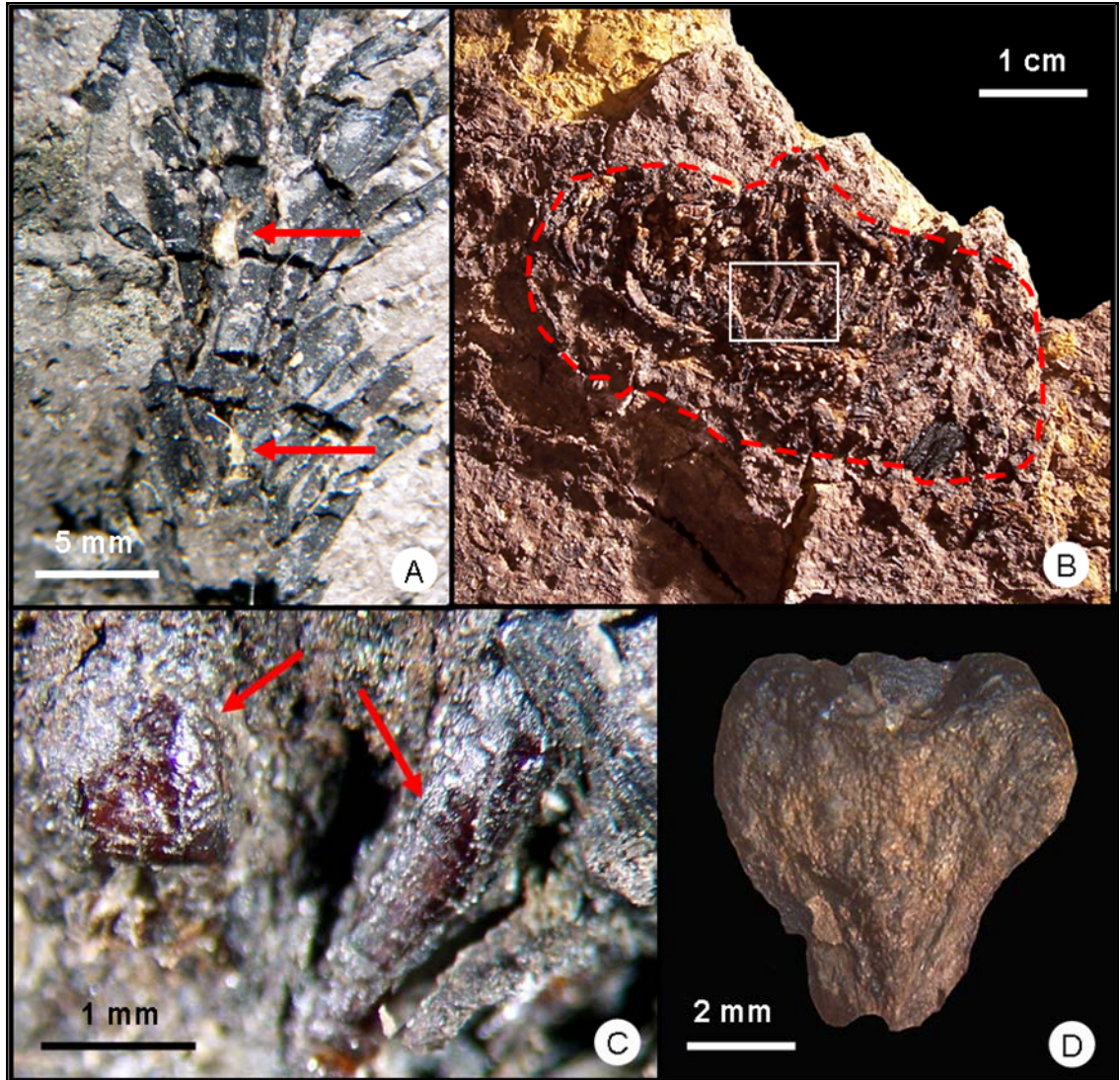


FIGURE 28—Plant macrofossils directly associated with amber. (A) Conifer foliage type 4 (KIS-118) showing *in situ* amber rods inside the stem (indicated by the red arrow). (B) Poorly preserved conifer fossil (KIS-127), possibly a cone or cone scale, showing *in situ* amber rods. (C) Close-up of amber rods from Fig. 1B. (D) “*Dammara*” cone-scale (KIS-161).

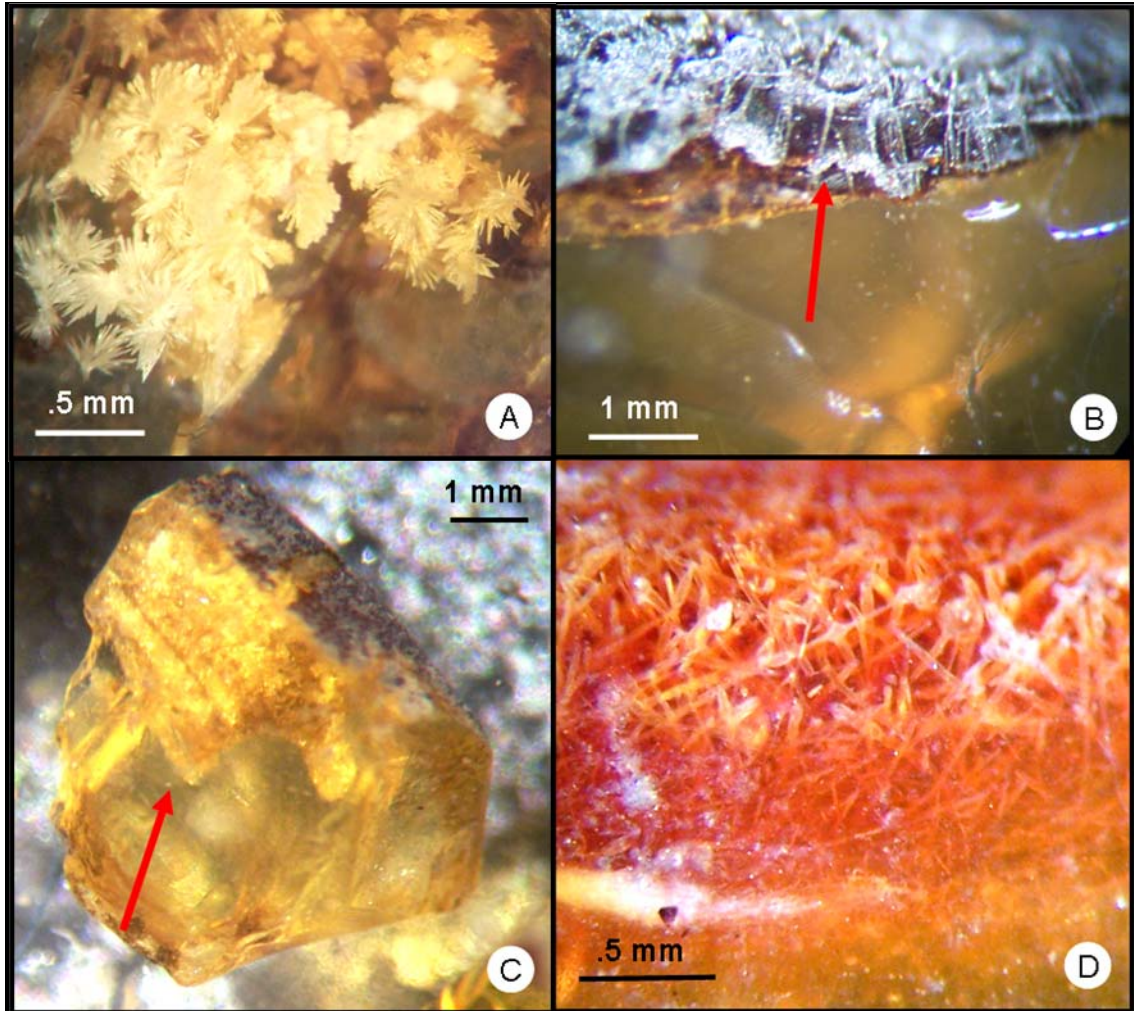


FIGURE 29—Inorganic amber inclusions. (A) Opaque white mineral in tufts of acicular crystals (gypsum?). (B) Pyrite infilling shrinkage cracks (indicated by red arrow). (C) Pyritized organic fossil within amber nodule (indicated by red arrow). (D) Unidentified fibrous organic fossils (possibly moss or bark fibers).

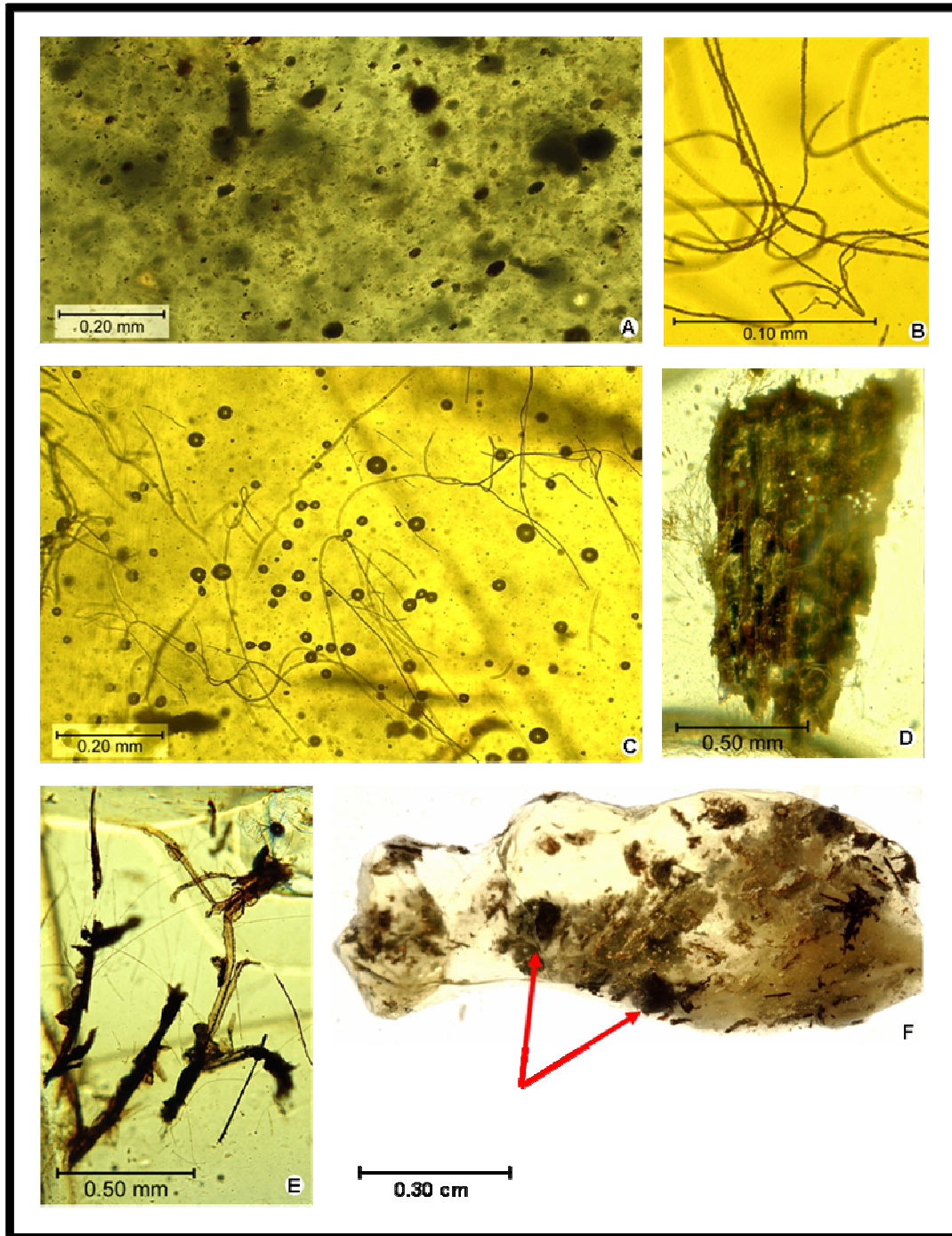


FIGURE 30—Non-arthropod amber inclusions. (A) Unidentified organic particles in a turbid piece. (B) Fungal mycelia and fine bubbles. (C) Detail of mycelia. (D) Wood fragment with mycelia overgrowth. (E) Wood and/or plant inclusions. (F) Wood and/or plant fibers and insect fecal pellets (indicated by red arrows). Photographed and identified by David Grimaldi (American Museum of Natural History).

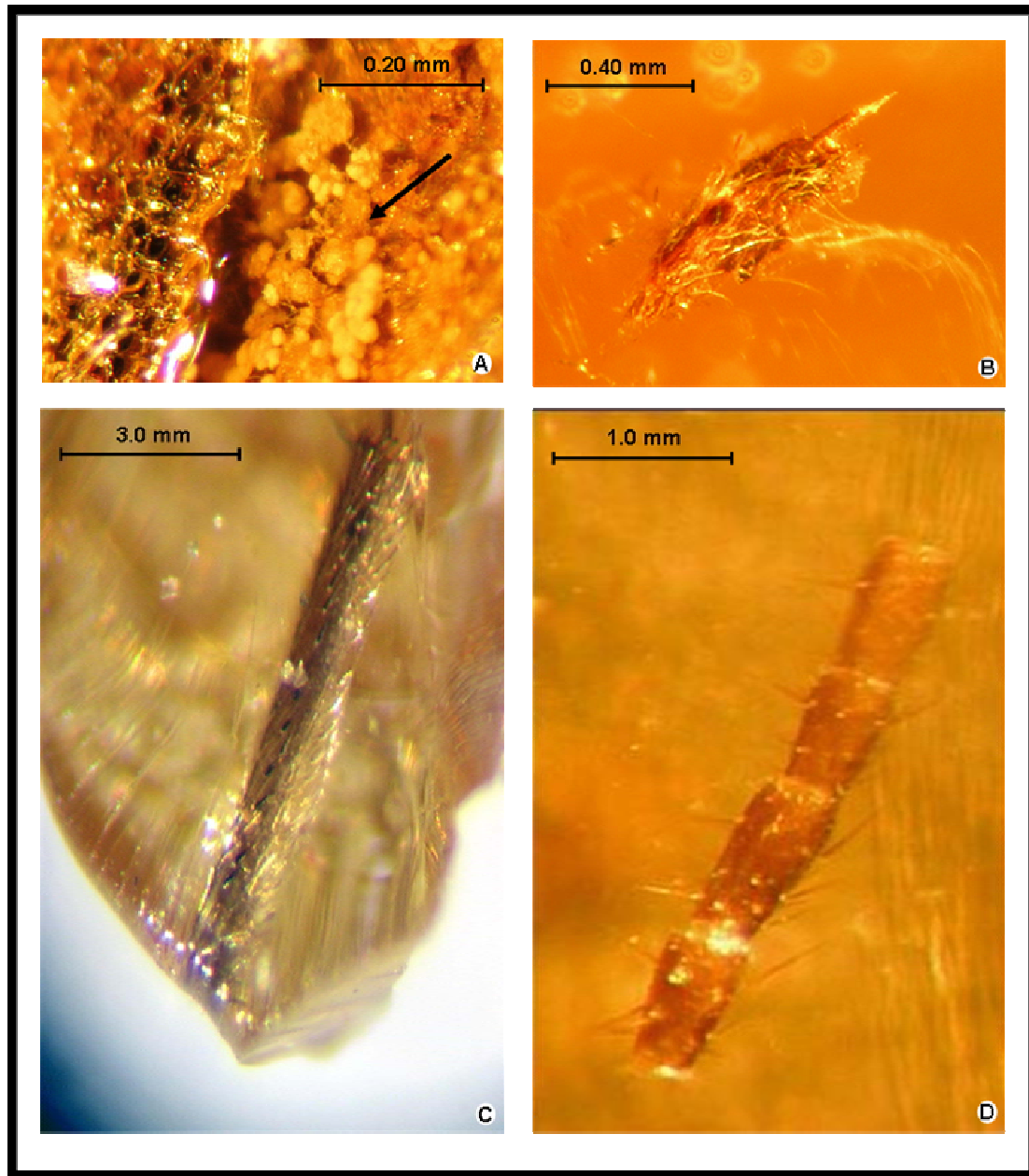


FIGURE 31—Fungal, plant, and arthropod inclusions. (A) Possible fungal hyphae (indicated by black arrow). (B) Fibrous organic inclusions (possibly a seed or flower). (C) Disarticulated insect appendage; well preserved spines indicate tibia. (D) Disarticulated flagellum segment of an insect antenna; notice the well-preserved sensory hairs. Photographed by Patrick Bingham (Auburn University).

were found associated with plant debris (Fig. 30F). Several amber pieces contained arthropod remains. Unidentifiable, disarticulated arthropod appendages were present (Figs. 31C and 31D), as well as identifiable arthropod remains, which include two mites (Acarina) (Figs. 32A and 32B), one spider (Araneae) (Figs. 32D and 32E), and one scale insect (Fig. 32F). The amber clast containing the spider also contains parts of the web (Figs. 32C and 32D). The preserved web contains sticky droplets adhering to the silk strands, indicating that it was made by the associated araneid spider (David Grimaldi, personal communication, 2006).

INTERPRETATION AND DISCUSSION

Ingersoll shale amber is always found in association with macerated plant debris and often in clusters. The amber clusters formed by settling into small depressions during transport within the bedload of the tidal channel, or when it settled from suspension during slack water. These amber clusters are similar to what Grimaldi et al. (2000a) reports from the Raritan Formation (Turonian) amber deposits of New Jersey. The hydraulically sorted amber clusters found in the Ingersoll shale are evidence that at least some of the amber was transported from upstream, and deposited in the lower energy meander of the tidal channel. This interpretation is strengthened by the rounded edges on irregularly shaped pieces that suggest reworking in abrasive sediment prior to final deposition (David Grimaldi, personal communication, 2006). Reworking within the substrate is further demonstrated by the rarity of fragile slender rivulet pieces.

The high fractility of the Ingersoll shale amber indicates that it is very physically mature. According to David Grimaldi, this may be the result of clay compaction. The

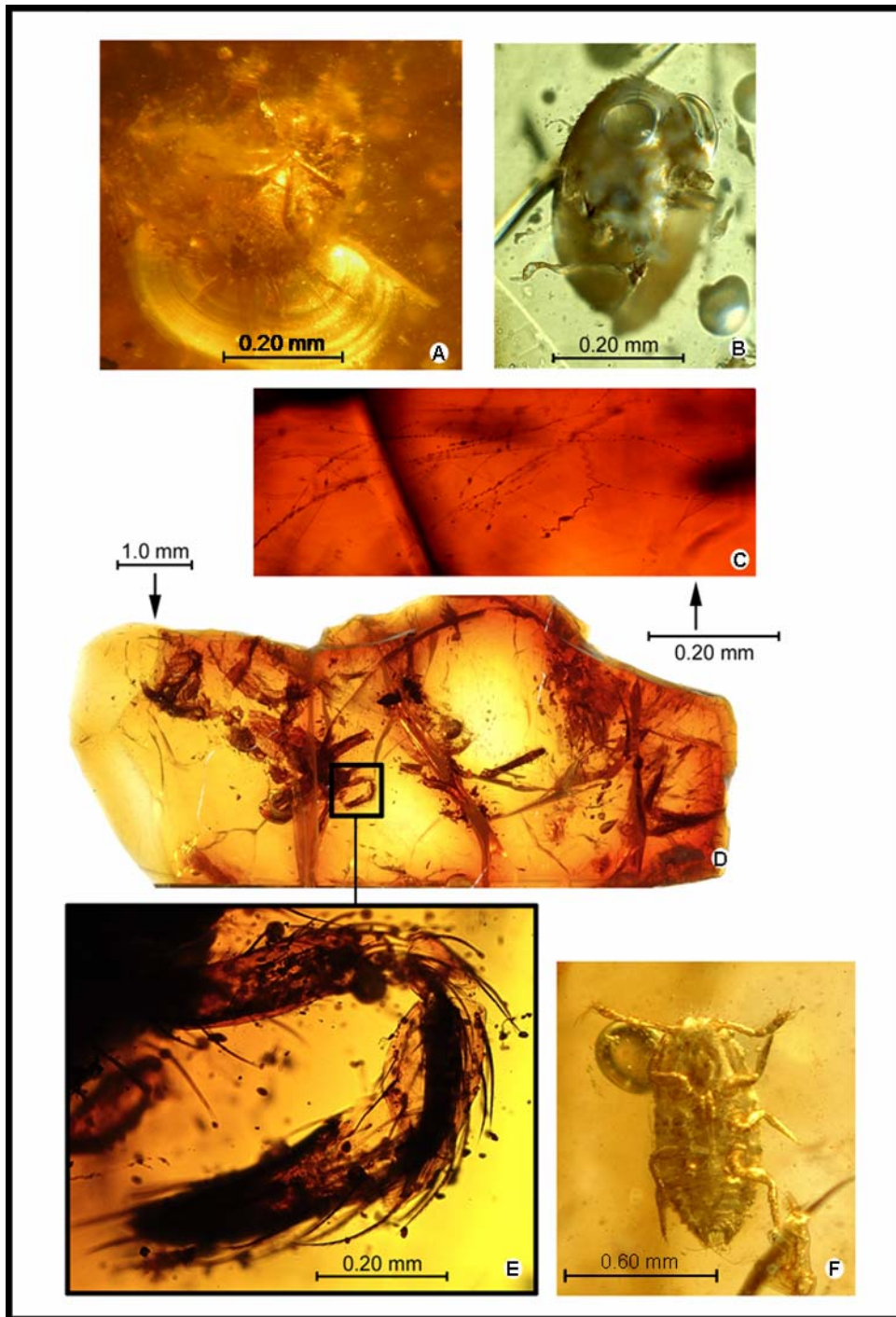


FIGURE 32—Arthropod inclusions. (A and B) Unidentified mites. (C) Spider webbing; notice the sticky droplets adhering to the silk strands. (D) Disarticulated araneoid spider and associated webbing. (E) Details of spider appendage. (F) Female coccoid (scale) insect. Photographs and identifications made by David Grimaldi (American Museum of Natural History).

high fractility of the Ingersoll shale amber is similar to most Mesozoic ambers, and is a consequence of age. Less polymerized amber can become flattened because it is still plastic (Alonso et al., 2000; Martínez-Delclòs et al., 2004). The amber pieces that are compressed in the Ingersoll shale were deposited quickly and compacted prior to complete polymerization, while the resin was still ductile. Since these larger pieces take longer to polymerize, they would be buried before they completely hardened. The release of pressure when the amber is exhumed would cause the larger flattened amber pieces to fracture (Martínez-Delclòs et al., 2004), and form haloes around inclusions (Fig. 32A). Smaller hardened pieces would retain their three-dimensional shape.

With respect to color, the resin was possibly clear originally. The dark, frothy amber was possibly produced during fires. Furthermore, this amber was found in association with fusainized plant remains, so it is likely that resin was exuded from the source plants as a result of fire/heat. The viscosity of the resin was lowered with an increase in temperature allowing it to froth with air bubbles and flow more readily (Martínez-Delclòs et al., 2004). The red amber found within the highly compacted, unoxidized portions of the shale is probably a result of oxidation prior to deposition (Martínez-Delclòs et al., 2004). Considering the quality of preservation seen in other fossils from these layers, oxygen was not abundant. The white, chalky, highly-degraded amber may have been oxidized after deposition as groundwater filtered through the sandy, organic-rich, lower portions of the shale lens.

At least some of the amber in the Ingersoll shale appears to be from taxodiaceous conifers in the family Cupressaceae. The *in situ* amber rods in the Ingersoll shale occur in association with conifer foliage type 4 (Fig. 28A), which is conformable to *Sequoia*

reichenbachi. The leaf characteristics of this plant suggest that it has a taxodiaceous affinity (Robert Gastaldo, personal communication, 2006). The affinity of “*Dammara*” cone-scales from New Jersey is probably taxodiaceous, not araucarian. Nevertheless, a cuticular examination of these amber producers needs to be performed before they can confidently be placed in families.

The abundance of pyrite inclusions in amber pieces results from exposure to sulfate-reducing conditions. This indicates that either replaced inclusions extended out of the resin or waters penetrated fine fractures within the amber. The organic matter subsequently acted as a nucleation site for pyritization. This is demonstrated by fine fractures filled with dendritic pyrite. Nonpyritiferous crystals similar to the ones identified in the Ingersoll shale have been described in the New Jersey amber (Grimaldi et al., 2000a). These were thought to be either jarosite [$\text{KFe}^{3+}_3(\text{SO}_4)_2(\text{OH})_6$] or selenite ($\text{CaSO}_4 \cdot 2\text{H}_2\text{O}$) (Grimaldi et al., 2000a).

The mycelia isolated within some amber pieces suggest that fungus grew on the exposed surface of the fresh resin before being covered by a fresh flow. Arthropod inclusions are rare in the Ingersoll shale but the relative abundance is comparable to other major Cretaceous sites. Mites are rare in the New Jersey amber but are common in the Burmese amber (David Grimaldi, personal communication, 2006). The high diversity of mites makes identification difficult, and the Ingersoll shale mites have yet to be identified. Spider inclusions are common in all major Cretaceous deposits (Penney et al., 2003). The Ingersoll shale spider specimen is disarticulated and poorly preserved but it does retain microscopic detail of its cuticle. Early Cretaceous araneoid spiders and webs also were found in Albian deposits of Spain (Peñalver et al., 2006) but previously have

never been found in the same piece. Taking this into account, the Ingersoll shale spider is the earliest araneoid associated with its web.

The scale insect is exceptionally preserved. The specimen is a wingless female with well-developed legs and antennae; these features indicate that it belongs to a basal lineage of Coccoidea (Grimaldi and Engel, 2005). Primitive Coccoidea are abundant in the New Jersey and Myanmar ambers (David Grimaldi, personal communication, 2006); thus, finding the insect in the Eutaw Formation is consistent with the fossil record. Most Cretaceous scale insects are winged males, so it is unusual to have a single female specimen. Because of its limited mobility, it is almost certain that the insect was feeding on the tree when it was captured in the amber. It is possible to make an insect-plant association on the basis that the *in situ* amber is produced by a taxodiaceous conifer. The lack of winged arthropods in the Ingersoll shale amber suggests a taphonomic bias toward the capture of arthropods living on the trunks of trees or under the bark (David Grimaldi, personal communication, 2006).

CONCLUSION

Although the Ingersoll shale amber is restricted in abundance, it reveals useful information on Santonian life. Until now, arthropod-bearing Cretaceous ambers along the Atlantic Coastal Plain have been restricted to the amber *Lagerstätte* within the Raritan Formation of New Jersey. The Ingersoll shale amber expands the geographical distribution of Santonian mites, spiders, and scale insects to the southeastern U.S. Prior to the discovery of the Ingersoll shale, amber with inclusions was considered scarce in the Eutaw Formation and none revealed arthropods. Due to the exceptional plant macrofossil

preservation, the amber can be directly linked to the amber producer; the ability to make this connection is rare in the fossil record. This will help paleobotanists clarify Mesozoic amber producers in general, and specifically, in the southeastern U.S. One way this can be accomplished is to compare the chemical signature of the Ingersoll amber to that of other deposits. The Ingersoll shale has proven to be a rich site for paleontology, and amber adds another dimension to this deposit.

CHAPTER 10: INVERTEBRATES

MARINE INVERTEBRATES

Marine invertebrate fossils are rare within the Ingersoll shale lens and are restricted to the uppermost portions of zone 6. Low abundance of invertebrates is probably attributable to harsh benthic conditions during deposition. Near the top of the lens, clusters of infaunal bivalves are preserved mainly as external molds and casts (Fig. 33A) and rarely preserved via pyritization. Typical dimensions are ~1.1 cm in length, 0.6 mm in height, and ~0.5 mm in width.

Although not found in life position, all bivalve specimens are articulated, which suggests little or no transport. Concentric growth lines are faintly preserved on some casts indicating that sediment was compacted into the external mold after the shell dissolved. The bivalves left no trace fossils, unlike the producers of the sand-filled *Thalassinoides* and *Rhizocorallium* in zone 6, but their elongate morphology and weak ornamentation indicates an infaunal lifestyle (Stanley, 1990). The bivalves apparently burrowed into the clay lens after deposition, while the substrate was still relatively soupy but prior to firmground development and erosion.

The bivalve remains are similar in size and shape to *Nuculana* sp. (David Schwimmer, personal communication, 2007). However, due to their scarcity and a lack of biomineralized remains, their true biologic affinity is unclear.

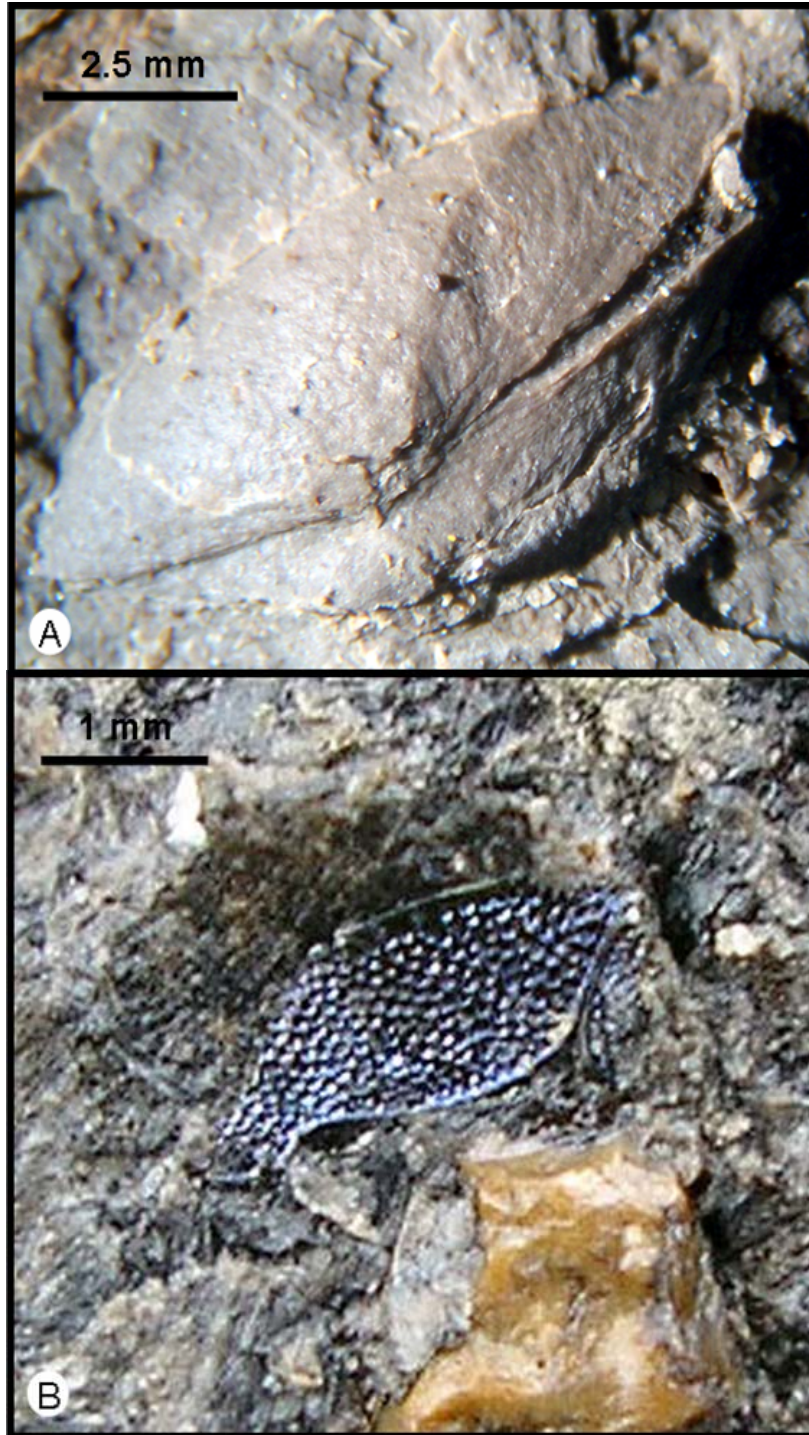


FIGURE 33—Invertebrates. (A) Cast of infaunal bivalve on the underside of a bedding plane, oriented dorsal edge up, lying almost perpendicular to bedding. Anterior end is on the left. (B) Possible beetle elytron showing irregular, coarse pitting (notice the blue iridescence).

TERRESTRIAL INVERTEBRATES

Remains of possible terrestrial invertebrates were found in association with plant macrodetritus in zone 2 of the clay lens. These remains are scarce but are recognizable by their iridescence. They deteriorate quickly and lose their color after exposure to open air. Some show irregular, coarse pitting, similar to that seen on the elytra (wing covering) of Coleoptera (beetles) (Fig. 33B).

Because of inadequate material to examine currently, this element of the Ingersoll fauna requires further attention in future research. If these fossilized remains are indeed from Coleoptera, they are of particular importance because of the rarity of insect fossils in sediments that also yield insect-bearing amber (Martínez-Delclòs et al., 2004).

CHAPTER 11: CTENOID FISH SCALES

INTRODUCTION

During excavation of the Ingersoll shale, 16 ctenoid fish scales were discovered. They represent 3 different morphologies, which vary in size and structure. They are preserved as carbonized and pyritized remains and as external molds, often preserving fine structural details. The detailed morphology of modern ctenoid fish scales is reviewed below in order to better explain the structural details that are preserved in the Ingersoll shale fish scales.

FISH SCALE ANATOMY

Today elasmoid scales are found in a large number of teleost species. They are composed of a plywood-like arrangement of collagen layers. There are two types of elasmoid scales: cycloid scales and ctenoid scales. Cycloid scales have a smooth exposed margin, whereas ctenoid scales have an irregular, tooth-like or spiny margin. Ctenoid scales are the focus of the comparison below.

The following descriptive terminology of ctenoid scales (Fig. 34) is from Lippitsch (1990). Ctenoid scales are characterized by *ctenial spines* (ctenii), which are arranged in rows along the free margin of the scale producing a comb-like appearance; ctenial spines are thought to reduce drag during swimming. Ctenoid scales are divided

Rostral field

Caudal field

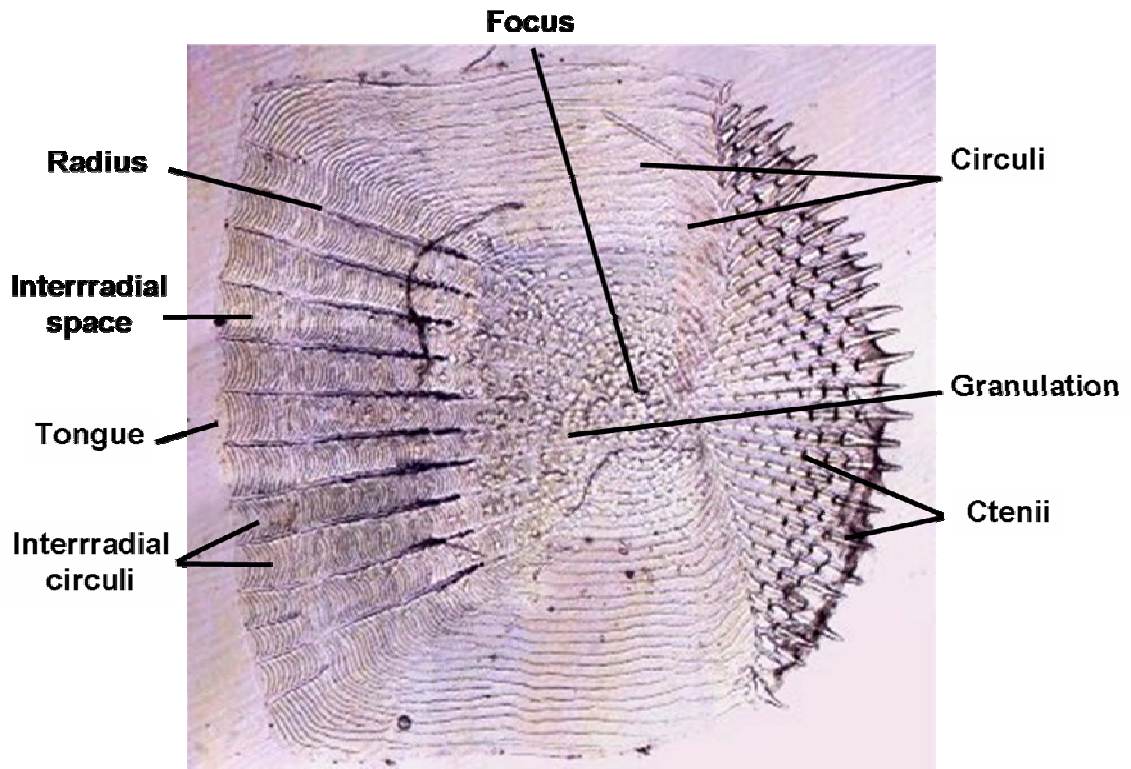


FIGURE 34—Photograph of ctenoid fish scale with most of the descriptive terms used in this chapter (modified from Cavanihac, 2002).

into an anterior rostral field (the attached end) and a caudal field in the posterior (the free margin). Because fish scales are partially overlapping in a shingle-like fashion; the rostral field of one scale is concealed by the caudal field of the overlying scale.

Scale surfaces have ridges and grooves that form concentric growth rings, or *circuli*, around a centrally located *focus*, which is the first formed part of the scale. The grooves between the circuli are called *circular grooves*. The boundary between the rostral and caudal fields is recognized by densely-spaced circuli in the rostral field, which terminates or become broader in the caudal field. The rostral field may have circuli that are partitioned at right angles by *radii*. The radii may be simple grooves or may be broad depressions and may be filled with fibrous tissue. If radii are present, the scale is considered to be *sectioned*; if radii are absent, the scale is considered to be *simple*. On the margin of the rostral field, the *interradial space* may have a projection (the tongue), which is free of circuli. The central caudal field has *granulation*, which may be composed of spike-like projections called *grains* or smoothly rounded projections called *tubercles*. The granulation can be inconspicuous or can consist of well-developed projections, such as those seen in sectioned scales. Simple scales may have absent or weak granulation. Simple scales are typically located on the head, while sectioned scales are located on the body.

A scale varies in thickness as a result of periodic variations in annual growth rates and other biological process. Growth ridges are called *annuli*. The caudal edge is weakly mineralized and may form a soft, basal fibrillary plate. In some specimens circuli are the only structures present in this field. In the caudal field, the circuli can become irregular and transform into the granulated area.

METHODOLOGY

Ingersoll-shale fish scales were discovered and prepared using the quarrying and curating techniques outlined in Chapter 5. Surface morphology of the scales was examined using a normal-light, binocular microscope and by SEM microscopy. Length measurements were taken along an anterior-posterior line through the focus, and width was taken at the caudal field (maximum width of scale).

RESULTS AND DESCRIPTIONS

Ctenoid scales were discovered throughout the thickness of the shale lens with the exception of zone 2 (Fig. 6). Lateral distribution was concentrated near the channel axis (Fig. 5 and 7). Occasionally, several fish scales were found associated on the same bedding plane, but more commonly they occurred in isolation. These scales, all of which are external molds, show detailed preservation of the circuli, granulation, radii, cteni, and the focus. Three distinctively different morphologies are described below. No endoskeletal fish remains were recovered from the deposit.

Fish Scale Morphotype 1

This morphotype is described from five specimens, which range from 0.75-2.00 cm wide and 1.15-2.00 cm long (Fig. 35A). The circuli are well preserved. In the rostral field, radii cut across the circuli forming a reticulate pattern. Some radii and circuli are filled with carbon (Fig. 36A). There are straight circuli in the interradial space, and some specimens show

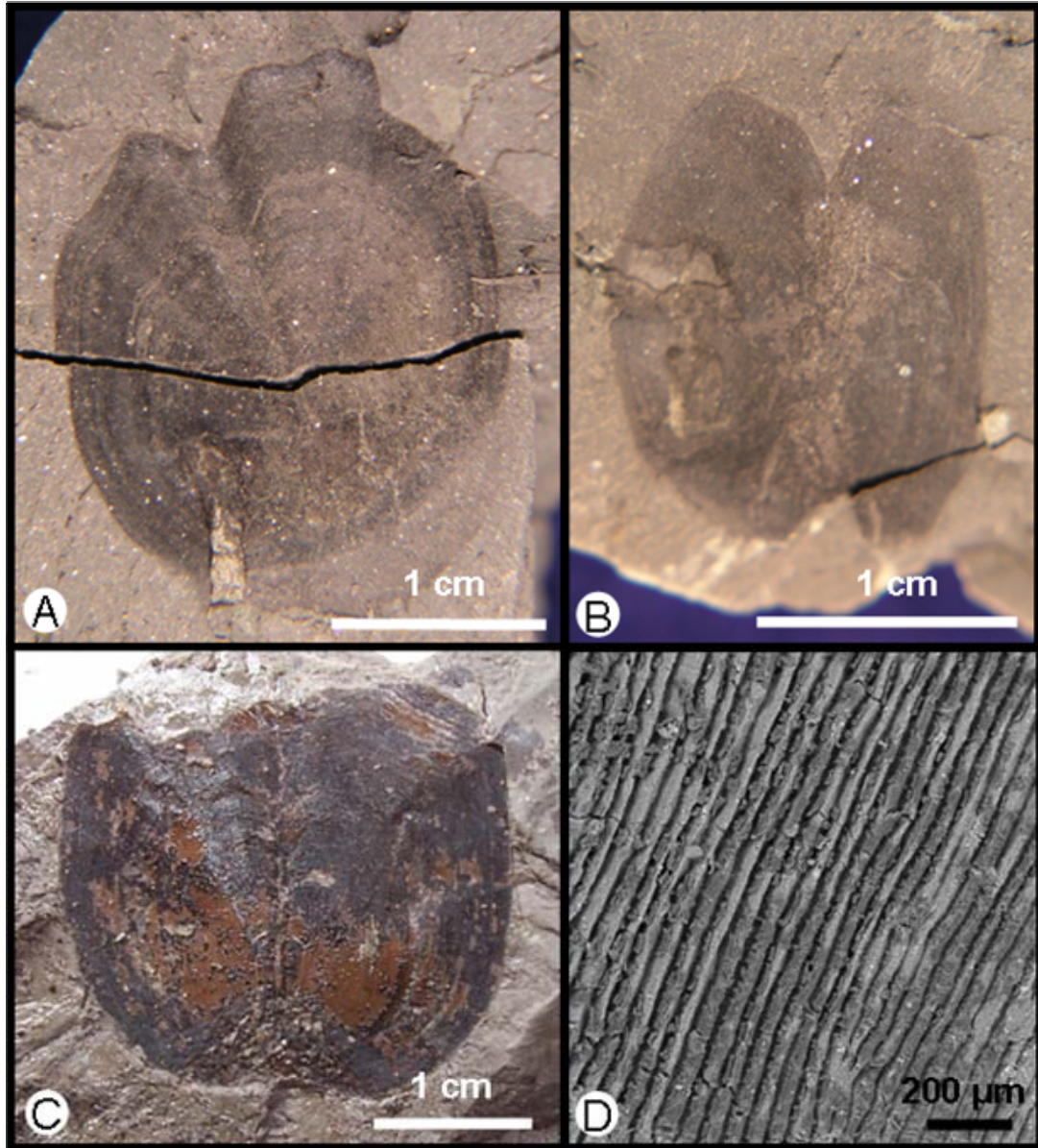


FIGURE 35—Ingersoll shale fish scales (external molds). (A) Fish scale morphotype 1 preserved as an external mold with residual carbon. (B) Fish scale morphotype 2 preserved as an external mold with residual carbon (notice the asymmetry). (C) Fish scale morphotype 3 preserved as an external mold with residual carbon (notice the brown film between the black carbonized remains and the matrix). (D) SEM image of KIS-228 (morphotype 2) showing fine detail of the circuli and carbon-filled grooves.

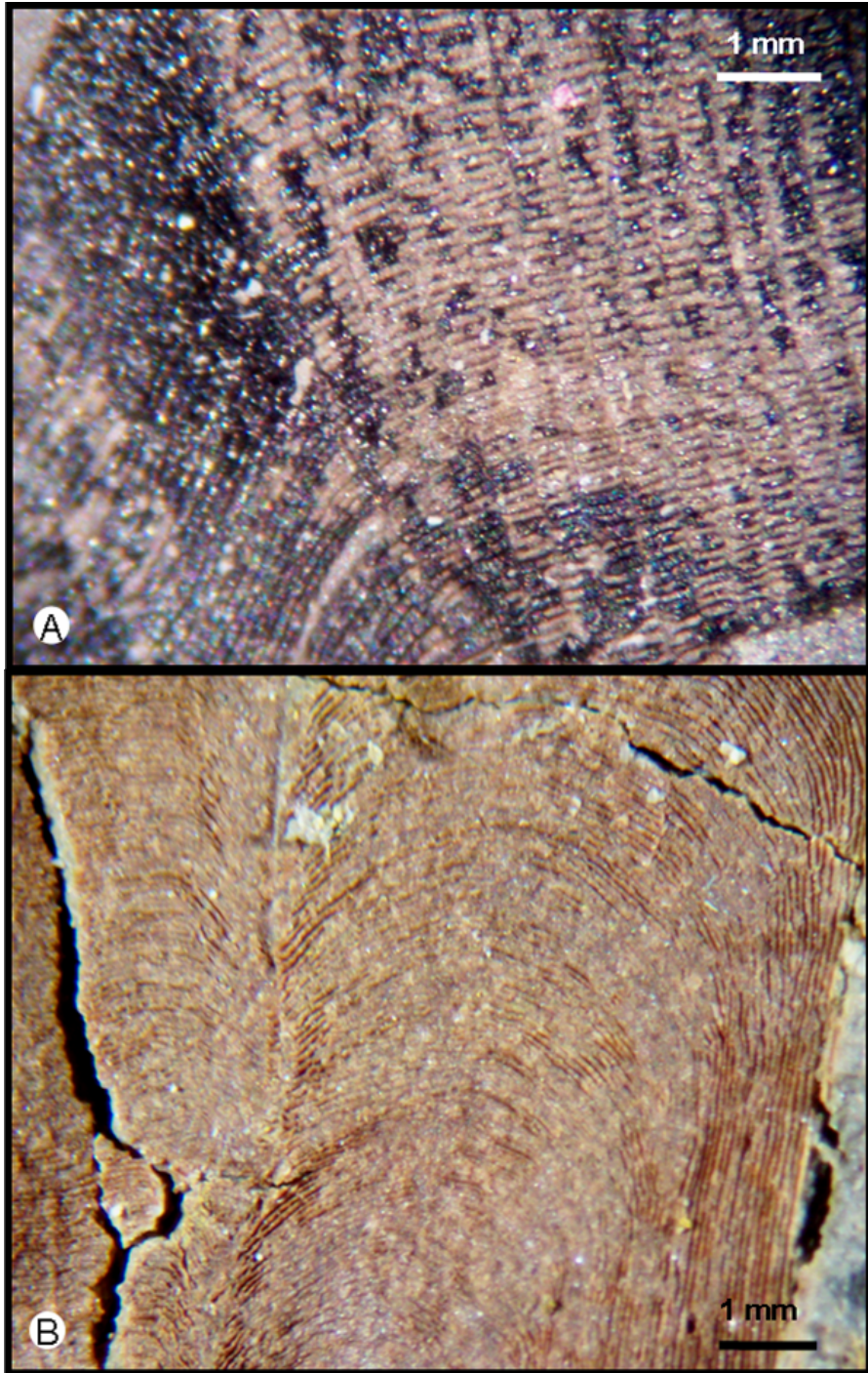


FIGURE 36—Rostral field of morphotype 1 and 2 (both are external molds). (A) KIS-209B showing circuli intersecting and crossing the radii (right) forming a reticulate pattern. (B) KIS-205B showing fine circuli curving sharply toward the caudal field at the midline (note the absence of radii). On the right, along the margin, the circuli become confluent.

separation along the circuli. Granulation can be observed in the caudal field in an area that is widest on the caudal margin and decreases in width toward the focus. This granulation is formed primarily by the circuli becoming more irregular, as in morphotype 3 below (Fig. 35D). A few small tubercles are seen on some specimens. The area of granulation varies between specimens.

Fish Scale Morphotype 2

This morphotype is distinctively bilobed and asymmetrical with one large and one smaller lobe; seven specimens measure 0.60-1.20 cm wide to 1.2-1.6 cm long (Fig. 35B). The prominent midline area widens near the focus. In the rostral field near the axis, the circuli curve sharply toward the anterior (Fig. 36B). The rostral field lacks radii. The caudal field has regular circuli with the granulation either completely absent or only occurring at the focus. Ctenal spines are preserved along a single row located directly on the caudal margin.

Fish Scale Morphotype 3

This morphotype is described from two specimens that average ~3.07 cm wide and ~2.62 cm long. They are bilobed with a prominent midline, and symmetrical (Fig. 35C and 36A). At the focus, the midridge is relatively wide. In the rostral field, near the axis, the circuli curve sharply toward the posterior (Fig. 37A). As the circuli go from the rostral to the caudal field, their pattern becomes irregular and granular (Fig. 37C). On the external mold, mounds on the matrix indicate that the sediment filled holes in the scale (Fig. 37B). This morphotype lacks radii in the rostral field. Ctenii along the margin of the caudal field are ~3.1 mm long. Annuli are preserved in the rostral field (Fig. 37D).

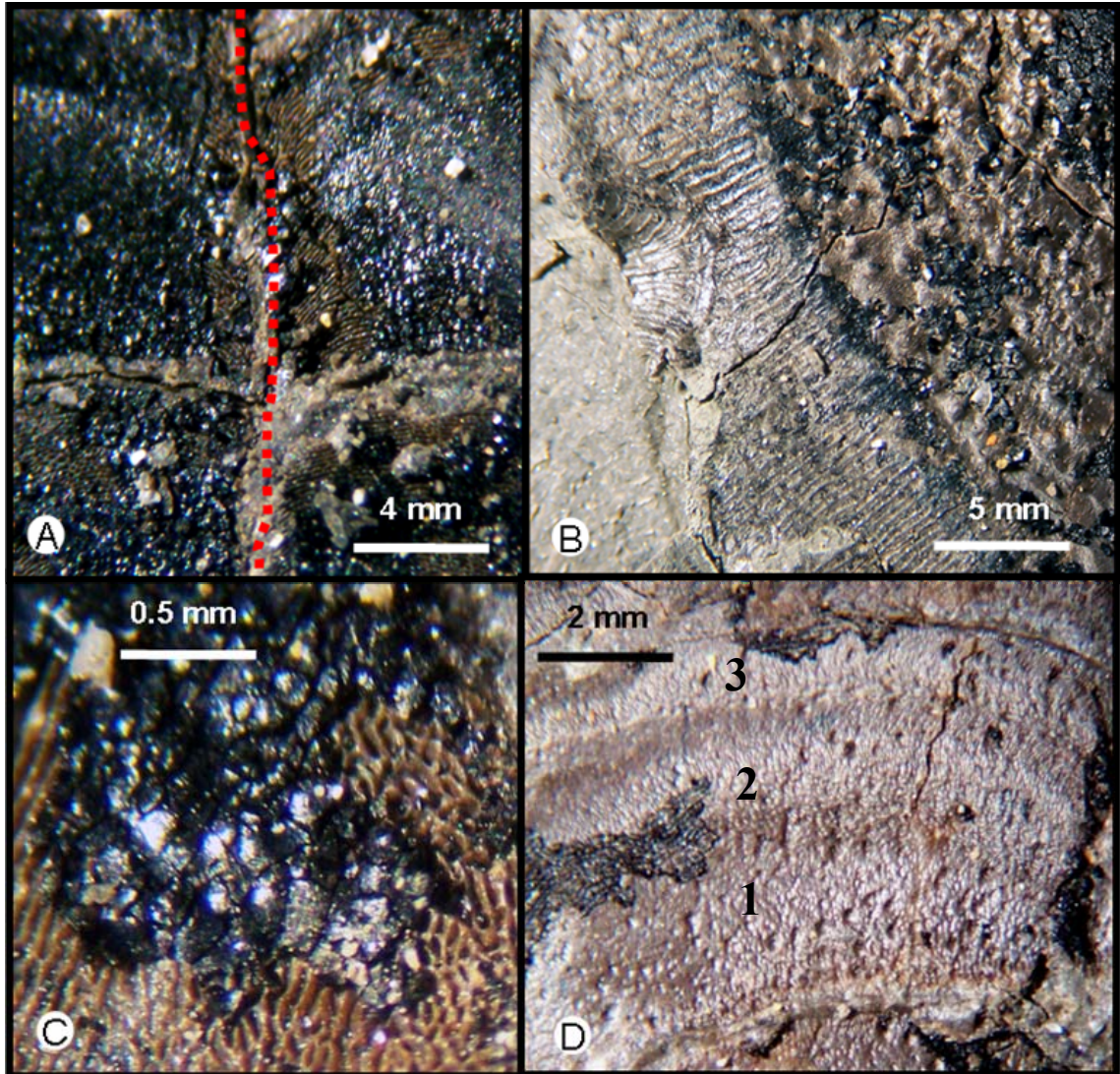


FIGURE 37—Close-up pictures of fish-scale morphotype 3. (A) KIS-227A showing circuli curving sharply toward the caudal field and prominent midline (red dashed line). (B) Portion of the caudal field of KIS-230A showing the ctenii (center) and granulation (right). (C) KIS-227A showing carbonized remains and external mold preserving regular circuli (left) and irregular circuli (right). (D) Preserved annuli on specimen KIS-230A (individual annuli are numbered).

TAPHONOMIC SUMMARY AND DISCUSSION

All three fish scale morphotypes appear to exhibit the same mode of preservation. Most specimens occur as thick, carbonized remains, which break into blocks, giving the appearance of coalification. Pyritization is commonly associated with the carbonized remains, especially within the circular grooves. Brown, translucent, cuticle-like coatings separate carbonized remains from the matrix. External molds preserve fine structural details, such as the circuli, radii, and granulation. Some scales appear to be torn along the circuli in the interradial space.

It is impossible to say with certainty whether or not these scales represent the allochthonous or autochthonous component of Ingersoll shale fossil assemblage. However, it is unlikely that the fish were living at the depositional site. We know the sediment-water interface was inhospitable and that sedimentation rates were high (Bingham, 2007). High-sedimentation rates would not support the idea that fish were living in the water of the channel. Furthermore, the isolated scales have no associated skeletal remains: no vertebrate skeletal remains were found anywhere in the shale lens.

If the fish were introduced into the abandoned tidal channel and died, the scales could have been dispersed during decay while the carcasses were floating, aided by tidal pumping. It is also possible that the scales floated into the depositional site as separate elements. However, from personal observation, fish scales will float if they are dry and if they are placed horizontally on the water. Surface tension is broken by wet scales and by dry scales that enter the water edge first. Alternately, scales could have been blown into the depositional site from the adjacent mudflat, eroded out of previous mudflat sediment, or were carried to the banks of the tidal channel by predators or scavengers.

CHAPTER 12: FEATHERS

INTRODUCTION

Feathers are rare in the fossil record. However, they are relatively common within the Ingersoll shale. Thus far, fourteen contour feathers have been collected, all from the channel axis (Chapter 6, Fig. 5). They range from 0.43 to 16.50 cm in length and resemble contour feathers seen on present-day birds. The feathers were replaced with bacteria and pyrite. Bacterial replacement has preserved fine structural detail, which is not usually retained in fossil feathers. Some originally hollow structures are preserved in three-dimensions, indicating that pyritization occurred prior to significant compaction. The detailed anatomy of modern bird feathers is reviewed below in order to better explain the structural details that are preserved in the Ingersoll shale feathers.

FEATHER ANATOMY

The following descriptive terminology is accepted by both paleontologists and ornithologists and is well explained by Lucas and Stettenheim (1972). Since typical body contour feathers have all the discernable structural components of other feather types, they are used for introducing feather terminology in general. Feathers are elaborately complex epidermal structures with hierarchical branching (Fig. 38). They essentially can be described as two flat *vanes* separated by a central *shaft* (Kellner, 2002).

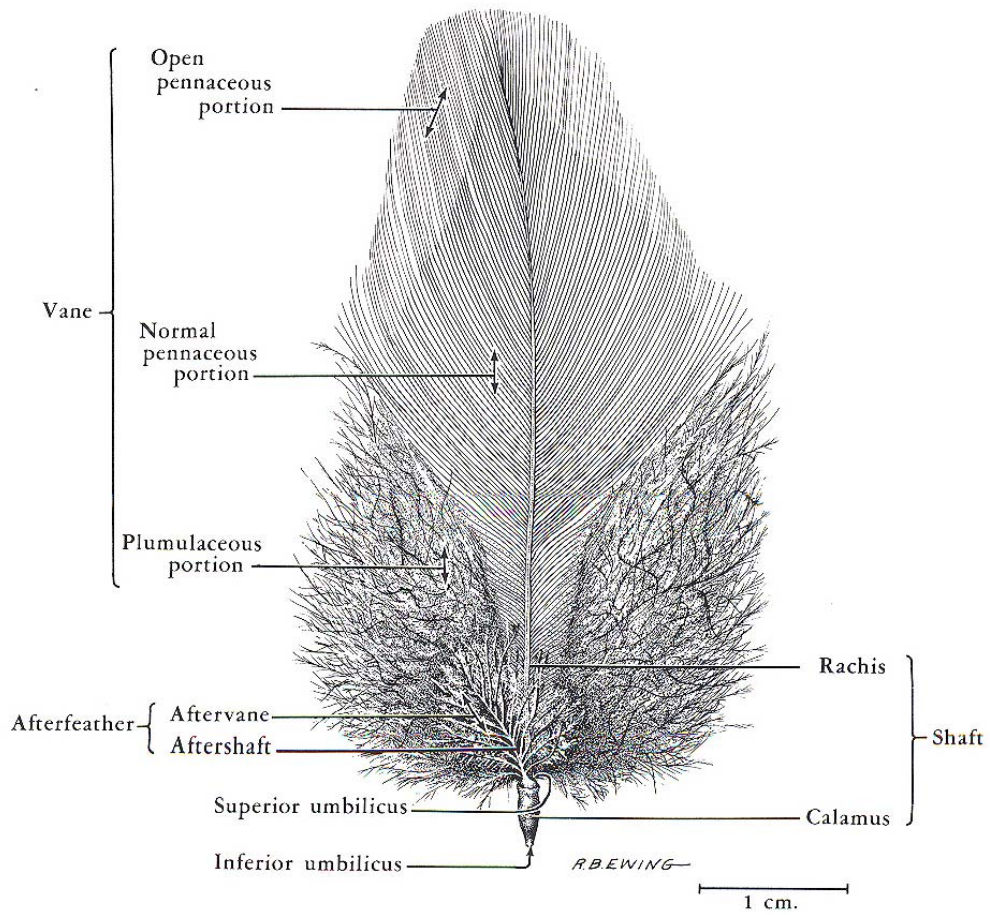


FIGURE 38—Structures found on a typical body contour feather (from Lucas and Stettenheim, 1972).

The shaft gives the feather its primary architecture. The short, tubular, hollow portion of the shaft that is embedded in the feather follicle when attached is referred to as the *calamus*. At the most proximal end of the calamus, there is a hole, known as the *inferior umbilicus*, through which nutrients are delivered to the feather. The remainder of the shaft, extending almost to the tip of the feather, is termed the *rachis*. It is pith filled, subrectangular in cross section (Fig. 39), and tapers distally. The term *dorsal surface* refers to the surface of the feather that faces away from the animal's body. The *ventral surface* faces the body. The ventral side of the rachis usually has a longitudinal groove that varies in width and depth and is referred to as the *ventral groove* (Fig. 39). The boundary between the rachis and the calamus has a small opening to the calamus on the ventral surface of the shaft known as the *superior umbilicus* (Fig. 38). Some feathers have downy outgrowths, referred to as *afterfeathers*, which form around the superior umbilicus (Fig. 38).

Each vane is composed of *barbs*, which branch from the rachis and form an essentially two-dimensional structure. A feather vane can either have a soft, loose, *plumulaceous* texture, or can have a closely knit texture referred to as *pennaceous* (Fig. 38). Toward the basal end of the barbs, near the feather rachis, the barbs lie closely parallel to one another, forming a normal or *closed pennaceous* texture (Fig. 38). Distally from the rachis, or toward the terminal end of the barbs, the closed pennaceous texture is abruptly replaced by an *open pennaceous* texture (Fig. 38). In extant bird species, the plumulaceous feather texture is thought to provide insulation, whereas the pennaceous portion of the feather is used for an airfoil, for water repellency, or to provide a mating

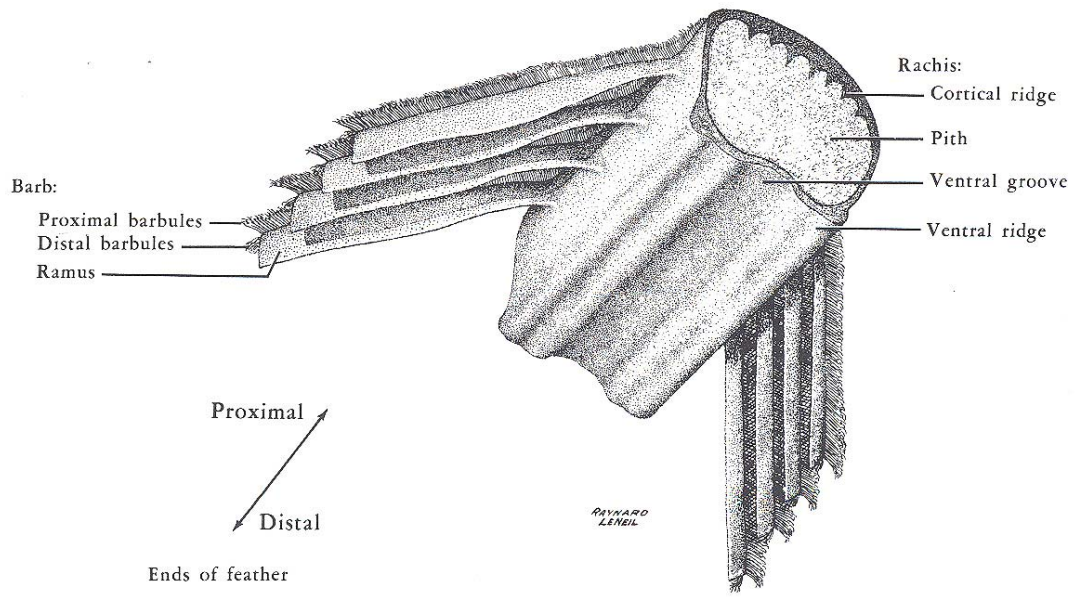


FIGURE 39—Segment of a contour feather in an oblique ventral view, showing the internal structure of the rachis, the attachment of the barbs to the rachis, and the orientation and structure of the barbs (from Lucas and Stettenheim, 1972).

display (Lucas and Stettenheim, 1972). Barbs are composed of a main shaft called a *ramus*, which is a compressed filament, as well as side branches termed *barbules*, which lie opposite to one another in a plane (Figs. 39 and 40). Collectively, barbules along one side of the ramus are referred to as a *vanule*. Barbules along the proximal side of each ramus are called *proximal barbules*, those on the distal edge are called *distal barbules*. The length of proximal and distal barbules decreases toward the tip or terminal end of the barb. All barbules have a thin projection called a *plate* (Fig. 40). Proximal barbules have a flange on the dorsal edge of their plate, and may or may not have fourth-order branching structures at the marginal area (*pennulum*) that are collectively called *barbicels* (Fig. 40). Distal barbules have no dorsal flange, but instead have fourth-order branching, which are hook-like tendrils collectively called *hooklets* (Fig. 40). Hooklets on distal barbules interlock with the dorsal flange on proximal barbules (Fig. 40), locking the feather vane in a plane, thus giving the feather the ability to maintain its integrity when stretched by air pressure. With the ventral side of an isolated feather facing downward, the distal vanules will always overlap the proximal vanules (Richard Prum, personal communication, 2007). This observation allows for the correct orientation of isolated feathers.

FEATHER TYPES

The main categories of feathers are based on variations in their structure, and each structural type serves a different function. The main structural types (Fig. 41A-F) are contour feathers, semiplumes, down feathers, filoplumes, bristle feathers, and powder feathers (Lucas and Stettenheim, 1972; Kellner, 2002). The classification of feathers can

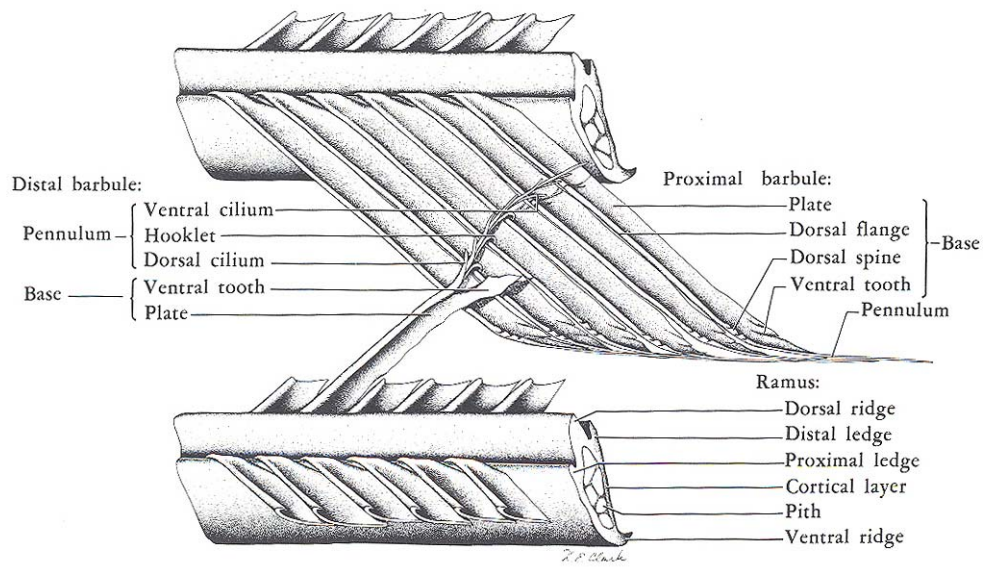


FIGURE 40—Two interlocking pennaceous barbs showing the structure of the ramus and the structure of the distal and proximal barbules (from Lucas and Stettenheim, 1972).

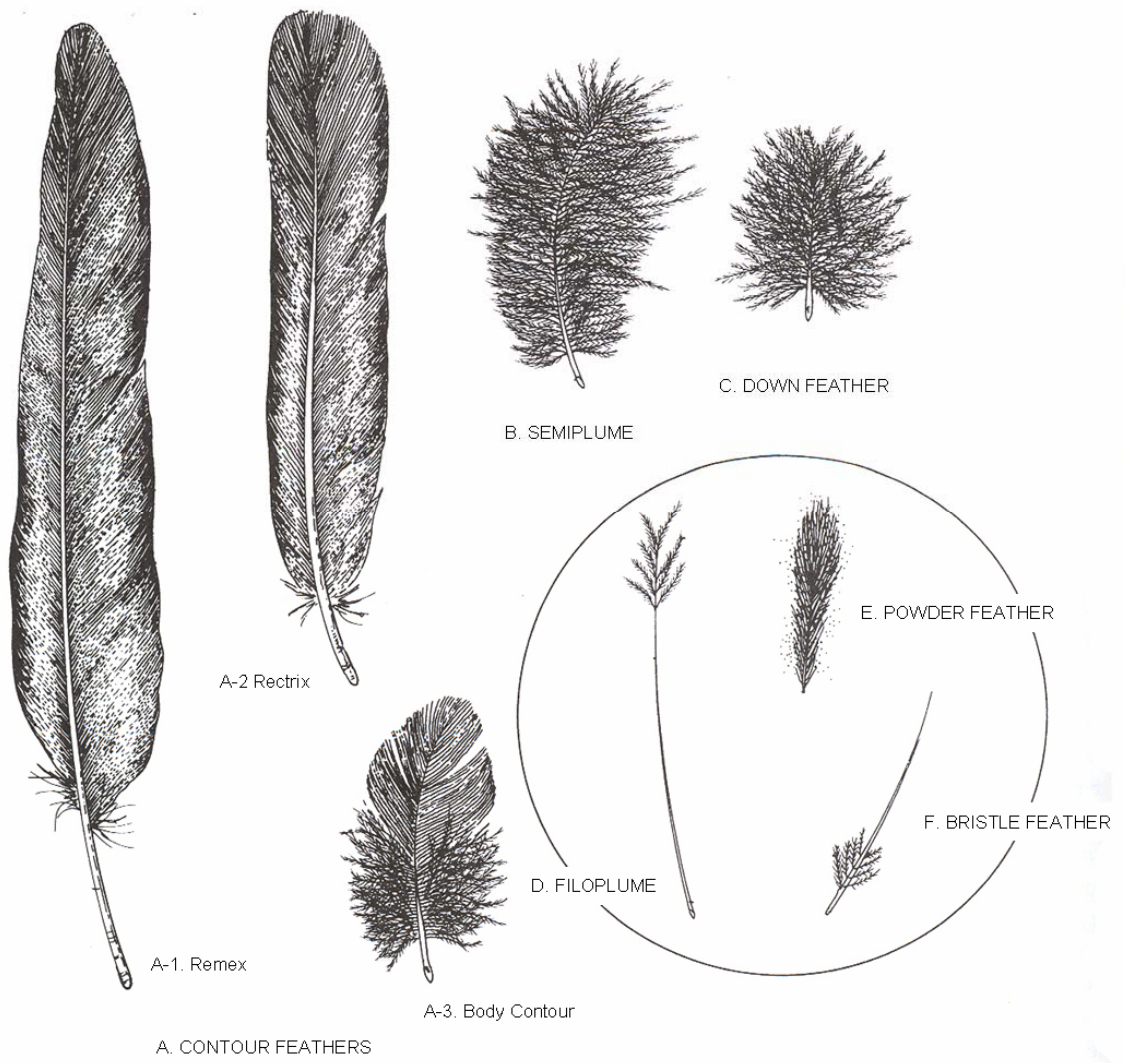


FIGURE 41—Different structural types of feathers (modified from Chatterjee, 1997).

overlap because some types are intermediates between other types (Lucas and Stettenheim, 1972).

Contour feathers are the most common type and are represented by three morphologies (Fig. 41A-1–41A-3). Body contour feathers (Fig. 41A-3) are the most common structural type and cover most of the body in extant theropods (Lucas and Stettenheim, 1972). They are usually medium-sized feathers with a basal plumulaceous portion and a distal pennaceous portion. Aside from body contour feathers providing a protective layer over the skin, they are also thought to provide water repellency (Lucas and Stettenheim, 1972; Stettenheim, 1972, Kellner, 2002). Types of contour feather that are large, stiff, and mostly pennaceous are remiges (wing feathers, Fig. 41A-1) and rectrices (tail feathers, Fig. 41A-2). The vanes of rectrices and remiges are usually asymmetrical, collectively providing the airfoil that gives birds their ability to fly (Lucas and Stettenheim, 1972).

Semiplumes have a long rachis with plumulaceous vanes (Fig. 41B). Semiplumes are insulating feathers and help fill the outer contour of the bird. Down feathers are small, fluffy, have a short rachis or none at all, and lack interconnecting barbs (Fig. 41C). These feathers help provide insulation (Stettenheim, 1972). Filoplumes are composed of a shaft with barbs only on their most distal portion (Fig. 41D). Filoplumes are thought to provide sensory input to aid in positioning the rectrices and remiges (Stettenheim, 1972). Powder feathers (Fig. 41E) shed a fine, non-wettable, keratin powder that is used in preening and possibly causes other feathers to become waterproof (Stettenheim, 2000). Bristle feathers have a stiff rachis and may or may not have barbs at the base (Fig. 41F). These feathers are commonly found around the eyes, the base of the bill, or elsewhere on the head, and

are thought to have a sensory function by transmitting air-pressure changes (Stettenheim, 1972).

FEATHER TAPHONOMY

Feathers are chemically very stable but do not typically endure in nature long enough to become fossilized because of decomposition caused by bacteria (Davis and Briggs, 1995; Lin et al., 1992). The major microstructural component of feathers is β -pleated sheet protein (β -keratin), which is twisted into microfilaments (Lin et al., 1992; Davis and Briggs, 1995; Burt and Ichida, 1999; Stettenheim, 2000), that are 3-4 nm in diameter (Schweitzer et al., 1999). These proteins are not digested by most bacterially-produced proteolytic enzymes such as trypsin, pepsin, or papain (Goddard and Michaelis, 1934; Harrap and Woods, 1964; Lin et al., 1992; Davis and Briggs, 1995; Shawkey, 2005). In order for bacteria to devour feather keratin, they must produce keratinase, an enzyme that catalyzes the hydrolysis of keratin (Lin et al., 1992). The bacterial glycocalyx (extra-cellular polymeric material) helps feather-decaying bacteria transfer nutrients from the substrate to the bacteria by acting as an ion-exchange medium. Glycocalyx also helps bacteria attach to inert surfaces, protects bacteria from attack by other bacteria, and helps bacteria digest insoluble nutrient substrates (Davis and Briggs, 1995).

Two bacteria that have been isolated from the feathers of extant bird species (Shawkey, 2005) are known to produce high quantities of keratinase: the anaerobic, coccus-shaped *Kocuria rhizophila* (Kovács et al., 1999) and the rod-shaped *Bacillus licheniformis* (Williams et al., 1990). *Bacillus licheniformis* can function in anaerobic and

aerobic environments but it is only known to affect feathers that have first been autoclaved (Davis and Briggs, 1995).

In the fossil record, feathers have been found to be preserved as carbonized traces, replaced by lithified bacteria, as imprints, as inclusions in amber, as external molds in coprolites, or possibly as original proteins (Davis and Briggs, 1995; Schweitzer et al., 1999). In 69% of feather-bearing deposits, the feathers are preserved as carbonized traces and are usually found in mudstone (Davis and Briggs, 1995). The carbonized traces have a honeycomb-like texture similar to that of the glycocalyx of modern feather-degrading bacteria. Carbonized glycocalyx can be restricted to the feather keratin, preserving feather details, or it can extend beyond the feather boundaries, which obscures the structural details by placing a film of carbon over the surrounding matrix. Bacterial autolithification occurs when the feather-degrading bacteria are themselves replaced with authigenic minerals prior to their decomposition, retaining their shape in three-dimensions. This type of preservation has been observed in the soft-tissue remains of the Messel Shale, Germany (Wuttke, 1983; Franzen, 1985). Within this deposit, feather-decaying bacteria are replaced by siderite and align themselves with the feather substrate giving the appearance of a “flowing mat” (Davis and Briggs, 1995). This alignment apparently maximizes the bacteria’s contact with the feather, thus, increasing their nutritional intake (Wuttke, 1983; Davis and Briggs, 1995).

Feather preservation by imprintation is restricted to the Jurassic Solnhofen Limestone, the fossil locality famous for preserving feathers of *Archaeopteryx* (Davis and Briggs, 1995). In this mode of preservation, no organic carbon remains. Bacteria are thought to have colonized the underside of the feather, causing changes in the

microenvironment and promoting the lithification of the underlying sediments (Davis and Briggs, 1995). Subsequently, the bacteria completely consumed the feathers, and the overlying substrate was then pressed into the void space preserving a mold and a cast of the feather's ventral surface (Davis and Briggs, 1995). Feathers can also be preserved as external molds composed of apatite within coprolites. This mode of preservation has been reported in marine deposits of the Miocene Chesapeake Group, Maryland (Wetmore, 1943).

Amber is the best preservational medium for feathers (Davis and Briggs, 1995). Preservation of feathers as organic inclusions within amber is achieved through the dehydration of keratin (Grimaldi et al., 1994; Davis and Briggs, 1995; Martínez-Delclòs et al., 2004). Feather preservation in amber shows exquisite structural details such as barbules and barbicels; in some rare cases, amber has been shown to preserve color variations (Kellner, 2002).

The final mode of feather preservation is known from only one specimen. Small, fibrous structures, possibly feathers, were found associated with an articulated specimen of *Shuvuuia deserti*, a small coelurosaurian dinosaur, from Late Cretaceous sediments in southwestern Mongolia (Schweitzer et al., 1999). The fibers were morphologically consistent with feathers, and the immunological techniques that were employed suggested original protein preservation (Schweitzer et al., 1999).

Feathers from Mesozoic strata have been discovered in a wide range of environments. Most fossil feathers are found in lake sediments, where they are dominantly preserved as carbonized traces (Davis and Briggs, 1995; Kellner, 2002). Second in abundance are non-aquatic terrestrial environments. Most feathers from these

environments are entombed in amber (see Kellner, 2002). The major feather-producing environments discussed above show a taphonomic bias toward preserving feathers from theropods that inhabited inland freshwater and adjacent environments (Davis and Briggs, 1995; Kellner, 2002).

In 77% of depositional sites with fossilized feathers, no biomineralized theropod material is preserved (Davis and Briggs, 1995). This statistic has been taken to mean that the feathers were deposited in acidic environments in which bones would have dissolved (Hedges, 2002; Clayburn et al., 2004).

FEATHERS FROM MESOZOIC STRATA

As shown in Table 1, there are 19 confirmed deposits worldwide that preserve fossil feathers in Mesozoic strata (Kellner, 2002). Only 2 of these occurrences are in North America (Kellner et al., 1994; Davis and Briggs, 1995). One of these is from the Turonian sediments of the Raritan Formation in New Jersey (Grimaldi and Case, 1995). Here a semiplume feather, as well as other feather fragments, have been preserved in amber. The Campanian sediments of the Foremost Formation in Southern Alberta, Canada, has preserved at least four feathers, also in amber, one of which possibly retains its original color pattern (Kellner, 2002). One unconfirmed occurrence in North America is from the carbonate-rich Niobrara Formation in Kansas. These feathers were reported to be articulated on *Hesperornis* (Williston, 1896), but the specimen has been lost (Davis and Briggs, 1995; Kellner, 2002). The only two known occurrences of Mesozoic fossil feathers from estuarine facies are from Kazakhstan. One single, isolated feather was found within the upper Turonian-Coniacian sediments of the Zhirkindeck Formation, and

TABLE 1—Confirmed occurrence of fossil feathers from Mesozoic strata (modified from Kellner, 2002).

DEPOSIT	GEOLOGIC AGE	DEPOSITIONAL ENVIRONMENT
Southern Alberta, Canada	Campanian	Terrestrial
Taldysay, Kazakhstan	Santonian-Campanian	Estuarine
Northern Siberia, Russia	Santonian	Terrestrial
Kuji, Japan	Santonian	Terrestrial
Tjulkeli, Kazakhstan	Upper Turonian-Coniacian	Estuarine
New Jersey, United States	Turonian	Terrestrial
Chaibu-Sumi, Inner Mongolia, China	Early Cretaceous	Lacustrine (?)
Khurit-Ulan-Bulak, Mongolia	Early Cretaceous	Lacustrine
Gansu Province, China	Early Cretaceous	Lacustrine
Araripe Basin, Brazil	Aptian	Lacustrine
Koonwarra, Australia	Barremian-Aptian	Lacustrine
Las Hoyas, Spain	Barremian	Lacustrine/palustrine
Transbaikalia, Russia	Hauterivian-Barremian	Lacustrine
Sheen Khuduk, Mongolia	Hauterivian-Barremian	Lacustrine
Jessine, Lebanon	Hauterivian	Terrestrial
El Montsec, Spain	Berriasian-Valanginian	Lacustrine
Gurvan Eren, Mongolia	Berriasian	Fluvial/lacustrine
Liaoning, China	Tithonian-Berriasian	Lacustrine
Solnhofen, Germany	Lower Tithonian	Lagoonal

another small asymmetrical feather was described from the Santonian-Campanian sediments of the Bostobe Formation (Kellner, 2002).

The oldest fossil feather was found in the Late Jurassic, Solnhofen Limestone, southern Germany. This structurally modern, primary flight feather was first reported by von Meyer (1861) and named *Archaeopteryx lithographica*. *Archaeopteryx* is considered to be the oldest undisputed fossil avian. Feathers were formerly considered to be the diagnostic character of the class Aves. The idea that feathers were exclusive to birds remained accepted until the late 1990's but changed with the discovery of exceptionally well-preserved theropods in the Early Cretaceous lacustrine strata in the Liaoning province of China. These non-avian theropods have integumentary structures that strongly resemble feathers. The feather structures seen in these dinosaurs range from simple filaments, as seen in *Sinosauropteryx prima* (Currie and Chen, 2001), to branched filamentous protofeathers in tyrannosaurids (Xu et al., 2004), to retrices with symmetrical vanes, as seen in *Caudipteryx* and *Protoarchaeopteryx* (Ji et al., 1998). *Microraptor gui* has the most advanced feathers seen in a non-avian theropod species. Their asymmetrical, pennaceous feathers probably served a primitive aerodynamic function such as gliding (Xu et al., 2003). Overall, feathers appear to increase in structural complexity from theropod dinosaurs to modern birds (Norell and Xu, 2005). The discovery of feathered dinosaurs has strengthened the hypothesis that birds evolved from theropod dinosaurs, a hypothesis that is now widely accepted in the paleontological community. This leads to the conclusions that feathers did not evolve for flight and that they are no longer a diagnostic feature of Aves (Ji et al., 1998). These feathered dinosaur discoveries have sparked new debates on why feathers evolved. Originally they may have served for water

repellency (Dyck, 1985), insulation (Ji et al. 1998), or thermoregulation (Xu et al., 2004), or other purposes.

METHODOLOGY FOR COLLECTING AND EXAMINING FOSSIL FEATHERS

The Ingersoll shale feathers were discovered by using normal quarrying techniques previously described in Chapter 5. Some feather specimens were coated with polyvinyl alcohol (PVA) to prevent deterioration via pyrite oxidation. Other specimens were slowly dried by placing them in containers with limited exposure to open air (containers with the lid unsealed). Due to the soft nature of the matrix, uncoated feather specimens were dried for approximately two months prior to preparation. Once dry, the overlying matrix was removed from the feather under a binocular microscope using a needle. All feathers and feather structures were measured with hand calipers. During preparation, feather samples were taken from the counterparts of six uncoated specimens for microscopic and elemental analysis via scanning electron microscopy (SEM) and energy-dispersive spectroscopy (EDS).

SEM and EDS analysis on two feather specimens (KIS-706 and KIS-709) was performed using a JEOL JSM-7000F (Field Emission Scanning Electron Microscope) in the Materials Engineering Department, Auburn University. Some feather samples were sputter-coated with gold to ensure conductivity. Sputter-coating was done for only 15 seconds in order to prevent obscuring fine details on the feather surface. The SEM was set to 20.0kv, and the specimens were examined under variable working distances.

Two different cataloging prefixes were given to the specimens. The prefix CSUK (Columbus State University Cretaceous) was given to the first three specimens recovered

from the deposit, discovered while the author was a student at Columbus State University. The prefix KIS (Cretaceous Ingersoll shale) was given to specimens collected while the author was attending Auburn University.

RESULTS AND DESCRIPTIONS

General Results

Fourteen contour feathers were collected from the channel axis of the Ingersoll shale; they are described below. The feathers were found throughout the entire thickness of the clay lens, excluding the higher energy zones 1 and 2 (see Fig. 6, Chapter 6). The feathers range from 0.43 cm to 16.50 cm in length and are 0.35-3.10 cm in width. Other measurements are given in Table 2. Twelve of the feathers are body contour feathers, one appears to be a rectrix (tail feather), and the other is a remix (wing feather). Some of the feathers are complete and include the rachis, calamus, and both vanes. Other feather specimens are incomplete due to partial decay prior to deposition and damage that occurred during excavation. Most of the feathers show the transition from a normal-pennaceous texture near the rachis to a closed-pennaceous texture distally. Although there is a taphonomic gradient between well-preserved specimens and poorly preserved specimens, they all show the preservation of rami and both distal and proximal barbules. Some fossil feathers are extraordinarily well preserved, and one even shows the fine detail of barbicular structures (hooklets), which is rarely seen in the fossil record. They range in color from black to dark brown and commonly have the rachis and calamus preserved in three-dimensions via pyritization.

TABLE 2—Measurements of Ingersoll shale feathers and their structures.

Specimen Number	Length (cm)	Width (cm)	Average Rachis Width (mm)	Average Calamus Width (mm)	Calamus Length (mm)	Average Barb Width (mm)	Longest Complete Barb (mm)	Shortest Complete Barb (mm)	Barbule Length (mm)	Angle of Barb to Rachis	Barb Density per mm of Rachis	Barbule Density per mm of Barb
CSUK-03-05-01	1.26	0.77	0.08	N/A	N/A	0.20	6.40	0.54	0.15	35°-15°	3	~25
CSUK-03-05-02	2.45	0.65	1.20	0.91	0.70	0.36	N/A	N/A	0.30	24°-22°	2-3	~30
CSUK-03-05-03	1.30	0.70	0.10	N/A	N/A	0.21	11.00	4.00	0.40	24°-10°	3	~16
KIS-700	4.71	0.80	0.22	N/A	N/A	0.29	15.00	1.44	0.25	80°-30°	3	25-30
KIS-701	1.27	0.78	0.15	N/A	N/A	0.41	8.00	1.66	0.36	40°	3	~35
KIS-702	3.25	1.75	N/A	N/A	N/A	N/A	N/A	N/A	N/A	30°	4	~25
KIS-703	0.43	0.36	0.32	N/A	N/A	N/A	N/A	N/A	N/A	36°-22°	4	N/A
KIS-704	3.16	0.73	0.46	1.20	7.05	0.22	7.64	4.90	0.54	33°	4	~30
KIS-705	0.84	0.64	0.71	N/A	N/A	0.53	N/A	N/A	0.50	38°-33°	3-4	~26
KIS-706	1.650	3.10	1.77	N/A	N/A	0.55	21.80	8.4	0.56	35°	2-3	~23
KIS-707	2.68	0.65	1.22	1.22	4.50	0.55	8.26	1.65	0.38	40°	4	~30
KIS-708	3.10	2.08	0.48	0.90	8.14	0.52	6.55	0.40	0.24	52°	3	~30
KIS-709	8.35	2.24	3.18	3.26	2.12	0.49	18.20	16.76	0.51	42°-24°	3	~28
KIS-710	1.28	0.35	0.19	N/A	N/A	0.32	5.20	1.90	0.23	30°	3	~32

Specimen CSUK-03-05-1F, Body Contour Feather

This feather is small, obovate, dark brown, with a rounded tip, and a slightly curved, very thin rachis (Fig. 42A). The proximal portion of the feather is missing, and the barbs from the left vane are still enclosed in the matrix. The basalmost barbs do not appear to be interlocking. Vanes near the rachis have a closed-pennaceous texture at the basal ends of the barbs and an open-pennaceous texture terminally. Barbs are of variable length and curve slightly upward. Distal vanules overlap the proximal vanules, indicating the feather was fossilized with its dorsal side facing upward.

Specimen CSUK-03-05-2F, Body Contour Feather

This feather is dark brown and has a slightly curved, pyritized rachis (Fig. 42B). The rachis tapers distally and is preserved in three-dimensions. Remnants of the calamus are pyritized. The terminal ends of both vanes are enclosed in the matrix, both basally and distally. The right vane was damaged in its middle portion during excavation, and the distal portion of the right vane was damaged during preparation. Portions of the left and right vane that are exposed have a consistent closed-pennaceous texture. The barbs curve slightly downward. Proximal vanules overlap distal vanules, indicating the feather was fossilized with its ventral side facing upward.

Specimen CSUK-03-05-3F, Body Contour Feather

This feather is small, ovate, black, fluffy in appearance, and has a slightly curved, very thin rachis (Figs. 42C and 42D). The proximal portion of the feather is missing, and barbules on the distal end are still enclosed in the matrix. On the counterpart, the basal portion of the feather is still embedded in the matrix. The basal most barbs are long and curve upward. Both vanes have a closed-pennaceous texture at the basal end of the barbs

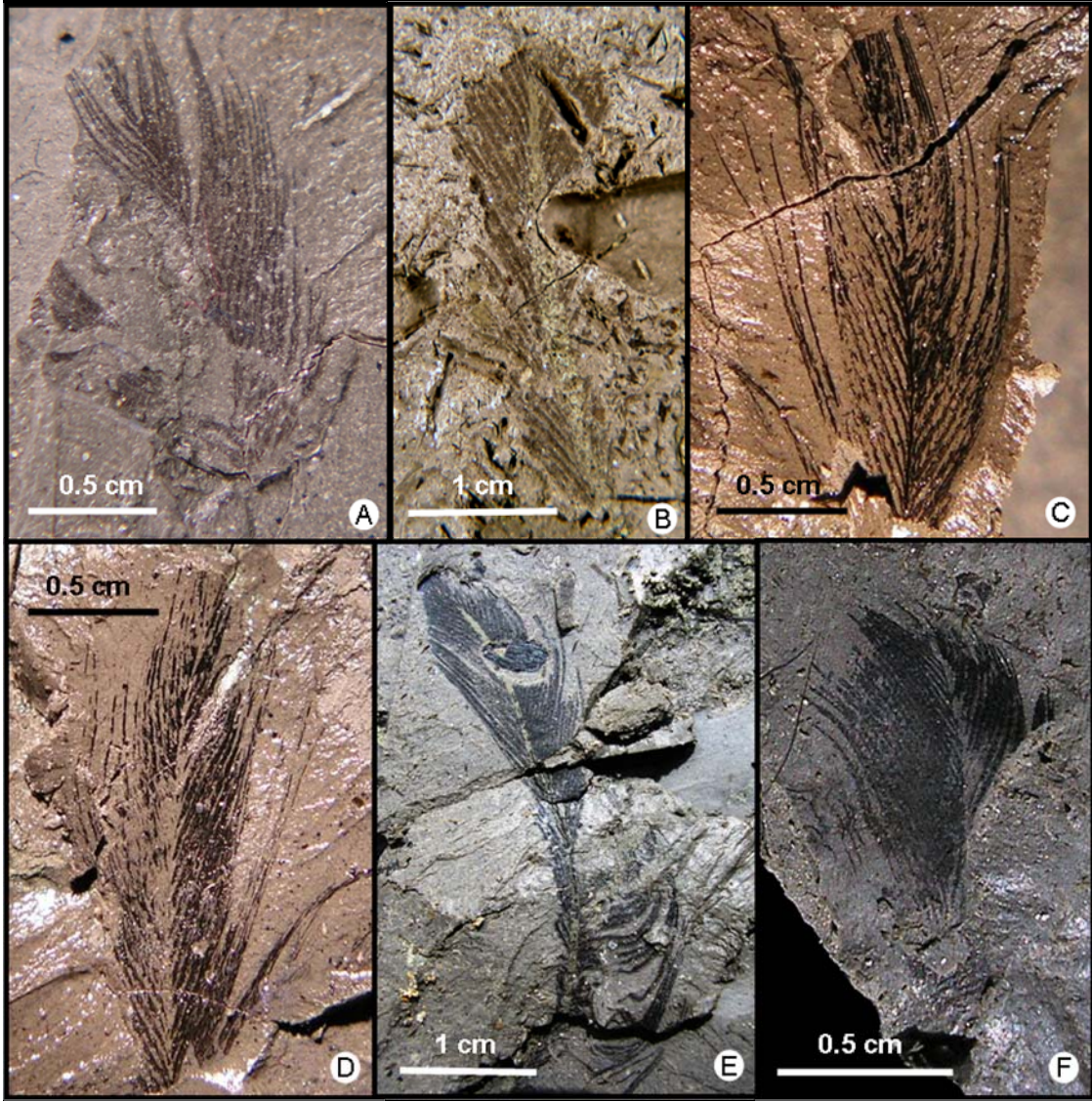


FIGURE 42—Body contour feathers. (A) CSUK-03-05-1F. (B) CSUK-03-05-2F. (C, D) CSUK-03-05-3F part and counterpart, respectively. (E) KIS-700. (F) KIS-701. Photographed by Patrick Bingham (Auburn University).

and an open-pennaceous texture terminally. Distal vanules overlap proximal vanules, indicating the feather was fossilized with its dorsal side facing upward.

Specimen KIS-700, Body Contour Feather

This feather is large, ovate, black, and has a curving rachis (Fig. 42E). The feather has a pennaceous portion distally that measures 2.16 cm in length, and a plumulaceous portion basally that measures 2.55 cm in length. Most of the feather is preserved except for the calamus, and a portion of the upper right vane came off during excavation; this portion was not recovered. The rachis is mostly pyritized, with some portions still having a black, apparently carbonized film covering, possibly the cortex (see Fig. 39). The vanes on the pennaceous portion of the feather have a closed-pennaceous texture at the basal ends of the barbs, and open slightly terminally. The barbs curve upward on the right vane and downward on the left vane. On the pennaceous portion of the feather the barbs branch from the rachis at 30°, gradually decreasing distally, until they become nearly parallel to the rachis at the acute tip. The distal vanules overlap proximal vanules, indicating the feather was fossilized with its dorsal side facing upward.

Specimen KIS-701, Body Contour Feather

This feather is small, obovate, black, with a slightly curved, very thin rachis (Fig. 42F). The proximal portion of the feather is missing, as is the lower half of the right vane. The feather tip is round. The vanes have a closed-pennaceous texture at the basal ends of the barbs, and an open-pennaceous texture at the terminal ends of the barbs. Barbs curve upward on the right vane and downward on the left vane. Both the proximal and distal barbules are preserved; they decrease in length terminally until they align parallel to the

ramus. The proximal vanules overlap distal vanules, indicating the feather was fossilized with its ventral side facing upward.

Specimen KIS-702, Body Contour Feather

This large feather is oblong, black, and poorly preserved (Fig. 43A). It appears that only the distal portion of the feather is preserved, so its true length is undeterminable. The basal and distal portions of the feather are missing. The longitudinal middle section, including the rachis, is obstructed by a thin sheet of matrix and an angiosperm leaf. The barbs curve slightly upward. The angle at which they diverge from the rachis remains consistent throughout the entire length of the vanes. Both proximal and distal barbules are present along some portions of the rami. Most barbules appear to be preserved as a thick pyritized and carbonized sheets.

Specimen KIS-703, Body Contour Feather

This black, partial feather (closed-pennaceous portion) is the smallest of the Ingersoll shale feathers (Fig. 43B). There are 13 barbs on the right vane curving slightly outward and faint traces of the rachis and 10 barbs on the left vane. Both proximal and distal barbules are preserved, but could not be measured. The feather orientation could not be deciphered.

Specimen KIS-704, Body Contour Feather

The feather is black, obovate, dark brown, and has a slightly curved, very thin rachis (Fig. 43C). The rachis and calamus are preserved with pyrite. The rachis tapers distally. Distal portions of the feather are missing and the left vane is only preserved as an impression. The right vane is carbonized and pyritized. Both vanes have a closed-pennaceous texture basally, and an open-pennaceous texture terminally. The barbs curve

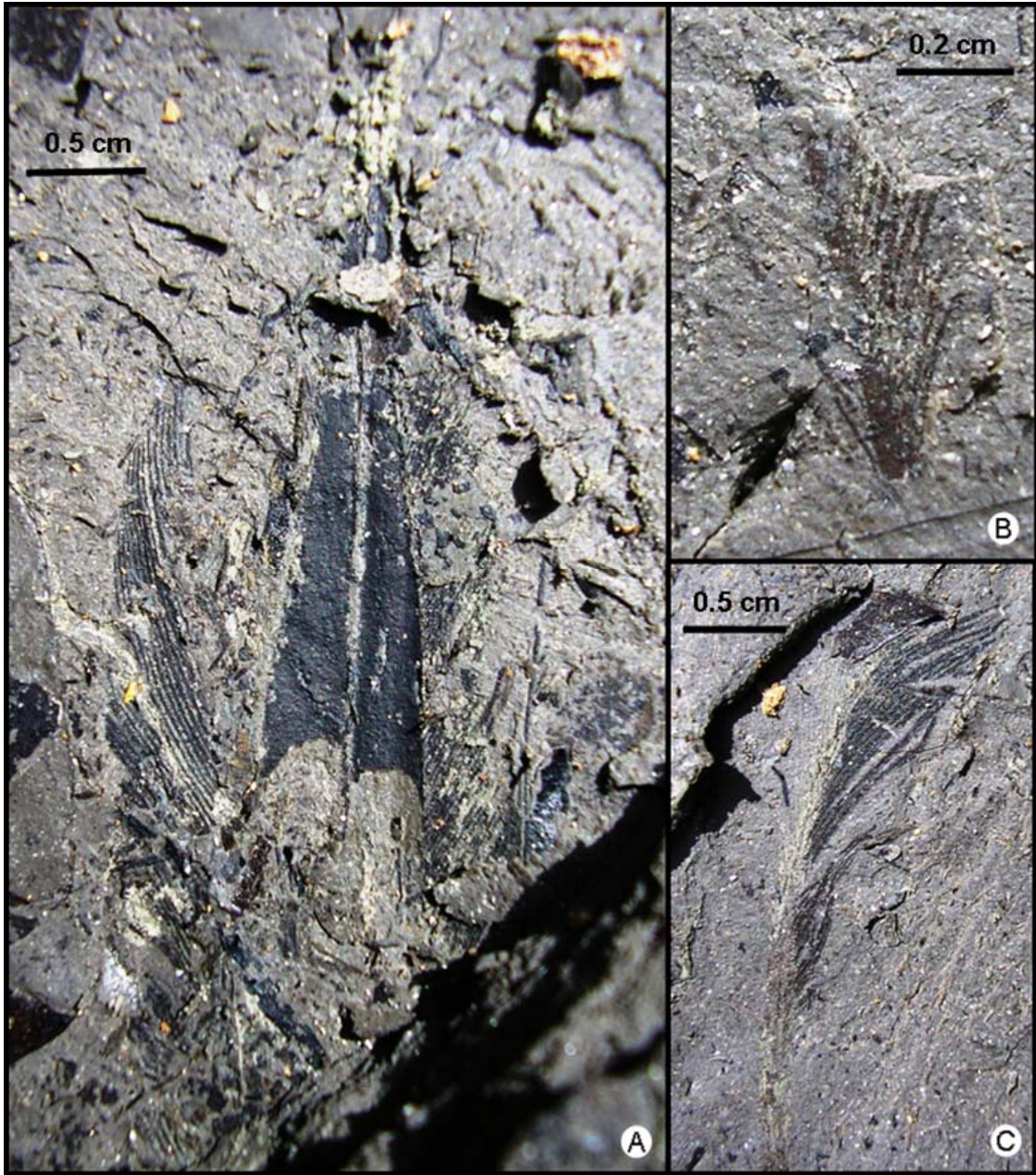


FIGURE 43—Partial contour feathers. (A) KIS-702. (B) KIS-703. (C) KIS-704. Figures A and C photographed by Patrick Bingham (Auburn University).

slightly downward. Both proximal and distal barbules are preserved and decrease in length terminally. The distal vanules overlap proximal vanules, indicating the feather was fossilized with its dorsal side facing upward.

Specimen KIS-705, Body Contour Feather

This partially preserved feather is small and dark brown (Fig. 44A). The proximal and distal portions of the feather are missing and there are 7 barbs comprising the left vane and 9 barbs comprising the right vane. The vanes have a closed-pennaceous texture and the angle of their barbs remains constant along the entire rachis. Both proximal and distal barbules are preserved and have equal lengths that stay consistent along the entire portion of the rami. The terminating ends of the barb on the left vane shows damaged barbules (Fig. 45D). Barbicel structures (possibly hooklets) branch from the pennulum of the distal barbules (Fig. 45C). The proximal vanules overlap distal vanules, indicating the feather was fossilized with its dorsal side facing upward.

Specimen KIS-706, Tail Feather

The black, oblong feather is the largest to be discovered in the Ingersoll shale (Fig. 46). The rachis has the ventral groove preserved. The proximal portion of the feather is missing, and some portions of the vanes are still enclosed in the matrix. There are several barbs on both vanes that appear to be ‘unzipped’ (Fig. 45B). Vanes on the entire length of the feather has a closed-pennaceous texture. Both proximal and distal barbules are preserved and decrease in length at the terminal end of the barb. The proximal vanules overlap distal vanules, indicating the feather was fossilized with its ventral side facing upward.

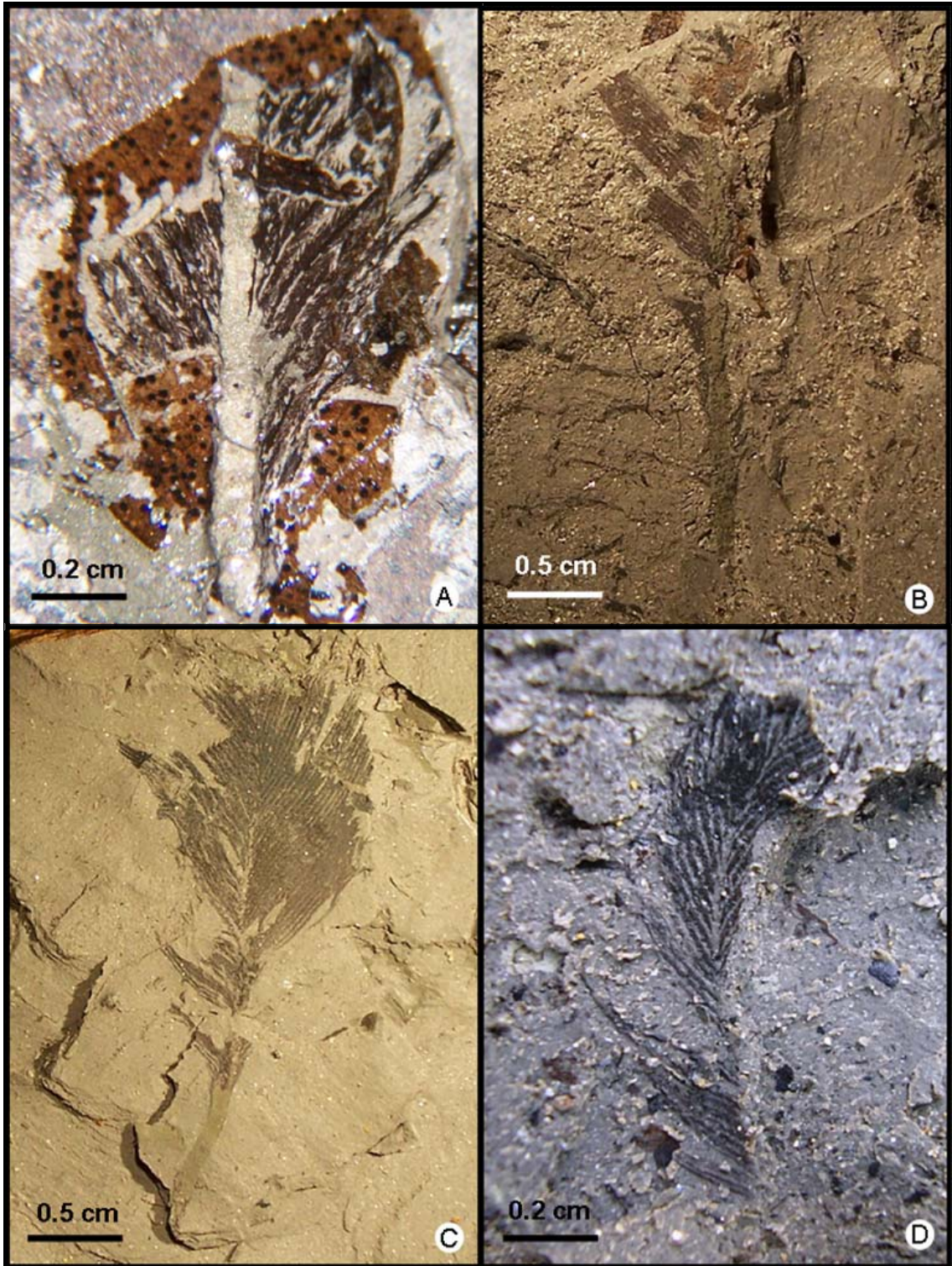


FIGURE 44—Body contour feathers. (A) KIS-705. (B) KIS-707. (C) KIS-708. (D) KIS-710. Figure D was photographed by Patrick Bingham (Auburn University).

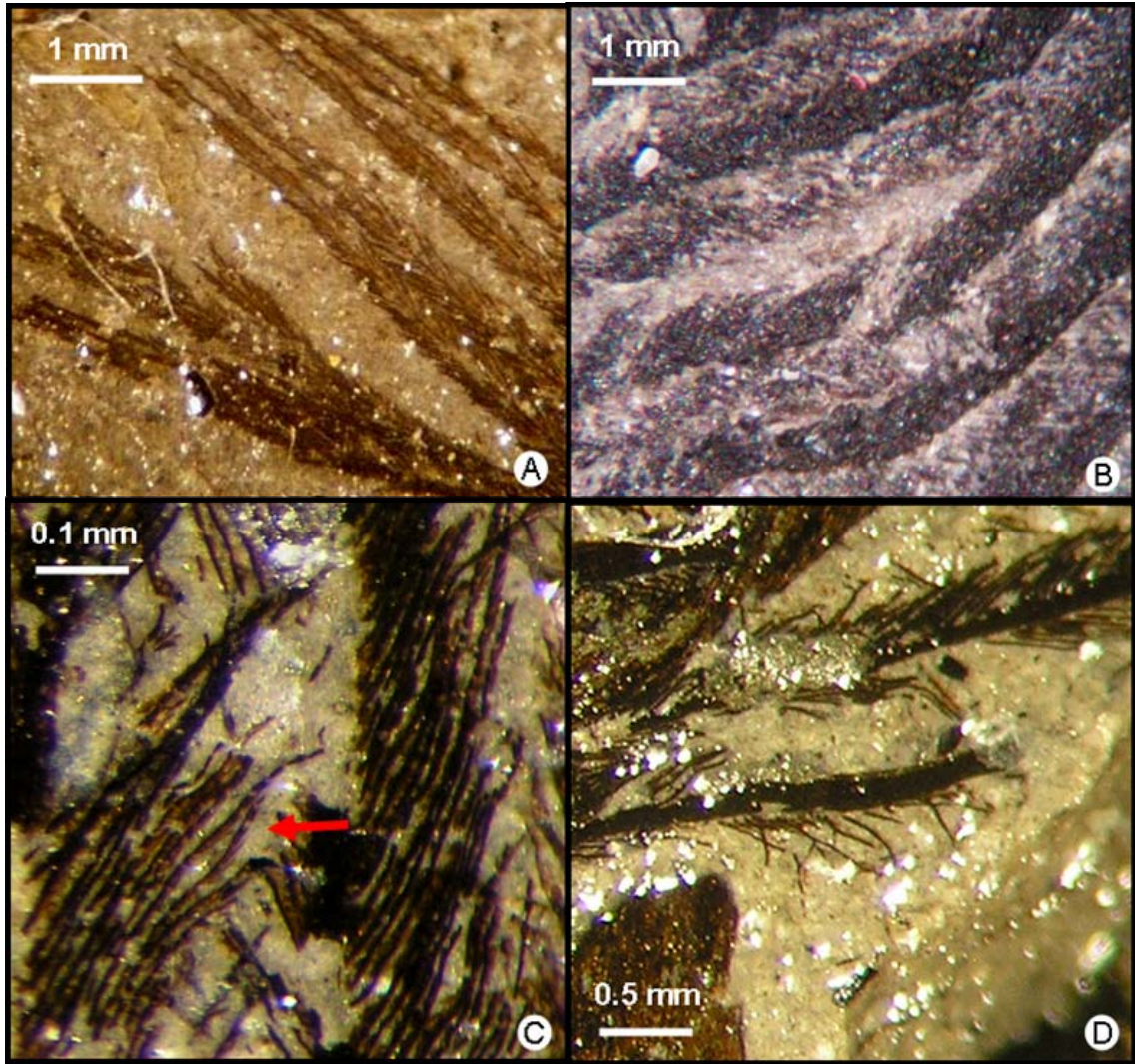


FIGURE 45—Structural and taphonomic features of Ingersoll shale feathers. (A) Tip of the barbs on CSUK-03-05-1F, showing a decrease in length of the distal and proximal barbules. (B) “Unzipping” of the proximal and distal barbules in KIS-706. (C) Close-up photograph of distal barbules on KIS-705 (red arrow points to barbicels). (D) Barb on the right vane of KIS-705 showing degradation of the barbules prior to deposition.



FIGURE 46—Composite image of KIS-706, the longest contour feather discovered in the Ingersoll shale (possibly a rectrix). Photographs and composite image made by Patrick Bingham (Auburn University).

Specimen KIS-707, Body Contour Feather

The feather is dark brown and has a straight rachis that is preserved via pyritization and tapers distally (Fig. 44B). The calamus is also pyritized. Only the left vane is preserved and it has a closed-pennaceous texture. Both proximal and distal barbules are preserved and decrease in length terminally. Proximal vanules overlap distal vanules, indicating the feather was fossilized with its ventral side facing upward.

Specimen KIS-708, Body Contour Feather

The feather is dark brown, obovate, and almost complete (Fig. 44C). The calamus and rachis are both preserved with pyrite. Black carbonized material on the outside of the calamus indicates that remnants of the cortex are preserved. Only the distal-most portion of the feather is missing and the tip appears to be rounded. The left vane appears to have been damage prior to deposition. The vanes have a closed-pennaceous texture basally, and an open-pennaceous texture terminally. The barbs are curving slightly upward on the right vane and downward on the left vane. Both proximal and distal barbules are preserved and decrease in length terminally. The orientation of the feather is undeterminable because the left vane has proximal barbs overlapping distal, and on the right distal overlapping proximal.

Specimen KIS-709, Wing Feather

This poorly preserved, oblong, asymmetrical feather is the second largest recovered from the deposit (Figs. 47A and 47B). The rachis and calamus are pyritized in three-dimensions and the calamus tapers towards the base. Both vanes have a closed-pennaceous texture. The barbs curve slightly upward on the right vane and downward on the left vane. The barbs branch from the rachis at 42° on the left vane and 24° on the right



FIGURE 47—Part and counterpart of KIS-709 (A) Asymmetry of the left and right vanes. (B) Three-dimensionally preserved rachis.

vane. Both the proximal and distal barbules are present and decrease in length terminally. The distal vanules overlap proximal vanules, indicating the feather was fossilized with its dorsal side facing upward.

Specimen KIS-710, Body Contour Feather

The feather is small, ovate, dark brown, and has a slightly curved, very thin rachis (Fig. 44D). The feather tip is rounded and parts of the right vane are missing. The basal most barbs have an open-pennaceous texture. The vanes near the middle of the rachis have a closed-pennaceous texture at the basal ends of the barbs, and an open-pennaceous texture at the terminal ends of the barbs. The barbs range in length and curve slightly upward. Both proximal and distal barbules are preserved and have equal lengths. Both decrease in length terminally. The proximal vanules overlap distal vanules, indicating the feather was fossilized with its dorsal side facing upward.

TAPHONOMIC PROCESSES

SEM analysis at relatively low magnifications revealed fine details of the rachis, rami, and barbules, indicating that some of the feathers preserve relief (Fig. 48A). As seen previously, pyritization in the Ingersoll shale biota was rapid enough to preserve specimens in three dimensions. SEM analysis at high magnification revealed the presence of framboidal pyrite, individual clusters of rhombohedral pyrite crystals, and microcrystalline pyrite crystals (Fig. 48D). With a light microscope, pyrite could be seen dispersed throughout the feather calamus, rachis, and vanes.

Most of the feathers are dark brown to black and significantly darker than the rock matrix, giving the appearance that they are preserved by concentrations of carbonized

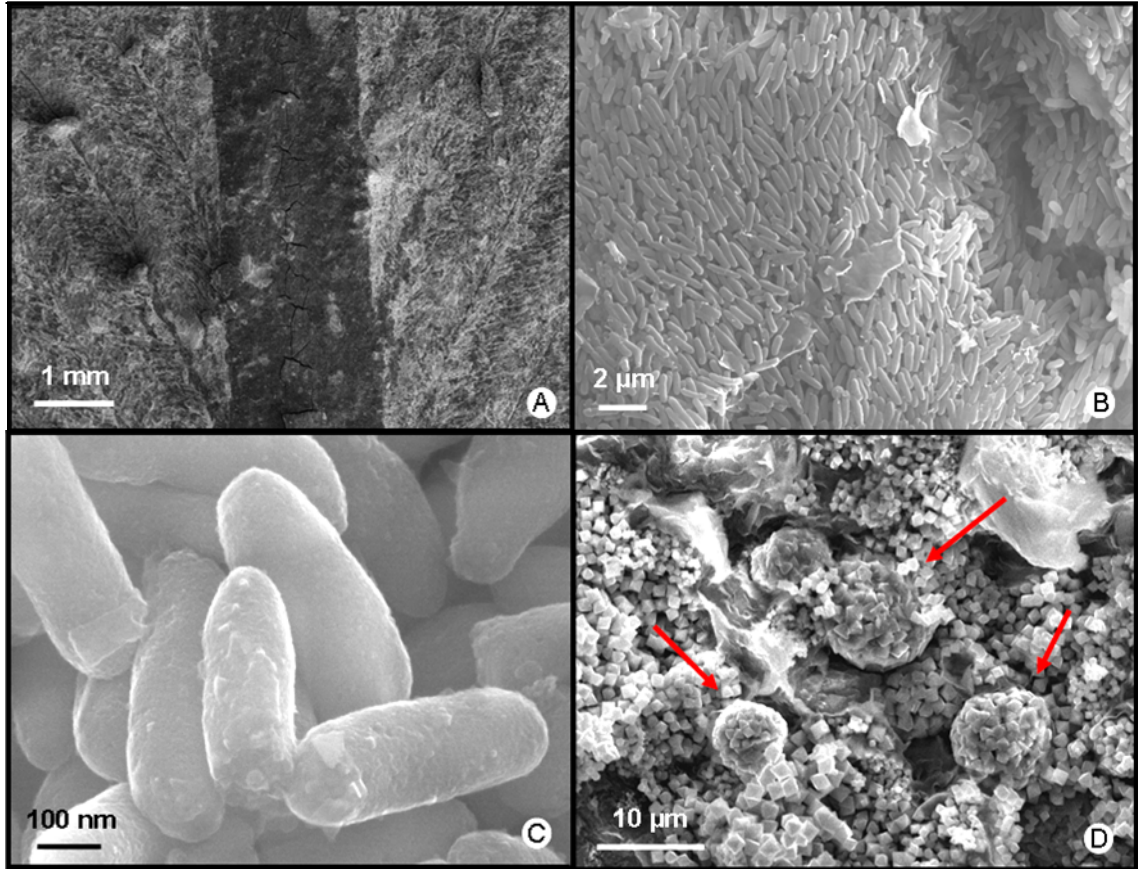


FIGURE 48—SEM images of KIS-706 and KIS-709. (A) SEM image of KIS-706 showing rachis (center), barbs, and barbules. (B) SEM image of KIS-709 showing the “flow-mat” alignment of bacilliform bacteria at a branching intersection of the ramus (lower right) and a barbule (notice how the bacilliform bacteria have reoriented themselves at the intersection). (C) Close-up image of the bacteria in KIS-706. (D) SEM image of KIS-709 showing framboids (red arrows) and cluster of pyrite crystals .

residue (carbonization) from the original feather. SEM examinations at high magnifications reveal that at least two of the fossil feathers are replaced by mats of small, rod-shaped structures (Figs. 48B and 48C) that compare favorably to *Bacillus*-like bacteria. These rod-shaped bacteria are preserved in three dimensions and are $\sim 1 \mu$ in length. Intermittently dispersed throughout the bacilliform bacterial mats are coccoid-shaped bacteria (Fig. 49). Some of the bacteria appear to have a clay coating, but they do not penetrate the clay barrier between the barbules (Fig. 49). The spaces between the bacteria are void of sediment matrix. Glycocalyx (extra cellular polymeric material) does not seem to be preserved. However, it is possible that some fibrous structures connecting some of the fossilized bacteria are glycocalyx.

Although not quantitative, EDS results from the bacteria and surrounding matrix reveal an increase in carbon in the bacteria when compared to the amount of carbon in the surrounding matrix (Figs. 50 and 51). This increase of carbon implies that original bacterial carbon may be preserved. The bacteria and clay showed high silica and aluminum peaks not seen in the pyrite sample. The bacteria did not contain high amounts of sulfur or iron, as did the EDS results on the pyrite crystals, indicating that the bacteria are not pyritized.

INTERPRETATION AND DISCUSSION

Taxonomic Affinity

Structurally the Ingersoll shale feathers can all be classified as contour feathers. The vertical stratigraphic distribution of the feathers shows that they almost certainly did not come from a single individual; rather, they were deposited throughout the deposition

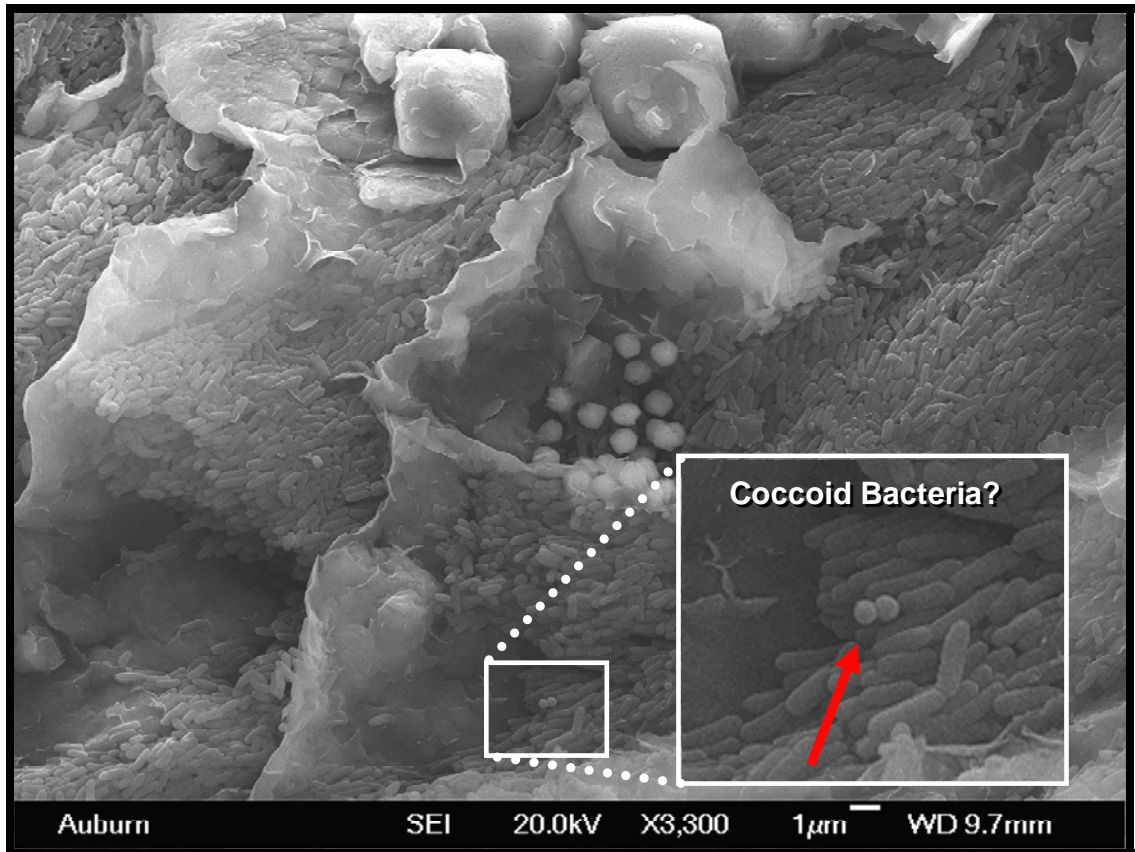


FIGURE 49—SEM of barbules on KIS-709. Notice the fine clay between the barbules and the void space between bacteria. Inset image shows coccoidforms of bacteria (indicated by the red arrow) on the tips of bacilliform bacteria.

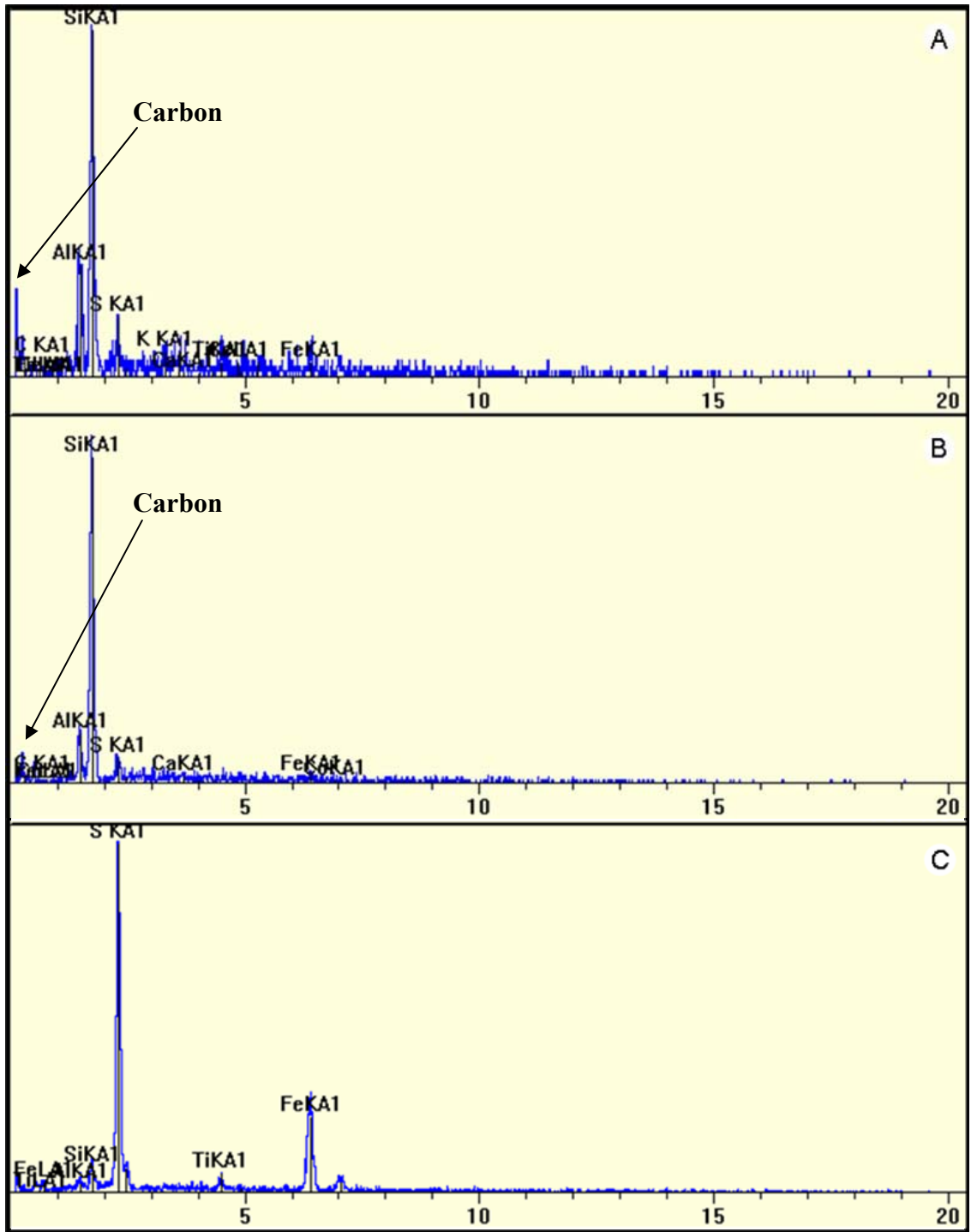


FIGURE 50—EDS results of KIS-706. (A) EDS results from the bacteria. (B) EDS results from the surrounding clay matrix. (C) EDS results from an associated pyrite crystal.

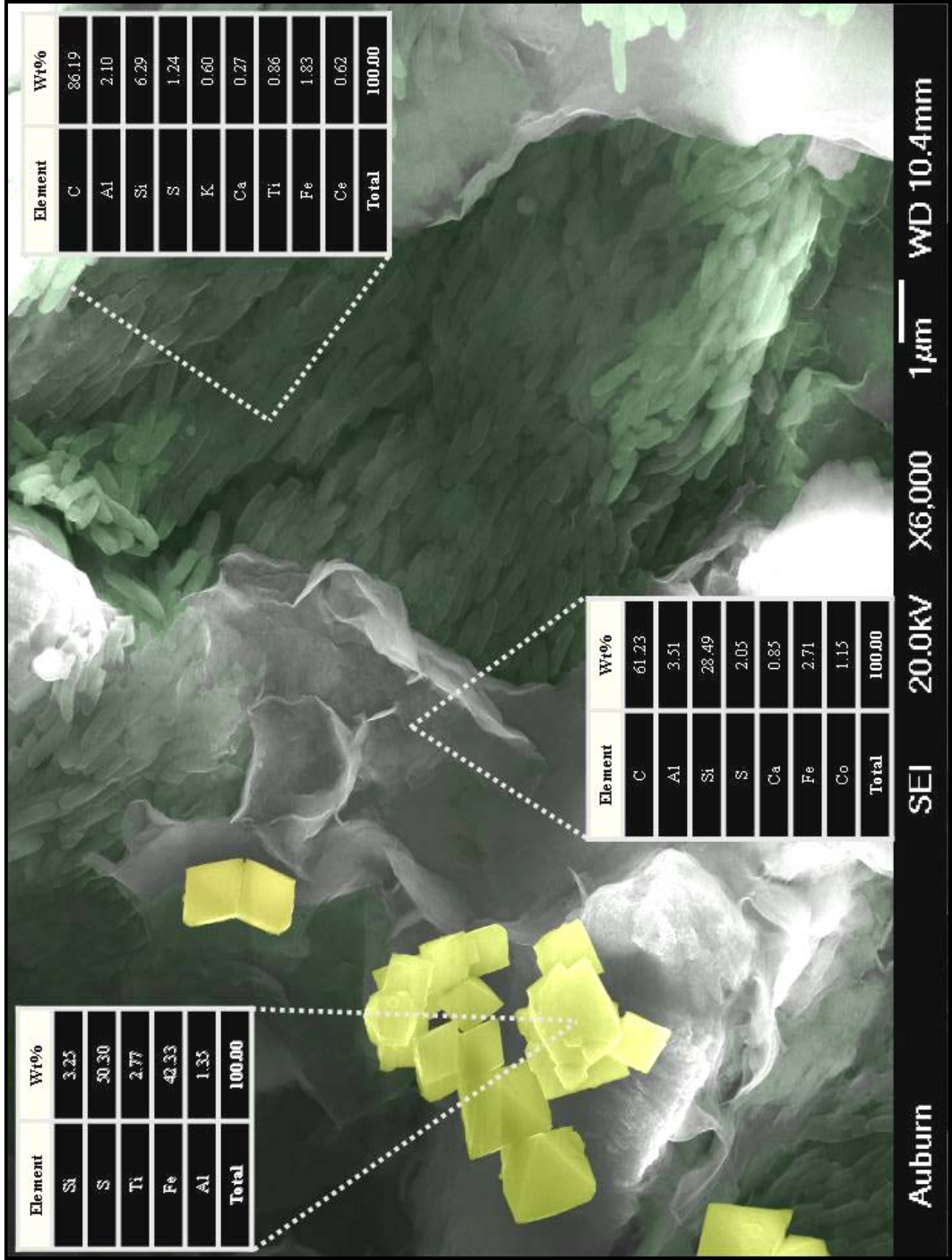


FIGURE S1—False-color SEM image of KIS-706 showing EDS results from analysis on bacteria (right), clay (middle), and pyrite (left)

of the Ingersoll shale. Size variations also suggest that the feathers came from more than one species of theropod. However, it is possible that the feathers represent adult and juvenile forms from the same species. Nonetheless, this begs the question, were these avian or nonavian species? This question cannot be answered based on the presence of isolated feathers as demonstrated by the nonavian feathered dinosaurs of China, because the microstructure of these Chinese specimens has not been studied in detail.

We can no longer say with any certainty that an isolated, structurally modern feather indicates the presence of a bird and not a dinosaur (Ji et al., 1998). However, we can speculate on possible feather bearers that were living in the southeastern United States during the Late Cretaceous. *Ichthyornis* was a small-medium sized seabird that inhabited the eastern shoreline of the Western Interior Seaway during the Late Cretaceous. Skeletal remains of *Ichthyornis* have been recovered from the Mooreville Chalk in Alabama (Lamb, 1993). Based on its known size range, *Ichthyornis* could have possibly been the producer of thirteen of the feathers, but it is highly unlikely that it produced the largest specimen, KIS-706. *Halimornis thompsoni* (Enantiornithes) is a primitive bird that was also recovered from the Mooreville Chalk in Alabama (Chiappe, et al., 2002). This nearshore marine bird could possibly have been the producer of thirteen of the feathers, but it also is highly unlikely that this bird produced KIS-706.

Due to its large size, it is probable that KIS-706 came off a dromaeosaurid dinosaur (Julia Clarke, personal communication, 2007). One dromaeosaurid dinosaur tooth was also found in the Mooreville Chalk, so they are known to have inhabited the southeastern United States during the Late Cretaceous (Kiernan and Schwimmer, 2004). Fossil bones from the dinosaur family Ornithomimidae have been found in the mid-late

Campanian sediments of the Blufftown Formation (Schwimmer et al., 1993). Although no feathers have been recovered with skeletal remains of ornithomimidids, we can infer the presence of feathers in this group, based on its cladistic position, making it possible that at least some of the Ingersoll shale feathers came from this dinosaur (see Prum and Brush, 2004). Hesperornithid bones have been found in the Late Cretaceous sediments of Georgia (David Schwimmer, personal communication, 2007); this relatively large seabird could also have produced KIS-706. It is highly unlikely that any of the Ingersoll shale feathers were produced by the tyrannosaurid *Appalachiosaurus montgomeriensis*, discovered in the Demopolis Formation of Alabama (Carr et al., 2005). Although tyrannosaurids have been discovered with feathers in China, they had branched, filamentous protofeathers that are not consistent with the structurally modern feathers from the Ingersoll shale (Xu et al., 2004).

Taphonomy

The main preservational mode of the Ingersoll feathers appears to be bacterial autolithification. The most common form of bacteria is bacilliform, and these are similar to the modern feather-degrading bacterium, *Bacillus lichenformis*. The preservational mode and the bacterial forms are very similar to those seen in the Messel Shale, Germany (Wuttke, 1983). The preserved coccoid-shaped bacteria seen in SEM, which are very similar in form to the modern feather-degrading bacterium *Kocuria rhizophila*, do not appear to have played a major role in feather replacement. However, these bacteria could have played a role in feather decay. The feather-degrading bacilliform bacteria were obviously capable of producing keratinase in order to digest the feather keratin, because the feather itself has been completely consumed. The bacteria are preferentially aligned

flow mats similar to those seen by other researchers (Wuttke, 1983; Franzen, 1985; Davis and Briggs, 1995). In water with neutral pH, modern feather-degrading bacteria can completely consume a feather within just a few days (Matthew Shawkey, personal communication, 2007). During this rapid consumption, the Ingersoll bacteria would have changed their microenvironmental conditions, causing minerals to precipitate from solution and causing their own fossilization. It is unclear exactly what mineral(s) have replaced the original bacteria. Fossil bacteria from the Messel Shale are preserved as siderite, but the conditions in the Ingersoll shale would not have allowed carbonates to form, and to date have not been found. EDS revealed no pyrite replacement, but it did indicate that a carbon component remains. Because the feather was completely consumed, it is possible that the carbon spike on the EDS is a result of original carbon from the bacteria itself. This type of preservation is seen in feathers from the Crato Formation, Brazil, where the bacteria that replaced the feathers are preserved as the original organic remains of the microbial cell wall (Briggs, 2003).

The Ingersoll shale feathers show a range in their quality of preservation. The well-preserved specimens appear to have been deposited on clay-rich laminations, whereas, the poorly preserved feathers were deposited on silty laminations. Thus it seems that the nature of the substrate plays a role in the quality of preservation of feathers; however, this needs further study. If the clay substrate were soupy, then it would have infiltrated all void space when the feather was first deposited. This would have separated even the finest structures, as seen in Fig. 49. The bacteria would have then consumed the feather but apparently were unable to pass through the clay barrier. If the feather were deposited on a silty substrate, the sediment might not have been able to infiltrate all of the

void space. This would possibly cause the bacterial colony to ‘spill over’ onto the adjacent sediment prior to fossilization. This would make the feather difficult to decipher, because the proximal and distal barbules would be morphed into a carbonized sheet, as was observed on KIS-702.

The pyrite that preserves some structures of the Ingersoll shale feathers probably formed very early in diagenesis. This is demonstrated by the pith-filled rachis found in three-dimensions on several specimens. Pyrite had to precipitate before any significant compaction took place. Actualistic experiments involving the precipitation of authigenic minerals via microbial decay have shown that mineralization can occur within a few days (Briggs, 1995; Grimes et al., 2001). Considering this fact as well as the rapid deposition of the Ingersoll shale (Bingham et al., 2006; Bingham, 2007), it is possible that the authigenic mineralization of pyrite also occurred within just a few days.

Although the micro-taphonomy of the Ingersoll feathers is relatively clear, the macro-taphonomic processes remain in question. Studies have shown that isolated feathers can float for many days and travel over great distances (Schäfer, 1972). An avian carcass can float for several days, losing feathers from decay as it drifts (Schäfer, 1972). This can also cause the distribution of feathers from a decaying carcass to be very widespread. Scavenging can also distribute feathers over an area and isolate them from a carcass (Davis and Briggs, 1995). The absence of avian skeletal remains within the Ingersoll shale, and the fact that these feathers were found in isolation, suggest they were produced during preening or molting. However, they could have been lost during decay and transported separately. Furthermore, if they originated from preening or molting, it is

still unclear whether they fell directly into the depositional site, or were introduced after considerable water transport.

CLOSING REMARKS

Despite the uncertainties discussed above, the Ingersoll-shale feathers are a major contribution to North American paleontology. Of the handful of feather specimens that have been discovered on this continent, the Ingersoll shale has yielded the largest collection from the Mesozoic strata. Aside from the one report of feathers in the Niobrara Formation in Kansas (Williston, 1896), the Ingersoll feathers are the only Mesozoic feathers from the North American continent preserved in a non-amber host. Furthermore, they considerably add to the sparse fossil record of feathers from Mesozoic strata worldwide, especially within Late Cretaceous strata. In addition, the Ingersoll shale is only the third site worldwide to preserve feathers in an estuarine setting.

CHAPTER 13: FOSSIL CONTENT AND PRESERVATION IN RELATION TO THE DEPOSITIONAL HISTORY OF THE INGERSOLL SHALE

In an extensive study of the stratigraphy and depositional history of the Ingersoll shale, Bingham (2007) interpreted the initial phase as subaerial erosion of the Tuscaloosa Formation during sea-level lowstand (Fig. 52A). As sea level rose, the river system was flooded, creating an estuary with a bayhead delta (Fig. 52B). This interpretation accounts for the coarse-grained, cross-bedded tidal sands and clay drapes of the Eutaw Formation unit beneath the Ingersoll shale. The next stage of development is the formation and subsequent filling of the Ingersoll tidal channel within the bayhead delta (Figs. 52C and 53). The channel-fill is characterized by rhythmically bedded sands and clays reflecting tidal processes. During infilling of the tidal channel there was apparently a decrease in energy as indicated by textural data. This decrease in energy could be attributed to a variety of local factors including obstruction of flow by an obstacle (e.g., fallen log across the channel). It is also possible that there was a shift from a shallow intertidal to a deeper subtidal channel caused by the transgression. The last stage in development of the Ingersoll shale is a continuation of transgression, which resulted in the landward migration of the bay shoreline (Fig. 52D). This interpretation accounts for the presence of central-bay deposits on top of the truncated Ingersoll shale lens. In addition, palynological and geochemical evidence indicates that the Ingersoll shale accumulated beneath normal to near-normal marine water (Bingham, 2007). The purpose of this

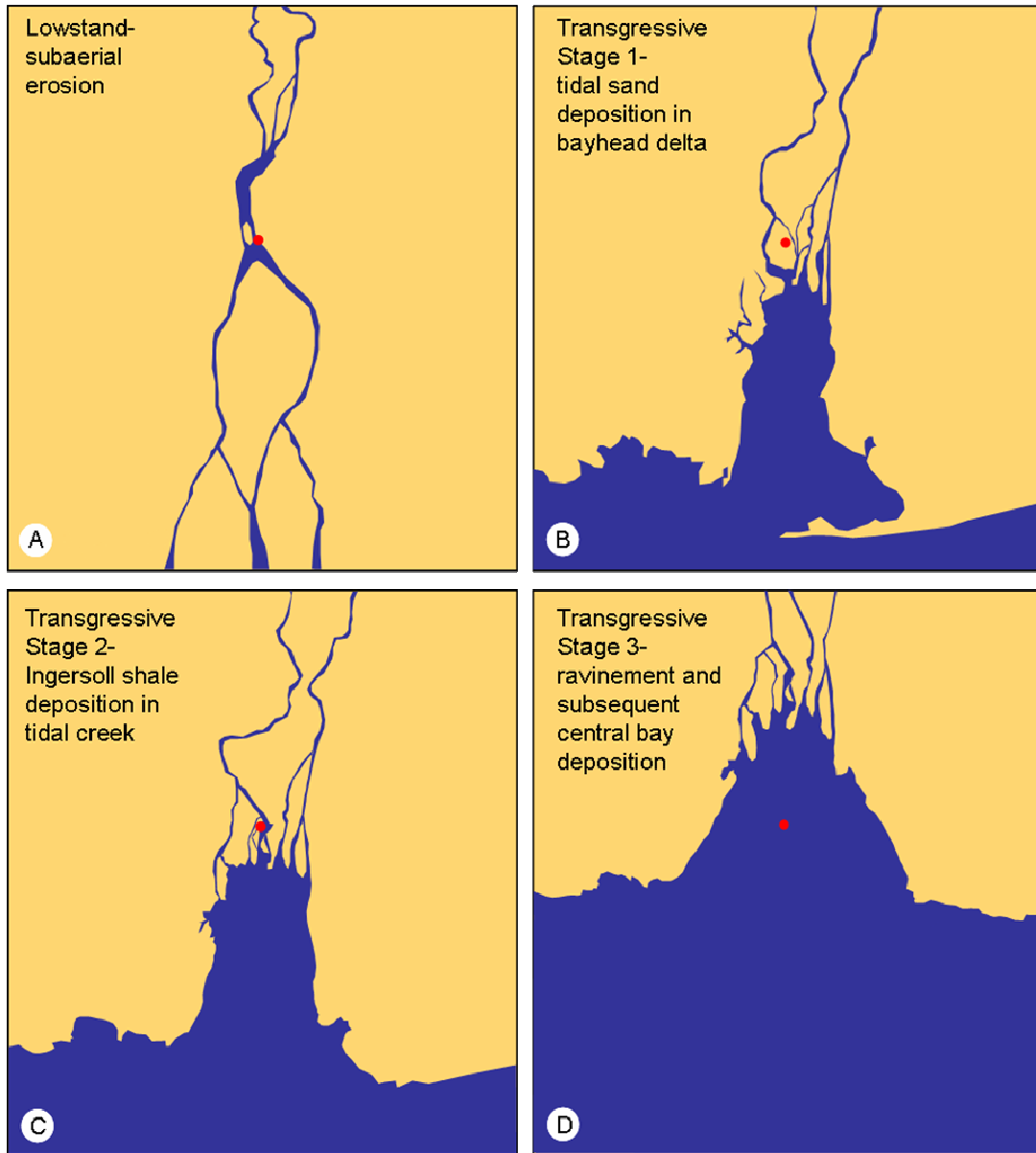


FIGURE 52—Reconstruction of estuary development in relation to the study area (red dot). (A) Subaerial erosion of the Tuscaloosa Formation during sea-level lowstand. (B) Initial transgression with flooding of the incised valleys and development of the estuary and bayhead delta. (C) Creation and filling of the Ingersoll tidal creek in the bayhead-delta plain as transgression continues. (D) Landward migration of shoreline and deposition of central-bay deposits on top of the Ingersoll shale (from Bingham, 2007).

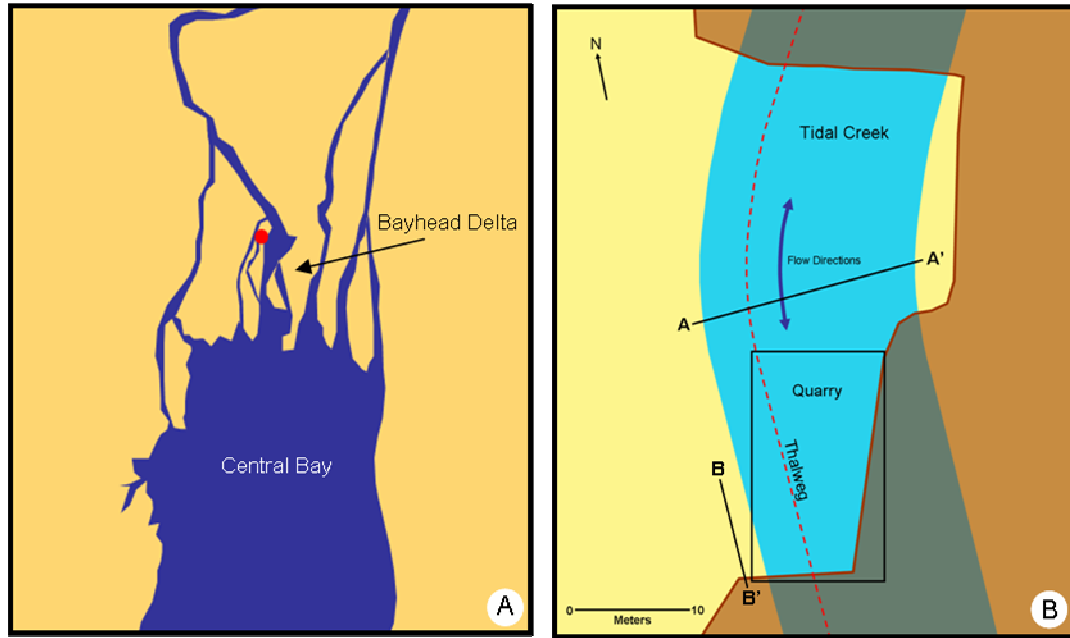


FIGURE 53—Detailed view of the interpreted estuarine setting of the Ingersoll shale. (A) Estuarine complex includes bayhead delta (red dot indicates inferred tidal creek for the deposition of the Ingersoll shale). (B) Outcrop scale reconstruction of Ingersoll tidal creek in relation to the quarry and trenches (both figures from Bingham, 2007).

chapter is to relate the occurrence and taphonomic conditions of the fossil biota to Bingham's stratigraphic and paleoenvironmental interpretation.

The vertical distribution of the Ingersoll shale fossil biota and taphonomic conditions can be explained largely by variations in water and wind energy responsible for introducing and transporting fossil elements. In general, energy levels decreased stratigraphically up section. When the tidal channel cut through the bayhead delta sands, energy levels within the channel were at their highest, as indicated by the high weight percent of sand in the lowermost part of the lens (Fig. 54; Bingham, 2007). This high-energy zone corresponds to zones 1 and 2.

In zone 1, the total organic carbon is at the lowest levels in the Ingersoll shale. This is explained by organic carbon being leached and oxidized by the flow of groundwater, which preferentially infiltrated this sandy zone. This groundwater flow can still be seen happening today. Fossils from the upper portions of zone 1 are usually preserved only as impressions with iron stains partially filling the voids.

At the boundary between zones 1 and 2, there is a sharp decrease in weight percent sand (Fig. 54) indicating a decrease in energy. This decrease in energy could have allowed enough clay to settle from suspension, acting as a boundary between these zones, thus protecting the carbon in zone 2 from the leaching process that occurs in zone 1. Within zone 2 (~6 cm thick), amber clasts and many highly durable plant reproductive organs are preserved; both components are thought to have been transported within the bedload of macerated plant detritus. This indicates that many of the fossils within this zone are allochthonous. The few whole leaves preserved within this zone are thought to

FIGURE 54— General stratigraphic column of the Ingersoll shale lens divided into six zones based on the relative abundance and taphonomic condition of fossils. Curves show weight percent sand and total organic carbon (modified from Bingham, 2007). Relative fossil abundance is based on qualitative data and indicated by the thickness of the red bars. Included in zone 5 are two intervals (cross-hatched) denoting subzones with multiple layers of macerated plant detritus. Shown in zone 6 are *Thalassinoides* and *Rhizocorallium* borrows. The dashed lines represent sand-dominated lamina. Blue dotted line marks the triplet of sand layers used as a vertical datum. TOC represents total organic carbon.

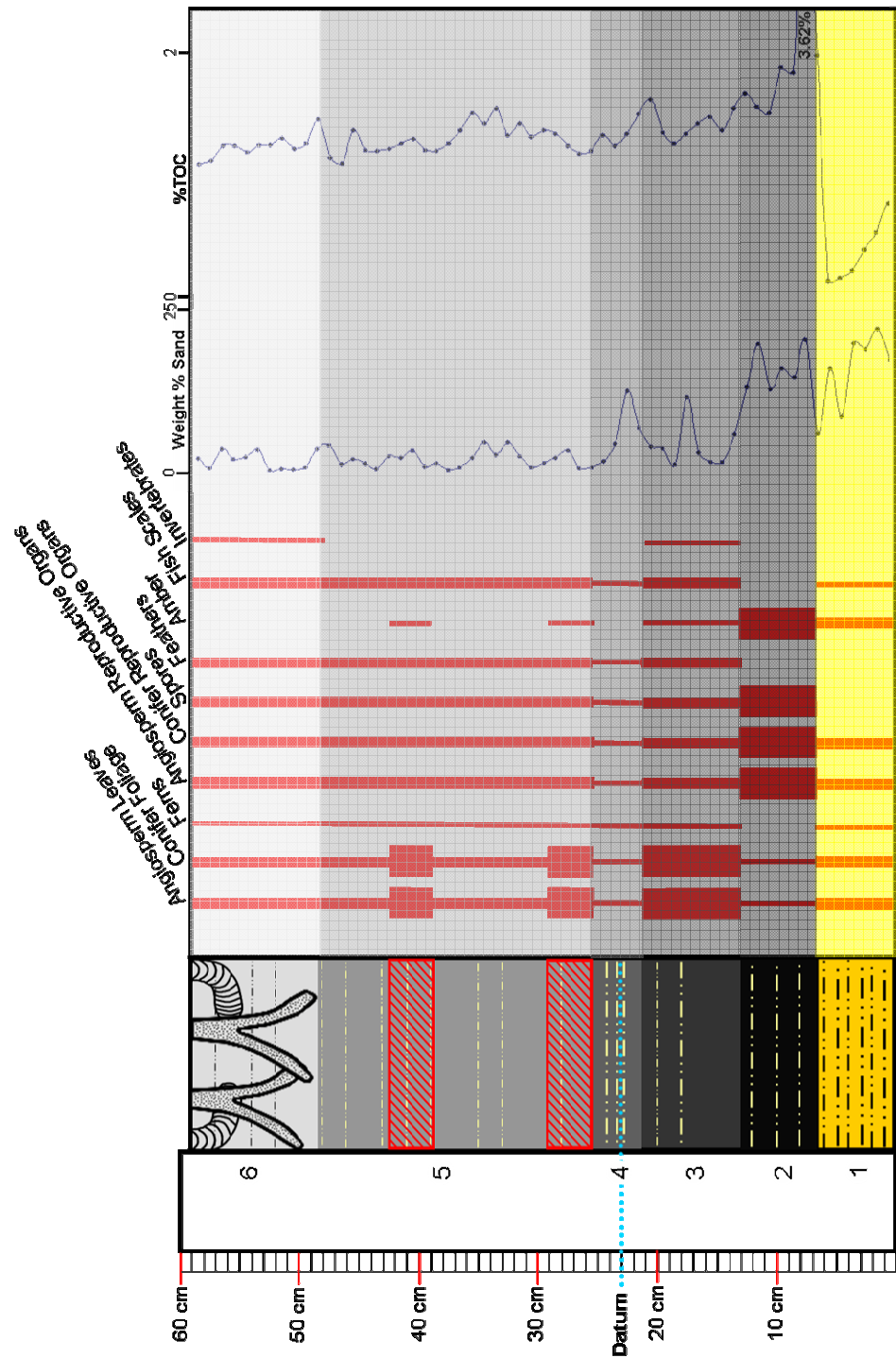


Fig. 54

be from the constant supply of angiosperm and conifer leaves falling or being blown directly into the tidal channel. This zone also contains authigenically mineralized pyrite nodules as well as pyritized fossils. This demonstrates that reducing conditions were prevalent within the sediment regardless of the daily influx of marine waters via tidal pumping.

The amber clusters found within zones 1 and 2 were deposited in small depressions while the amber pieces were being transported within the bedload of the tidal channel, or when it settled from suspension during slack water. The hydraulically sorted amber clusters found in the Ingersoll shale are evidence that at least some of the amber was transported. This interpretation is strengthened by the rounded edges on irregularly shaped pieces, which suggest reworking in abrasive sediment prior to final deposition (David Grimaldi, personal communication, 2006). Reworking within the substrate is further demonstrated by the rarity of fragile, slender rivulet pieces.

Since extant members of the source plants of megaspores found within zones 1 and 2, the families Marsileaceae and Isoetaceae, are not salt tolerant, it is likely that the Cretaceous representatives were living in nearby freshwater lakes or rivers and were washed into the depositional site (Richard Lupia, personal communication, 2006). These megaspores could have been transported from the forest floor or washed into the estuarine system from a fluvial source and later brought into the tidal channel by high tides. The high abundance of megaspores within these high-energy zones and the decrease in megaspores as energy levels decreased within the tidal channel suggest the latter: spores brought to the estuary in distributary channels were later concentrated at the depositional site via tidal pumping. Once the channel began to fill, energy levels

decreased, causing a decrease in the number of megaspores that made it into the tidal channel.

Zone 3 is ~8 cm thick and contains layers of large plant macrodetritus such as angiosperm leaves and conifer foliage that are mostly well preserved. Corresponding quantitative data show a sharp decrease in weight percent sand as well as total organic carbon compared to the zone below (Fig. 54). The decrease in energy indicated by these data is also reflected in the lower abundance of macerated plant layers when compared to zones 1 and 2. Amber within zone 3 is sparse, and when found, the pieces are smaller than those of zone 2 (personal observation). Many of the leaves are complete and appear to have undergone very limited transport within the channel. Some conifer fossils within this zone are preserved in three-dimensions. The three-dimensional preservation of conifers is attributed to two factors: rapid pyritization in reducing conditions, and deposition in a soupy substrate.

The increase in pristine angiosperm leaves and conifer foliage within this zone could be the result of (1) lack of dilution by large amounts of macerated plant detritus, or (2) transportation to the site by high winds. A high-wind event would increase the amount of these fossils into the depositional site without a corresponding increase in water energy. Because of the relatively heavy whole leaves, it is unlikely that they were transported by low-velocity water flow. Since the suspected beetle remains found in zone 3 were in association with macerated plant detritus, it is possible that they washed into the tidal channel from the forest floor during a storm.

Zone 4 is ~4 cm thick and contains the vertical datum known as the “triplet.” Fossils within this zone are sparse, but when found, they include all Ingersoll fossils with

the exception of amber inclusions. Intermittently there are lamina with macerated plant detritus. Textural data from this zone, directly at the vertical datum reflects a significant increase in energy levels. However, at this energy peak there is a decrease in total organic carbon. Taking this in conjunction with the overall rarity of fossils within this zone, this could be explained by scouring/flushing of biotic remains within the channel during higher-energy events. The increase in water energy within the channel could have been caused by a storm event out at sea that simply never made landfall. The lack of wind and rain onshore would explain the scarcity of new, whole leaves in this zone.

Zone 5 is ~19 cm thick and contains a large number of lamina that contain whole leaves. It has relatively few, intermittently dispersed sand/silt lamina. The high clay content within this zone may represent low energy as the channel filled with sediment. In spite of the overall low flow velocity, there were occasional higher-energy events. Layers of macerated plant detritus found within the fine sand-silt lamina were possibly washed in from the forest floor during a rain event or by water-energy levels increasing enough to transport debris from another portion of the channel. These macerated plant layers are current-oriented, which indicates water flow, so they were most likely transported along the channel bed as part of the traction load.

Zone 5 contains bundles with multiple layers of macerated plant detritus including seeds, small clasts of amber, small cones, as well as whole leaves. These bundles are interpreted to be high-energy wind events because there is little increase in weight percent sand at these horizons. It is also possible that these zones represent an absence of leaves due to seasonality, but this does not correlate with the interpretation made by Wolfe and Upchurch (1987) on the relatively low seasonality during the Santonian.

Zone 6 has an average thickness of 8 cm. This zone is similar to zone 5 in almost every aspect; it was differentiated on the bases that it contained a *Thalassinoides* and *Rhizocorallium* dominated firmground ichnofossil assemblage that has damaged many of the fossils.

The erosional surface between the Ingersoll shale and the overlying central-bay sediments is considered to be a transgressional erosion surface. Within these central-bay sediments, rip-up clasts of the Ingersoll shale are common. It is unclear how much of the Ingersoll shale is missing. It is possible that only the lower portions of a larger channel complex are preserved. Thus, the reason no *in situ* root traces have not been found may be that overbank deposits with root traces have been destroyed by subsequent erosion.

The bivalves, which were also found in zone 6, left no trace fossils, although, based on comparison to modern species, their morphology indicates an infaunal lifestyle. Therefore, the bivalves may have burrowed into the clay lens after clay deposition, while the substrate was still relatively soupy and prior to firmground development and erosion. However, further investigation is needed in order to fully understand the emplacement of these fossils.

The absence of avian skeletal remains within the Ingersoll shale and the fact that feathers were found in isolation suggest they were produced during preening or molting. The occurrence of feathers throughout the clay lens suggests that there was a constant input of feathers into the depositional site. However, they could have been lost during the decay of carcasses from some distance away and transported into the tidal channel by high tides. Furthermore, if they originated from preening or molting, it is still unclear

whether they fell directly into the depositional site, or were introduced via water transport.

It is unclear as to whether or not the fish scales represent the allochthonous or autochthonous component of Ingersoll shale fossil assemblage. As stated above, it is possible they are from fish living in the water column. However, it is also possible that the fish scales were dispersed from a decaying carcass that floated into the tidal channel or were reworked out of adjacent mudflats and transported by water or wind into the channel.

CHAPTER 14: COMPARISONS WITH SIMILAR *KONSERVAT-LAGERSTÄTTEN* AND A MODERN ANALOG

INTROCUCTION

The Ingersoll shale *Konservat-Lagerstätte* is similar to several other deposits of comparable age and setting, but it has its own unique combination of depositional environment, modes of preservation, and biotic composition. In this chapter, I will compare and contrast the Ingersoll shale with three other *Konservat-Lagerstätte* and one analogous modern setting.

SIMILAR FOSSILS DEPOSITS

The Messel Shale, Germany

The mid-Eocene Messel Oil Shale is best known for its completely articulated vertebrates (Franzen, 1985). In some specimens, it is possible to distinguish structural details such as the eye, liver, hair, and veins (Wuttke, 1983; Franzen, 1985). Articulated bird specimens often have their feathers preserved (Wuttke, 1983). Bat wing membrane and mammal fur is commonly preserved (Wuttke, 1983; Franzen, 1985). Typically, these articulated fossils have silhouettes of their bodies preserved as carbonized external molds.

The Messel Shale is thought to have been deposited in a lake approximately 10 m deep (Franzen, 1985). The lake apparently had a fluvial component, with two inflows and one outlet. Organisms transported to the lake by rivers settled out on the stagnant,

argillaceous, lake bottom. Occasionally, dinoflagellate blooms would drive anoxic benthic conditions (Franzen, 1985). The presence of alligator and palm fossils in the lake sediments along with oxygen-isotope data from molluscs indicates that the climate at the time was tropical to subtropical (Franzen, 1985). These harsh benthic conditions prevented bioturbation, thus allowing the decaying carcasses to remain undisturbed by scavengers. At the lake bottom, reducing conditions produced poisonous substances like hydrogen sulfide and ammonia. When the lake overturned, the rising poisonous gases caused mass killings of aquatic vertebrates, including turtles, fish, and crocodilians, as well as semiaquatic mammals. Birds and bats that were flying over the lake were poisoned by a thin layer of carbon dioxide near the water surface, which is thought to have been produced by volcanic outgassing (Franzen, 1985).

Bacterial mats formed on the underside of the carcasses shortly after putrefaction. These now are seen as blackened body outlines, shown by SEM to consist of mats of bacilliform bacteria that have been replaced by siderite. The production of CO₂ and the presence of iron caused the precipitation of the siderite. This process was dubbed bacterial autolithification by Wuttke (1983). The black stain was caused by the migration of plant kerogens through the sediments (Wuttke, 1983; Franzen, 1985).

The Messel Shale *Konservat-Lagerstätte* is similar to the Ingersoll shale in that the feathers in both deposits have been preserved by bacterial autolithification. That is, both deposits have preserved feathers by the bacterial replacement process, and the bacteria preserving feathers in both deposits are rod-shaped or bacilliform. The Messel Shale fossil bacteria were subsequently replaced with siderite. In contrast, bacteria preserving the feathers in the Ingersoll shale appear to contain original carbon and are

apparently unmineralized. The comparison of these two fossil deposits demonstrates that this particular mode of preservation of feathers can occur in different depositional settings and under either rapid or slow sedimentation.

The Grès à Voltzia Formation, France

Etter (2002) reviewed the Triassic Grès à Voltzia Formation of northern France. This deposit is a *Konservat-Lagerstätte* that exhibits a high degree of soft-tissue preservation. Labile tissues of jellyfish and annelid worms are preserved. The unit also contains complete spiders, insects, and crustaceans, and well-preserved plants such as horsetails, ferns, and gymnosperms (Etter, 2002).

The lower part of the formation, which is the focus of this review, contains silty clays, sandstones, and carbonates (Gall, 1985; Etter, 2002). The sandstone facies is typically devoid of fossils. The silty-clay lithology is green to red and occurs as lenses up to several decimeters thick, which are intercalated with sandstones. The fossiliferous lenses are finely laminated and commonly exhibit mud cracks and plant-root traces at their tops. The carbonate facies occurs as interbedded dolomitic sandstones that rarely show soft-tissue preservation.

Overall, the Grès à Voltzia Formation is thought to represent an alluvial to deltaic transition associated with transgression. Channel deposits within this setting are represented by the sandstone facies (Gall, 1985). The sediments in the fossil-bearing silty-clay lenses are interpreted to be overbank deposits, formed by the settling of silt and clay from suspension during flood events or strong tides (Gall, 1985). The resulting floodplain ponds and abandoned channels contain brackish-water species and salt clasts

indicating that salinity levels periodically were high. They were thought to have been filled quickly due to the presence of mudcracks and plant-root traces.

Plant remains are very well preserved and consist of horsetails, ferns, gymnosperms, and many of their reproductive organs. Structural details are usually preserved with a crust of iron oxides. Marine species such as lingulid brachiopods, fish, bivalves, jellyfish, and annelids also occur in this facies (Etter, 2002). The terrestrial invertebrate assemblage is characterized by scorpions, spiders, myriapods, and insects (Etter, 2002). Many of these marine and terrestrial animals are fully articulated and show minimal signs of decay. They are commonly preserved as organic material (carbonization) or as iron oxide crust (Briggs and Gall, 1990). In some fossils, siderite initially precipitated around the fossils. However, all of the original calcareous material has been dissolved, leaving only carbonized remains (Etter, 2002). Organic-rich horizons show the preservation of microbial mats (Briggs and Gall, 1990). The autochthonous assemblage is thought to have been transported in from the immediate vicinity, with the marine component transported by storms or high tides.

There are similarities between the Grès à Voltzia Formation and the Ingersoll shale. The biota in both were deposited in restricted clay-rich sites, within a deltaic setting, and were buried by rapid sedimentation. They also share similarities in modes of preservation, such as in carbonization, precipitation of iron crust, and an absence of carbonate fossils. However, the Grès à Voltzia Formation contains no pyrite or compressions. Instead, some of its fossils have been sideritized, which is not observed in the Ingersoll shale fossils.

The differences between these two fossil deposits are in the biotic composition of the organisms that are preserved, transport of the fossils to the depositional site, and the main factors that led to exceptional preservation. The Ingersoll shale preserves very few marine species with the exception of the isolated fish scales, rare post-depositional bivalves, and marine dinoflagellates. In contrast, the Grès à Voltzia Formation contains an abundance of marine fauna. This could be attributed to the Ingersoll shale being deposited in a restricted tidal channel further from open marine waters. In the Ingersoll shale, most of the biota, especially the plants, were living in close proximity to the depositional site. The exceptional preservation within the Ingersoll shale biota is attributed to rapid sedimentation and reducing substrates, whereas preservation in the Grès à Voltzia Formation is attributed largely to bacterial sealing of organic remains prior to burial.

The South Amboy Fire Clay, New Jersey

The South Amboy Fire Clay Member of the Raritan Formation, New Jersey, is very similar to the Ingersoll shale *Konservat-Lagerstätte*. Although no comprehensive study of this Turonian-age *Konservat-Lagerstätte* has yet been published, selected elements of the biota are described. This includes the plant fossils (Newberry, 1896), feathers in amber (Grimaldi and Case, 1995), and insects in amber (Grimaldi et al., 2000a).

The Raritan Formation consists of interbedded gravels, sand, and clay, representing a prograding alluvial fan and nearshore marine environments (Gandolfo et al., 2001). It is composed of seven sand and clay beds, one of which is the South Amboy Fire Clay, which formed as fine sediment settled in slack water streams within a deltaic

complex (Gandolfo et al., 2001). Peat layers are intercalated with layers of fine sand and clay beds, all of which contain large amounts of pyrite (Grimaldi et al., 2000a).

The peat layers consist of large clasts of wood, partially decayed angiosperm leaves, conifer needles, stems of equisetaleans, and fine fusanized flowers in complete relief (Grimaldi et al., 2000a). Over 100 taxa of plant fossils have been described from this deposit, including members of the families Magnoliidae, Lauraceae, and Capparales (Grimaldi et al., 2000a). Ferns, pines, and monocotyledon angiosperms are also present within the deposit. Many of these plant remains are intact and preserved as compressions or as pyritized and carbonized remains (David Grimaldi, personal communication, 2006). This deposit is considered to be an insect *Konservat-Lagerstätte* because it preserves insects within the sediments, as well as in amber (Grimaldi et al., 2000a). To have both of these modes of preservation within the same deposit is extremely rare (Martínez-Delclòs et al., 2004). Floral remains and several feathers also have been found in the amber. These feathers include a semiplume and feather fragments (Grimaldi and Case, 1995); several other feathers that were discovered but have yet to be described (David Grimaldi, personal communication, 2006).

The biota of both the South Amboy Fire Clay and the Ingersoll shale are preserved within clays that formed in channels in marine coastal environments. These low-energy deposits were reducing in both cases. Evidence that both depositional sites were dominated by sulfate-reducing conditions includes common pyrite nodules and pyritization of the fossils. Both sites have amber with included plant and animal fossils. If the Ingersoll shale terrestrial invertebrate remains do indeed turn out to be beetle elytra, then both deposits will have insects preserved both within the sediment and in amber. In

the South Amboy Fire Clay, fossils are found and concentrated within peat layers. These peat layers could be compared to the macerated plant layers within zones 1 and 2 of the Ingersoll shale. Many of the whole leaves in the Ingersoll shale are morphologically similar to plants described in the monographic work by Newberry (1896) on the Amboy Clay Flora (see Chapter 8). Both sites have produced “*Dammara*” cone scales with *in situ* amber and angiosperm fruit/seed coats preserved within the peat layers. One of the most significant similarities between these two fossil deposits is that they both have produced fossil feathers, although they are preserved in different media. Feathered theropods are thus documented as living in close proximity to coastal settings in both cases.

MODERN ANALOG TO THE INGERSOLL SHALE

Mahakam River Delta (Indonesia)

Since Miocene time, the Mahakam river has been forming a major deltaic complex on the eastern shore of Borneo, Indonesia. Gastaldo and Huc (1992) studied the delta in order to gain a better understanding of the generation, incorporation, and preservation of plant parts in this type of environment. They described a number of specific depositional environments, including major tidal channels that were isolated from fluvial input. Plant detritus and the taphonomic condition of plants within these modern tidal channels will be the focus of this comparison.

Gastaldo and Huc (1992) found that the bases of the tidal channels are often in contact with delta-front sands. These channels often contain sand-mud couplets, which reflect fluctuating water conditions. As flow is progressively restricted, a fining-upward sequence may develop as the channel fills with sediment. These channel deposits also

contain horizontally bedded plant litter. Gastaldo and Huc (1992) recognized plant parts that were reworked into millimeter size, unidentifiable organic debris, mainly dispersed leaf cuticle. The cuticle may be whole and pristine or may show decay structures. Most cuticle is from coriaceous, broad-leaved evergreens. The parenchymatous tissues in many leaf specimens had undergone a considerable amount of decay. Wood clasts were flattened and rounded, with framboidal pyrite forming in open spaces. Plant resin was found transported as bedload along with macerated plant detritus, as indicated by their rounded edges. Some of these resin pieces showed signs of microinvertebrate traces such as borings. Seeds and fruits were encountered, but were rare. Disarticulated insect parts, including ant heads and beetle elytra, were found within plant-bearing beds. Vertebrate remains such as fish vertebra were a minor component of the biota within this modern analog.

Dicotyledon angiosperm leaves represent the parautothous component of the tidal channel deposits. These leaves were produced by vegetation growing adjacent to the tidal channel, and the size of the leaves reflects the mechanical processes that they had gone through prior to burial. Tidal channels have a high species diversity (e.g., dicotyledon angiosperms mixed with palms), which distinguishes them from low-diversity mangrove swamps, which have low species diversity. However, Gastaldo and Huc (1992) state that it would be difficult to distinguish fluvial channels from tidal channels based on biotic composition alone.

These characteristics are very reminiscent of the Ingersoll shale *Konservat-Lagerstätte*. Like the tidal channels studied by Gastaldo and Huc (1992), the Ingersoll shale clays are in contact with bayhead delta sands (see Bingham, 2007). The

sand-mud couplets within the tidal channel deposits of the Mahakam River Delta could possibly be compared to the tidal rhythmites seen in the Ingersoll shale. Textural analysis of the sediments of the Ingersoll shale also reveals a fining upward sequence.

The general and specific nature of the plant fossils and resin clasts are also strikingly similar. One difference between the fossils of these two depositional environments lies in the resins of the Mahakam River Delta. These resins showed borings from microinvertebrates, which are not seen in the amber clasts of the Ingersoll shale. This could possibly be attributed to the inferred inhospitable benthic conditions at the sediment-water interface during the deposition of the Ingersoll shale, which would exclude many of the microinvertebrates. It could also be attributed to the high rates of sedimentation of Ingersoll shale deposition, which would have minimized the residence time of resin at the sediment-water interface.

CLOSING REMARKS

Comparison of the Ingersoll shale with other *Konservat-Lagerstätten* demonstrates that it represents a unique combination of environmental setting, fossil biota, and taphonomic states. The preservation of feathers within the Messel Shale and the Ingersoll shale are very similar, despite differing depositional setting and sedimentation rates. This shows that bacterial autolithification can occur under extremely different conditions. Comparison with the Grès à Voltzia Formation shows that *Konservat-Lagerstätten* can form in clay lenses that accumulated in vastly different settings within the delta complex. The Ingersoll shale is most similar to the South Amboy Fire Clay of New Jersey. The similarities between these deposits demonstrate that

Konservat-Lagerstätten formed in reducing, low-energy tidal channels within a delta complex may be more common than was previously thought. Tidal channel deposits within the Mahakam River Delta of Indonesia are an excellent modern analog to the Ingersoll shale both sedimentologically and taphonomically. Although the sedimentation rates in the Ingersoll shale were probably higher than that of the tidal channels studied in the Mahakam River Delta, the continuation of actualistic studies within deltaic settings may provide further insight into understanding how *Konservat-Lagerstätten* form within a deltaic setting and aid in prospecting for similar fossil deposits.

The Ingersoll shale project indicates that *Konservat-Lagerstätten* can form in very small, isolated tidal channels within incised bayhead delta sands. In such settings, plants growing in close proximity to the rapidly filling tidal channel show exceptional preservation because of limited transport and fragmentation. In addition, the close proximity of vegetation to the depositional site allowed for amber to be deposited. Rapid deposition in this setting prevents scavenging and limits bioturbation. Reducing conditions also limit scavenging and bioturbation and promote early diagenetic mineralization of fossils.

The author encourages future researchers to test these conclusions by going to ancient deltaic environments and looking closely for similar, small clay lenses within incised bayhead delta sand deposits. Researchers should look for evidence of rapid deposition under reducing conditions, and fossils found should be closely examined in the field while still fresh. This future exploration for well-preserved fossils in small clay lenses could lead to the discovery of other Ingersoll shale-like deposits and more rarely seen biotas.

CHAPTER 15: SUMMARY AND FUTURE RESEARCH

Fossils from this newly discovered *Konservat-Lagerstätte* provide an opportunity to observe and document rare, ancient life from the Santonian age, some of which never seen before and thus warrant future systematic studies. The taphonomic conditions of these fossils, combined with the well-documented depositional history of the deposit, have led to a better understanding of the conditions required to form nearshore *Konservat-Lagerstätten* deposits. Furthermore, archived bulk samples were collected from this *Konservat-Lagerstätte* deposit to be used in future research. Continued investigations of the Ingersoll shale biota have the potential of making many more significant paleobiologic contributions.

The Ingersoll shale is composed of rhythmically bedded sands and clays that were deposited in a tidal channel under progressively decreasing water-energy levels as the channel filled. Six zones within the shale lens were distinguished based on their biotic composition and the taphonomic condition of the fossils. These taphonomic zones are largely explained by variations in water and wind energy, which is responsible for introducing and transporting fossil elements. Higher energy, as indicated by weight percent sand, corresponds to an increase in mechanically degraded plant detritus.

During the excavation of the Ingersoll shale, 321 macrofossils were recovered from the deposit, additional smaller fossils were recovered from sediment, and amber

samples with biologic inclusions. These fossils include a variety of palynomorphs, assignable sediment and amber samples. These fossils include a variety of palynomorphs, assignable to the *Sohllipollis* Taxon Range Zone (mid-Turonian-Santonian). In addition, several megaspores from heterosporous water ferns as well as isoetalean and selaginellean lycopsids were recovered, indicating a nearby freshwater source.

Lower vascular plants are rarely found in the Ingersoll shale lens and are represented by horsetails and seven fern-like morphotypes. Although fern remains are rarely found, they are highly diverse.

Gymnosperms are represented by seven morphotypes, representing four form genera. These morphotypes are tentatively assigned to three families: the extant Araucariaceae, and Cupressaceae (including Taxodiaceae), and the extinct family Cheirolepidiaceae. Both the Araucariaceae and Cupressaceae, and possibly the Cheirolepidiaceae, also are represented by isolated or articulated cones and cone scales. Gymnosperm elements are variably carbonized and pyritized, and three-dimensional preservation is common. The systematic position of the Ingersoll conifers will be the focus of research by Brian Axsmith, University of South Alabama.

Thus far, 41 distinctive angiosperm leaf morphotypes (39 dicotyledon and 2 monocotyledon) are reported from the Ingersoll shale. Fossil leaves are commonly found whole and, in some cases, are found articulated on branched stems. These branched stems occasionally have articulated reproductive organs. Reproductive organs are represented by 4 flower morphotypes, 2 miscellaneous seed types, a fruit type, fruit coatings, and a fruit/seed wing. These fossils are lignified, pyritized, coalified, preserved as impressions, and/or mummified. Due to the good cuticular preservation of fossil leaves and articulated

reproductive organs, future research on the Ingersoll flora may reveal species that have not been previously described and may provide more details on previously described taxa.

The isolated amber clasts, common in the lowermost part of the shale lens, have already yielded important discoveries. Inclusions within amber pieces are dominated by plant debris but also include fecal pellets, well-preserved fungal mycelia, mites, a female scale insect with well-developed legs and antennae, and an araneoid spider that may be the oldest found in association with its web. The Ingersoll shale amber expands the geographical distribution of Santonian mites, spiders, and scale insects to the southeastern U.S. Prior to the discovery of the Ingersoll shale, Eutaw Formation amber with inclusions was scarce and was not known to contain arthropods. Conifer remains, possibly from the family Cupressaceae, contain *in situ* amber rods within their ducts. Due to such exceptional plant macrofossil preservation, the amber can be directly linked to the amber producer; the ability to make this connection is rare in the fossil record.

Comparative geochemical studies will help paleobotanists identify Mesozoic amber producers in general, and specifically, in the southeastern U.S. Bulk samples of amber from the Ingersoll shale were sent to David Grimaldi, Curator of Entomology at the American Museum of Natural History, for detailed analysis.

Marine invertebrate remains within the Ingersoll shale lens are rare. They are represented by articulated, infaunal bivalves, preserved mainly as external molds and casts, and rarely preserved via pyritization. Remains of a possible terrestrial invertebrate (beetle elytra) were found in association with plant macrodetritus. If identification as

beetle remains is confirmed, then this discovery is of particular significance, because of preservation of insects in both sediments and amber is rare.

Ctenoid fish scales are commonly found in the Ingersoll shale, and consist of 3 different morphotypes. The scales preserve the fine fingerprint-like texture (circuli) on the external molds and contain some carbonized material.

Of major significance is the discovery of feathers. Fourteen isolated feathers have been found in the Ingersoll shale to date, making this the largest collection known from Mesozoic strata in North America. Feather specimens range from 0.4 to 16.5 cm in length and are all contour feathers. The discovery of these feathers documents the existence of feathered theropods in the southeastern United States during the Late Cretaceous.

Furthermore, the Ingersoll shale is the only known Late Cretaceous deposit in the United States to have theropod feathers in a clay host. This allows for detailed study of feather surfaces by SEM, which has already revealed that the feather keratin was replaced with rod-shaped bacteria in which the original bacterial cell-wall carbon was preserved.

The extraordinary preservation of the Ingersoll-shale biota is attributed to reducing conditions (stagnation), rapid burial (obstruction), and entombment in relatively sterile media (amber). Reducing depositional conditions and rapid burial also prevented disturbance by benthic organisms and enhanced microbial processes (e.g., bacterial autolithification) and early diagenetic mineralization (e.g., pyritization).

Preservation of the Ingersoll biota most closely resembles the Turonian-age South Amboy Clay of New Jersey and the modern Mahakam River Delta (Borneo), both of which are low-velocity channel deposits. However, the feathers of the Ingersoll shale are uniquely different from the South Amboy Fire Clay feathers in that they are preserved in

sediment. The Mahakam River Delta is an excellent modern analog to the Ingersoll shale both sedimentologically and taphonomically. However, Ingersoll resins lack borings from microinvertebrates, which reflects a higher degree of inhospitable conditions when compared to channel deposits from this modern analog.

REFERENCES

- ALLISON, P.A., 1988a, *Konservat-Lagerstätten*: Cause and classification: *Paleobiology*, v. 14, p. 331–344.
- ALLISON, P.A., 1988b, The role of anoxia in the decay and mineralization of proteinaceous macro-fossils: *Paleobiology*, v. 14, p. 139–154.
- ALONSO, J., ARILLO, A., BARRON, E., CORRAL, J.C., GRIMALT, J., LOPEZ, J.F., LOPEZ, R., MARTÍNEZ-DELCLÓS, X., ORTUNO, V., PENALVER, E., and TRINCAO, P.R., 2000, A new fossil resin with biological inclusions in Lower Cretaceous deposits from Alava (Northern Spain, Basque-Cantabrian Basin): *Journal of Paleontology*, v. 74, p. 158–178.
- BATTEN, D.J., 1996, Palynofacies and palaeoenvironmental interpretation, in Jansonius, J., and McGregor, D.C., eds., *Palynology: Principles and Application*: American Association of Stratigraphic Palynologists Foundation, v. 3, p. 1011–1064.
- BERRY, E.W., 1914, The Upper Cretaceous and Eocene floras of South Carolina and Georgia: United States Geological Survey Professional Paper 84, 200 p.
- BERRY, E.W., 1919, Upper Cretaceous floras of the eastern Gulf Region in Tennessee, Mississippi, Alabama, and Georgia: United States Geological Survey Professional Paper 112, 177 p.
- BINGHAM, P.S., 2007, Stratigraphic and paleoenvironmental context of the Ingersoll shale, an Upper Cretaceous Konservat-Lagerstätte, Eutaw Formation, eastern Alabama: Unpublished M.S. thesis, Auburn University, Auburn, Alabama, 134 p.
- BINGHAM, P.S., and KNIGHT, T.K., 2005, Terrestrial fauna and flora of the Ingersoll shale: An Upper Cretaceous Konservat-Lagerstätte, Eutaw Formation, eastern Alabama: *Geological Society of America, Abstracts with Programs*, v. 37, n. 2, p. 3.
- BINGHAM, P.S., SAVRDA, C.E., KNIGHT, T.K., and LEWIS, R.D., 2006, Paleoenvironmental factors controlling fossil preservation in an upper Cretaceous Konservat-Lagerstätte (Ingersoll shale, Eutaw Formation, eastern Alabama): *Geological Society of America, Abstracts with Programs*, v. 38, n. 3, p. 306.

- BOTTJER, D.J., ETTER, W., HAGADORN, J.W., and TANG, C.M., 2002, Fossil-Lagerstätten: Jewels of the fossil record, *in* Bottjer, D.J., Etter, W., Hagadorn, J.W., and Tang, C.M., eds., *Exceptional Fossil Preservation: A Unique View on the Evolution of Marine Life*, Columbia University Press, New York, p. 1–10.
- BRIGGS, D.E.G., 1995, Experimental taphonomy: *Palaios*, v. 10, p. 539–550.
- BRIGGS, D.E.G., 2003, The role of decay and mineralization in the preservation of soft-bodied fossils: *Annual Review of Earth and Planetary Sciences*, v. 31, p. 275–301.
- BRIGGS, D.E.G., and GALL, J.C., 1990, The continuum in soft-bodied biotas from transitional environments: A qualitative comparison of Trassic and Carboniferous Konservat-Lagerstätten: *Paleobiology*, v. 16, p. 204–218.
- BRIGGS, D.E. and KEAR, A.J., 1994, Decay and mineralization of shrimps: *Palaios*, v. 9, p. 431–456.
- BRIGGS, D. E. G. and WILBY, P. R., 1996, The role of the calcium carbonate-calcium phosphate switch in the mineralization of soft-bodied fossils: *Journal of the Geological Society, London*, v. 153, p. 665–668.
- BRIGGS, D.E., CLARKSON, E.N., and ALDRIGE, R.J., 1983, The conodont animal: *Lethaia*, v. 16, p. 1–14.
- BROCK, F., PARKES, J.R. and BRIGGS, D.E.G., 2006, Experimental pyrite formation associated with decay of plant material: *Palaios*, v. 21, p. 499–506.
- BURTT, E.H. JR, and ICHIDA, J.M., 1999, Occurrence of feather-degrading bacilli in the plumage of birds: *The Auk*, v. 116, p. 364–372.
- BUTTERFIELD, N.J., 1990, Organic preservation of non-mineralizing organisms and taphonomy of the Burgess Shale: *Paleobiology*, v. 16, p. 272–286.
- CARR, T.D., WILLIAMSON, T.E., and SCHWIMMER, D.R., 2005, A new genus and species of tyrannosauroid from the Late Cretaceous (middle Campanian) Demopolis Formation of Alabama: *Journal of Vertebrate Paleontology*, v. 25, p. 119–143.
- CAVANIHAC, Fishes and Scales, January 2002, <http://www.microscopy.uk.org.uk/mag/indexmag.html?http://www.microscopy.uk.org.uk/mag/artjan02/fishes.html>.
Checked 16 March 2007
- CHATTERJEE, S., 1997, *The Rise of Birds: 225 Million Years of Evolution*: Johns Hopkins University Press, Baltimore, 312 p.

- CHIAPPE, L.M., LAMB, J.P., and ERICSON, G.P., 2002, New enantiornithine bird from the marine Upper Cretaceous of Alabama: *Journal of Vertebrate Paleontology*, v. 22, p. 170–174.
- CHRISTOPHER, R.A., SELF-TRAIL, J.M., PROWELL, D.C., and GOHN, G.G., 1999, The stratigraphic importance of the Late Cretaceous pollen genus *Sohlipollis* gen. nov. in the Coastal Plain Province: *South Carolina Geology*, v. 41, p. 27–44.
- CLAYBURN, J.K., SMITH, D.L., and HAYWARD, J.L., 2004, Taphonomic effects of pH and temperature on extant avian dinosaur eggshell: *Palaaios*, v. 19, p. 170–177.
- CURRIE, P.J., and CHEN, P., 2001, Anatomy of *Sinosauropteryx prima* from Liaoning, northeastern China: *Canadian Journal of Earth Science*, v. 38, p. 1705–1727.
- DAVIS, P.G., and BRIGGS, E.G., 1995, Fossilization of feathers: *Geology*, v. 23, p. 783–786.
- DYCK, J., 1985, The evolution of feathers: *Zoologica Scripta*, v. 14, p. 137–154.
- ETTER, W., 2002, Grès à Voltzia: Preservation in Early Mesozoic deltaic and marginal marine environments, in Bottjer, D.J., Etter, W., Hagadorn, J.W., and Tang, C.M., eds., *Exceptional Fossil Preservation: A Unique View on the Evolution of Marine Life*: Columbia University Press, New York, p. 1–10.
- FELDMAN, H.R., ARCHER, A.W., KVALE, E.P., CUNNINGHAM, C.R., MAPLES, C.G., and WEST, R.R., 1993, A tidal model for Carboniferous *Konservat-Lagerstätten* formation: *Palaaios*, v. 8, p. 485–498.
- FERGUSON, D.K., 2005, Plant taphonomy: Ruminations of the past, the present, and the future: *Palaaios*, v. 20, p. 418–428.
- FRANZEN, J.L., 1985, Exceptional preservation of Eocene vertebrates in the lake deposit of Grube Messel (West Germany), in Whittington, H.B., and Morris, S.C., eds., *Extraordinary Fossil Biotas: Their Ecological and Evolutionary Significance*: *Philosophical Transactions of the Royal Society of London, series B: Biological Sciences*, v. 311, p.181–186.
- FRAZIER, W.J., 1997, Upper Cretaceous strata in southwestern Georgia and adjacent Alabama: *Atlanta Geological Society Field Trip, Guidebook*, 22 p.
- FRIIS, E.M., PEDERSEN, K.R., CRANE, P.R., 2006, Cretaceous angiosperm flowers: Innovation and evolution in plant reproduction: *Palaeogeography, Palaeoclimatology, Palaeoecology*, v. 232, p. 251–293.

- GABBOTT, S.E., NORRY, M.J., ALDRIGE, R.J., and THERON, J.N., 2001, Preservation of fossils in clay minerals: A unique example from the Upper Ordovician Soom Shale, South Africa: *Proceedings of the Yorkshire Geological Society*, v. 53, p. 237–244.
- GALL, J.C., 1985, Fluvial depositional environment evolving into deltaic setting with marine influences in the Buntsandstein of northern Vosges, *in* Mader, D., ed., *Aspects of Fluvial Sedimentation in the Lower Triassic Buntsandstein of Europe: Lecture Notes in Earth Sciences*, no. 4: Springer Verlag, Berlin, p. 449–477.
- GANDOLFO, M.A., NIXON, K.C., CREPET, W.L., and RATCLIFFE, G.E., 1997, A new fossil fern assignable to Gleicheniaceae from Late Cretaceous sediments of New Jersey: *American Journal of Botany*, v. 84, p. 483–493.
- GASTALDO, R., 1986, Land plants, Notes for a short course, ed., *Studies in Geology: University of Tennessee, Department of Geological Sciences*, v. 15, p. 1–212.
- GASTALDO, R.A., 1992, Plant taphonomic character of the Late Carboniferous Hamilton Quarry, Kansas, USA: Preservational modes of walchian conifers and implied relationships for residency time in aquatic environments, *in* Kovar-Eder, J., ed., *Palaeovegetational Development in Europe and Regions Relevant to its Palaeofloristic Evolution: Museum of Natural History, Vienna*, p. 393–399.
- GASTALDO, R.A., and HUC, A.Y., 1992, Sediment facies, depositional environments, and distribution of phytoclasts in the recent Mahakam River delta, Kalimantan, Indonesia: *Palaios*, v. 7, p. 574–590.
- GODDARD, D. R., and MICHAELIS, L., 1934, A study of keratin: *Journal of Biological Chemistry*, v. 106, p. 604–614.
- GOMEZ, B., BAMFORD, M., and MARTÍNEZ-DELCLÒS, X., 2002, Lower Cretaceous plant cuticles and amber (Kirkwood Formation, South Africa): *Comptes Rendus Palevol*, v. 1, p. 83–87.
- GREENWOOD, D. R., 1991, The taphonomy of plant macrofossils, *in* Donovan, S. K., ed., *The processes of fossilization: Belhaven Press, London*, p. 141–169.
- GRIMALDI, D. A., and CASE, G. R., 1995, A feather in amber from the Upper Cretaceous of New Jersey: *American Museum Novitates*, v. 3126, p. 1–6.
- GRIMALDI, D., and ENGEL, M.S., 2005, *Evolution of the Insects: Cambridge University Press, New York*, 755 p.

- GRIMALDI, D.A., BONWICH, E., DELANNOY, M., and DOBERSTEIN, S., 1994, Electron microscopic studies of mummified tissues in amber fossils: *American Museum Novitates*, v. 3097, p. 1–31.
- GRIMALDI, D., SHEDRINSKY, A., and WAMPLER, T.P., 2000a, A remarkable deposit of fossiliferous amber from the Upper Cretaceous (Turonian) of New Jersey, *in* Grimaldi, D., ed., *Studies on Fossils in Amber, With Particular Reference to the Cretaceous of New Jersey: Paleontology of New Jersey Amber Part VII*: Backhuys Publishers, Leiden, p. 1–76.
- GRIMALDI, D., LILLEGRAVEN, J.A., WAMPLER, T.W., BOOKWALTER, D., and SHEDRINSKY, A., 2000b, Amber from Upper Cretaceous through Paleocene strata of the Hanna Basin, Wyoming, with evidence for source and taphonomy of fossil resin: *Rocky Mountain Geology*, v. 35, p. 163–204.
- GRIMALDI, D.A., ENGEL, M.S., and NASCIMBENE, P.C., 2002, Fossiliferous Cretaceous amber from Myanmar (Burma): its rediscovery, biotic diversity, and paleontological significance: *American Museum Novitates*, v. 3361, p. 1–72.
- GRIMES, S.T., BROCK, F., RICKARD, D., DAVIES, K.L., EDWARDS, D., BRIGGS, D.E.G., and PARKES, R.J., 2001, Understanding fossilization: Experimental pyritization of plants: *Geology*, v. 29, p. 123–126.
- GRIMES, S.T., DAVIES, K. L., BUTLER, I. B., BROCK, F., EDWARDS, D., RICKARD, D., BRIGGS, D.E.G., and PARKES, R. J., 2002, Fossil plants from the Eocene London Clay: The use of pyrite textures to determine the mechanism of pyritization: *Journal of the Geological Society, London*, v. 159, p. 493–501.
- HARRAP, B. S., and WOODS, E.F., 1964, Soluble derivatives of feather keratin. 2. Molecular weight and conformation: *Biochemical Journal*, v. 92, p. 19–26.
- HARRIS, T.M., 1969, Naming a fossil conifer, *in* Santapau, H., ed, *J. Sen Memorial Volume*: Botanical Society of Bengal, Calcutta, p. 243–252.
- HEDGES, R.E.M., 2002, Bone diagenesis: An overview of processes: *Archaeometry*, v. 44, p. 319–328.
- HENWOOD, A., 1992, Exceptional preservation of dipteran flight muscle and the taphonomy of insects in amber: *Palaaios*, v. 7, p. 203–212.
- HERENDEEN, P.S., MAGALLÓN-PUEBLA, S., LUPIA, R., CRANE, P.R., and KOBYLINSKA, J., 1999, A preliminary conspectus of the Allon flora from the Late Cretaceous (Late Santonian) of central Georgia, USA: *Annals of the Missouri Botanical Garden*, v. 86, p. 407–471.

- HILGARD, E.W., 1860, Report on the geology and agriculture of the state of Mississippi: Mississippi State Geological Survey, E. Barksdale, State Printer, Jackson, Mississippi, 391 p.
- HOOKS, G.E., III, SCHWIMMER, D.R., and WILLIAMS, D.G., 1999, Synonymy of the pytondont *Phacodus punctatus* and its occurrence in the Late Cretaceous of the southeastern United States: *Journal of Vertebrate Paleontology*, v. 19, p. 588–590.
- KELLER J. A., HERENDEEN, P.S., and CRANE, P.R., 1996, Fossil flowers and fruits of the Actinidiaceae from the Campanian (Late Cretaceous) of Georgia: *American Journal of Botany*, v. 83, p. 528–541.
- KELLNER, A.W.A., 2002, A review of avian Mesozoic fossil feathers, *in* Chiappe, L.M., and Witmer, L.M., eds., *Mesozoic Birds: Above the Heads of Dinosaurs*: University of California Press, Berkeley, p. 389–404.
- KELLNER, A.W.A., MAISEY, J.G., and CAMPOS, D.A., 1994, Fossil down feather from the lower Cretaceous of Brazil: *Paleontology*, v. 37, p. 489–492.
- KIERNAN, C.R., and SCHWIMMER, D.R., 2004, First record of a velociraptorine theropod (Tetanurae, Dromaeosauridae) from the eastern gulf coastal United States: *The Mosasaur*, v. 7, p. 89–93.
- KING, D.T., JR., and SKOTNICKI, M.C., 1986, Facies relations and depositional history of the Upper Cretaceous Blufftown Formation in eastern Alabama and coeval shelf sediments in central Alabama, *in* Reinhardt, J., ed., *Stratigraphy and Sedimentology of Continental, Nearshore, and Marine Cretaceous Sediments of the Eastern Gulf Coastal Plain: Guidebook – Georgia Geological Society*, v. 6, n. 3, p. 10–18.
- KING, D.T., JR., 1990, Facies stratigraphy and relative sea-level history-Upper Cretaceous Eutaw Formation, central and eastern Alabama: *Transactions, Gulf Coast Association of Geological Societies*, v. 40, p. 381–387.
- KNIGHT, T.K., BINGHAM, P.S., and SCHWIMMER, D.R., 2004, The Ingersoll shale, an Upper Cretaceous Konservat Lagerstätte in the Eutaw Formation of east central Alabama: *Geological Society of America, Abstracts With Programs*, v. 36, n. 2, p. 109.
- KNOLL, A.H., 1985, Exceptional preservation of photosynthetic organisms in silicified carbonates and silicified peats: *Philosophical Transactions of the Royal Society of London, Series B: Biological Sciences*, v. 311, p. 111–122.

- KOVÁCS, G., BURGHARDT, J., PRADELLA, S., SCHUMANN, P., STACKEBRANDT, E. and MARIALIGETI, K., 1999, *Kocuria palustris* sp. nov. and *Kocuria rhizophila* sp. nov., isolated from the rhizoplane of the narrow-leaved cattail (*Typha angustifolia*): International Journal of Systematic Bacteriology, v. 49, p. 167–173.
- LAMB, J. P., Jr., 1993, A review of Cretaceous birds of Alabama and initial report of a possible new species: Journal of the Alabama Academy of Science, v. 64, p. 1–88.
- LEAF ARCHITECTURE WORKING GROUP (ASH, A., ELLIS, B., HICKEY, L.J., JOHNSON, K.R., WILF, P., and WING, S.L.), 1999, Manual of leaf architecture: Morphological Description and Categorization of Dicotyledonous and Net-Veined Monocotyledonous Angiosperms: Smithsonian Institution, Washington, D.C., 65 p.
- LESQUEREUX, L., 1892, The flora of the Dakota Group, a posthumous work, in Knowlton, F.H., ed.: United States Geological Survey Monograph 17, 400 p.
- LIPPITSCH, E., 1990, Scale morphology and squamation patterns in cichlids (Teleostei, Perciformes): a comparative study: Journal of Fish Biology, v. 37, p. 265–291.
- LIN X., LEE, C.G., CASALE, E.S., and SHIH, J.C., 1992, Purification and characterization of a keratinase from a feather-degrading *Bacillus licheniformis* strain: Applied and Environmental Microbiology, v. 58, p. 3271–3275.
- LUPIA, R., SCHNEIDER, H., MOESER, G.M., PRYER, K.M., and CRANE, P.R., 2000, Marsileaceae sporocarps and spores from the Late Cretaceous of Georgia, U.S.A.: International Journal of Plant Sciences, v. 161, p. 975–988.
- LUCAS, A. M. and STETTENHEIM, P. R., 1972, Avian anatomy: Integument. Part II: U.S. Department of Agriculture Handbook 362, Washington, D. C., 340 p.
- MAGALLÓN, S., HERENDEEN, P.S., and CRANE, P.R., 2001, Floral diversity in Hamamelidoideae (Hamamelidaceae): *Androdecidua endressi* gen. et sp. nov. from the late Santonian (Late Cretaceous) of Georgia, U.S.A: International Journal of Plant Sciences, v. 162, p. 963–983.
- MANCINI, E.A., PUCKETT, M.T., TEW, B.H., and SMITH, C., 1995, Upper Cretaceous sequence stratigraphy of the Mississippi–Alabama area: Transactions, Gulf Coast Association of Geological Societies, v. 45, p. 377–384.
- MARTÍNEZ-DELCLÒS, X., BRIGGS, D.E.G., and PEÑALVER, E., 2004, Taphonomy of insects in carbonates and amber: Palaeogeography, Palaeoclimatology, Palaeoecology, v. 203, p. 19–64.

- MCALPINE, J.F., and MARTIN J.E.H., 1969, Canadian amber: A paleontological treasure chest: *Canadian Entomologist*, v. 101, p. 819–838.
- MEYER, H., VON, 1861, *Archaeopteryx lithographica* (Vogel-Feder) und *Pterodactylus* von Solenhofen: *Neues Jahrbuch für Mineralogie: Geognosie, Geologie und Petrefakten-Kunde*, p. 678-679.
- MICHENER, C. D., and GRIMALDI, D.A., 1988, The oldest fossil bee: Apoid history, evolutionary stasis, and antiquity of social behavior: *Proceedings of the National Academy of Science*, v. 85, p. 6424–6426.
- NAGALINGUM, N. S., SCHNEIDER, H., and PRYER, K. M., 2006, Comparative morphology of reproductive structures in heterosporous water ferns and a reevaluation of the sporocarp: *International Journal of Plant Sciences*, v. 167, p. 805–815.
- NASCIMBENE, P., and SILVERSTEIN, H., 2000, The preparation of fragile Cretaceous ambers for conservation and study of organismal inclusions, *in* Grimaldi, D., ed., *Studies on Fossils in Amber, with Particular Reference to the Cretaceous of New Jersey*: Backhuys Publishers, Leiden, p. 93–102.
- NEL, A., PERRAULT, G., PERRICHOT, V., and NÉRAUDEAU, D., 2004, The oldest ant in the Lower Cretaceous amber of Charente-Maritime (SW France) (Insecta: Hymenoptera: Formicidae): *Geologica Acta*, v. 2, p. 23–29.
- NÉRAUDEAU, D., ALLAIN, R., PERRICHOT, V., VIDET, B., and DEBROIN, F.L., 2003, Découverte d'un depot paraliqúe á bois fossils, amber insectifère et restes d'Iguanodontidae (Dinosauria, Ornithopodia) dans le Cénománian inférieur de Fouras (Charente-Maritime, Sud-ouest de la France): *Comptes Rendus Palevol*, v. 2, p. 221–230.
- NEWBERRY, J.S., 1896, *The flora of the Amboy Clays*: United States Geological Survey Monograph 26, 260 p.
- NORELL, M.A., and XU, X., 2005, Feathered dinosaurs: *Annual Review of Earth and Planetary Sciences*. v. 33, p. 277–299.
- PEÑALVER, E., GRIMALDI, D.A., and DELCLÓS, X., 2006, Early Cretaceous spider web with its prey: *Science*, v. 312, p. 1761.
- PENNEY, D., WHEATER, C.P., and SELDEN, P.A., 2003, Resistance of spiders to Cretaceous-Tertiary extinction events: *Evolution*, v. 57, p. 2599–2607.
- PERRICHOT, V., 2004, Early Cretaceous amber from south-western France: Insight into the Mesozoic litter fauna: *Geologica Acta*, v. 2, p. 9–22.

- PLOTNICK, R.E., 1986, Taphonomy of a modern shrimp: Implications for the arthropod fossil record: *Palaios*, v. 1, p. 286–293.
- POINAR, G., 1998, Trace fossils in amber: A new dimension for the ichnologist: *Ichnos*, v. 6, p. 47–52.
- POINAR, G.O. JR., 1993, Insects in amber: *Annual Review of Entomology*, v. 46, p. 145–159.
- POINAR, G.O. JR., and MASTALERZ, M., 2000, Taphonomy of fossilized resins: Determining the biostratigraphy of amber: *Acta Geologica Hispanica*, v. 35, p. 171–182.
- POINAR, G.O. JR., and MILKI, R., 2001, Lebanese amber: The Oldest Insect Ecosystem in Fossilized Resin: Oregon State University Press, Corvallis, 96 p.
- PRUM, R.O., and BRUSH, A.H., 2004, Which came first, the feather or the bird?: *Scientific American*, v. 14, p. 72–81.
- JI, Q., CURRIE, P.J., NORELL, M.A., and JI, S., 1998, Two feathered dinosaurs from northeastern China: *Nature*, v. 393, p. 753–761.
- REINHARDT, J., and DONOVAN, A.A., 1986, Stratigraphy and sedimentology of Cretaceous continental and nearshore sediments in the eastern Gulf Coastal Plain, *in* Reinhardt, J., ed., *Stratigraphy and Sedimentology of Continental, Nearshore, and Marine Cretaceous Sediments of the Eastern Gulf Coastal Plain: Guidebook-Georgia Geological Society*, v. 6, n. 3, p. 3-9.
- REINHARDT, J., SCHINDLER, S., and GIBSON, T.G., 1994, Geologic map of the Americus 30'x 60' quadrangle, Georgia and Alabama: Department of the Interior, United States Geological Survey, map 1–2174.
- ROSS, A. J., 1997, Insects in amber: *Geology Today*, v. 13, p. 24–28.
- SAVRDA, C.E., LOCKLAIR, R.E., HALL, J.K., SADLER, M.T., SMITH, M.W., and WARREN, J.D., 1998, Ichnofabrics, ichnocoenoses, and ichnofacies: Implications of an Upper Cretaceous tidal-inlet sequence (Eutaw Formation, central Alabama): *Ichnos*, v. 6, p. 53–74.
- SAVRDA, C.E., and NANSON, L.L., 2003, Ichnology of fair-weather and storm deposits in an Upper Cretaceous estuary (Eutaw Formation, western Georgia, USA): *Palaeogeography, Palaeoclimatology, Palaeoecology*, v. 202, p. 67–83.
- SCHÄFER, W., 1972, *Ecology and Paleocology of Marine Environments*: University of Chicago Press, Chicago, 568 p.

- SCHIEBER, J., 2002, The role of an organic slime matrix in the formation of pyritized burrow trails and pyrite concretions: *Palaios*, v. 17, p. 104–109.
- SCHWEITZER, M. H., J. A. WATT, R. AVCI, L. KNAPP, L. CHIAPPE, M. NORELL, and M. MARSHALL., 1999, Beta-keratin specific immunological reactivity in feather-like structures of the Cretaceous alvarezsaurid, *Shuvuuia deserti*: *Journal of Experimental Zoology (Molecular and Developmental Evolution)*, v. 285, p. 146–157.
- SCHWIMMER, D.R., 1981, A distinctive Upper Cretaceous fauna, 3-4 meters below the Blufftown-Cusseta contact in the Chattahoochee River Valley: *in* Reinhardt, J., and Gibson, T.G., eds., *Upper Cretaceous and Lower Tertiary geology of the Chattahoochee River Valley, Western Georgia and Eastern Alabama: Georgia Geological Society Field Trip Guidebook*, v. 1, n. 1, p. 81–88.
- SCHWIMMER, D.R., 1988, Late Cretaceous fish from the Blufftown Formation (Campanian) in western Georgia: *Journal of Paleontology*, v. 62, p. 290–301.
- SCHWIMMER, D.R., PADIAN, K. and WOODHEAD, A.B., 1985, First pterosaur records from Georgia: Open marine facies, Eutaw Formation (Santonian): *Journal of Paleontology*, v. 59, p. 674–676.
- SCHWIMMER, D.R., WILLIAMS, G D., DOBIE, J.L., and SIESSER, W.G., 1993, Late Cretaceous dinosaurs from the Blufftown Formation in western Georgia and eastern Alabama: *Journal of Paleontology*, v. 67, p. 288–296.
- SCHWIMMER, D.R., STEWART, J.D., and WILLIAMS, G.D., 1997, Scavenging by sharks of the genus *Squalicorax* in the Late Cretaceous of North America: *Palaios*, v. 12, p. 71–83.
- SCHWIMMER, D.R., HOOKS, G.E., and JOHNSON, B., 2002, Revised taxonomy, age, and geographic range of the large laniform shark *Cretodus Semiplicatus*: *Journal of Vertebrate Paleontology*, v. 22, p. 704–707.
- SEILACHER, A., 1970, Begriff and Bedeutung der Fossil-Lagerstätten: *Neues Jahrbuch für Geologie und Paläontologie. Abhandlungen*, v. 1, p. 34–39.
- SEILACHER, A., REIF, W.-E., and WESTPHAL, F., 1985, Sedimentological, ecological and temporal patterns of *Fossil-Lagerstätten*: *Philosophical Transactions of the Royal Society of London, Series B: Biological Sciences*, v. 311, p. 5–23.
- SHAWKEY, M.D., 2005, Feathers at a fine scale, Unpublished Ph.D. dissertation, Auburn University, Auburn, Alabama, 198 p.

- SIMS, H.J., HERENDEEN, P.S., LUPIA, R., and CHRISTOPHER, R.A., 1999, Fossil Flowers with *Normapolles* pollen from the Upper Cretaceous of southeastern North America: *Review of Palaeobotany and Palynology*, v. 106, p. 131–151.
- SIRE-JEAN-YVES and HUYSSEUNE, A., 2003, Formation of dermal skeletal and dental tissues in fish: a comparative and evolutionary approach: *Biological Reviews*, v. 78, p. 219–249.
- SMITH, E.A., and JOHNSON, L.C., 1887, Tertiary and Cretaceous strata of the Tuscaloosa, Tombigbee and Alabama Rivers: *United States Geological Survey Bulletin* 43, 189 p.
- SPICER, R.A., and GREER, A.G., 1986, Plant taphonomy in fluvial and lacustrine systems, *in* Land plants, Notes for a short course, ed., *Studies in Geology*: University of Tennessee, Department of Geological Sciences, v. 15, p. 10–26.
- STANKIEWICZ, B.A., POINAR, H.N., BRIGGS, D.E.G., EVERSLED, P.R., and POINAR, G.O. JR., 1998, Chemical preservation of plants and insects in natural resins: *Philosophical Transactions of the Royal Society London, Series B: Biological Sciences*, v. 265, p. 641–647.
- STANLEY, S.M., 1970, Relation of shell form to life habits in the Bivalvia (Mollusca): *Geological Society of America Memoir* 125. Boulder, Colorado, 296 p.
- STEPHENSON, L.W., 1957, Fossils from the Eutaw Formation, Chattahoochee River Region, Alabama-Georgia: *United States Geological Survey Professional Paper* 274, p. 227–250.
- STETTENHEIM, P. R., 1972, The integument of birds, *in* FARNER, D.S., KING, J.R., and PARKES K.C., eds., *Avian Biology*, v. 2: Academic Press, New York, p. 1–63.
- STETTENHEIM, P. R., 2000, The integumentary morphology of modern birds-An overview: *American Zoology*, v. 40, p. 461–477.
- TAKAHASHI, M., HERENDEEN, P.S., and CRANE, P.R., 2001, Lauraceous fossil flowers from the Kamikitaba locality (Lower Coniacian; Upper Cretaceous) in northeastern Japan: *Journal of Plant Research*, v. 114, p. 429–434.
- WETMORE, A., 1943, The occurrence of feather impressions in the Miocene of Maryland: *The Auk*, v. 60, p. 440–441.
- WILLIAMS, C.M., RICHTER, C.S., MACKENZIE J.M., and SHIH, J.C.H., 1990, Isolation, identification and characterization of a feather-degrading bacterium: *Applied and Environmental Microbiology*, v. 56, p. 1509–1515.

- WILLISTON, W.S., 1896, On the dermal covering of *Hesperornis*: Kansas University Quarterly, v. 5, p. 53–54.
- WOLFE, J.A., and UPCHURCH, G.R., JR., 1987, North American nonmarine climates and vegetation during the Late Cretaceous: Palaeogeography, Palaeoclimatology, Palaeoecology, v. 61, p. 33–77.
- WUTTKE, M., 1983, ‘Weichteil-Erhaltung’ durch lithifizierte Mikroorganismen bei mittel-eozänen Vertebraten aus den Ölschiefern der ‘Grube Messel’ bei Darmstadt: Senckenbergiana. Lethaea, v. 64, p. 509–527.
- XU, X., NORELL, M.A., KUANG, X., ZHAO, Q., and JIA, C., 2004, Basal tyrannosauroids from China and evidence for protofeathers in tyrannosauroids: Nature, v. 431, p. 680–683.
- ZHERIKHIN, V.V., and ESKOV, K.Y., 1999, Mesozoic and Lower Tertiary resins of former USSR: Estudios Museo Ciências Naturales de Alava, v. 14, n. 2, p. 119–131.